THE APPLICATION OF HIGH POWER LASERS TO THE WELDING OF TEE SECTION JOINTS IN SHIP PRODUCTION

Volume I

Stephen John BROOKE, B.Sc.

NEWCASTLE UNIVERSITY LIBRARY
087 11608 7
Thesis L3253

Department of Naval Architecture and Shipbuilding
May 1987

University of Newcastle upon Tyne
Newcastle upon Tyne NE1 7RU

Thesis submitted for the degree of Doctor of Philosophy
Prepared in two volumes

To Karen

ABSTRACT

The use of computers by naval architects has revolutionised ship design and construction management. The use of high power laser technology could similarly revolutionise production processes to produce a quantum leap in productivity.

Facilitating low heat input materials processing, the laser is suited to various cutting, welding and heat treatment applications in shipbuilding to increase productivity through improved product accuracy. From these processes, the Author has concentrated on the application of high power lasers to the welding of tee section joints - the most common joint configuration in ship structures - by a single sided method (skid welding) to give both the lowest possible heat input and greatest flexibility.

Using a 10kW laser, single pass fully penetrating skid welds may be produced for joints in plate of up to 15mm thick, but using this size of laser, production parameter envelopes to produce visually and structurally sound joints reduce in size as plate thickness increases to greater than 10mm. It is shown that fully penetrating laser skid welds produced in steel conventionally used for surface vessel construction are

of superior structural quality to fillet welds as required by classification society rules.

The work has shown that achieving process consistency in an automated production based skid welding workstation operating with existing levels of joint tolerance will be dependent not only on well designed laser and beam delivery harware but also on suitable on-line adaptive control systems.

It has been demonstrated that by employing laser skid welding for steelwork fabrication, an increase in productivity can be gained, principally through increased processing speed and improved product accuracy.

CONTENTS

Volume I

ACKNOWLEDGEMENTS xiii

NOMENCLATURE xvi

LIST OF FIGURES xx

1 INTRODUCTION 1

1.1 LASER MATERIALS PROCESSING IN SHIPBUILDING - THE WAY AHEAD 1

1.2 GENERAL HISTORY AND DEVELOPMENT OF THE CO2 HIGH POWER LASER 4

1.2.1 Brief Overview of the Development of Industrial High Power CO2 Lasers 4

1.2.2 High Power Laser Beams for Materials Processing 12

1.3 LASER MATERIALS PROCESSING IN SHIPBUILDING - THE STATE OF THE ART 23

1.3.1 A Review of works by Authors on Ship Production Based Laser Processing 23

1.3.2 Summary of Conclusions Drawn by D.R.Martyr 26

2 PRINCIPLES OF LASER WELDING 31

2.1 INTRODUCTION 31

2.1.1 High Power and Low Power Laser Welding 31

2.1.2 The Simplest High Power Laser "Weld" 32

2.1.3 Development of the Melt Run to Produce Practical Weld Configurations 33
2.1.4 Classificaiton of Welding Techniques 34
2.1.5 Laser Welding Terminology 34
2.2 GENERAL PRINCIPLES OF HIGH POWER LASER WELDING 41
2.2.1 Manipulation of a Laser Beam to the Workpiece 41
2.2.2 Beam Absorption to Form a Keyhole 42
2.2.3 Energy Transfer from the Keyhole 45
2.2.4 Dynamics of a moving keyhole system to form a continuous fusion zone 47
2.2.5 Controlling the Plasma Density Balance in the Keyhole 48
2.3 THEORETICAL ANALYSIS OF WELD ZONE CHARACTERISTICS 51
2.3.1 Heat Flow Analysis 53
2.3.2 Heat Flow From Point and Line Heat Sources 54
2.3.3 Correlation of Linear Heat Source Analysis with Practical Welds 59
2.4 PRACTICAL WELD JOINT CONFIGURATIONS 63
2.4.1 Butt Welding 64
2.4.2 Laser Through-Weld 68
2.4.3 Laser Keyhole Welds with Reinforcement or Smoothing Bead Additions 73
2.5 LASER SKID WELDING 74
2.5.1 Principal Parameter Assessment 76
2.5.2 Plasma Control Requirements 78
2.5.3 Filler Requirement 78
2.5.4 Laser Skid Welding - Summary of D.R. Martyr's Trials

and Conclusions 79

2.5.5 Laser Skid Welds - Review of Recent Literature 81

2.5.6 Laser Skid Weld - Reasons for further investigation in this Weld 82

3 WELDING TRIALS TO PRODUCE "SKID" WELDS IN TEE BUTT JOINTS 84

3.1 OBJECTIVES OF LASER SKID WELDING TRIALS 84

3.2 PREREQUISITES FOR TRIALS PROGRAMME 86

3.2.1 Choice and Scheduling of Laser Welding Test Facility 86

3.2.2 Design of a Focus Unit for Skid Welding 88

3.2.3 Design of a Shroud Unit for Skid Welding 91

3.2.4 Wire Feed Unit Design 94

3.2.5 Sample Support Table Design 96

3.3 SAMPLE SELECTION AND PREPARATION 96

3.3.1 Plate Selection and Preparation 96

3.3.2 Jig Construction 99

3.3.3 Sample Pretacking 101

3.4 PREPARATION OF LASER, BEAM LINE AND WORKSTATION PRIOR TO TRIALS 102

3.4.1 Laser Start Procedure and Stabilisation 102

3.4.2 Beam Line Alignment 103

3.4.3 Beam Diameter and Intensity Distribution Measurement 104

3.4.4 Power Measurement 106

3.4.5 Wire Feed Alignment 107

3.4.6 Shroud Unit Alignment 108

3.4.7 Focus Unit Positional Alignment 108

3.4.8 Focus Position Assessment 110

3.4.9 System Calibration 112

3.5 PRACTICAL WELDING PROCEDURES 113

3.5.1 Parameters to be Considered for each Weld Run 113

3.5.2 Workpiece Positioning in Workstation 113

3.5.3 Plasma Control Jet Positioning 117

3.5.4 Filler Feed Positioning 119

3.5.5 Interlocks 121

3.5.6 Operation of the Laser System for each Weld Run 123

3.5.7 Sample Identification 124

3.6 Trial Programme Scheduling 125

3.6.1 Review of Processing Variables 125

3.6.2 Selection of Programme Priorities 125

3.6.3 Trial Schedule Development 126

3.6.4 Dominant Milestones in the Welding Programme 127

4 SKID WELDING PARAMETERS, PROCESS EFFECTS AND TOLERANCES 133

4.1 LASER POWER AND SKID WELDING TRAVERSE SPEEDS 134

4.1.1 Traverse speeds for skid welding flat plate webs 138

4.1.2 Effect of joint gap on skid weld traverse speeds 146

4.1.3 Effect of plate edge shape on skid weld traverse speeds 150

4.1.4 Effect of plate coatings on skid weld traverse speed 151

4.1.5 Effect of skidwelding through tack welds 154

4.1.6 Traverse speeds for skid welding at powers less that 9kw 155

4.1.7 Correlation of laser power and traverse speed to joint shapes 157
4.2 FILLER WIRE INPUT 164
4.2.1 Assessment of filler wire input rate 164
4.2.2 Filler Wire Thickness 173
4.2.3 Filler Wire Alignment 173
4.3 LASER BEAM SPOT POSITIONING AND FOCUS 174
4.3.1 Incident Beam Angle 176
4.3.2 Incident Beam Spot Height 182
4.3.3 Beam Mode 191
4.3.4 Focal Depth of Operation 193
4.4 PLASMA CONTROL AND WELD SHROUDING 195
4.4.1 Gas Flow Rates to Achieve Plasma Control and Weld Shielding 196
4.4.2 Position of Plasma Control Unit 198
4.5 SUMMARY OF LASER WELDING PARAMETER SPECIFICATIONS AND TOLERANCES 200

Volume II

5 WELD CLASSIFICATION - MECHANICAL TESTING 204
5.1 THE REQUIREMENTS SET BY CLASSIFICATION SOCIETIES 204
5.1.1 Standards for conventional testing of fillet welds 205
5.1.2 Alternative test procedure ratification by classification societies 206
5.1.3 Non-Destructive Testing 208
5.2 CRUCIFORM TEST 211
5.2.1 Preparation of Test pieces for Cruciform Tests 211

5.2.2 Cruciform Test Results 213

5.3 FILLET WELD FRACTURE TEST 216

5.3.1 Fracture test specimen manufacture 217

5.3.2 Fracture testing details 219

5.3.3 Fracture testing results and discussion 219

5.4 IMPACT TESTING 224

5.4.1 Use of Sub-sized Charpy specimens 225

5.4.2 Alternative procedures to all-weld-metal consumable testing 227

5.4.3 Charpy testing of narrow weld sections 230

5.4.4 Charpy specimen manufacture 232

5.4.5 Charpy test results and discussion 238

5.4.6 Recommendations for Charpy value assessment 247

5.5 FATIGUE TESTING 249

5.5.1 Tee Joint Classification within B.S.5400 254

5.5.2 Fatigue test specimen manufacture 258

5.5.3 Fatigue Testing Details 261

5.5.4 Fatigue Testing Results 263

5.5.5 Alternative method for assessment of comparative fatigue properties 272

6 METALLURGICAL EXAMINATION AND CLASSIFICATION 277

6.1 HARDNESS TESTING 278

6.1.1 Classification Requirement for Hardness Testing 279

6.1.2 Hardness test specimen manufacture and testing 284

6.1.3 Hardness Test Results and Discussion 284

6.2 WELDABILITY OF SHIP STEEL FOR LASER SKID WELDING 291

6.3 GENERAL ASSESSMENT OF WELD MICROSTRUCTURE 304

6.3.1 Classification of Laser Weld Microstructural Constituents 304

6.3.2 Grain Growth Microstructure 307

6.3.3 Transformed Microstructure 314

6.3.4 Relationship of microstructure to Charpy Values 324

6.4 WELD FLAWS HIGHLIGHTED BY MICRO EXAMINATION 330

6.4.1 Solidification Cracking 331

6.4.2 Lack of Fusion 333

6.4.3 Porosity 335

7 EVALUATION OF SHIPYARD BASED FACILITIES EMPLOYING LASER SKID WELDING 339

7.1 APPRAISAL OF LASER BASED EQUIPMENT FOR SKID WELDING IN SHIPYARDS 340

7.1.1 Production line laser generators 340

7.1.2 Beam line transmission equipment 345

7.1.3 Manipulation devices 348

7.2 APPRAISAL OF SKID WELDING FACILITY ON-LINE MONITORING AND ADAPTIVE CONTROL EQUIPMENT 364

7.2.1 Beam structure and delivery monitoring 365

7.2.2 Process monitoring 367

7.2.3 Seam Tracking 370

7.3 SAFETY REQUIREMENTS RELATING TO LARGE SHIPYARD BASED LASER SYSTEMS 373

7.3.1 Operational Considerations 374

7.3.2 Laser Affected Zone Monitoring 375

7.3.3 System Shut-Down Time 377

7.3.4 Proposed safety procedures for the shipyard based skidwelding facility 378

7.4 ECONOMIC EVALUATION OF SKID WELDING FACILITIES 379

7.4.1 Analysis of welding facility and operational costs to compare laser skid and semi-automatic fillet welding 381

7.4.2 Synthesis and economic evaluation of a matrix line 387

7.4.3 Synthesis and economic evaluation of a minor assembly line 407

8 SUMMARY, CONCLUSIONS AND RECOMMENDATIONS 420

8.1 Summary 420

8.2 Conclusions 423

8.3 Recommendations 429

REFERENCES 431

Appendix A : APPENDICES ASSOCIATED WITH CHAPTER 3 449

Appendix B : APPENDICES ASSOCIATED WITH CHAPTER 4 457

Appendix C : APPENDICES ASSOCIATED WITH CHAPTER 5 475

Appendix D : APPENDICES ASSOCIATED WITH CHAPTER 6 505

Appendix E : APPENDICES ASSOCIATED WITH CHAPTER 7 527

ACKNOWLEDGEMENTS

The Author is indebted to Dr James Teasdale whose supervision, encouragement and suggestions contributed to the success of this work.

The advice and stimulating ideas of many members of the University of Newcastle are acknowledged with gratitude. Particularly of Professor J B Caldwell, the Authors colleagues Kevin Hudson, Philip Dalton, Roauf Kattan, Dr Yang Yong-Soon and John Rouse and Chief Technician Alan Buckham in the Department of Naval Architecture. Thanks is also due to members of other departments, namely Dr John Congleton and Don Maxwell in Metallurgy and Judith Hunter in Computing, whose facilities enabled the Author to type and format this thesis.

Particular thanks go to the Laser Applications Group at the UKAEA Culham Laboratories, Oxfordshire whose facilities were made avaialble to the Author to produce the laser skid welds. The encouragement, helpful advice and technical assistance of Dr Ian Spalding, Dr Harry Megaw, Brooke Ward, Chris Nicholson, Ian Stares and Malcolm Terry are gratefully acknowledged.

The Author would like to take this opportunity of thanking various organisations and people for their inspiration during many technical discussions. From The Welding Institute Dr Martin Watson, Peter Oackley, Ian Norris Norman Bailey and Chris Punshon; Peter Boothby of British Gas, Derrick Camsey, Don Cuthbert and Chris Baxter of BMT; Dr Roger Vaughan, Frank Wylie and Tommy Dent of Swan Hunter Ltd; Einor Pederson of TTS, Norway; Dr Armin Gukelburger of Spectra Physics, Germany; Ed Metzbower of NRL, USA; Dr Liane Smith of Shell Research, Dick Ashcroft and Gerry Parsons of Control Laser; John Chadwick and Brian Moody of ILS and Alec Milne of International Paints. A special thanks must go to Dr David Martyr of Ferranti, formerly of British Shipbuilders.

Members of the following testing facilities are thanked for their co-operation in enabling critical tests to be made within the NACRO Standards: Les Brown of British Steel, Keith Murray of NEI International Research and Development, Ted Wilkinson of Dunelm Testing and Peter Tubby of the Welding Institute.

For the constructive observations made by classification organisations the Author thanks Mr Frank Watkinson, Dr Peter Lane, and Tom Close of Lloyds Register of Shipping; John Bird and John Galsworthy of the MOD(Navy).

The financial and administrative support of British Shipbuilders and the Science and Engineering Research Council are gratefully acknowledged, particularly to Ray Adams of MDC and Jim Heaton formerly of British

Shipbuilders for securing the administrative aspects and Peter Orrick for his technical oversight to the project.

The Author also wishes to pay tribute to Tony Smith, Director of Technology at British Shipbuilders unitl his untimely and tragic death in October 1983. His inspiration and motivation was surely a substantial driving force in facilitating this adventurous project.

Finally the most important thanks go to the members of the Author's family and friends for their support and positive help. Clearly this work would not have been possible had it not been for the patience, support and practical help of Karen, the Author's wife, the true value of which cannot be adequately expressed.

NOMENCLATURE

A	Weld cross-section area (m^2)
a	Weld pool depth (m)
amax	Maximum depth of penetration for a given laser power (m)
b	Weld pool average width (m)
CE	Material Carbon equivalent (% weight) as calculated by the equation of a particular author.
c	Specific heat ($J.kg^{-1}.K$)
d	*Wire diameter (m)*
D	Thermal diffusivity ($m2.s^{-1}$)
E	Young's modulus ($N.m^{-2}$)
Em	Melt ratio
Eht	Heat transfer efficiency
FILo	Basic filler rate, no reinforcement (m/sec)
FIL1	Basic filler rate, one joint side reinforced (m/sec)
FIL2	Basic filler rate, both joint sides reinforced (m/sec)
FILLY	Filler rate as computed (m/sec)
f	Distance apart of supports for fatigue testing (m)
G	Joint gap (m)
h	Plate thickness (m)
HvM	Material hardness once 100% martensite formed (Hv)
Hvmax	Maximum hardness within the heat affected zone (Hv)

I	Second moment of area (m^4)
K	Thermal conductivity ($J.m^{-1}.s^{-1}..K^{-1}$)
Ko	Bessel function of the first kind, zero order.
k	Constants relating to maximum penetration
k_1	capacity calculations
Lf	Latent heat of fusion ($kJ.kg^{-1}$)
l	Reinforcing bead effective leg length (m)
M	Bending moment (N.m)
Plo	Laser power at the laser output (kW)
Pm	Laser power to melt a volume of material (kW)
Pwp	Laser power at the workpiece (kW)
p	Material density ($kg.m^{-3}$)
Q	Heat input per unit length ($J.m^{-1}$)
q	Rolled section bar edge radius (m)
R	Radius of gyration (m)
r	Distance from weld centre line (m)
S	Heat funcion (kW/m)
s	Laser spot height above face the face plate (m)
σ_1	Stress measured at the weld toe (N/m^2)
σ_2	Stress measured in the weld throat (N/m^2)
T	Temperature at a point (°K)
DT	Temperature change (°K)
To	Original temperature (°K)
Tm	Melting temperature (°K)
t	Time (seconds)
Dt8-5	Time for temperature to drop from 800-500°C (sec)

UTS Ultimate tensile stress ($N.m^{-2}$)

v Traverse speed ($m.s^{-1}$)

w Peak power intensity within the laser beam (Watts)

X Normalised power input per unit depth function

Y Normalised speed-weld width function

x Distance along the joint line (m)

y Perpendicular distance from joint centre line (m)

yn Distance from the neutral axis (m)

z Depth into the plate (m)

α_1, α_2)Constants used in point and line heat source

ϕ)equations.

ABBREVIATIONS

BRITE Basic Research into Industrial Technology

AC Martensite with aligned martensite, austenite or carbide.

AF Acicular ferrite.

GF Grain boundary ferrite.

PF Polygonal ferrite.

FATT Fracture Appearance Transition Temperature (°C)

HAZ Heat affected zone.

IIW International Institute of Welding

LARS Laser Articulated Robot System

LO Laser output)- used when referring to the position at

WP Work piece.) which laser power is measured.

MMA Manual metal arc welding process

MIG/MAG Metal inert / active gas welding.

SAW Submerged arc welding.

TIG Tungsten inert gas welding.

TWI The Welding Institute

MOD(N) Ministry of Defence (Navy).

LIST OF FIGURES

No	Title	Page
1.01	- Examples of typical commercial CO2 lasers of greater than 5kW output	8
1.02	- Stable and unstable optical resonators	13
1.03	- The electromagnetic spectrum	13
1.04	- Laser beam modes	15
1.05	- Typical laser generation paths	17
1.06	- The UKAEA Culham Laboratory designed CL5, 5kW laser	28
2.01	- Comparison of conventional fillet welding processes used in shipbuilding	36
2.02	- Butt and tee joint; conventional and laser terminology	39
2.03	- Use of mirrors and lenses for focusing a laser beam	43
2.04	- Stages in the formation of a keyhole	44
2.05	- Beam reflections within the keyhole	46
2.06	- Heat flow from the keyhole to the parent plate	46
2.07	- Forces acting to maintain the keyhole	49
2.08	- Production of a weld from a moving keyhole system	49
2.09	- Directions of heat flow from a point and line heat source	55

2.10 - Penetration weld geometry with a linear heat source . . 57

2.11 - Comparison of idealised and practical butt edges . . . 65

2.12 - Plasma control shoe positioned for butt welding 67

2.13 - Laser butt weld joint surface profiles 69

2.14 - Laser keyhole welds with smoothing beads 75

2.15 - Limiting beam positional considerations for skid welding 77

2.16 - Laser to sample orientation for Martyr's and Brooke's work 80

3.01 - UKAEA Culham Laboratory laser facility 87

3.02 - Focusing unit positioned for butt welding 89

3.03 - Skid welding shroud unit positioned at the. workpiece 93

3.04 - MIG welding wire feed drive unit used for the skid welding trials 95

3.05 - Workpiece support jig with leveling adjuster mechanism 97

3.06 - Sample preparation jig with a sample supported for tack welding 100

3.07 - A shallow beam print made in way of a beam line folding mirror 105

3.08 - A Joule Stick positioned in the beam line for power measurements 105

3.09 - Position of the gas shroud unit at the workpiece . . . 109

3.10 - Effect of the off axis focused beam to assist in identifying the relative position of the beam focus . 111

3.11 - A pre-tacked sample positioned on the welding stand and aligned to worktable datum, plasma control unit positioned 116

3.12 - The shroud position relative to the joint for butt welding and skidwelding 118

3.13 - Position of the filler wire for butt and skid

welding 120

3.14 - Mechanical and electronic interlocks controlling access to the workstation ans beam line 122

3.15 - Programme of laser welding trials at UKAEA Culham Laboratory 128

4.01 - Heat inputs needed to enable blind melt run penetrations of 6-15mm at various powers using a CL10 laser - data from Kaye et al 136

4.02 - Traverse speed envelope for skid welding flat plate tee section joints: power(WP)9kW for 6-15mm plate, 5kW for 3mm plate 141

4.03 - Balanced plasma on both sides if an 8mm joint during skidwelding 143

4.04 - Traverse speed envelope for skid welding gap joints (1-2 mm gap):laser power 9kW(WP) 148

4.05 - Skid weld produced in a joint in 6mm thick plate containing a gap of 2mm and showing well balanced beads (X4.8) 149

4.06 - Traverse speed envelope for skid welding rolled section tee section joints : laser power 9kW (WP) . . 152

4.07 - Traverse speed envelope for skid welding tee section joints with primer on the plate surface : laser power 9kW(WP) 152

4.08 - The effect of reducing laser power from 9kW(WP) on traverse speed maintaining a visually acceptable joint : 6mm plate 156

4.09 - Normalised efficiency analysis for melt runs showing the differential for blind and penetrating melt runs 159

4.10 - Normalised efficiency analysis for skid welds in various plate thickness : laser power 9kW(WP), various traverse speeds 160

4.11 - Normalised efficiency analysis for skid welds of varying joint gaps ; laser power 9kW(WP), various traverse speeds 160

4.12 - Normalised efficiency analysis for skid welds in

6mm plate using various power inputs 162

4.13 - Melt ratios of joints in 6mm plate calculated with respect to the weld zone area for various heat inputs 162

4.14 - Comparison of predicted and actual weld penetration for skid and blind melt runs using a laser power of 9kW(WP) 163

4.15 - Filler rates calculated by the Skidfill prediction for various joint gaps as measured. Actual rates used for a nominal gap shown 170

4.16 - Predictions of speeds at which smoothing bead sizes will reduce for 6mm, 10mm and 15mm thick joints : laser power 9kW(WP) 170

4.17 - Comparison of FIL1/FIL2 and FILLY predicted filler rates for each plate thickness welding at the recommended production speed 171

4.18 - Variations between FIL2 and FILLY predictions of weld filler rates in 8mm plate and various joint gaps 171

4.19 - Total included beam angle for laser beams of various focal numbers 177

4.20 - Keyhole root forming at the emergent bead root 179

4.21 - Formation of the keyhole side-shoot to form a fully fused emergent bead 181

4.22 Effect of the laser spot height on autogenous skid welds : 8mm plate thickness 184

4.23 - Comparison of tested spot heights, the tolerance envelope and a plot calculated heights from equation 4.07 186

4.24 - Skid weld in 8mm & 12mm plate, excessive spot height causing a lack of fusion mext to the incident bead . 188

4.25 - Comparison of incident bead face angles for varying spot heights 190

4.26 - Laser spot heights for use in skid welding joint of varying gaps : laser power 9kW 190

4.27 - Beam prints taken at various positions within the beam line from the source to the workstation . . 192

4.28 - Output from the SKIDWELD program for interactive process control 201

5.01 - Dimensions of test samples used for tensile testing . . 212

5.02 - Ultimate tensile strenght of laser skid welds compared with parent plate carbon equivalent 214

5.03 - Laser skid welded cruciform samples failed in the parent plate during tensile testing 215

5.04 - Flaws (lack of fusion) identified in the skid weld during tensile testing 215

5.05 - Dimensions of the samples used for fillet fracture type testing 218

5.06 - Loading of the fracture test samples 218

5.07 - Sound joints after fillet fracture 221

5.08 - Various types of failure observed in skid weld fracture testing 221

5.09 - Charpy test specimen extraction from a cruciform welded sample 229

5.10 - Rotation of the face plate for an alternative configuration to Charpy test tee section joints . . 229

5.11 - ISO and ASTM standard stricker geometries for Charpy testing 233

5.12 - Charpy transition and fracture appearance curves for laser butt and skid welds in 8 and 10mm plate 9kW laser power, A31 filler wire 239

5.13 - Flow diagram for the proposed revised charpy testing schedule 248

5.14 - Three principle modes of fatigue loading for tee joints and respective modes of failure 255

5.15 - Two alternative arrangements for applying a fatigue load for the Mode 2 failure 259

5.16 - Dimensions of fatiuge test specimens 260

5.17 - Fatigue S-N curves results for Mode 1 loading: non-loaded stiffener 264

5.18 - Fatigue crack surfaces 265

5.19 - Comparative results of a non-loaded stiffener for control results in bending and torsion 267

5.20 - Fatigue results for Mode 2 fatigue testing - loaded stiffener 270

5.21 - Fatigue crack surfaces showing areas of weld defects . 270

5.22 - Surface roughness measuring device with a fine stylus type probe 274

5.23 - Male replicas of the weld profile 274

6.01 - Hardness traverse test positions for fillet and laser skid welds 281

6.02 - Hardness traverse test positions for fillet and laser skid welds 283

6.03 - Hardness traverse results for skid weld tee section joints in each plate thickness; 9kW laser power . . . 285

6.04 - Hardness traverse results for 6mm plate (P6/01/CS) skid welds; varying power 289

6.05 - Hardness traverse results for 6mm plate (P6/02/SHS) skid welds; varying power 290

6.06 - Skid weld HAZ cooling rates (800 - 500) for various traverse speeds as calculated form the max. hardness in the HAZ 294

6.07 - Predictions of max. hardness in the HAZ assumming fully martensitic micro structure 297

6.08 - Predictions of max. hardness in the HAZ for various cooling rates using equations of Suzuki 298

6.09 - HAZ cooling rates (800 - 500) for laser skid welds, MMA and MIG fillet welds in the HAZ for various plate thickness 298

6.10 - Predictions of max. hardness in the HAZ for laser skid and MMA/MIG fillet welds assuming an average plate composition 301

6.11 - Variation of hardness levels for varying plate compositions and skid weld plate thickness 301

6.12 - Percentage of equiaxed grains to columnar grains for 6mm plate skid welds with varying heat input . . 308

6.13 - Weld widths and ratio of equiaxed/columnar grains measured at various points across the weld transverse section 310

6.14 - Prior austenite grain sizes measured for skidwelds of various plate thickness 311

6.15 - Skid weld longitudinal section: 8mm plate (x12.8 & x64) 313

6.16 - Phase counts in 6,10 & 15mm plate skid weld, weld metal 315

6.17 - Continuous cooling transformation curves and the influency of various parameters 318

6.18 - Impact toughness of various microstructures 318

6.19 - 8mm skid weld microstructure 320

6.20 - 8mm MMA weld fillet microstructure 322

6.21 - Fusion line in 6mm skid weld (plate P6/01/CS) showing inclusions (x1000) 327

6.22 - Relationship of acicular ferrite levels and Charpy transition values for various wire feed compositions. 327

6.23 - Solidification crack in 12mm skid weld incident bead, columnar grains joining at weld centreline (x20). . . 332

6.24 - Solidification crack in 12mm skid weld, formed in weld centre (x40) 332

6.25 - Lack of fusion with the face plate due to too high laser beam height in a 12mm skid weld (x64) 334

6.26 - Lack of fusion at the web plate edge due to too low laser beam height in a 10mm skid weld (x80) 334

6.27 - Emergent bead of a 12mm skid weld. Molten material has been forced out at the molten zone without full fusion (x32) 336

6.28 - Emergent bead of a 6mm skid weld with insufficient

fusion with a rolled section web (x50). 336

6.29 - 10mm skid weld joint emergent zone with a lack of flow of filler to a rolled section web edge (x50) . . 337

6.30 - Porous emergent bead in a 6mm skid weld (x20) 337

7.01 - Microprocessor control unit attached to a 1.5kW laser . 344

7.02 - 75m beam line for testing long beam path propogation . 346

7.03 - Beam line optics for laser beam columnation 346

7.04 - Robot moves a part under a fixed laser nozzle 350

7.05 - Laser based articulating robot, the beam guide forms an integral part of the robot arm 350

7.06 - Flexible beam guide linking the laser to the robots end 352

7.07 - Gantry mounted beam delivery and manipulation system. . 353

7.08 - CO2 laser connected to the end of a robot arm 355

7.09 - Proposed gantry mounted laser 355

7.10 - Laser integrated into an existing machine tool design . 357

7.11 - Boom type robot attached to a static laser. 359

7.12 - Robot on rails serving a number of workstations 359

7.13 - Gantry based production welding robot using MIG 361

7.14 - Gantry based LARS laser processing system 361

7.15 - Design of the multiaxis beam manipulator head to be incorporated into the European laser demonstrator . . 362

7.16 - Output from the laser beam analyser in orthogonal plains 366

7.17 - 3D output from a beam analyser sensing through a hole matrix mirror 366

7.18 - Seam tracking using a scanning HeNe laser 372

7.19 - Comparative costs for laser welding and MIG welding a continuous stiffener divided into four

cost headings 384

7.20 - Comparative total cost for laser or MIG welding a continuous stiffener 385

7.21 - Advanced method of assembling a matrix panel 388

7.22 - Traditional method of assembling amatrix panel 388

7.23 - Conventional matrix panel assembly flow line 390

7.24 - Proposed flow line for a matrix panel line incorporating laser skid welding. 392

7.25 - Laser on times for the example matrix line: utilisation in total = 75% 396

7.26 - Included angle distortion of welded tee joints 402

7.27 - Comparison of included angles of distortion measured for laserr skid and MMA fillet welds in unconstrained joints 402

7.28 - NPV for various levels of productivity savings when using a laser based matrix assembly line. 406

7.29 - Cost analysis of a laser matrix line: yield on extra capital as a result of increased productivity 406

7.30 - Principle minor assembly structures identified within a design of lightweight ferries 408

7.31 - Flow line for a minor assembly facility using conventional and laser welding processes 410

7.32 - Laser on times for the example minor assembly line for one batch: utilisation = 75% 413

7.33 - NPV for various productivity savings for alser based minor assembly line 418

7.34 - Cost analysis for an example laser based minor assembly line: yield on extra capital as a result of increased productivity 418

B4.01 - Bead surface profiles and macrosection of
B4.06 skid weld in 3 -15mm plate 457

C5.01 - Charpy transition curves and fracture appearance curves for 6-15mm plate, A31 filler wire 480

C5.02a - Charpy transition curves and fracture appearance curves for butt welds in 6,10 and 15mm plate, various filler wires 485

D6.01 - Weld microstructure of a 3mm skid weld 517

D6.02 - Weld microstructure of a 6mm skid weld 519

D6.03 - Weld microstructure of a 10mm skid weld 521

D6.04 - Weld microstructure of a 12mm skid weld 523

D6.05 - Weld microstructure of a 15mm skid weld 525

List of Tables Included in the Text

1.01 - Principal types of lasers 6

1.02 - Typical laser applications 7

1.03 - Characteristic of each principal type of laser resonator 11

1.04 - Comparative advantages and disadvantages of using high power lasers for materials processing 21

2.01 - Welding process classification 35

2.02 - Potential laser butt welding faults reasons and remedies 70

3.01 - Parameters considered for each weld run and their principle effects 114

4.01 - Estimates of the minimum powers required to achieve laser skid welding without excessive plasma interaction 139

4.02 - Positional distance of the filler wire in front of the HeNe spot 175

cost headings 384

7.20 - Comparative total cost for laser or MIG welding a continuous stiffener 385

7.21 - Advanced method of assembling a matrix panel 388

7.22 - Traditional method of assembling amatrix panel 388

7.23 - Conventional matrix panel assembly flow line 390

7.24 - Proposed flow line for a matrix panel line incorporating laser skid welding. 392

7.25 - Laser on times for the example matrix line: utilisation in total = 75% 396

7.26 - Included angle distortion of welded tee joints 402

7.27 - Comparison of included angles of distortion measured for laserr skid and MMA fillet welds in unconstrained joints 402

7.28 - NPV for various levels of productivity savings when using a laser based matrix assembly line. 406

7.29 - Cost analysis of a laser matrix line: yield on extra capital as a result of increased productivity 406

7.30 - Principle minor assembly structures identified within a design of lightweight ferries 408

7.31 - Flow line for a minor assembly facility using conventional and laser welding processes 410

7.32 - Laser on times for the example minor assembly line for one batch: utilisation = 75% 413

7.33 - NPV for various productivity savings for alser based minor assembly line 418

7.34 - Cost analysis for an example laser based minor assembly line: yield on extra capital as a result of increased productivity 418

B4.01 - B4.06 Bead surface profiles and macrosection of skid weld in 3 -15mm plate 457

C5.01 - Charpy transition curves and fracture appearance curves for 6-15mm plate, A31 filler wire 480

4.03 - Comparison of plasma control/weld shrouding rates . . . 197

4.04 - Summary of skid welding parameter specifications and tolerances 202

5.01 - Material mechanical property specification as defined by classification bodies 209

5.02 - Fillet fracture test results 220

5.03 - Guidelines for sub-sized Charpy specimen. 226

5.04 - Charpy acceptance criteria for skid weld toughness testing 226

5.05 - Specification composition and mechanical properites of filler wires used during the skid welding trial. . 236

5.06 - Summary of Charpy transition data for a comparison of the result for testing similar skid and butt weld metal 241

5.07 - Charpy transition data for butt weld metal to compare the affect of using various filler wires 245

5.08 - Summary of the surface topography measurements of weld surfaces measured on 8mm plate joints 276

6.01 - Max carbon levels so as not to exceed 350Hv hardness (Optimum speed using a constant power of 9kW) 302

6.02 - Max carbon levels so as not to exceed 400Hv hardness (Optimum speed using a constant power of 9kW) 302

6.03 - Nomenclature for the classification of laser weld microstructural constituents 306

6.04 - Microstructural/mechanical properties of butt and skid welds; optimum speed, 9kW laser power 325

6.05 - Microstructural/mechanical properties of 10mm thick laser butt welds to compare the affect of varying filler wires. 328

7.01 - Synthesis of a conventional matrix panel line 391

7.02 - Synthesis of a matrix panel line incorporating laser skid welding 393

7.03 - Estimate of facility costs for a conventional matrix assembly line 397

7.04 - Estimates of facility costs for a laser based matrix assembly line 398

7.05 - Operational costs of conventionasl and laser based matrix assembly lines 400

7.06 - Savings accruing to man-hours/tonne 405

7.07 - Manhours per tonne ratings for general cargo vessel steelwork manufacture 405

7.08 - Synthesis of a laser line to produce, minor assemblies. 411

7.09 - Synthesis of a conventional line to produce minor assemblies 412

7.10 - Estimated costs for a laser based minor assembly line 414

7.11 - Estimated cost for an example conventional minor assembly line 414

7.12 - Operational costs of a conventional and laser based minor assembly line 415

7.13 - Potential consequential savings as a function of manhours per tonne work improvement 416

7.14 - Manhour per tonne ratings for light scantling warship structures contruction 416

A3.01 - Variables of material and equipment affecting skid welding performance 449

C5.01 - Results of cruciform tensile tests on laser skid welds 479

D6.01 - Chemical analysis of the plate steels used in skid welding trials 515

D6.02 - Chemical analysis of the rolled section steels used in skid welding trials 516

E7.01 - Consumable costs for laser and conventional

welding processes 528

E7.02 - Assumptions used for the economic evaluation 530

E7.03 - Prices of some commercial lasers of greater than 5kW noting respective generator configurations . . . 531

E7.04 - Net present value calculations for the additional cost of a laser based matrix line, assuming 5 manhr/t savings 532

E7.05 - Net present value calculations for the additional costs of a laser based minor assembly line, assuming 7 manhr/t savings 533

CHAPTER ONE

INTRODUCTION

1.1 LASER MATERIALS PROCESSING IN SHIPBUILDING - THE WAY AHEAD

During the past decade the increasing use of computers by naval architects has revolutionised ship design procedures. They have also given shipbuilders a new asset for management and control of ship production. However, while computers might be capable of operating the varied array of sophisticated shop floor machines now available, a new means of revolutionising the existing processing techniques is needed for any quantum leap in overall productivity improvements. The use of high power laser technology could create such a means.

Since the first demonstration of laser action in 1960, laser generation technology has been applied to producing laser light of varied wavelengths each with a particular characteristic. This characteristic then determines how the light can be manipulated and ultimately used. Diverse applications, from holographic photography and micro-surgery to space weaponry have been found.

Just as each laser type is at a unique stage of development, so is the attributable process and application technology. Today, industry in general is just starting to accept mid-powered (0.5-5.0kW) laser generators as reliable power sources. Particular applications for laser

cutting, heat treatment and thin section welding have been researched and developed in parallel with the laser to this power range so there is now a demand for reliable industrial turnkey systems.

In contrast, at higher powers (>5kW), laser generators still tend to be associated only with research projects. However, with production units now becoming available and process and application technology being developed in parallel, industry can to look more seriously at the use of high power laser technology as a viable option for materials processing.

By assessing the use of high power lasers for welding in ship production most previous authors have been naturally constrained by the relevant "state of the art". Primarily they were restricted to assessing the use of autogenous laser welding so that prepared and close fitting piece parts became an essential pre-requisite [1] [2] . Later, for filler welds, the joint gap was restricted by the focused laser beam diameter.

By using the wire filling means as a beam interceptor Martyr [3] showed how process tolerances could be increased. This meant that the process could be applied viably to ship production even with the types of conditions and joint fit-up experienced conventionally (<3mm unintentional joint gap).

Virtually all published procedural analysis of laser welds, together with their property assessment, has concentrated on plane butt welds, "melt runs" and to a lesser extent on twin fillet type, tee section

welds. In comparison, the highest proportion of weld length used in ship production is for tee section joints where a low heat input, single sided process would have greatest flexibility and potential cost savings.

Martyr [3] only indicated the potential for producing such a joint under shipbuilding simulated conditions. Therefore the Author has concentrated his research on analysing the procedural requirements for producing a tee section "skid weld" which would be acceptable within the limits of normal shipbuilding practice.

To achieve this goal, to compare the weld against classification institution requirements and relate process parameter limits and tolerances to assess workstation design, the Author set the following objectives:

1. Produce laser filler skid welds in plate thicknesses to 15mm acceptable to normal shipbuilding practice for surface vessels.
2. Determine the limitations, tolerances, and inter-relationships between the main process input parameters so that these may in turn be related to the requirements imposed on a workstation design.
3. Compare the requirements of shipbuilding classification institutions for conventionally welded tee section joints to the properties achieved when testing the laser skid welded joint.
4. Assess the inadequacies of "conventional" classification requirements for assessing laser skid welds, providing evidence of some alternative assessment to compare weld properties acceptable to classification institutions .

5. Develop some methods of relating skid weld metallurgical characteristics to physical properties.
6. Investigate typical weld defects and associated remedies.
7. Use some theoretical simulations of welds to compare and predict skid weld characteristics and thus develop basic process parameter equations which could be used as the basis of workstation software.
8. Calculate the economic viability of a skid welding workstation.

1.2 GENERAL HISTORY AND DEVELOPMENT OF THE CO2 HIGH POWER LASER

1.2.1 Brief Overview of the Development of Industrial High Power CO2 Lasers

From Einstein's initial ideas of 1917 and the invention of the MASER (Mircrowave Amplification by Stimulated Emission of Radiation) in the early 1950's, the first laser (acronym for Light Amplification by Stimulated Emission of Radiation) demonstrated by Maiman [4] in 1960 extended the principles used on microwaves to optical radiation.

The first laser used a ruby rod as the "laser medium", which, when excited by a flash lamp emitted a pulse of light which had initially built up between the rods silvered ends. The first gas laser, the laser medium being a mixture of Helium and Neon, was produced in 1962and was the fore-runner to the type of laser now used for alignment purposes in shipbuilding [5] . Patel [6] demonstrated the first CO2 laser in 1965,

the principles of which are the basis for today's high power CO2 laser.

The range of lasers utilising many various mediums and excitation methods still increases. Table 1.01 classifies the principal types of lasers in general use today with a more detailed break-down being given for those likely to be encountered for shipbuilding applications marked "*". Table 1.02 shows the diversity of application associated with the more common laser types.

While designers and builders of high power CO2 lasers still spend time looking to producing "even higher" power outputs [7] , the greatest commercial emphasis today seems to be on refining machines to meet the requirements of the industrial end user and examining alternative laser wavelengths.

The refinement process takes many forms but primarily it is being directed to provide a more reliable and cost effective power source for the end user. Prototype units are being value engineered before being produced commercially; new methods of excitation or resonator oscillation are being developed to improve output beam stability [8] ; manufacturers are attempting to modularise component parts [9] or develop new gas flow methods [10] . Examples of presently available commercial lasers are shown in figure 1.01.

The three basic components for obtaining laser action, however, still remain. A "Laser Medium" (a collection of atoms, molecules or ions

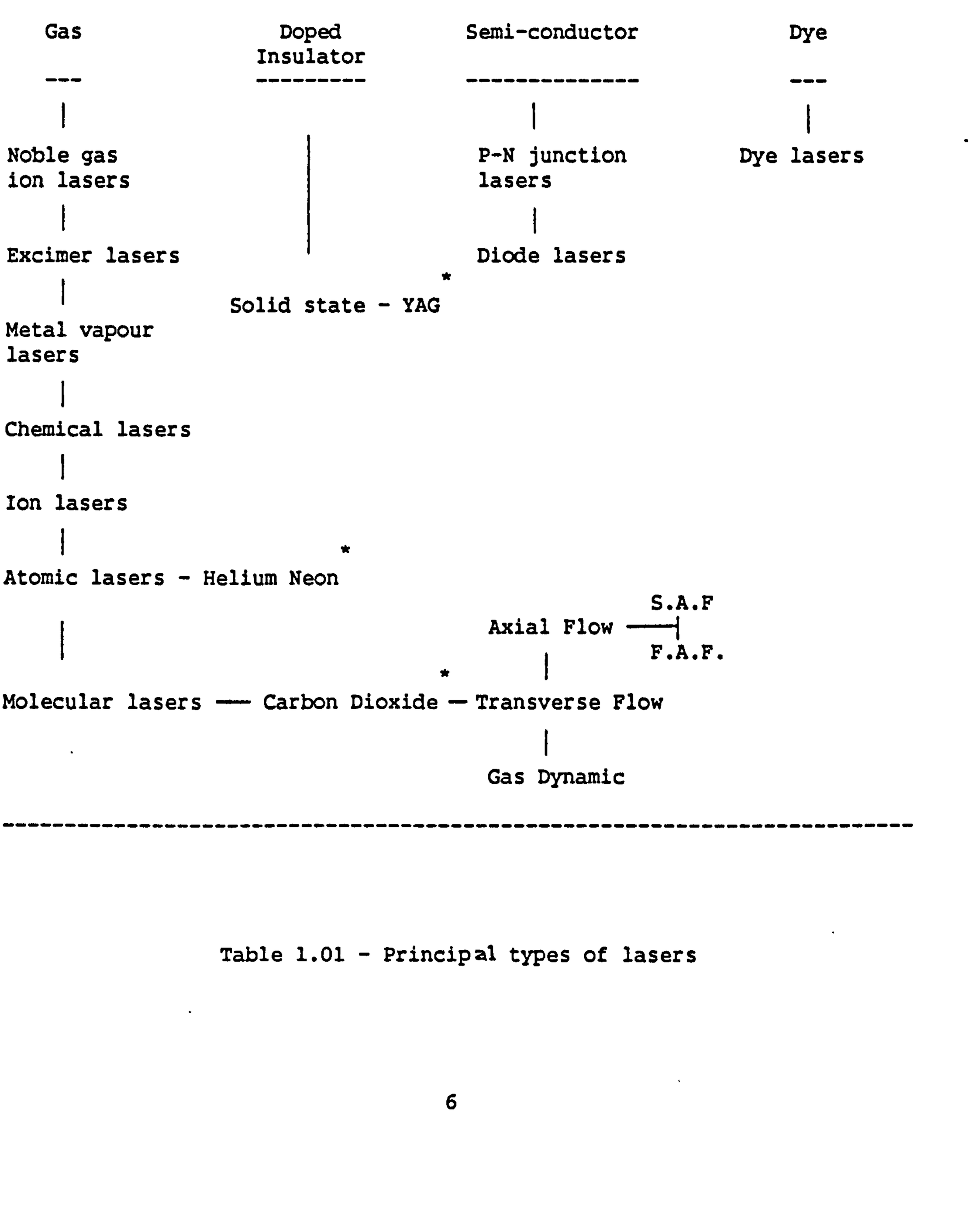

Table 1.01 - Principal types of lasers

Laser Type	Applications
Gas(General)	Research & development, photochemistry, materials processing, laser radar, infrared beacons & scanners, plasma diagnostics.
Ion	Pumping dye lasers, recording, reprographics, medical photocogulation, multi-colour lightshows & displays.
HeNe	Construction aligning, holography, general measurement, atmospheric research, surgery, photochemistry
Doped Insulator	Holography, materials working, reseach & development, range finding, target designation.
YAG	Materials processing
Semi-conductor	Fibre-optic communications
Dye	Spectroscopy, Research and Development.

Table 1.02 - Typical laser applications

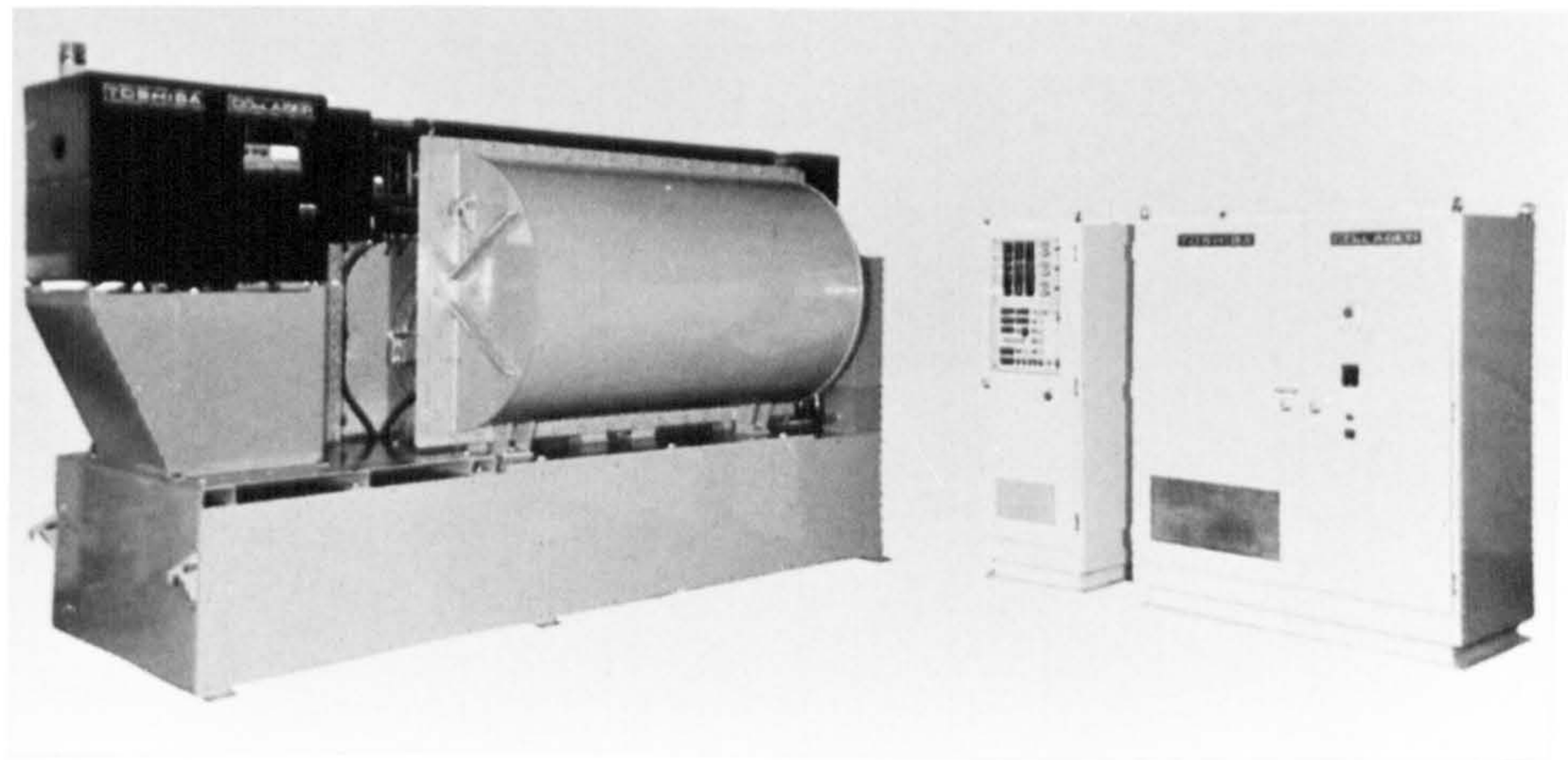

a) 5kW laser - Toshiba, Japan

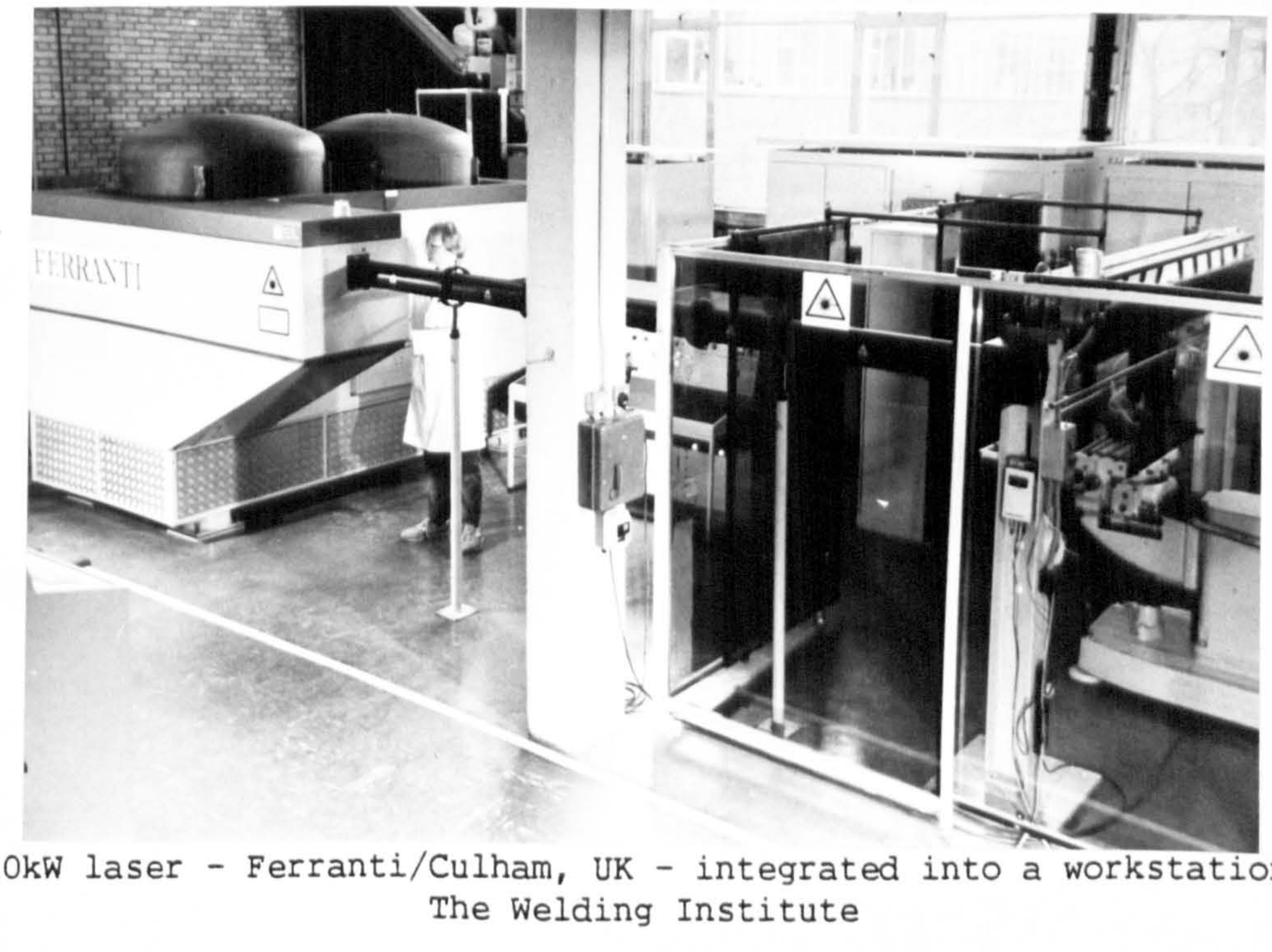

b) 10kW laser - Ferranti/Culham, UK - integrated into a workstation at The Welding Institute

Figure 1.01 - Examples of typical commercial lasers of greater than 5kW output

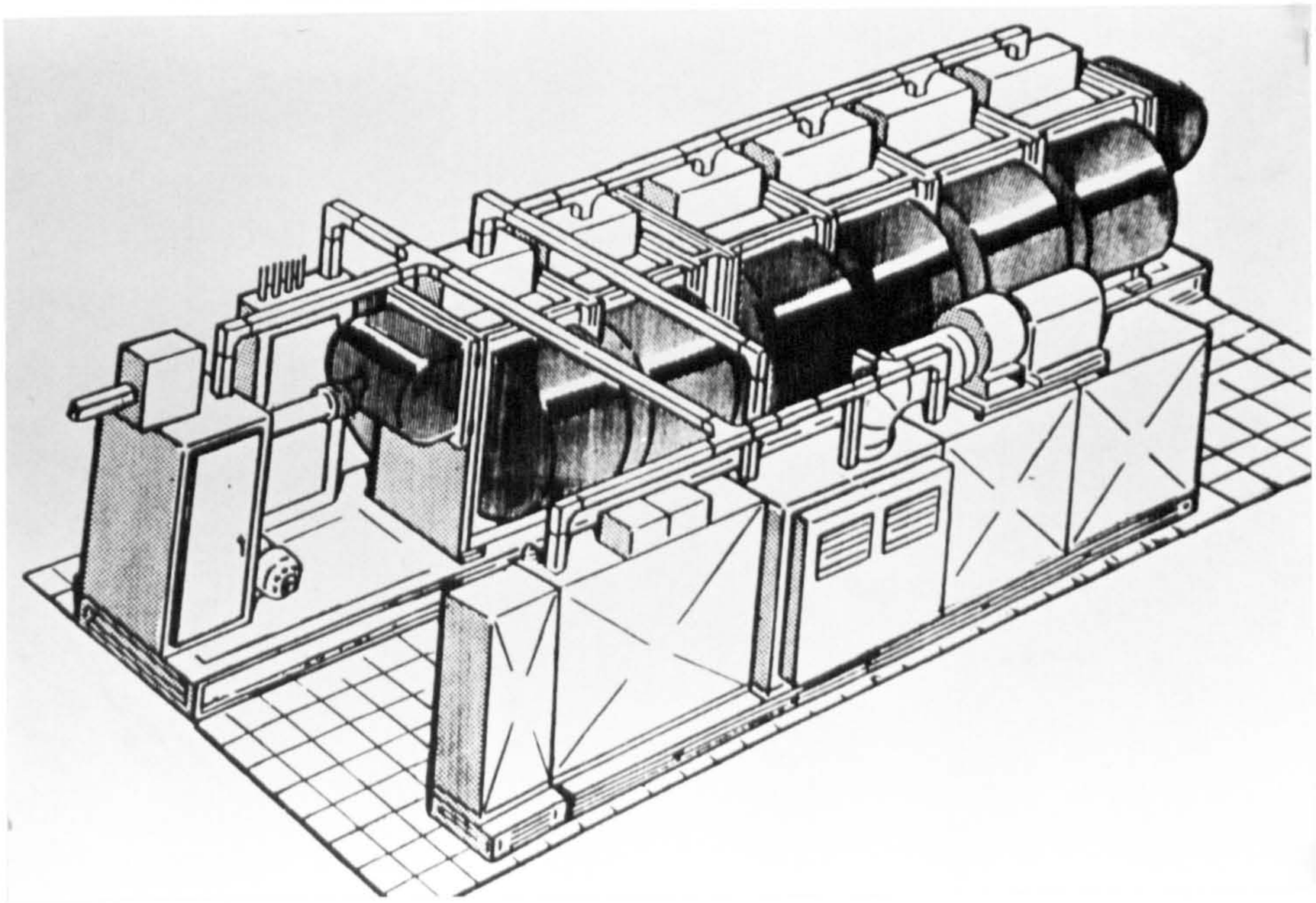

Figure 1.01c - 15kW laser - United Technologies Research Centre, USA

capable of emitting radiation of a frequency within the optical part of the electromagnetic spectrum) has to be influenced by a "Source of Excitation". This must create a situation where the atomic energy of the medium changes from its normal level to a higher level, an action called pumping.

Lasing action occurs as the atoms then revert to their normal energy levels. The lasing action is amplified by enclosing the laser medium in an optical beam generation path to create an "Optical Resonator". The output beam is then formed by allowing a proportion of the built-up energy to escape, either through a semi-reflective mirror or by a particular arrangement of the resonator mirrors.

Industrial CO2 lasers can be sub-divided in accordance with the configuration of these three basic components. Axial flow lasers have the laser gas flowing along the same axis as that of the exciting electric field, normally enclosed within a heat resistant glass tube. End mirrors form the optical resonator, normally with one end semi-reflective to allow the beam to pass through, i.e. the beam is generated along the same axis as the gas flow.

Transverse flow or cross flow lasers have the gas circulated along an axis perpendicular to both the electric field and optical resonator, hence the beam is generated perpendicular to these axes.

	Axial Flow		
	Slow Axial Flow	Fast Axial Flow	Transverse Flow
Laser resonator configuration	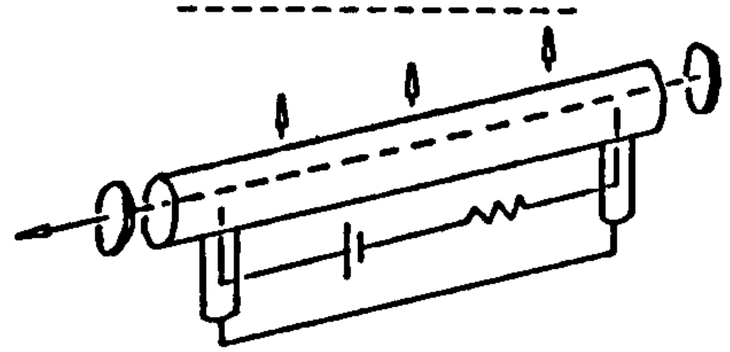	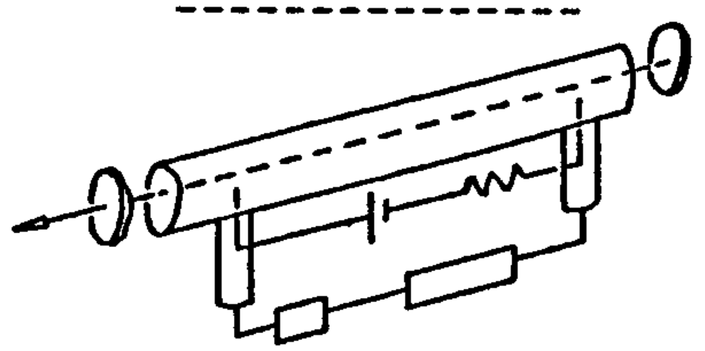	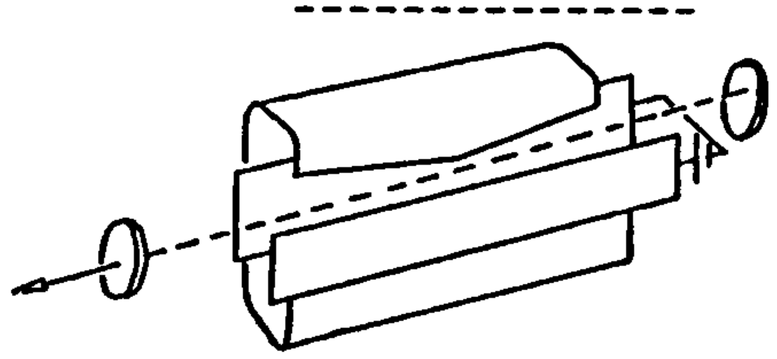
Typical laser cavity optical arrangements	Stable resonator	Stable/unstable resonator	Stable/unstable resonator
Typical power output range (Watts)	100 - 1,500	100 - 6,000	1000 - >25,000
Typical power output per metre length	100W/m	1000W/m	5000W/m
Typical Ancillary Equip.	Controller Power supply Cold water supply	Controller Power Supply Chiller unit	Controller Power supply/ Ballast unit Chiller unit
Advantages	Stable beam Small and compact Lightweight Ideal for moving laser systems	Stable beam Ease of modular assembly for large power range	High powers Short length per unit power output
Disadvantages	Power output restricted	Heavy expensive roots type blower	Large power packs and ballast resistor units
Key to parts in laser diagrams	1.Mirrors 2.Gas flow 3.High tension power supply to cathodes and anodes 4.Output laser beam 5.Heat exchanger 6.Heat escape through cooling jacket 7.Pump		

Table 1.03 - Characteristic of each principal type of CO2 laser resonator

Table 1.03 summarises the principal characteristics of each type indicating their particular advantage or disadvantage as power sources for materials processing in a shipbuilding environment. Axial flow lasers have been further divided between Slow Axial Flow (SAF) and Fast Axial Flow (FAF) showing how they differ. Figure 1.02 presents a further explanation of two different optical resonator configurations commonly used, both stable and unstable.

1.2.2 High Power Laser Beams for Materials Processing

Light is characterised within the electromagnetic radiation spectrum which extends from long wavelength radio waves to shorter wavelength gamma rays. The wavelengths associated with laser light range from near infra-red, through visible, to ultra-violet. Figure 1.03 shows these relationships identifying specific wavelengths associated with particular lasers.

Incandescent light produced by a light bulb comprises all colours within the "visible" spectrum, radiating in all directions. By comparison, the laser emits light of one frequency (monochromatic) in a coherent and almost perfectly collimated beam i.e. the beam is unidirectional with only a small divergency (typically 1-2 milliradians). It has high intensity or brightness and can be focused to a comparatively small spot size, typically less than 0.5mm in diameter.

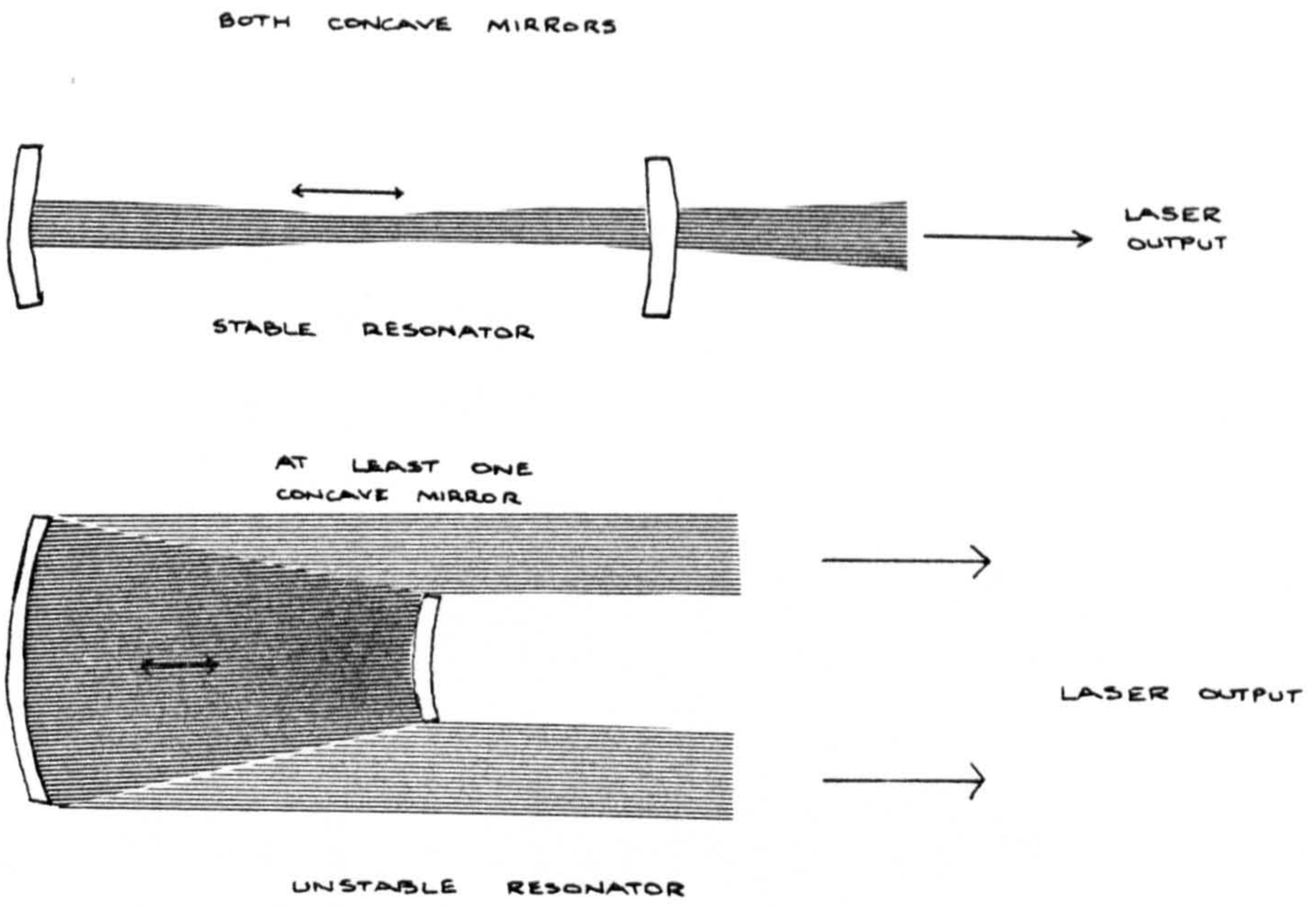

Figure 1.02 - Stable and unstable optical resonators

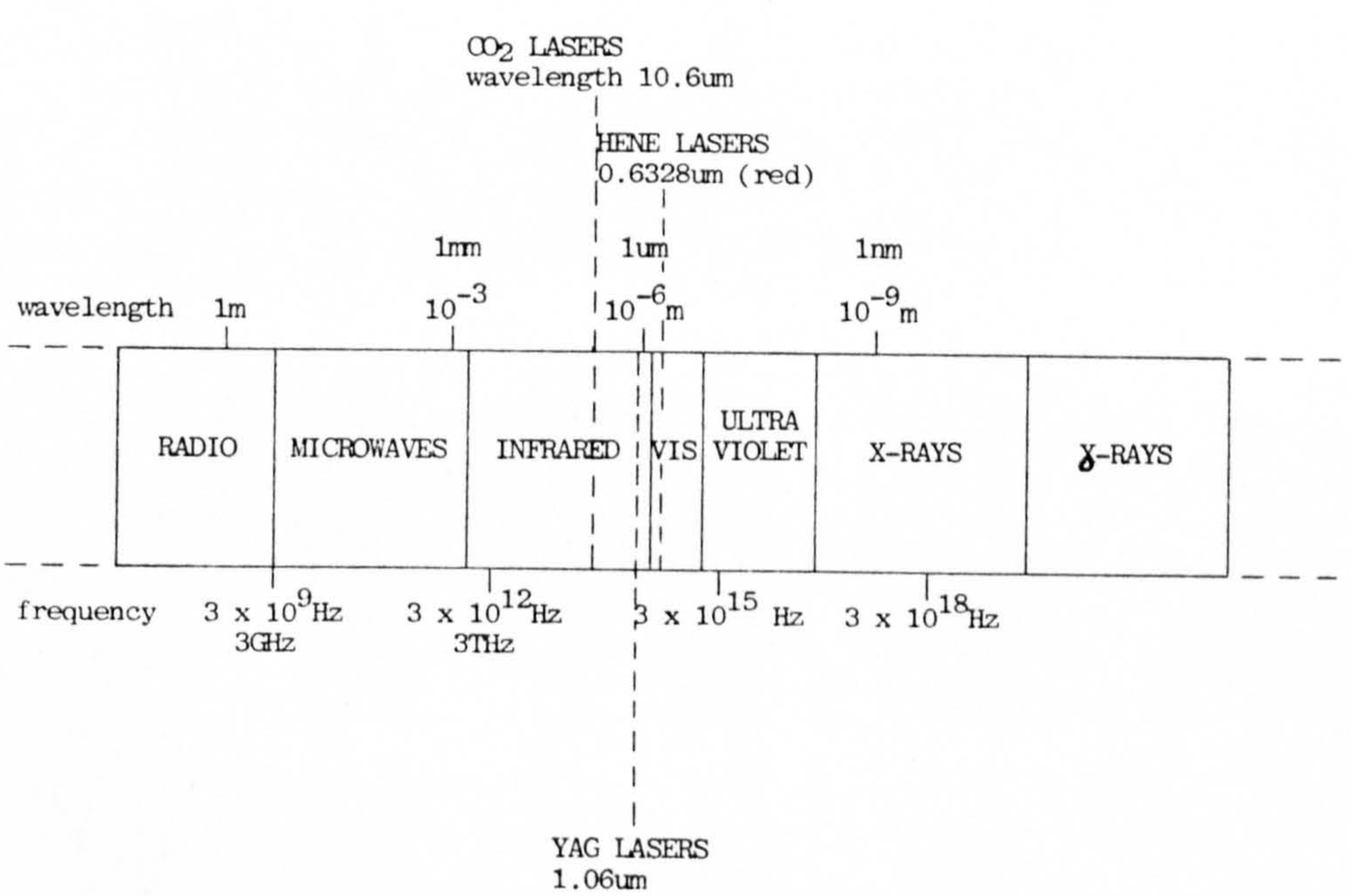

Figure 1.03 - The electromagnetic spectrum

While these characteristics are inherent to laser light itself, the additional properties associated with the optical cavities' effect on the beam structure, namely the beam mode and its degree of polarisation should also be considered for materials processing .

The Transverse Electromagnetic (TEM) Mode of a high power CO2 laser is a term associated with the shape of the electromagnetic field formed within the laser discharge tube. This is especially dependent on the photon wavelength, the shape of the laser cavity and on the mirror alignment, curvature and spacing. However, identification of a particular transverse mode may be made by examining the intensity distribution of the output beam.

The lowest order mode experienced in CO2 lasers with stable resonators is "TEMoo", which gives a "Gaussian" output power intensity distribution. Another mode commonly employed for materials processing is "TEM01*" with a "doughnut" shaped output distribution, figure 1.04a.

For an unstable resonator system, when at least one of the mirrors has a negative radius of curvature, the output takes the form of an annulus which leaks past one of the mirrors, producing a multimode configuration. A typical example of this is for the mode produced by the CL series of lasers shown in three dimensions, figure 1.04b.

A TEMoo mode produces a beam which can be focused to the smallest possible spot size giving high power density hence is ideal for most

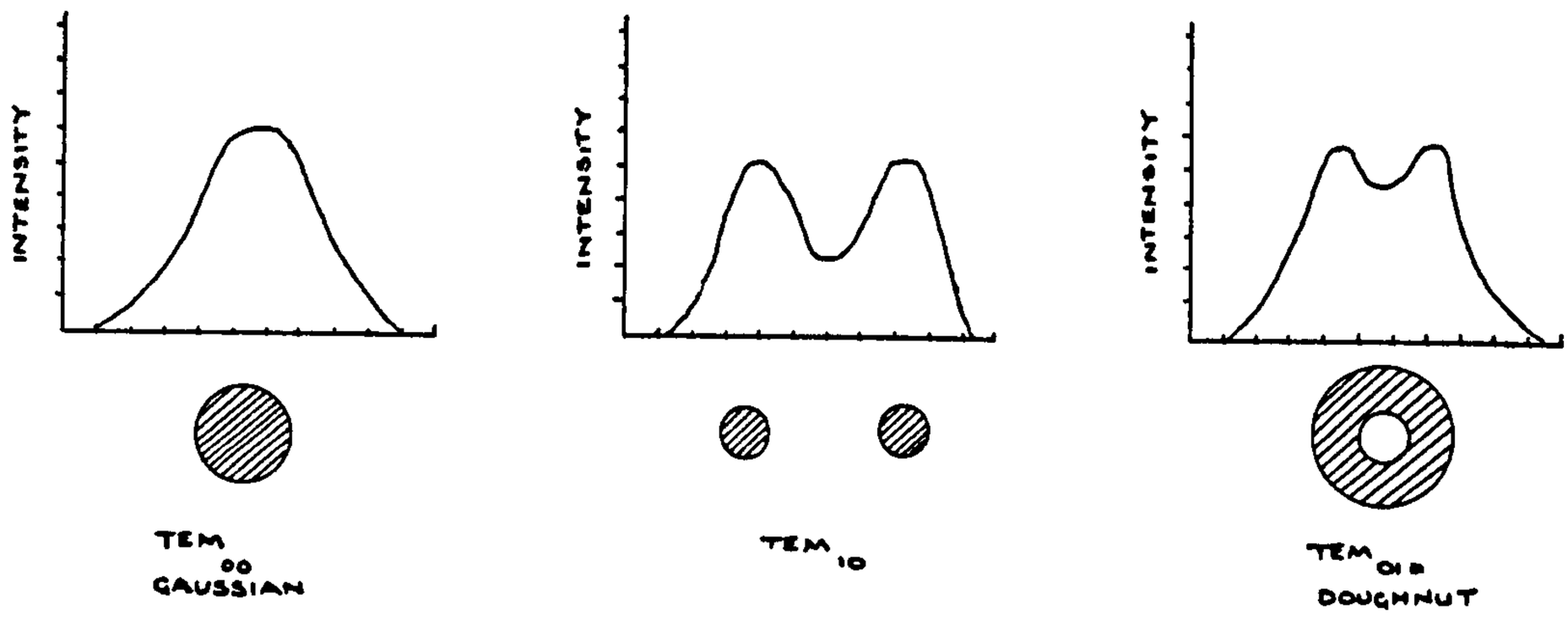

Figure 1.04a - Beam mode power intensities for stable resonators.

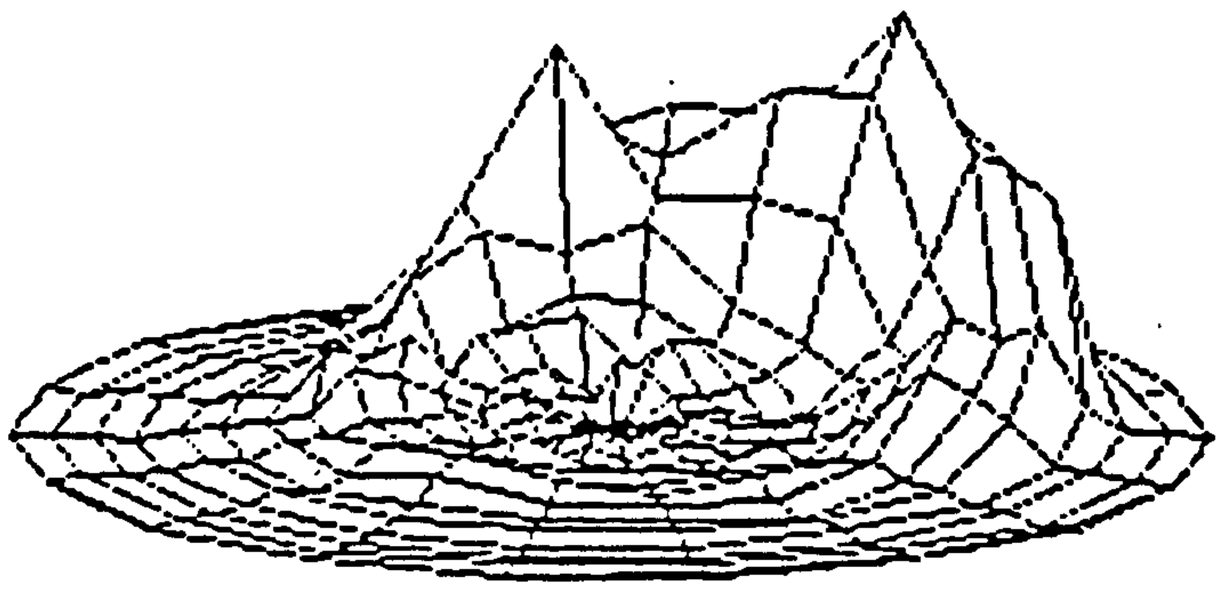

Figure 1.04b - 3D interpretation of the power intensity for an unstable resonator.

cutting, drilling and welding applications, especially where precision is required. TEM01* mode can be controlled to give a larger but more even power intensity distribution and therefore it tends to be favoured more for welding and heat treatment applications.

"Polarisation" of light is a function of the wave nature of electromagnetic radiation. As transverse waves vibrate at right angles to the direction of propagation, so the plane of vibration can be defined. If all component rays of a laser beam vibrate in a fixed plane the beam is described as "linearly polarised", just as "random polarisation" occurs when the plane of polarisation varies in an indeterminate manner.

The inherent degree of polarisation formed within the laser cavity will depend on the fold mirror (mirror placed in the beam path to facilitate a change in direction) configuration within the laser. Generally, lasers employing 45° "roof-edge" folding mirrors have a fixed polarisation, while those with "Z" folding or with no folds have a polarisation which can vary. To fix the polarisation of the latter two, a polarising element (Brewster window) is fixed at such an angle to the laser beam that one plane of polarisation dominates. Figure 1.05 shows some of the most different beam generation arrangements found in commercial lasers.

The state of polarisation , in addition to the the angle of incidence, will affect the characteristics of absorption when a beam strikes a

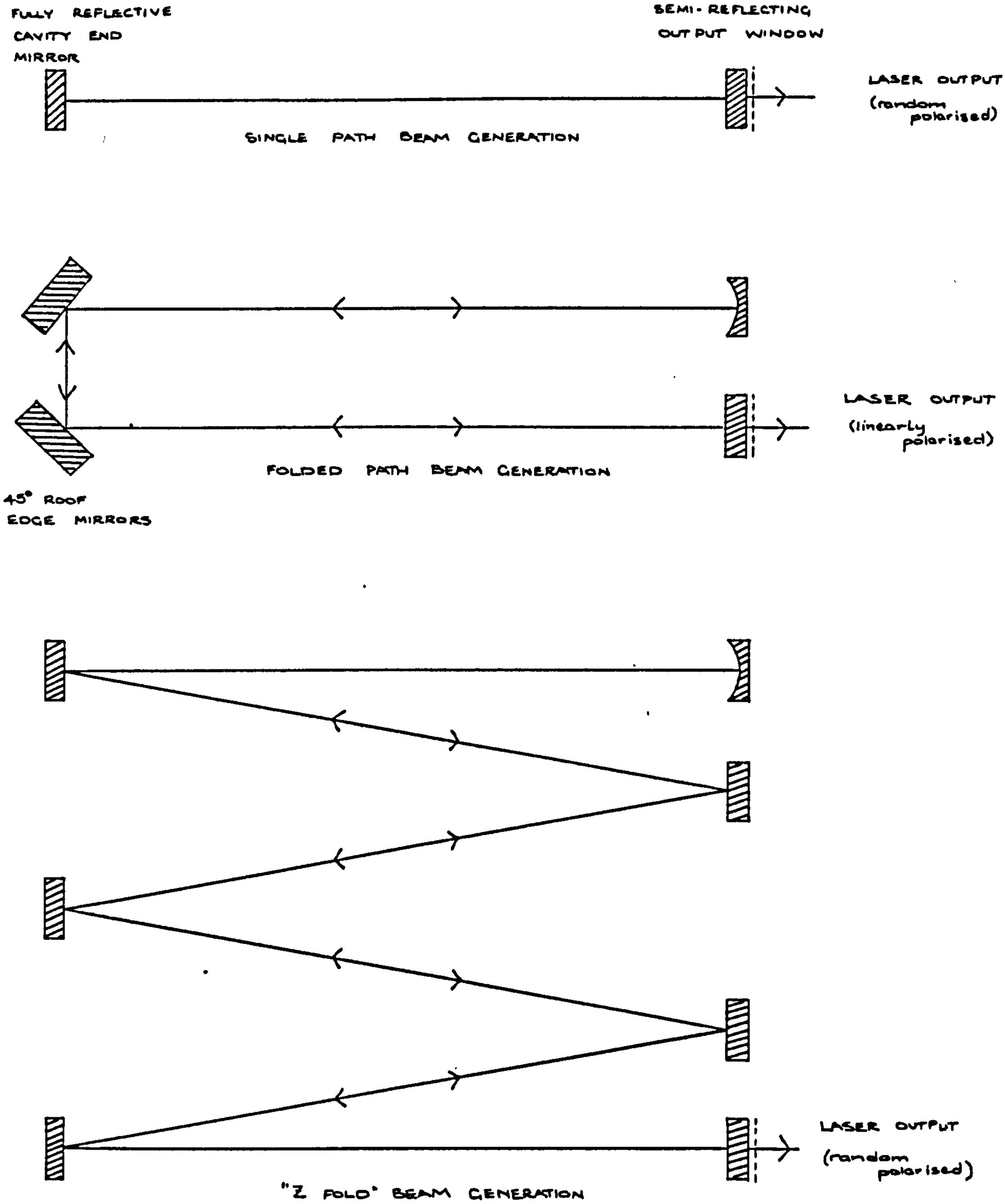

Figure 1.05 - Typical laser generation paths

target. Various trials [11] [12] [13] note the detrimental effects of linear polarisation on multidirectional laser cutting, when cut quality showed a directional bias. This effect may be successfully overcome by effecting "circular polarisation" by introducing phase retarding optics into the beam line.

Similar effects in laser welding have not been found. Trials to investigate the effect [13] emphasised the differences between the processes. For welding the predominant energy transfer to the keyhole walls is through the entrapped plasma i.e. conduction. However for cutting, the plasma is dislodged by the assist gas hence the dominant form of heat transfer is directly into the kerf walls i.e. radiation, when reflective properties, hence polarisation, affect energy coupling.

For the transmission of the beam from the laser generator to a workpiece, beam propagation and manipulation should be considered also.

Laser beams will propagate through normal dry air with minimal attenuation, though the longer the distance, the greater the care required in designing the beam line. Trials to simulate the effect of industrial environments on beam paths of up to 75 metres [14] [15] have highlighted the main features affecting long beam path propagation, summarised as follows:

Aperturing	- Ratio of beam diameter/aperture
Diffraction	- Fresnel number
Thermal distortion	- De-focusing
	Aberration
Pointing error	- Servo control
Vibration	- Isolation/fast servo
Absorption	- Mirror surfaces
Scattering	- Apertures
Turbulence	- Flow, Convection, Scintillation
Thermal blooming	- Impurity of gas.

The trials have shown that once power losses (approximately 20% over a 75m beam line) and changes in beam structure are taken into consideration, "far field" welds comparable to those produced in the "near field" can be produced.

From inception to the workpiece the use of optics to manipulate the beam may take various forms. Mirrors and windows -either solid or aerodynamic - will be used in the beam generation; the beam may be prepared for transmission - beam expanders, collimators, phase shifting mirrors; folding mirrors, either stationary or moving, will be used to reflect the beam to the working head and after final transmission adjustments, mirrors or lenses will be used to create the required focal arrangement for processing. Optics for beam transmission must have both good reflective qualities and the substrate must remain stable within the particular operating environment. The most widely used mirrors for CO2

beam transmission consist of a diamond machined copper substrate coated in gold. Various authors and optics manufacturers provide guidance to using these and other products to produce efficient beam line optics design [16] [17] [18] [19] .

Cost effective use of the energy beam described is then dependent on being able to utilise its properties to advantage and either minimise or preferably overcome any disadvantages. Table 1.04a lists some of the advantages available to the shipbuilder of using high power CO2 lasers, particularly for cutting and welding. Table 1.04b lists the most commonly quoted disadvantages and explains their validity.

Wherever possible the work programme reported in this thesis has been designed to optimise the advantages to be gained from using the high power laser beam as a means of welding. However the Author has been aware also of constraints placed by "normal shipbuilding practice", either in documented physical terms , for example the rules set by classification societies which do not mention laser welds, or in psychological terms; e.g. labour's initial reaction to using lasers with its connotations of "Star Wars". Appreciation of all aspects was needed therefore to encourage the success of introducing the system to a shipyard situation.

Advantages	Potential Exploitation
Low heat input - low distortion	
Intensive energy applied to a localised area for a short period hence distortion is minimised.	All heat input processes; welding and cutting where conventional processes cause significant distortion; heat line bending; heat treatment.
High speed	
High power density and efficient energy transfer permit fast traverse speeds	Cutting processes requiring square edge, accurate profiling with a minimal kerf width. Welding processes where conventional automated speeds are lower.
Accuracy	
Small focused spot can be directed with high precision. Laser power and hence heat input can be precisely controlled.	Process where conventional method accuracy is less than ideally required by follow-on processes.
Fexibility of energy source	
An unfocused laser beam can be projected in air in excess of 70m without serious loss of power. Therefore several workstations can be sited in the beam path and time share a single laser source. Manipulative transmission e.g. along a robot arm gaining single sided access.	Flow line production areas having many different "heat input" processes e.g. cutting, welding. These could be served by a standard but flexible power source. Joint configurations inaccessible to conventional methods.
Suitability for automation	
Precise control of the energy source coupled with high processing speeds and flexibility of transmission is ideally suited to automation.	Trends to the standardisation of work packages lends itself to automated processing. Automated working will compensate for the present reduction in craft skills.

Table 1.04a - Comparative advantages of using high power lasers for materials processing.

Perceived disadvantages	Validity
Workhandling	
Either precise work handling or beam handling equipment is necessary to ensure good alignment of the laser beam to the workpiece	Standard workhandling equipment and robotic units are becoming more accurate because of demands set by conventional processes. Joint tracking devices further set defined tolerance limits within those for laser processing. Laser quality assessment and feedback units now becoming available to enable accurate beam control.
Consumables	
C02 lasers consume N2,C02 and particularly expensive He. He is used as a sheilding gas. Electrical power is used inefficiently. Beam transmissive and focusing optics are expensive and may have a limited service life.	Laser consumables appear expensive individually but when considered as a function of processing length, with high processing speeds and potentionally high utilisation factors the net cost effectively reduces.
High equipment costs	
Laser generators are expensive compared with conventional processing power sources.	Correct, but only in regard to capital items. Comparison can be made effectively only for a complete system when cost is related to processing capacity and savings. In future relevant costs are likely to reduce with value engineered products.
Workpiece fit-up	
Close fitting joints are required to ensure high weld quality.	Whilst true for autogenous welds, filler and beam interceptor techniques can now be used to effect joints in low tolerance connections.

Table 1.04b- Perceived disadvantages of using high power lasers for materials processing.

1.3 LASER MATERIALS PROCESSING IN SHIPBUILDING - THE STATE OF THE ART

1.3.1 A Review of works by Authors on Ship Production Based Laser Processing

References to the use of high power lasers in shipbuilding are scarce. In addition to those mentioned by Martyr [3] , reports and articles have concentrated on the use of research laser facilities by shipbuilders rather than reporting on the actual use of high power lasers on a ship production line .

Facilities at the United Technologies Research Centre UTRC have been used by various authors to provide experimental data for their studies. The Aker Group (Norway) provided shipyard information in 1976 [20] to evaluate laser welding in merchant shipbuilding. The resulting report [21] predicted viability for panel line type systems but specified an ability to laser weld typical shipyard joint tolerances as a pre-requisite. In further research the use of both electron beam and laser welding in shipyard construction have been researched showing a potential viability [22] .

As part of a "National Shipbuilding Research Programme" the Bethlehem Steel Corporation (USA) have produced reports of laser welding trials [23] which show a limited capability to produce butt and double sided tee welds using a filler wire together with tee joint preparations to obtain smooth reinforcing beads on tight fitting joints.

The Swedish shipyard, Kockums AB have produced evidence of some laser processing assessment. Having looked at the pre-requisites for using laser, electron beam and plasma welding in shipbuilding [2] , Hakansson [24] [25] reported tests in 1981 on laser welded tee butt joints in A36 high tensile steel. Their experiments with double sided welds using filler wire input examined the consequence of having different edge preparations. The results generally showed favourable results when compared with MMA welded control samples.

A journal article in 1982 [26] emphasised the priorities set by the U.S. Navy on laser welding. Their Naval Research Laboratory (NRL) has been researching the use of lasers in the production of guided missile launching systems using A36 steel. They are now overseeing the development of a prototype workstation [27] [28] known as the Laser Articulated Robotic System (LARS). This is primarily for munition production but could easily be used for small sub-assembly production work associated with ship production. A more novel idea for using this facility is in the heat line bending of plates [29] to replace a conventionally labour intensive process using gas heating torches for either shaping [30] or straightening of plates [31] .

Most of the processing research for the U.S. Navy's research, either by NRL or the United Aircraft Research Laboratories, appears to have concentrated on either the autogenous welding or the welding with shim inserts on high strength alloy steels [32] [33] [34] [35] [36] [37] [38] [39] . While the data provided in the reports indicate some procedural

envelopes for the laser welding of high tensile steel, they do not necessarily relate to mild steel welded in practical structural situations.

Few Japanese papers have discussed the use of lasers in shipbuilding directly even though some of their national companies involved in shipbuilding are also developing high power lasers . However, there is a growing number of authors relating laser processing to steel fabrication. Production systems for profile cutting steel plate of 6 x 2.4m are being employed [40] [41] and research is underway to increase the practical thickness of cut up to 25mm [42] . Various authors refer to research into laser welding using filler wire [43] [44] [45] .

Laser hardening of marine diesel engine cylinder liners [46] [47] is now being employed by a German engine builder taking advantage of the controlled nature of the process without the need to quench the heated zone with a cooling medium.

In the UK, Martyr has published various papers [48] [49] [50] based on his Ph.D thesis [3] . This contains the first published work that relates to the practical implications in applying high power laser to ship production. The author has therefore summarised Martyr's conclusions in the following section to enable initial assumptions to be deduced as starting points for the work contained in his thesis.

1.3.2 Summary of Conclusions Drawn by D.R.Martyr

Martyr, in his thesis "Application of High Power Lasers to Ship Production" [3] restricted a definition of "high power lasers" to those involved with materials processing, namely cutting, welding, transformation hardening and surface alloying/cladding although his efforts were concentrated in application studies of laser cutting and welding.

Martyr's research into laser cutting resulted in the manufacture of a moving optics Computer Numerical Controlled CNC laser profiling machine which made full use of the process advantages; low heat input,square edge with a kerf width of less than 0.5mm, minimal dross, ease of automation and speed . With an output power of 2kW, plates of up to 10mm thickness were successfully cut although there was potential to penetrate plates of greater thicknesses. However above 12mm thickness the edge quality tended to deteriorate. Cuts in material up to 75mm were observed on other laser equipment although edge quality was not comparable with conventional methods of cutting.

The process showed potential for cutting a wide range of materials making the machine suitable for application as a cutting tool for general outfit trades. The main problem found by Martyr when cutting steel was the detrimental effect of surface primers on cut quality . This effect has also been experienced with conventional cutting techniques [51] .

During more recent trials [52] the Author made successful cuts on primed steel by using a dual pass technique. The first pass, at traverse speeds of 200mm/sec "scorched" the primed surface in way of the cut path, the second penetrated the plate and cut with a good cut edge quality.

For his laser welding study, Martyr reviewed the considerable range of published work on laser weldable materials indicating the ease of processing with austenitic steels, a high titanium alloy and most mild steels. High strength steels and most aluminium or copper alloys proved the most difficult to weld by other experimenters. The literature search emphasised the lack of details on welding mild steels with thermally cut edges i.e. typical shipyard conditions.

Martyr mainly used the "CL5" 5kW laser ,figure 1.06, developed by the United Kingdom Atomic Energy Authority (UKAEA), Culham Laboratory for his welding experiments. He concentrated on the production of plane-butt and dual-sided tee-butt welds in low carbon steel, components being prepared with a variety of shipyard methods and using a filler input technique to infill for gaps and mismatch.

Plane-butt welds were perfected in steel thicknesses from 3mm to 8mm using CL5 and by a dual pass method on 15mm and 25mm thick plate using the 10kW CL10 which was developed from the joining of two CL5 modules. In attempting to weld joint gaps greater than the diameter of the focused beam (>0.5mm), the filler wire input was used to "intercept" the beam and facilitate the welding process with gaps up to 3mm in width.

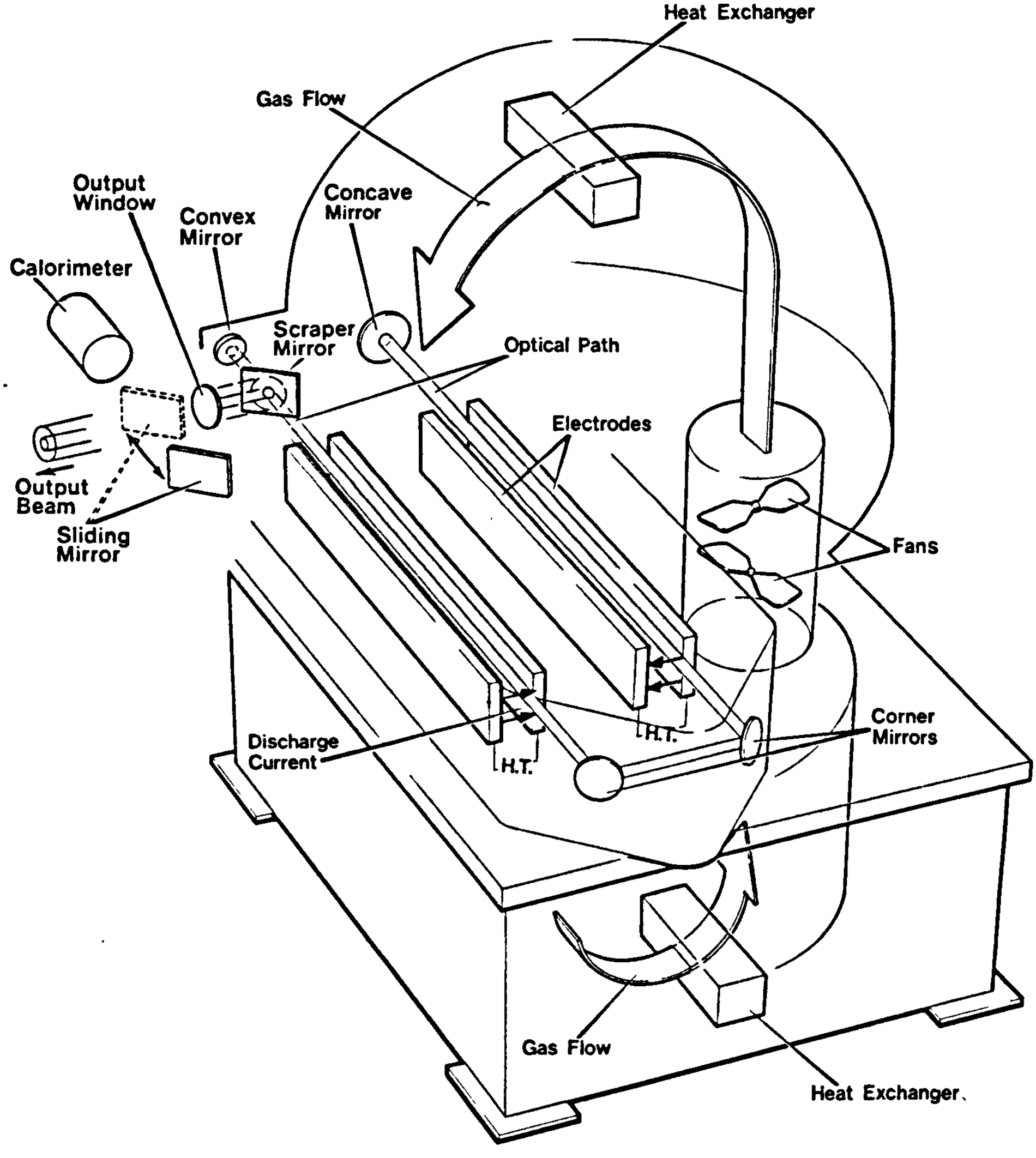

Figure 1.06 - The UKAEA Culham Lab. designed CL5 laser.

Butt welds were tested to Lloyds and MOD(N) guidance specifications after which Martyr concluded that the laser plane-butt welds either met or were superior to their requirements, both on joints with uncleaned edges, i.e. with oxide left from the cutting process and after being wire brushed.

Some skid welds were attempted using 6mm plate and 5kW of laser power at the workpiece, but with the sample orientated about a vertical beam. Gaps of 1.5mm were filled using the interceptor method. For larger gaps a lack of fusion occurred in the web. Welding of wider gaps (3-4mm) was achieved only by a dual pass method but with the incident angle increased to 13degrees to stop secondary penetration into the first bead surface.

The presence of primer appeared to have no noticeable effect on the finished weld quality. Martyr considered that the primer was ejected from the weld pool. However, only a limited number of macro and hardness scan tests were conducted on these samples.

Martyr investigated the distortion occurring in both butt and tee laser welded joints making comparisons with data for conventional welds. He showed a reduction of about 50% for the laser process even when a dual technique was used.

In addition to these trials (where the welds would directly replace conventional weld configurations) Martyr also attempted some novel joint configurations. "Through-welds" and "Lap-Welds" were made by using the

laser's high penetration characteristic to pin the components together. This type of weld is ideally suited for use in producing both existing and new types of structure e.g. the corrugated sandwich type [53] which is totally dependent on this type of joint to its assembly, but is particularly suited for automated methods of production.

Martyr based his laser welding workstation studies on the parameters derived from the experimental investigations which emphasised that any economic valuation of the process would be highly sensitive at present if viewed against initial direct costs. However when secondary savings were considered,e.g. savings as a result of the reductions in distortion, viable savings could be obtained

Therefore this provides the basis for further investigations into applying high power lasers to ship production materials processing. This is especially so for the work detailed in this thesis which describes investigations into producing a single sided tee section weld which is acceptable to ship construction and methods and design requirements.

CHAPTER TWO

PRINCIPLES OF LASER WELDING

2.1 INTRODUCTION

2.1.1 High Power and Low Power Laser Welding

There are two distinctly different types of laser commonly used for laser welding. The "Nd-YAG" laser, a solid state laser where the laser medium is neodymium doped Yttrium Aluminium Garnet (Nd-YAG) crystal, has a laser output wavelength of 1.06 micrometers, often pulsing, and with a power of generally below 500 watts, the processing is restricted to thin (<2mm thick) materials. The advantages of this welding method are obtained from the low and controlled heat input into the material with fine positional accuracy. Because of the particular optical wavelength, (near infra-red) normal visual optics can be used, the operator seeing the exact welding position along the same optics to which the laser will pass and thus weld positioning can be very precise. Also fibre optics can be used to transmit the beam in a flexible manner [54] .

The Nd-YAG process has been used on many fine electronic applications eg for television electron gun assemblies [55] headlamp filaments [56] , specialist metal packages [57] . It is ideal for spot welding, replacing micro-resistance spot welding which suffers from problems of electrode sticking. In a continuous mode the process has been used on sensitive

items where adjacent material must not be heated eg the casing for heart pacemakers [58] .

To obtain thicker weld penetrations, laser powers in excess of 500W are required. In the present stage of laser development this is best acheived using the CO2 laser. The work reported in this thesis investigates high power CO2 laser welding only as a basis for development.

2.1.2 The Simplest High Power Laser "Weld"

There is no need to have a joint present in a material to observe the action of the focused laser beam to form a keyhole - the basic pre-requisite in creating a fully penetrating laser joint. In fact, the welding action is often viewed in a solid block of material so that the simplest and idealised laser keyhole weld can be used to study initial processing parameter requirements.

For conventional welding where a weld bead is run on a solid block of material, requiring the deposit of filler material on the plate the result is termed a "bead-on-plate". Because of the deep penetration of the laser weld the term bead-on-plate could be confusing. More appropriately a laser run should be termed a " bead-in-plate ". A term used by the Author as being applicable to all processes, conventional and laser, is simply a "melt run".

This melt run can be produced either in a plate of thickness less than the depth of the keyhole penetration for a particular traverse speed and laser power producing a "penetrating melt run" , or in a plate of greater thickness when it can be termed a "blind melt run".

2.1.3 Development of the Melt Run to Produce Practical Weld Configurations

The Author has used the idealised properties of the melt run formation to explain the basic principles involved in laser welding (Section 2.2). From this idealised situation joints along the weld path can be considered as various types of discontinuities within the material and melt run structure to form different weld configurations.

Optimised joints have been considered as those where both faces to be joined are machined, degreased and clamped together with essentially no gap between them. A perfectly good weld can be made without needing to introduce any filling material and this is termed as an "autogenous" weld. At the other extreme there is likely to be a wide gap between faces to be joined with uneven and probably dirty surfaces. In this case additional material has to be introduced to fill the gap or produce reinforced beads. If the gap width is greater than the diameter of the focused laser beam a means of intercepting the beam is also necessary.

2.1.4 Classificaiton of Welding Techniques

Martyr [3] discusses the different welding processes used in shipbuilding and it is also important, in comparing weld structural properties and process suitability, to be aware of the alternative types of processes. Holdcroft [59] classifies welding into seven process types depending on the type of energy transfer. The Author has used these same headings but developed the table, table 2.01, to show how welding techniques used in general engineering and shipbuilding can be categorized. Technical terms for each method as detailed in B.S. 499 Part1:1983 "Welding Terms and Symbols,Glossary for Welding,Brazing and Thermal Cutting" [60] are presented, together with some of their colloquial titles. A diagramatic comparison of conventional fillet welding techniques is shown in figures 2.01(a-c). Each process is shown together with the relevant work situation and associated service requirements.

2.1.5 Laser Welding Terminology

Where possible all terms used in the thesis are as defined by the British Standards Institution. Conventional welding terminology is given in B.S.499 [60] . This reference now includes terms relating to Electron Beam Welding but due to their relative infancy laser welding and cutting have only a few terms defined.

Process	1.Solid Phase	2. Thermochemical	3.Electric resistance	4.Unshielded arc	5.Flux shielded arc	6.Gas shielded arc	7. Energy beam
Basic Principles	Two sides of a joint put in intimate contact by mechanical pressure or atomic diffusion or both	Joint heated by gas flame or exothermic reaction. Superheated molten metal then flows in joint	Heat produced by passing electric current across joint interface or induced in metal near joint	Passage of an arc within a joint - normally for a short period to stop contamination	Arch formed between a consumable metal electrode and joint. Flux from around electrode, as powder or within wire	Arc and weld pool shielded from the atmosphere by gas. The electrode may be 1) consumable or 2) non consumable	Heat energy created from a focused beam of radiation
Shipbuilding Application	Welding of dissimilar metals eg steel and aluminium blocks			Welding studs to bulkheads for cable trays, insulation or fairing	General stuctural welding, manual/ semi-automatic. Gravity welding from tripod or gantry for panel fabrication	General structural welding, pipe welding well suited to robotic application	1)R&D project use: panel line. 2)R&D project use: batch production of small parts
Particular welding techniques	Explosive cold pressure thermo-compression hot pressure friction ultrasonic	Plasma atomic-hydrogen Gas thermit	H.F. induction electro-slag flash-butt H.F. resistance	Bare wire stud spark discharge, percussion carbon arc	Covered electrode submerged arc, fuse arc, flux cored electrode	1)Inert gas metal arch,CO2 metal arc 2)Inert gas tungsten arc, gas/flux metal arc	1)Laser beam 2)Electron beam
General engineering descriptions	Explosive welding	Oxy-acetylene welding gas welding	Resistance spot welding	Stud welding	Manual metal arc (MMA), stick electrode electric arc welding, submerged arc welding (SAW)	Metal inert gas (MIG), metal active gas (MAG), gas metal arc welding (GMAW) CO^2 welding 2)Tungsten inert gas (TIG) arson arc welding	1)Laser beam welding (LBW) 2)Electron beam (EB) welding-EBW

Table 2.01 - Welding process classification

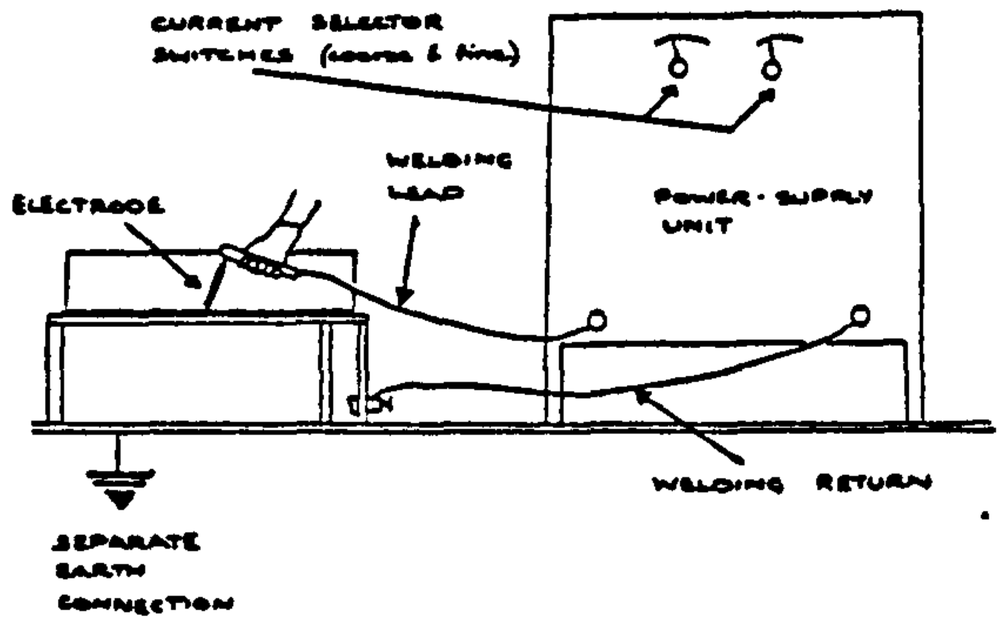

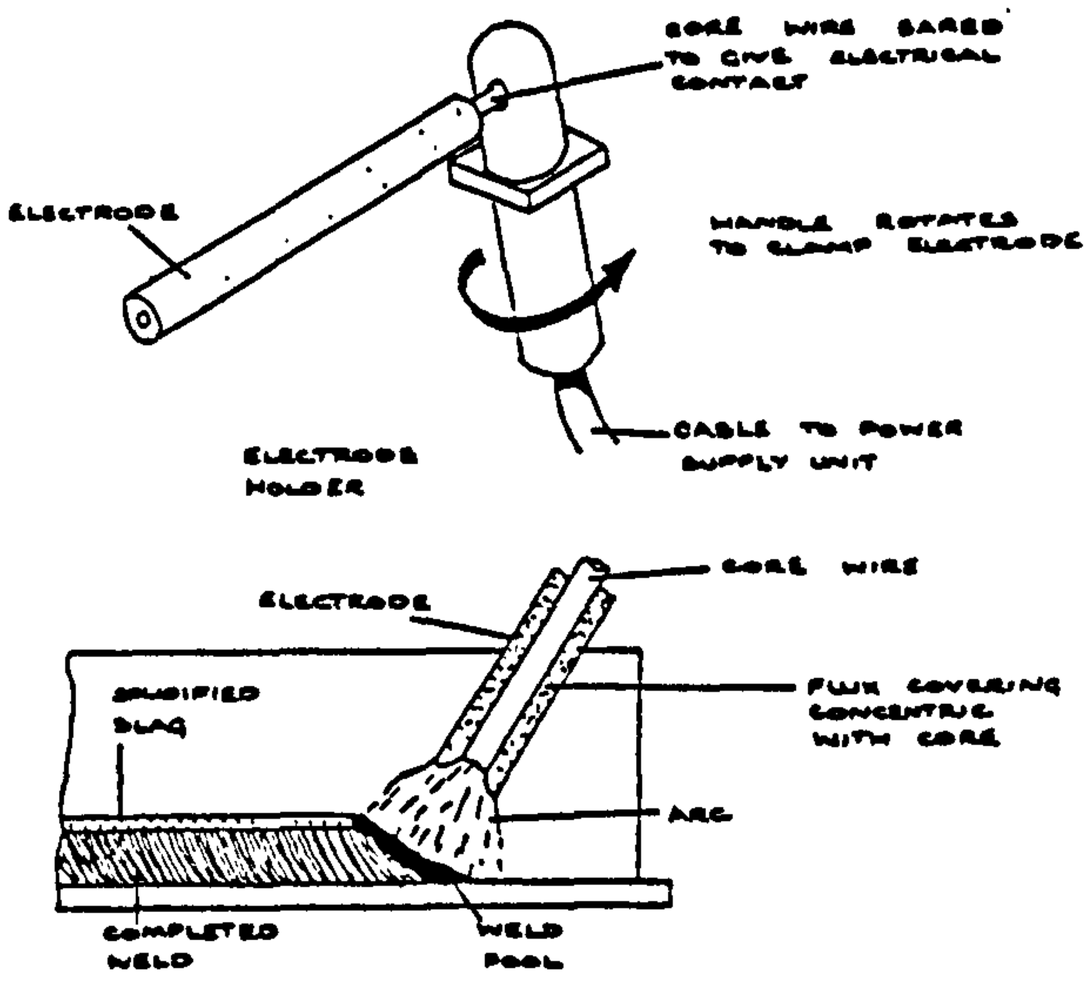

Figure 2.01a - Fillet welding processes : Covered electrode

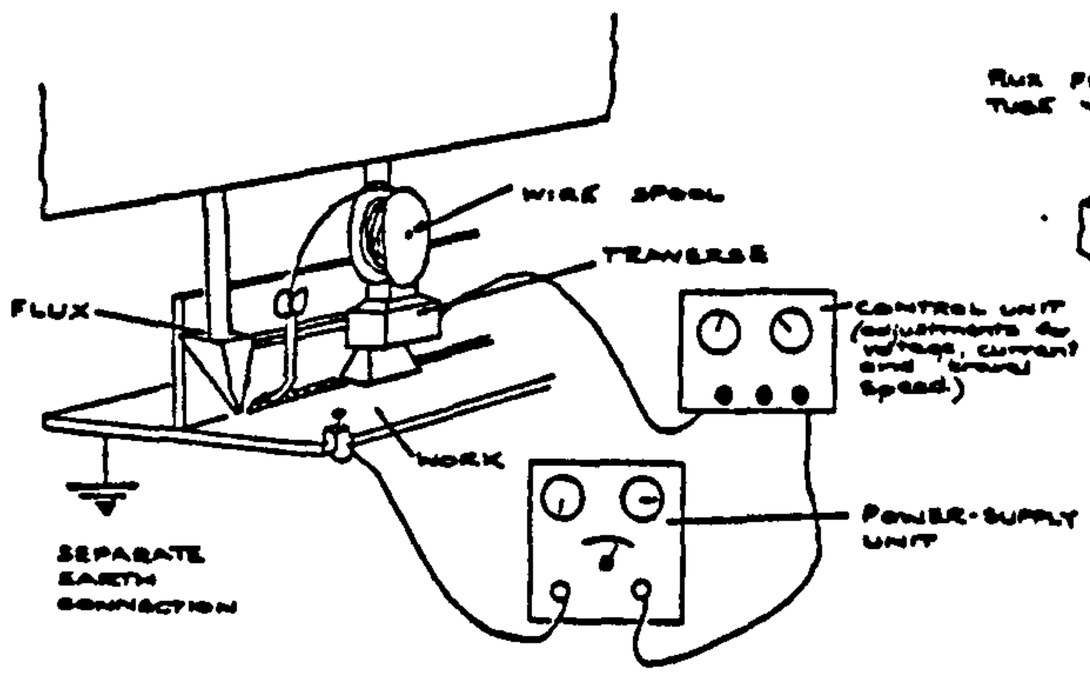

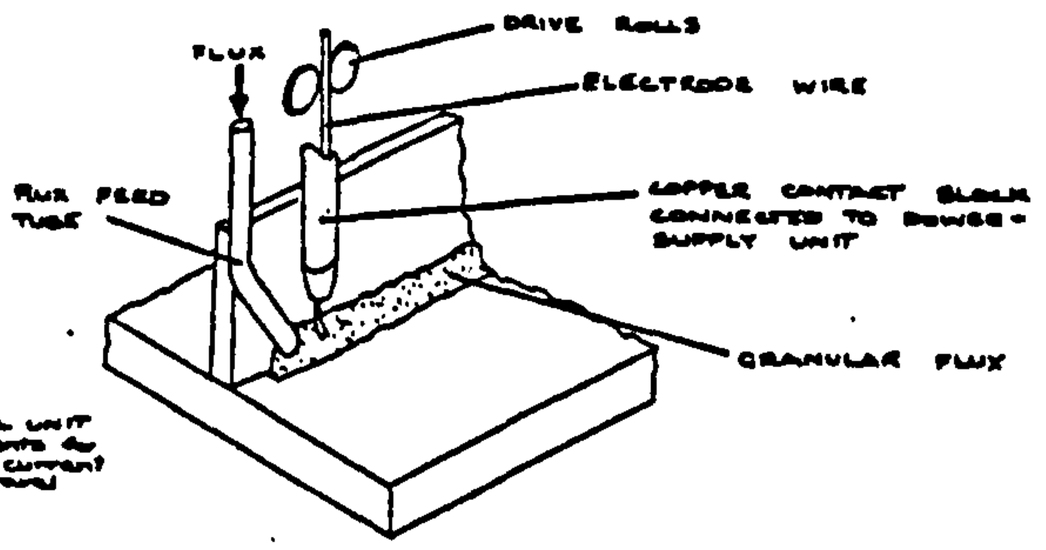

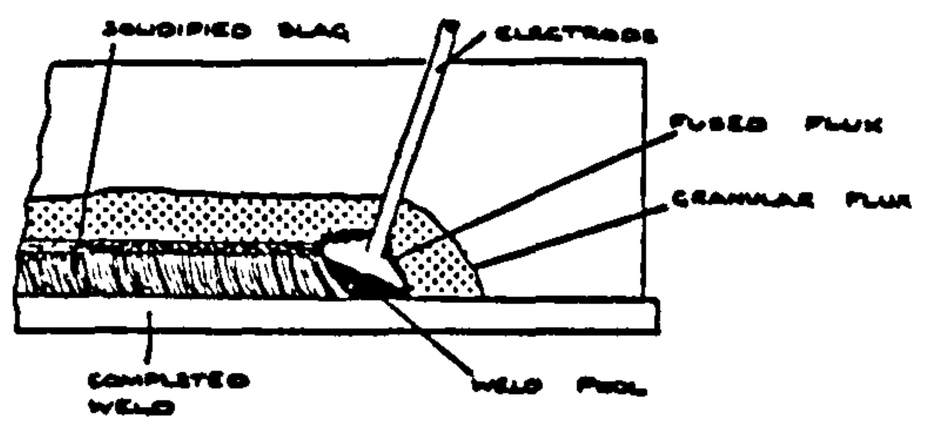

Figure 2.01b - Fillet welding processes : Submerged arc

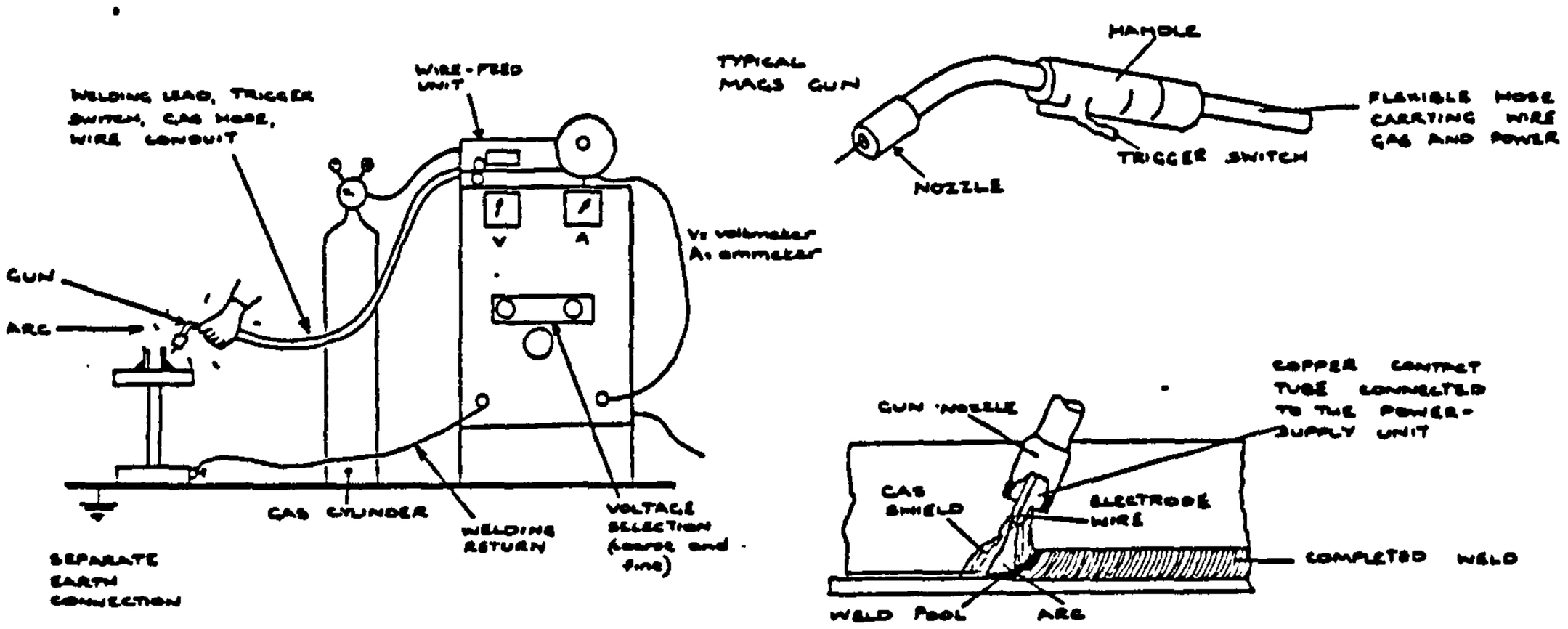

Figure 2.01c - Fillet welding processes - Inert gas/ CO2 metal arc

Additional reference to laser terminology can be derived from B.S.4803:Parts1-3 1983,"Radiation Safety of Laser Products and Systems" [61] . As the title describes this is directed to safety requirements for laser systems rather than the system terminology itself.

When a term is not quoted either as a conventional or established laser term, then terminology from the most recent publications is used as well as some novel terms. Wherever possible when choosing novel terms, a word relating to a practical or physical representation of the situation is used.

Figures 2.02a-b explain diagramatically some of the most important terms used to define the characteristics of butt and tee joints for conventional welds and for the laser weld comparison. Novel terms as named by the Author are now defined:

1. Incident bead - Relating to skid welding; the build-up of reinforcing material to the side of the joint where the laser beam is incoming (incident).
2. Emergent bead - Relating to a single sided skid weld; a build-up of reinforcing material to the side of the joint opposite the incident bead.
3. Laser spot height - the height at which the incident beam strikes the web plate above (or below) the face plate surface.

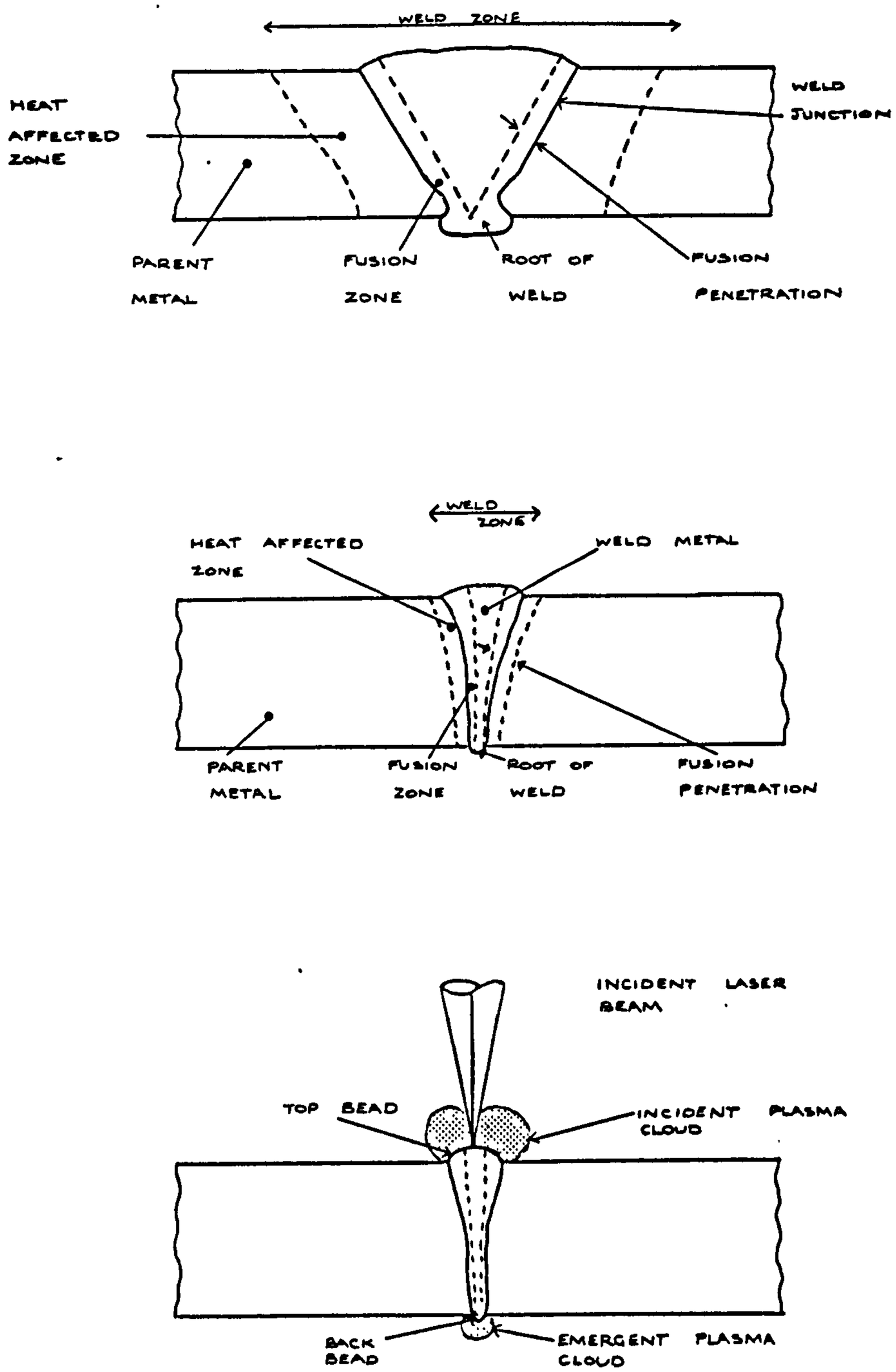

Figure 2.02a - Butt joint welding terminology

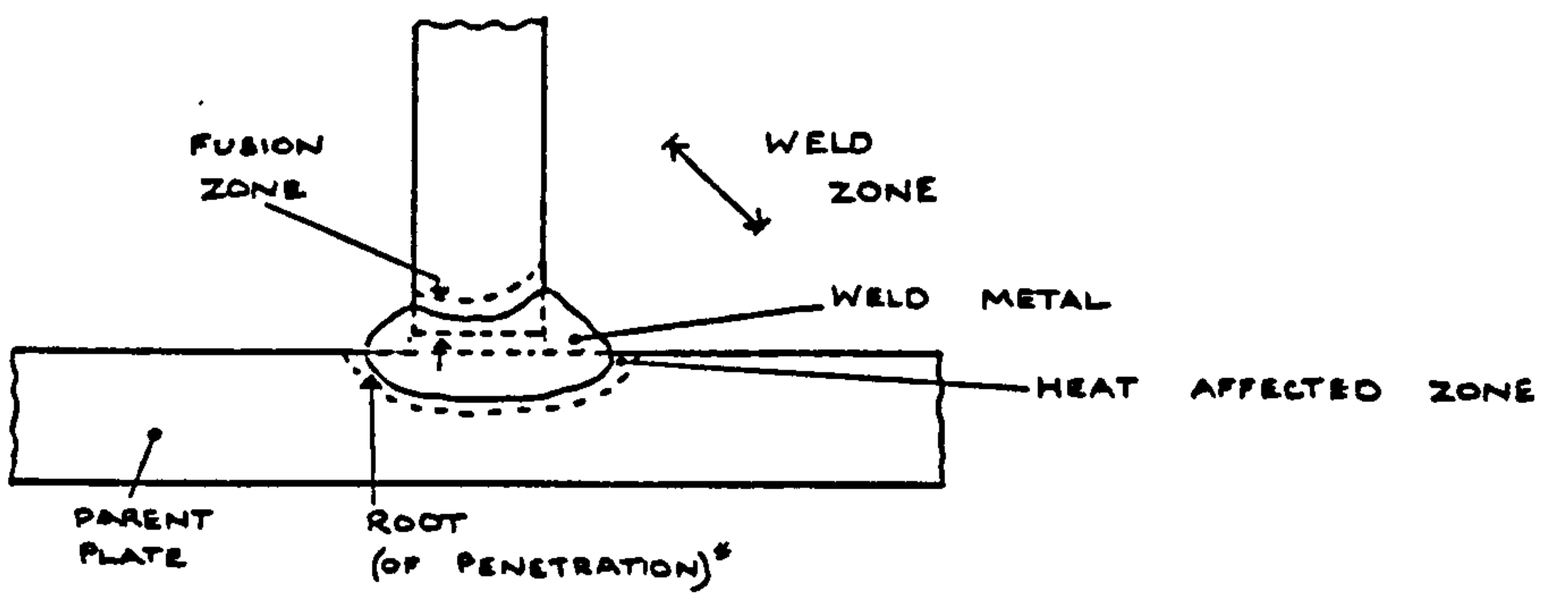

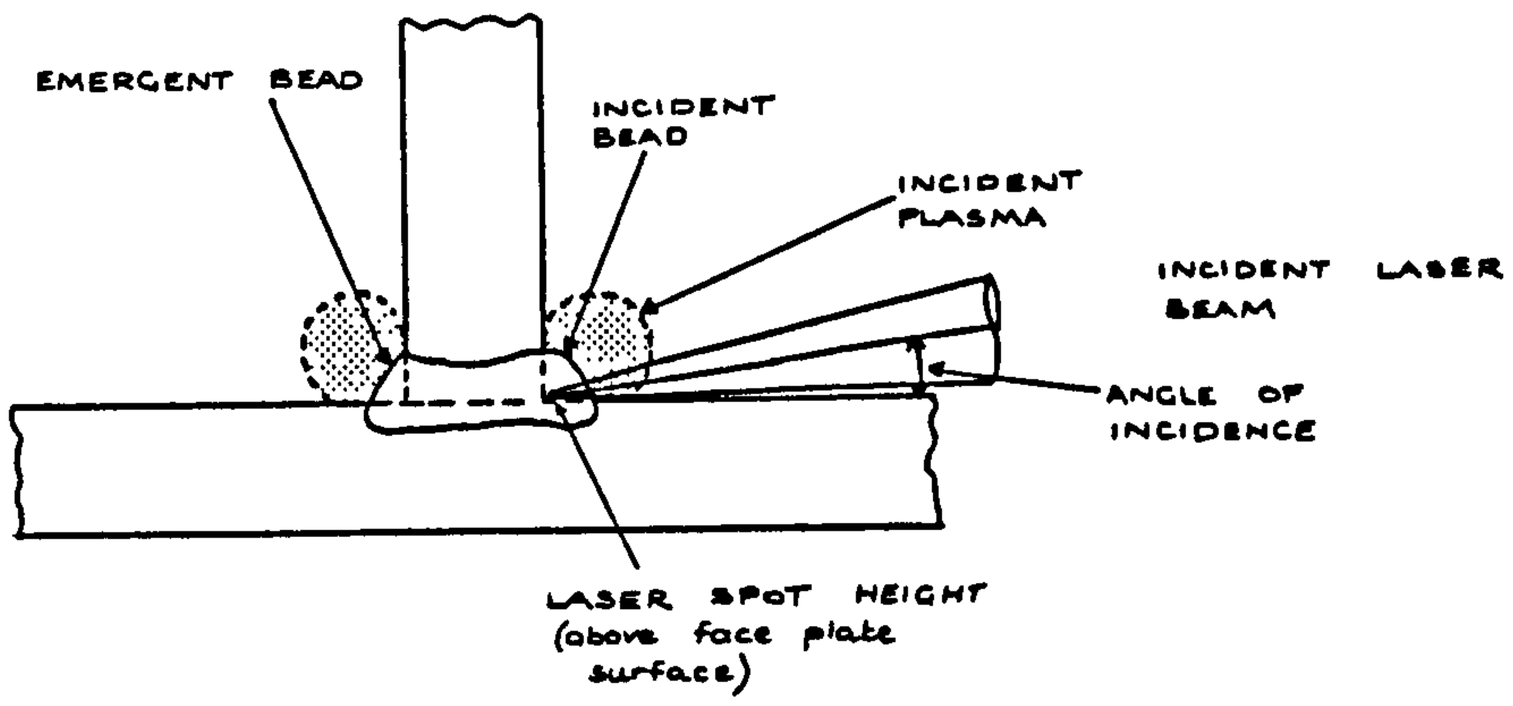

Figure 2.02b - Tee joint welding terminology

2.2 GENERAL PRINCIPLES OF HIGH POWER LASER WELDING

The simplest high power laser "weld" has been described as a bead-in-plate, or melt run. In order that the welding process may be fully understood before practical joint configurations are described, the Author has detailed the general principles involved in the formation of the laser keyhole melt run.

2.2.1 Manipulation of a Laser Beam to the Workpiece

The formation of a keyhole weld is dependent on supplying a point energy source to the workpiece of sufficient power density (>10^4 W/mm^2 for steel) to vaporise the material.

To achieve this the laser beam has to be passed through a beam delivery system. This comprises the laser beam generator - commonly described as "the laser" beam delivery line - which could also include various sections for turning the beam to manipulate it to the required position, and a focusing device - to converge the beam and provide the required power density on or near the workpiece surface.

In practice the system will also include associated devices e.g. a calorimeter used as both a "dump" for an unused beam and to measure beam power; a telescope to converge or diverge the beam as it leaves the laser (typically 20-50mm diameter) for efficient delivery dependent on the line length [14] ; beam surveillance equipment to monitor output

characteristics; and safety equipment.

Mirrors made of a substrate or with coatings to give optimum reflective characteristics for the particular laser wavelength (10.6um) are used to manipulate the beam either passively for a fixed system or dynamically for a moving optics system.

If the laser power is low enough so as not to cause distortion - less than 5kw - lenses are frequently used to focus the beam. For larger powers, curved mirrors are preferred. Various focusing methods are summarised in figure 2.03.

For safety reasons the complete "beam delivery system" must be encased in supported tubing and interlocking covers to prevent accidental access to the beam itself.

2.2.2 Beam Absorption to Form a Keyhole

Steel, in the solid state, is generally reflective to 10.6um wavelength CO2 laser radiation at room temperature. When the beam initially strikes the steel, 80-90% of the incident energy is reflected [62] [63] . The remaining 10-20% must be sufficient to heat and eventually melt the plate surface - melting point of steel is 1800 $^{\circ}$ K . The absorption process accelerates as surface temperature reaches the vaporisation temperature, figure 2.04.

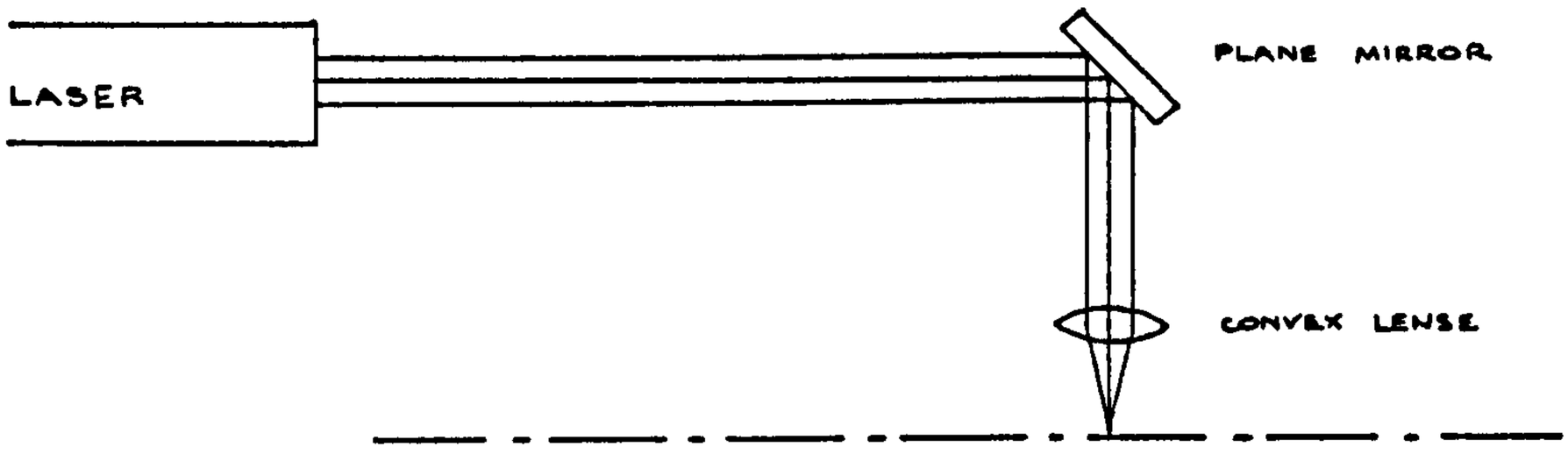

Figure 2.03 - Use of mirrors and lenses for focusing a laser beam

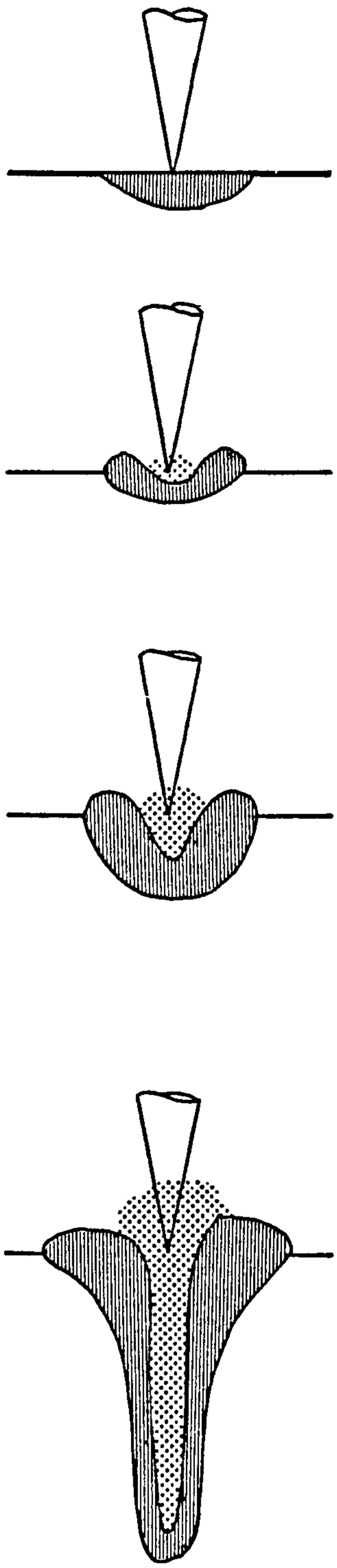

Surface melted.

Molten material is pushed to one side forming a crater as crater is filled with vapourised material or "plasma"

More molten material is pushed aside as the molten area deepens. Plasma increases above the deepening crater or "keyhole".

Sequence is repeated as the penetration increases to form a deep and narrow keyhole.

Figure 2.04 - Stages in the formation of a keyhole

Once a vaporised cavity forms, the energy transfer process increases further to give coupling levels in excess of 90%. This is due to the presence of the absorbent vaporised and ionised material called "plasma" and as a consequence of the cavity shape which results in multi-reflections of the incident energy on the side walls, figure 2.05. Hence the cavity grows, the predominant axis being along the line of incidence of the incoming beam.

The resulting deep but narrow cavity formed by applying the small point source of high power density is called the "keyhole". Parker and Luxon [64] estimate a time of 16us for steel to reach vaporisation temperature using a source with a power density of $10^8 W/mm^2$. The complete keyhole forming process probably takes between 0.1 and 1.0ms depending on penetration depth.

2.2.3 Energy Transfer from the Keyhole

The energy deposited in the keyhole, throughout its depth, is transferred to the surrounding molten zone by radiation and conduction, figure 2.06. The rates at which this occurs depend on the heat input characteristic and the materials thermal properties. Material reflectivity was observed as a dominant factor in the keyholing process. Heat transfer is subsequently influenced by the specific heat - the energy required to raise the temperature of unit mass by one degree K; thermal conductivity - the heat flow per unit area per unit thermal gradient; and latent heat - the amount of heat required to cause a change

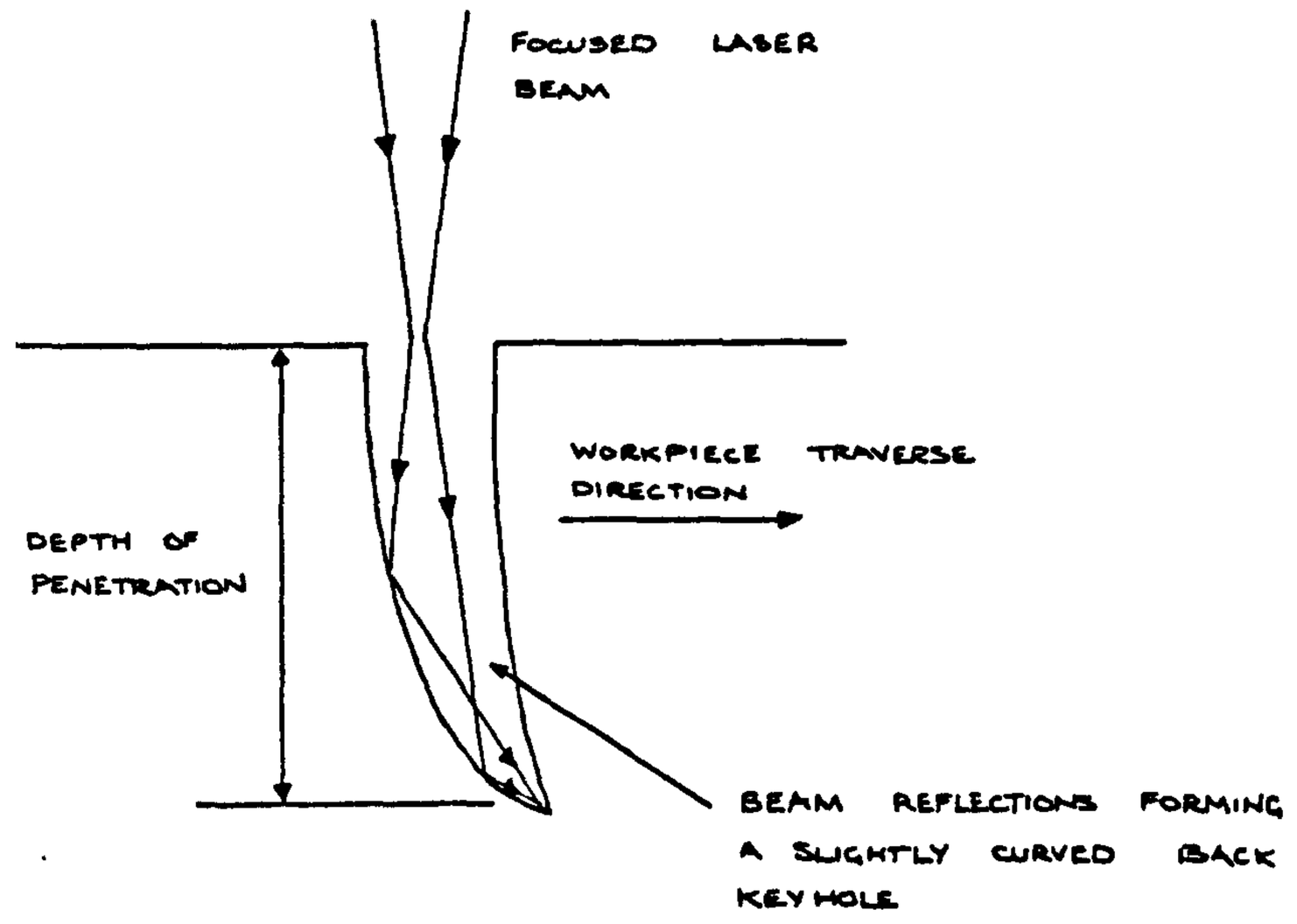

Figure 2.05 - Beam reflection within a keyhole

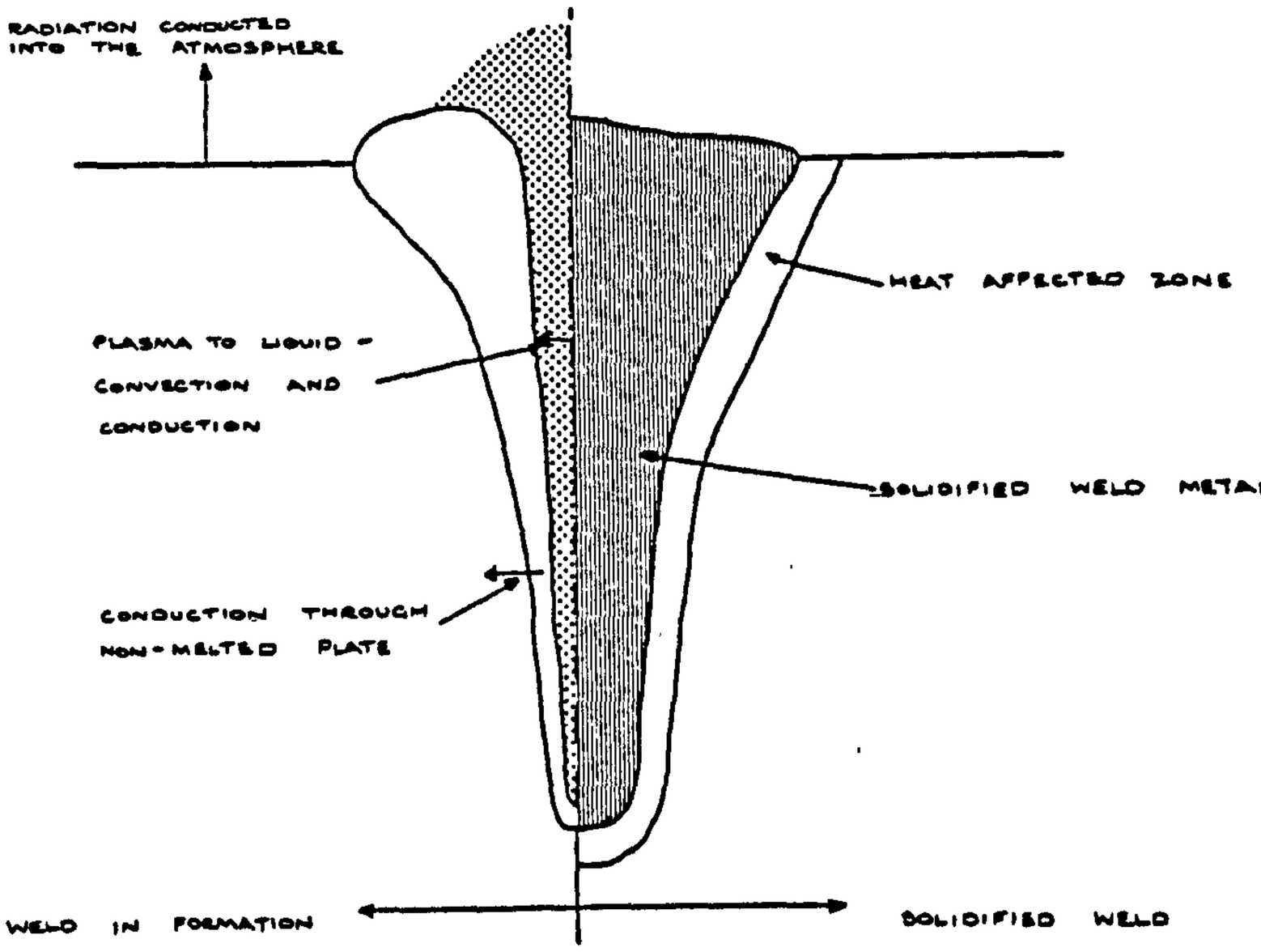

Figure 2.06 - Heat flow from the keyhole to the parent plate

of phase of unit mass of material.

2.2.4 Dynamics of a moving keyhole system to form a continuous fusion zone

The stationary keyhole examined so far is an idealised situation. If the system was kept stationary the ever-increasing molten zone would collapse into the keyhole until all available material had either been vaporised or had dropped through the bottom of the fully penetrated hole.

By moving the laser spot and subsequently the keyhole relative to the material, the leading sector will approach new material to maintain the molten pool. The sides will only be subjected to the heat source for a finite time, hence the molten zone will be of a finite size. As the heat source moves forward the material which has flowed to the back of the keyhole solidifies forming the fusion zone.

For laser cutting the plasma and molten material in a fully penetrating, moving keyhole are cleared by blowing a jet of assisting gas, usually oxygen or air, through the hole. However, for welding the principal requirement is to maintain a stable plasma-filled keyhole where the vapour pressure within the keyhole balances the collapsing forces within the molten pool.

Andrews and Atthey [65] examined the main forces acting within the keyhole system. In addition to gravity the hydrostatic pressure of the

molten material has to balance the recoil vapour pressure for the keyhole to be maintained, figure 2.07.

Having examined the stationary keyhole with a need for a hydrodynamic balance within the keyhole system , it is clear that there is likely to be a minimum advance speed to create a stable keyhole. Also for a fixed input power, speed will be the prime variable to obtain a particular weld characteristic.

Consider the physical flow of material within the balanced system, figure 2.08. In order that the molten pool can be maintained behind the forward moving keyhole material must flow either around the sides of the cavity or in the vapour phase across the cavity. Klemens [66] showed that the prime mechanism was of liquid transfer, a small proportion being vaporised to maintain the pressure already within the keyhole. The process also produces a slight pressure differential creating a driving force for the transfer of molten material around the sides.

2.2.5 Controlling the Plasma Density Balance in the Keyhole

Plasma is likely to escape from the keyhole through any discontinuity in the molten pool. Naturally the "mouth" of the keyhole is open as the incident beam penetrates and thus vapour can escape. In addition to creating losses in the plasma density balance, a plasma cloud can build up above the weld. Incident energy from the beam will be absorbed or reflected prematurely and the keyhole disrupted.

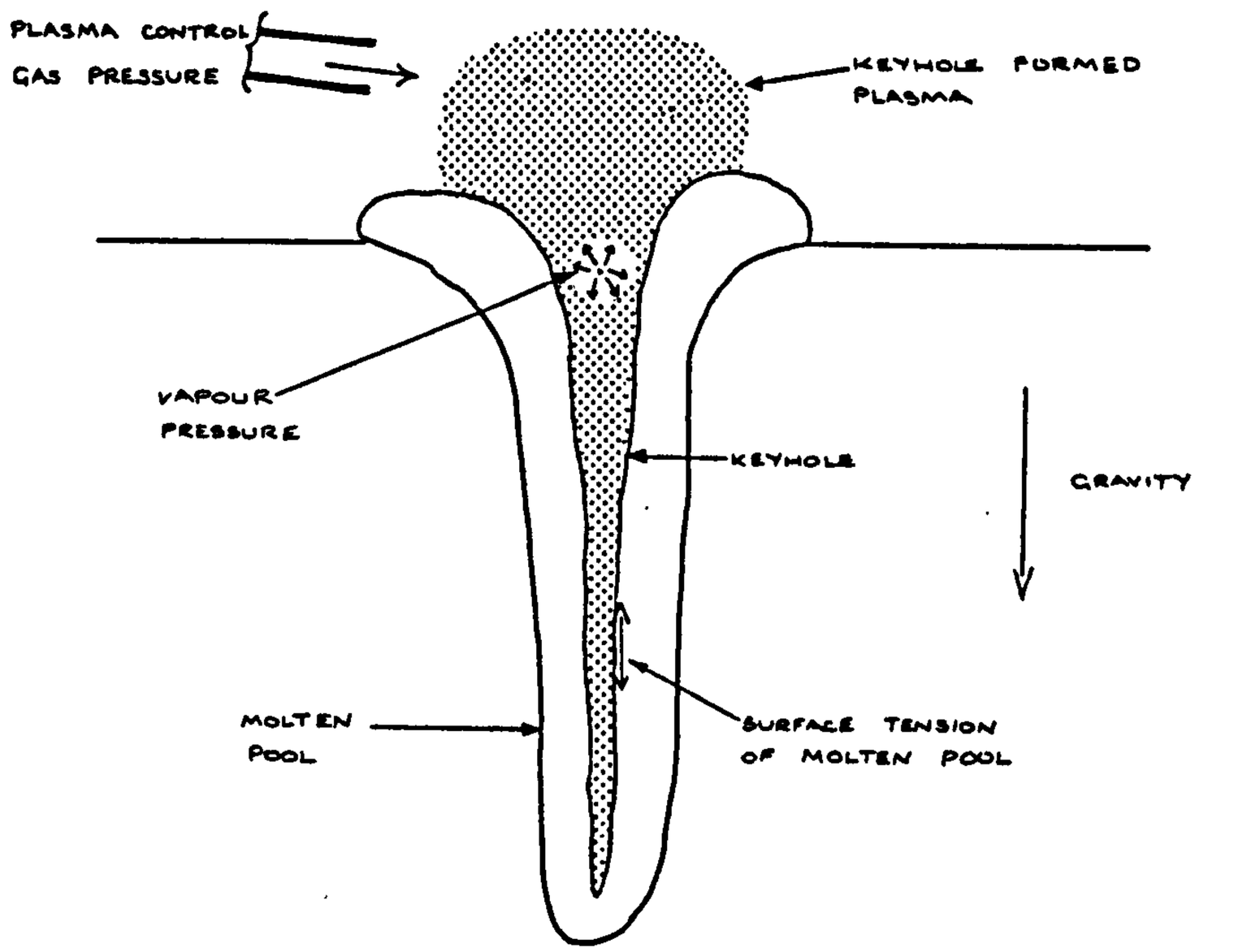

Figure 2.07 - Forces acting to maintain the keyhole

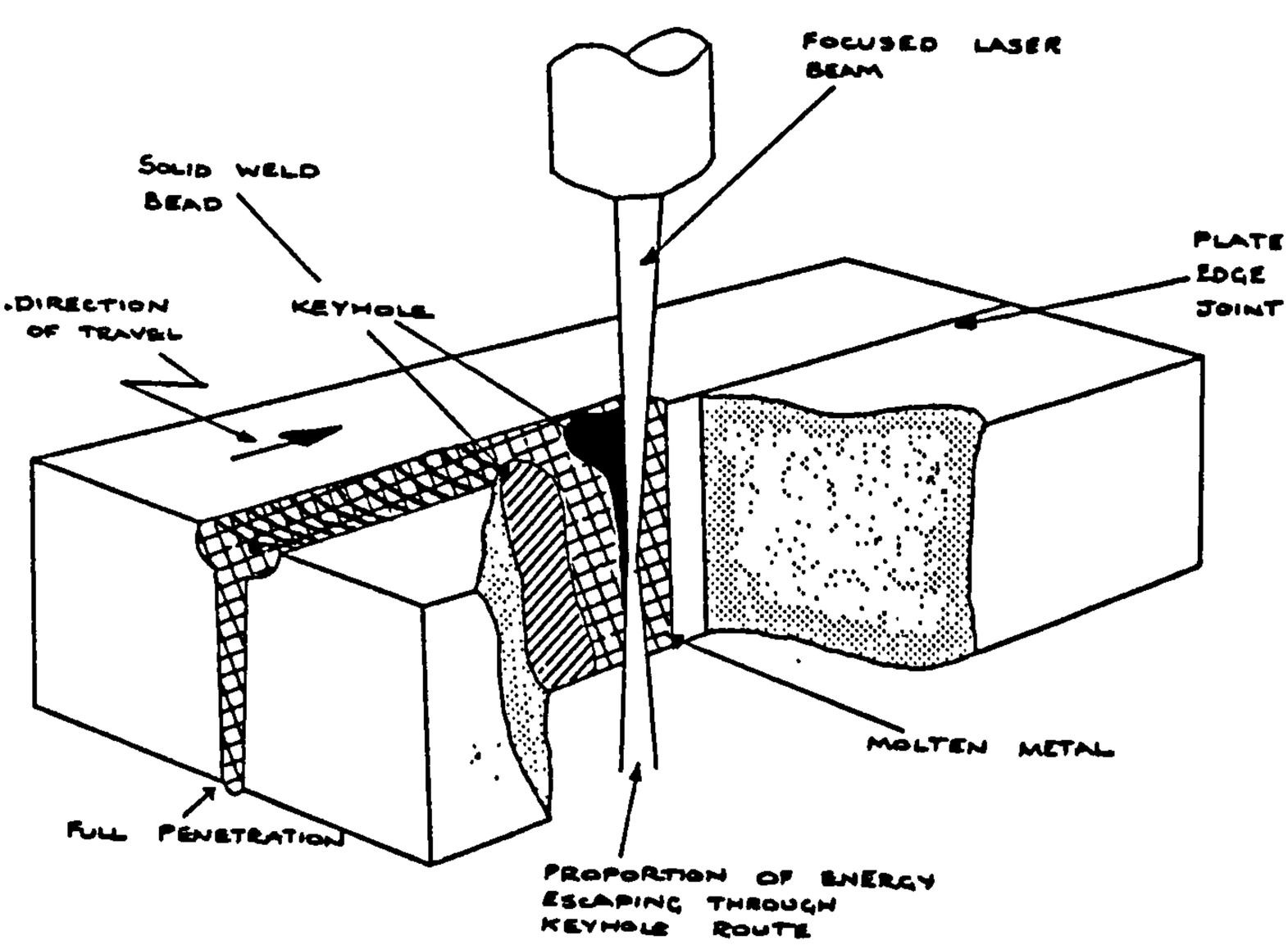

Figure 2.08 - Production of a weld from a moving keyhole system

Dowden et al [67] note the importance of maintaining an optimum plasma density - when too great, incident energy will either be absorbed by the plasma or reflected above the weld, when too little the process fails. The control method described, additionally by many other authors [68] [69] [70] , was that of blowing a stream of inert gas (helium or argon) at the interaction point. Whilst various configurations of plasma control units have been designed [71] [72] [73] , the predominant modes of gas flow are either coaxially to create a general positive pressure about the weld zone, or as a jet positioned at an acute angle to blow into the keyhole or across the weld surface, or a combination of them both.

Plasma density varies with the input parameters hence laser power, plate thickness and welding speed will effect the requirements for plasma control. Inherent methods have been proposed [74] where control is achieved by pulsing the laser power; though practically the gas control method is that most commonly used.

Losses will also be incurred from the root of a fully penetrating keyhole. Higher welding efficiencies have been reported in producing non-penetrating welds [75] [76] [62] [13] [43] both because of differences in heat flow and also because of loss of plasma. Efficiencies start to rise once the laser power and welding speed are balanced producing a stable keyhole to a depth which can be maintained in the molten zone formed. This does not necessarily mean just within the plate thickness as the molten zone could run or sag further than the line

of plate surface.

The methods for reducing losses at the keyhole mouth will be recalled. Similarly for a particular plate thickness there will be an optimum incident beam power and traverse speed to both reduce root loss and to determine the characteristics of an emergent bead.

2.3 THEORETICAL ANALYSIS OF WELD ZONE CHARACTERISTICS

So far the Author has characterised the formation of the weld in descriptive terms. It is necessary to further study the weld analytically to understand the effects of input parameters on the resulting weld characteristics.

Various researchers have attempted to make mathematical models of different aspects of laser and electron beam welds [66] [67] [63] [65] [77] [78] [79] which have emphasised their complicated nature.

Andrews and Atthey [65] analysed the hydrodynamic limit to penetration of a material by a high power beam. They analysed heat balance effects to show that the rate of keyhole formation was proportional to the incident beam power density, then by assuming firstly that the keyhole was formed at a steady state and secondly moving they produced dimensionless parameters which emphasised the dominant effects of gravity, molten pool surface tension and the vapour pressure within the keyhole.

At about the same time Klemens [66] was analysing heat balance and heat flow conditions for electron beam and laser welds. He showed how the keyhole plasma acted as a heat sink, conducting the energy to the surrouding molten zone.

Mazumber, Steen et al [63] [80] have developed a heat transfer model for general laser materials processing. The aim was to predict the dimensions of a weld, maximum welding speeds and the effect of supplementary heating or cooling, e.g. the effect of the plasma control jet and weld configurations.

Dowden et al. [67] [81] looked more recently at the influence of fluid dynamics on the molten pool and noted the effect which viscosity has on the weld characteristics.

While all these análogies helped in visualising the formation of the weld pool the Author wanted a practically based model to relate to the eventual metallurgical and mechanical properties of the weld in addition to the shape characteristics, i.e. a theoretical expression which would enable the temperature at a particular location in a component to be determined as a function of the welding parameters, position and time.

2.3.1 Heat Flow Analysis

The basis of predictions of temperature distribution and heat flow related equations within any weld is the differential equation of heat flow, theoretically developed for point, line and plane sources moving relative to a medium by Carslaw and Jeagar [82] , equation 2.01.

$$\frac{\partial^2 T}{\partial x^2} + \frac{\partial^2 T}{\partial y^2} + \frac{\partial^2 T}{\partial z^2} = \frac{c.p}{K} \cdot \frac{\partial T}{\partial t} \qquad (2.01)$$

where:

T = Temperature ($^{\circ}K$)

K = Thermal conductivity ($J.m^{-1}..s^{-1}.K^{-1}$)

c = Specific heat ($J.kg^{-1}..^{\circ}K^{-1}$)

p = density of the material ($kg.m^{-3}$)

x,y,z are directional vectors (m)

Rosenthal [83] developed practical solutions for this equation to examine the temperature distribution around a moving heat source by using the following assumptions:

1. The temperature distribution around the heat source will settle to a constant form - a "quasi-stationary" distribution i.e. for a practical situation acceleration and deceleration at the the start and end are not considered.
2. Specific heat and thermal conductivity of the material are constant.
3. Latent heats of melting and evaporation are ignored.

4. The plate is infinitely wide.

5. Heat dissipates only by conduction in the plate.

Whilst various authors have subsequently provided more refined solutions [84] Rosenthal's solution still remains a good basis for process modelling.

2.3.2 Heat Flow From Point and Line Heat Sources

Firstly the solution is expressed for a point heat source which gives three dimensional heat flow, figure 2.09. In addition to being referred to as the "thick plate" solution [85] , it also gives a model which could be used to examine heat flow in arc welds [86] . The equation gives the rise of temperature at a position relative to the weld centre line is given in terms of the material thermal properties and the heat input, equation 2.02.

$$T - To = \frac{Q}{2.\pi.K.t} \cdot \exp \frac{z^2 - y^2}{4.D.t} \qquad (2.02)$$

where:

T = Temperature at a point (°K)

To = Original temperature (°K)

Q = Heat input per unit length ($J.m^{-1}$)

t = Time after weld (s)

D = Thermal diffusivity ($m^2.s^{-1}$)

z = Depth in plate of the measured point (m)

y = Perpendicular distance from centre of joint (m)

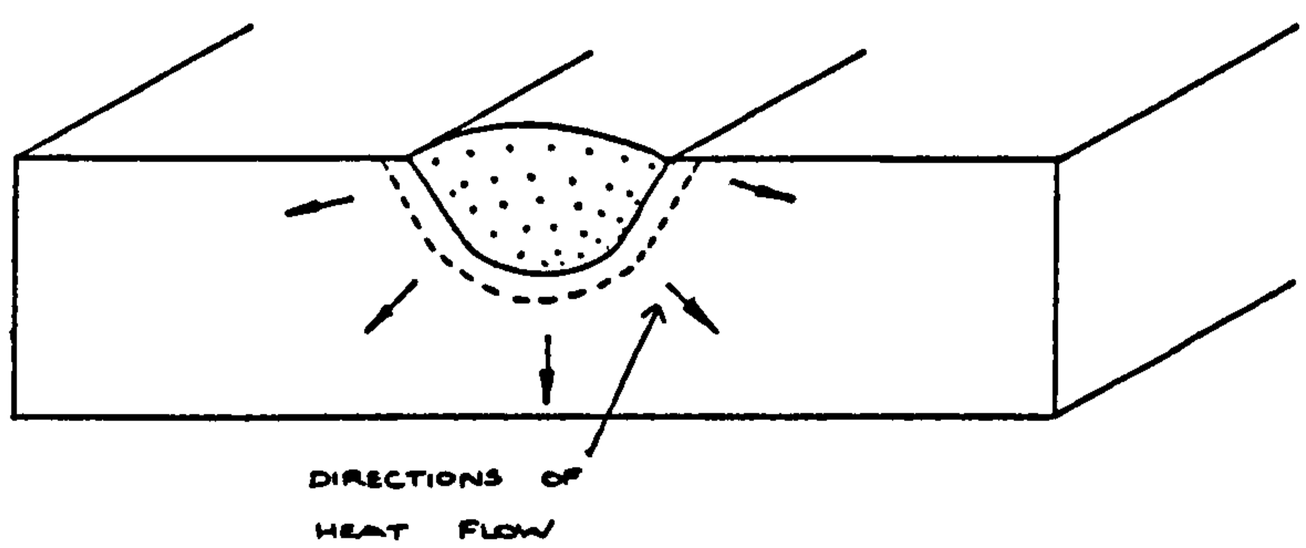

a) Heat flow from a point heat source producing 3 dimentional heat flow

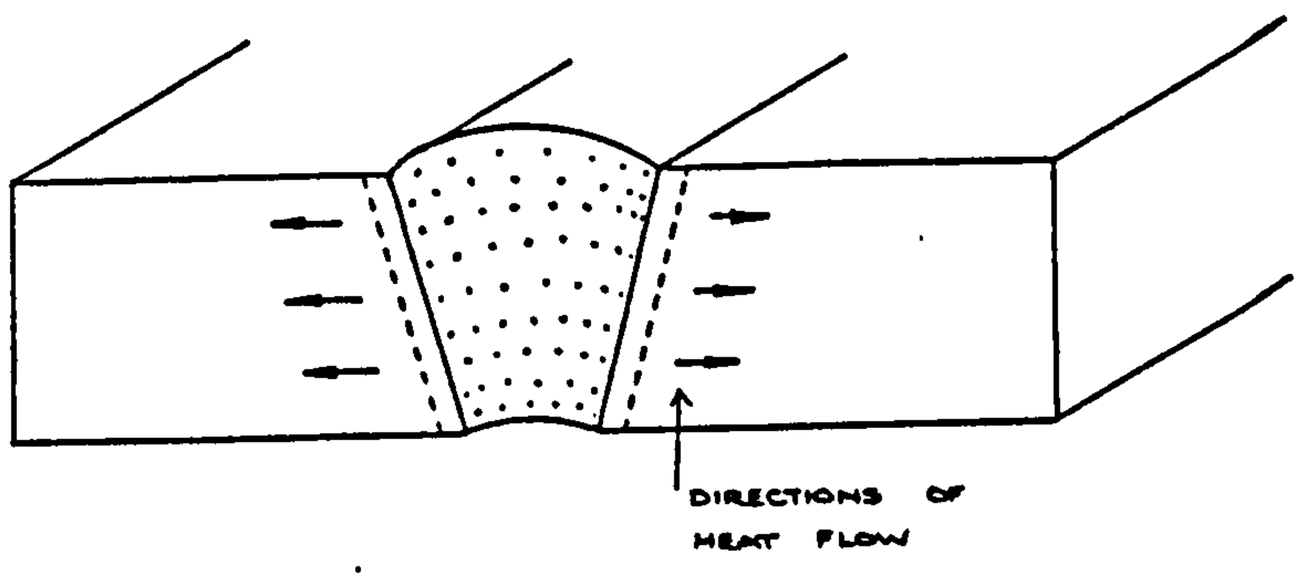

b) Heat flow from a line heat source producing 2 dimentional heat flow

Figure 2.09 - Directions of heat flow from a point and line heat source

Swift- Hook and Gick [76] report that the point source theoretical solution has been compared with practical results for conventional welds involving a surface pool with good correlation but propose that a line source, two dimensional heat flow simulation figure 2.09b, would be more suited to the keyhole type laser weld when the energy is deposited into a cylindrical line surrounded by a molten pool as shown in figure 2.10. Certainly trials on the similarly shaped EB welds have proved this to be valid [78] .

In the same way as for the point source, the equation can be developed to give a line source temperature - time distribution, equation 2.03.

$$T - To = \frac{Q}{2.h(\pi.K.p.c.t)^{1/2}} \exp\left(\frac{y^2}{4.D.t}\right) \qquad (2.03)$$

where h = thickness of material (m)

In addition, Easterling [85] has simplified equations 2.02 and 2.03 by considering the time taken for the weld to cool between 800°C and 500°C to give equations 2.04 and 2.05 respectively:

$$Dt8\text{-}5 = \frac{Q}{2.\pi.K.\alpha_1} \quad \text{(Point source)} \qquad (2.04)$$

where Dt8-5 = the time for the temperature to drop from 800°C to 500°C (sec)

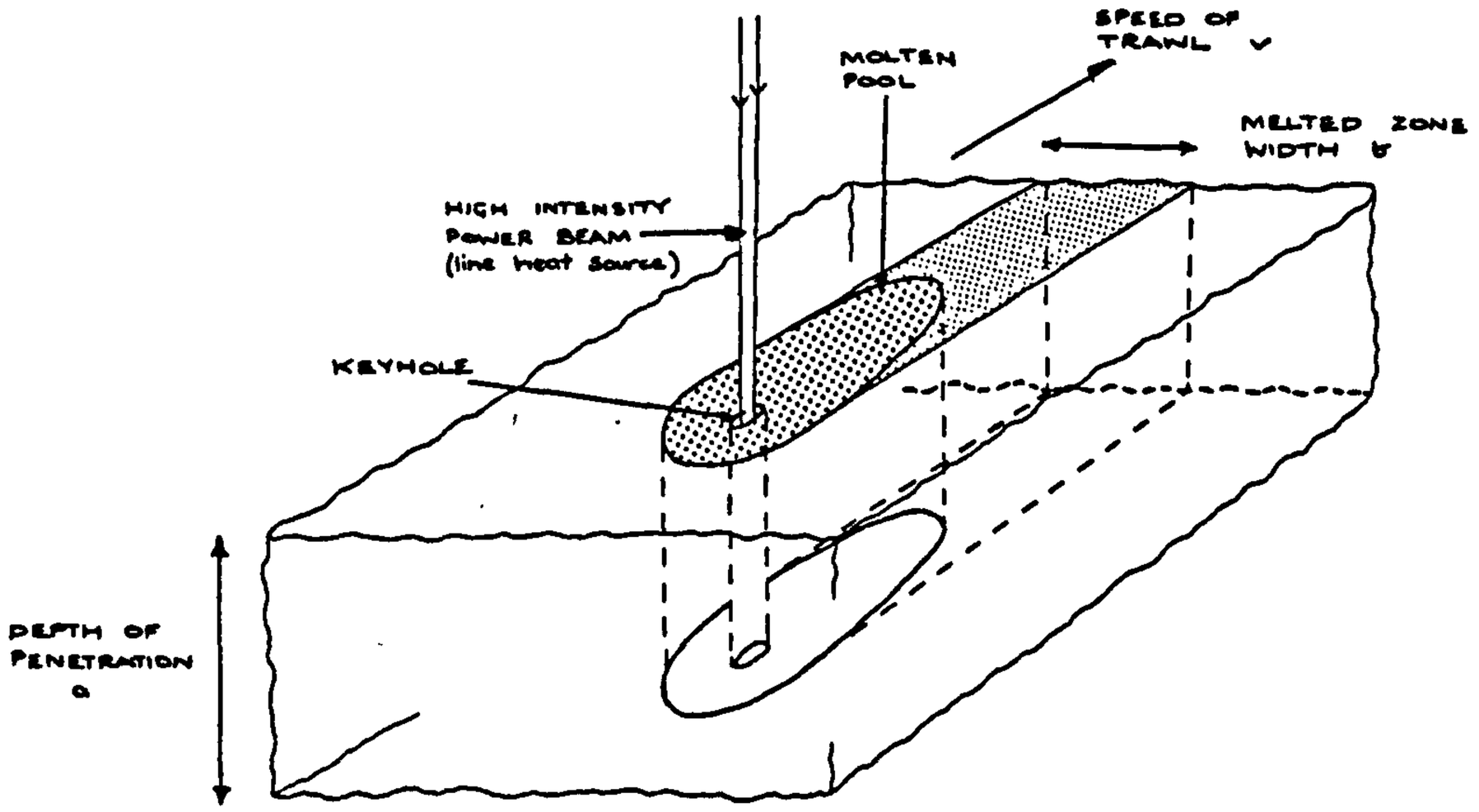

Figure 2.10 - Penetration weld geometry with a linear heat source representation

$$\frac{1}{\alpha_1} = \left(\frac{1}{773 - To} - \frac{1}{1073 - To}\right)$$

$$Dt8\text{-}5 = \frac{Q^{2}}{p.c.h^{2}.\alpha_1^{2}.K.\pi.4} \quad \text{(Line source)} \qquad (2.05)$$

where $$\frac{1}{\alpha_1^{2}} = \left(\frac{1}{773 - To} - \frac{1}{1073 - To}\right)$$

However, it is recognised that for a given welding process, weld geometry and material, the cooling time through the range 800-500°C is constant. Clearly, by equating equations 2.04 and 2.05 a boundary condition thickness may be derived (equation 2.06) determining the cross-over condition between point and line heat sources.

$$h = \left(\frac{Pwp}{2.p.c.v} \times \left(\frac{1}{773 - To} + \frac{1}{1073 - To}\right)\right)^{0.5} \qquad (2.06)$$

By assuming that for the laser weld this thickness represents the weld depth at which plate penetration is just initiated, plate thickness "h" may be substituted for the weld pool depth "a" to give an idealised estimate of the weld penetration for a particular laser power and traverse speed.

2.3.3 Correlation of Linear Heat Source Analysis with Practical Welds

The idealised method of analysing the laser weld has been examined. The difference between the ideal and practical results can now be assessed in terms of processing efficiency.

The simplest comparative function is that of melting efficiency or "melt ratio"; the ratio of the heat energy needed to cause melting of the material in the fusion zone compared with the potential energy provided from the heat source. For the laser weld it is the proportion of beam energy absorbed into the metal of the fusion zone. The principal losses include "energy transfer losses" and conduction of heat into the surrounding material. The melting ratio is given by equation 2.07.

$$Em = Pm/Pwp \qquad (2.07)$$

Where Em = Melting Ratio

Pm = Power required to melt a volume of metal (kW)

Pwp = Incident laser power at the workpiece (kW)

The power required to melt a volume of metal, "Pm", cross sectional area "A" (m^2) at a traverse speed "v" (m/s) is given by equation 2.08:

$$Pm = A \cdot v \cdot p. (c \cdot DT + Lf) \qquad (2.08)$$

where p = material density ($kg \cdot m^{-3}$)

c = Specific heat - averaged from room temperature to melting point ($J.kg^{-1}.K^{-1}$)

DT = temperature rise to melting point (°K)

Lf = latent heat of fusion ($kJ.kg^{-1}$)

Incident laser power Pwp, (Watts) is the power in the incoming laser beam, easily measured at the workpiece prior to welding using a "Joule Stick" if no on-line measuring device is available. Alternatively the value can be estimated by multiplying the laser output power by the beam line transmission efficiency value.

An alternative method for correlating welding variables and process efficiency using the analogy of the heat line source is presented by Swift-Hook and Gick [76] for laser welds after Hablanian [87] who made similar assessments of electron beam welds. They present normalised expressions which relate input power and traverse speed to penetration and weld width.

The expressions for normalised power input per unit depth of penetration "X" and normalised speed with weld width "Y" are shown as equation 2.9 and 2.10 respectively.

$$X = Pwp / a \,.\, S \qquad (2.09)$$

$$Y = v \,.\, b / D \qquad (2.10)$$

where Pwp=Power input (kW)

S = Heat function (kW/m)

v = Traverse speed of heat source ($m.s^{-1}$)

a = weld penetration (m)

b = average weld width (m)

D = thermal diffusivity ($m^2.s^{-1}$)

The idealised situation of all the incident power being absorbed to form the molten pool (melt ratio = 100%) would exist when X is equal to Y. However this is not possible due to conduction losses into the parent plate.

By examining the functions X and Y for both high and low speed welding situations Swift-Hook and Gick showed that the maximum possible melt ratio for a laser weld would be 48.4% and give experimental evidence to substantiate their claim. However Brainan and Banas in a later report [75] consider that as laser welds have been produced with higher melt ratios, the difference could be attributed to a reduced loss in the form of latent heat of fusion. For mild steel plate, where Lf= 250 $kJ.kg^{-1}$, this would increase the optimum to 56%.

Luxon and Parker [64] have equated the non-dimensional functions X and Y for the optimum melt ratio, using the theoretical maximum of 48.4% to obtain a relationship between weld pool penetration and the average weld width, equation 2.11:

$$b = 0.484 \cdot D \cdot Pwp / v \cdot a \cdot S \qquad (2.11)$$

The difference between the maximum possible melt ratio and that found for

an actual weld can be associated with the energy transfer losses eg. power lost within the plasma cloud above the weld. The ratio of the maximum possible melt ratio and that actually found for a particular weld is called the Heat Transfer Efficiency and is a measure of the proportion of the incident beam energy which is actually absorbed by the workpiece.

By graphically comparing X and Y values for a particular weld against curves for idealised conditions and the maximum possible melt ratio , relative efficiencies can be deduced for particular joint configurations and input parameters.

Comparison of other authors' work [43] [13] by this method or by simply calculating the melt ratio shows how melt ratio will generally be higher for a non-penetrating joint compared with a penetrating joint. Also as laser power and traverse speed increase, so melt ratio tends to the optimum. Comparison of similar welds produced using different lasers also shows different ratios . This will be due to the efficiency of beam focus as related to beam mode and to plasma control. Different materials will similarly give different values for the same parameters as shown by Megaw [13] due to the relative heating characteristics.

Although for normal reflection at a surface energy transfer efficiency for CO2 laser radiation is as low as 5%, once a keyhole is formed the resulting multiplying of reflections within the cavity containing vaporised and ionized metal causes the efficiency to increase. Whilst practical welds have shown the efficiency to be dependent on weld speed,

laser power, joint type and material Swift-Hooke and Gick quoted efficiencies of 50% at 8kw and 100% at 20kW (corresponding to a 50% melt ratio) though comparative results for welds in "thin" plate showed a reduction to between 10% and 20% efficiency.

Clearly, for the practical welding situation, the heat energy actually absorbed to form the joint is reduced in proportion to the heat transfer efficiency (Eht). Hence the Author has used equations 2.06 and 2.11 but included the factor for Eht to provide an estimate of the weld penetration and average weld width, equations 2.12 and 2.13 respectively, for practical joint configurations:

$$a = \left(\frac{Pwp \times Eht}{2.p.c.v} \times \left(\frac{1}{773 - To} + \frac{1}{1073 - To} \right) \right)^{0.5} \qquad (2.12)$$

$$b = 0.484 \,.\, D \,.\, Pwp \,.\, Eht \,/\, (v \,.\, a \,.\, S) \qquad (2.13)$$

2.4 PRACTICAL WELD JOINT CONFIGURATIONS

All practical laser keyhole welds are a development of the laser melt run, a discontinuity having been positioned relative to one of the axes of the keyhole. The principal keyhole weld configurations can be classified as "butt" - with the principal axis along the joint; "through" - with the joint perpendicular to the principal axis; and "reinforced" or "smoothed" where, in addition to the keyhole fusion zone within the plate, a reinforcing zone is formed externally to the plate within molten

filler material introduced to the joint. Each configuration is discussed briefly for practical weld requirements, the "skid" weld, which combines techniques from each welding principle configuration, is then examined in greater detail.

2.4.1 Butt Welding

To form a fusion zone with the principal axis of the keyhole parallel to the plate edges the laser beam is directed perpendicular to the plate surface and traversed along the joint line.

The idealised joint condition is to have machined, degreased joint faces with no gaps. A good quality weld can then be made autogenously at speeds similar to those for melt runs. As joint conditions deteriorate, e.g. with undulating and oxidized edges caused by prior cutting processes, gaps from inaccurate fit-up, dirt from environmental swarf, paint from protective coatings, autogenous weld or rolled section edges, figure 2.11, characteristics become unacceptable. A technique of introducing filler wire into the joint can be used as a method of counteracting losses, controlling fusion zone properties and, if the joint gap becomes excessive, as a beam interceptor to initiate the process [3] .

Weld shape may be characterised similarly to the melt run. However, to ensure complete fusion, the incident power and traverse speed must be balanced to give sufficient penetration and weld width, without excessive

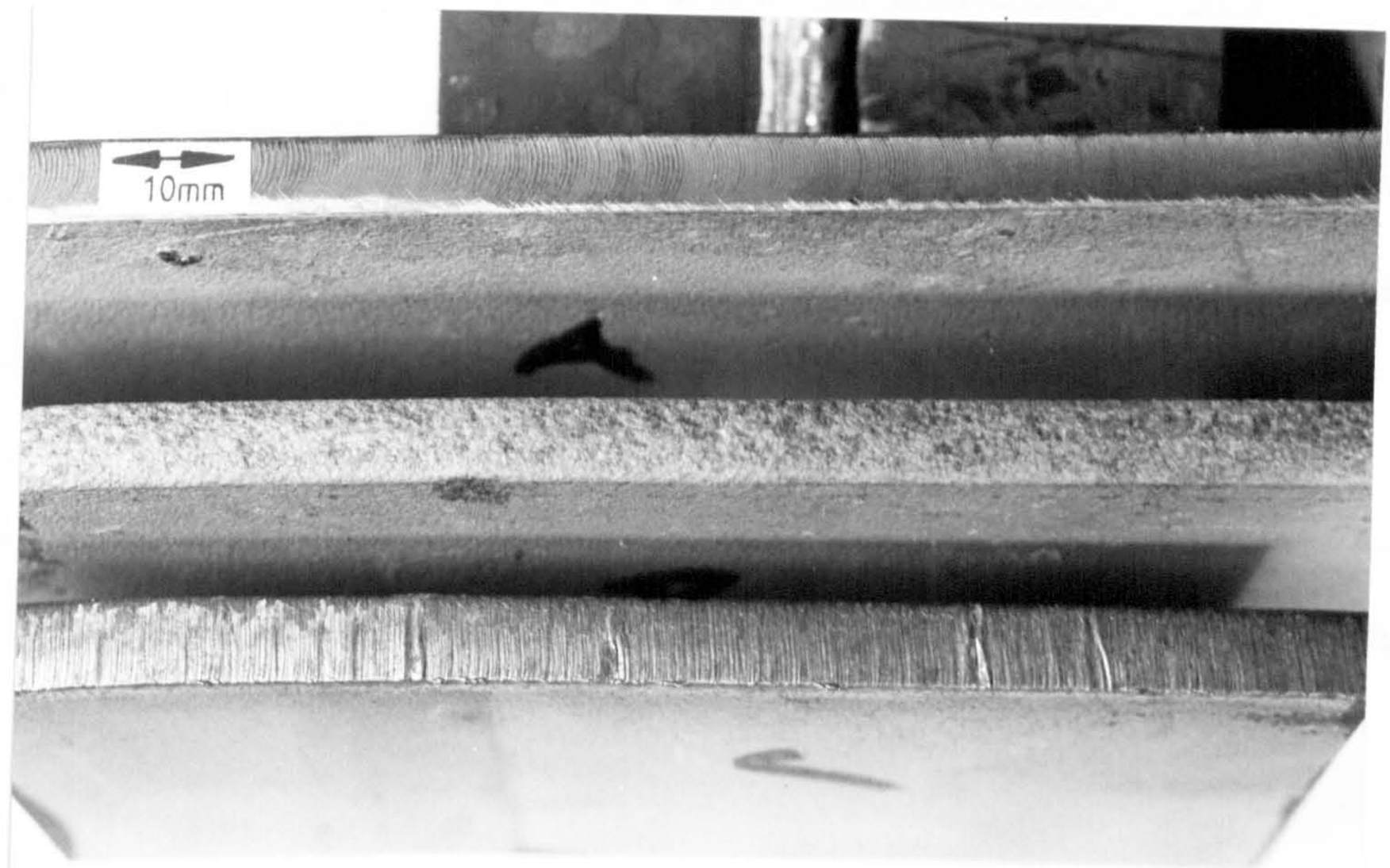

Figure 2.11 - Comparison of idealised and practical butt edges

sag from the emerging bead.

An optimised focus position for a particular plate thickness can be found by the melt run optimisation technique - producing melt runs at varying focal positions and selecting the one which gives the best penetration or weld shape. This is normally expected to be a position between the plate surface and one third plate thickness into the plate.

The control of excess plasma is achieved in the same way as for a melt run by blowing a jet of helium over the keyhole. A weld shroud "shoe" - the traversing unit delivering both the plasma control jet and a general shroud to stop surface oxidation - must give sufficient clearance over the workpiece to avoid collisions with any raised weld bead or tacks. At the same time the shoe must remain close enough to maintain jet pressure and shrouding continuity. A typical welding arrangement is shown in figure 2.12.

Filler wire may be introduced to the weld to control the weld structure by altering the chemical composition of the molten pool; to affect the weld surface shape by compensating for underfill or to produce re-inforced beads; or to counteract the onset of internal "volume" faults such as shrinkage cracks or certain types of porosity. Where the joint gap is greater than the focused beam diameter,the wire is essential for initiating the weld by intercepting with the beam to form the heat transmitting plasma.

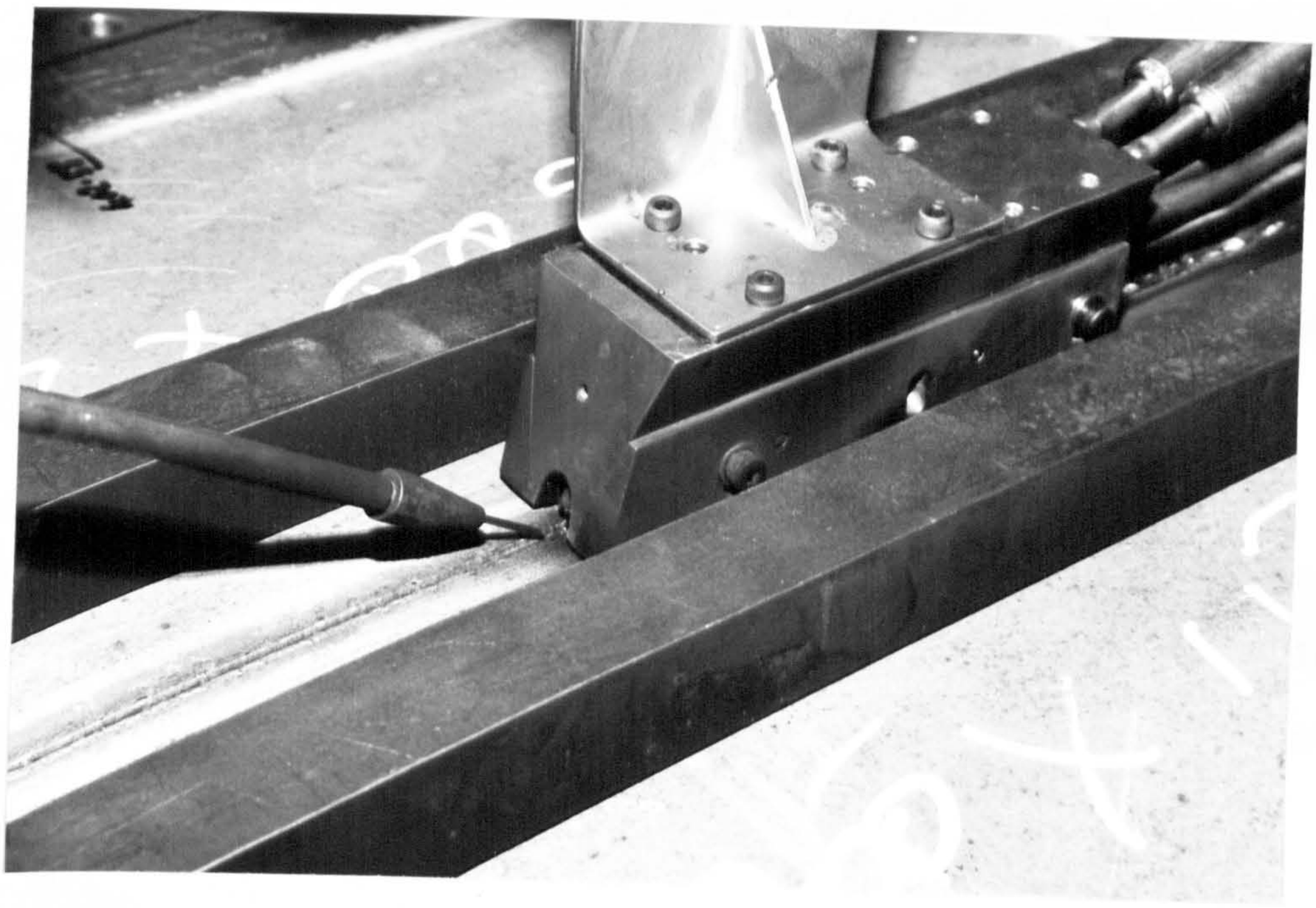

Figure 2.12 - Plasma control shoe positioned for butt welding

Figures 2.13a-b show examples of typical incident and emergent bead profiles for a laser butt weld. The top bead is characterised by a smooth, flat - relative to the normal reinforcement for an arc produced weld - and clean surface. Apart from a thin layer of "soot", formed as a combustion product from the welding process, there is no slag to be removed.

The back bead is comparatively narrower than an arc weld back bead and will tend to sag beyond the plate surface, this bead of material having formed the root envelope of the keyhole. Excessive penetration will result in the bead becoming too large with intermittent globules of material dropping from the main bead line.

The majority of laser welding references limit parameter data to the production of "good" welds. Therefore, the Author has assembled a summary of potential basic weld faults, their reasons and likely remedies as shown in table 2.02.

2.4.2 Laser Through-Weld

When the principal axis of the laser keyhole lies perpendicular to a joint discontinuity the resulting weld can be termed a "through-weld". The incident beam is directed perpendicular to the surface of two overlapping plates - the lower plate can have either its edge or surface butting to form a lap joint. The keyhole then penetrates through the top plate into the second plate, the solidified material between the surfaces

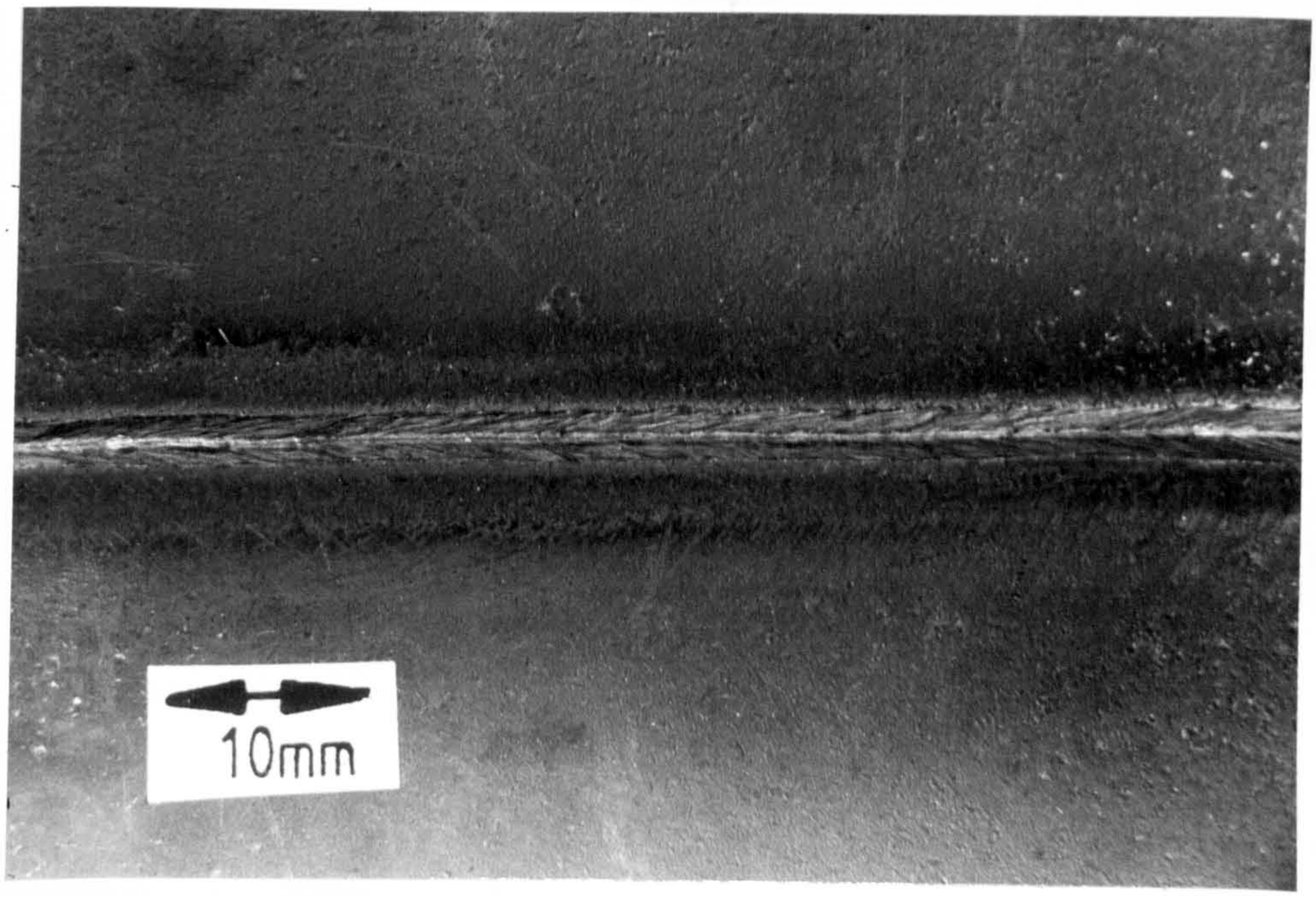

Figure 2.13a - Laser butt weld top bead surface profile

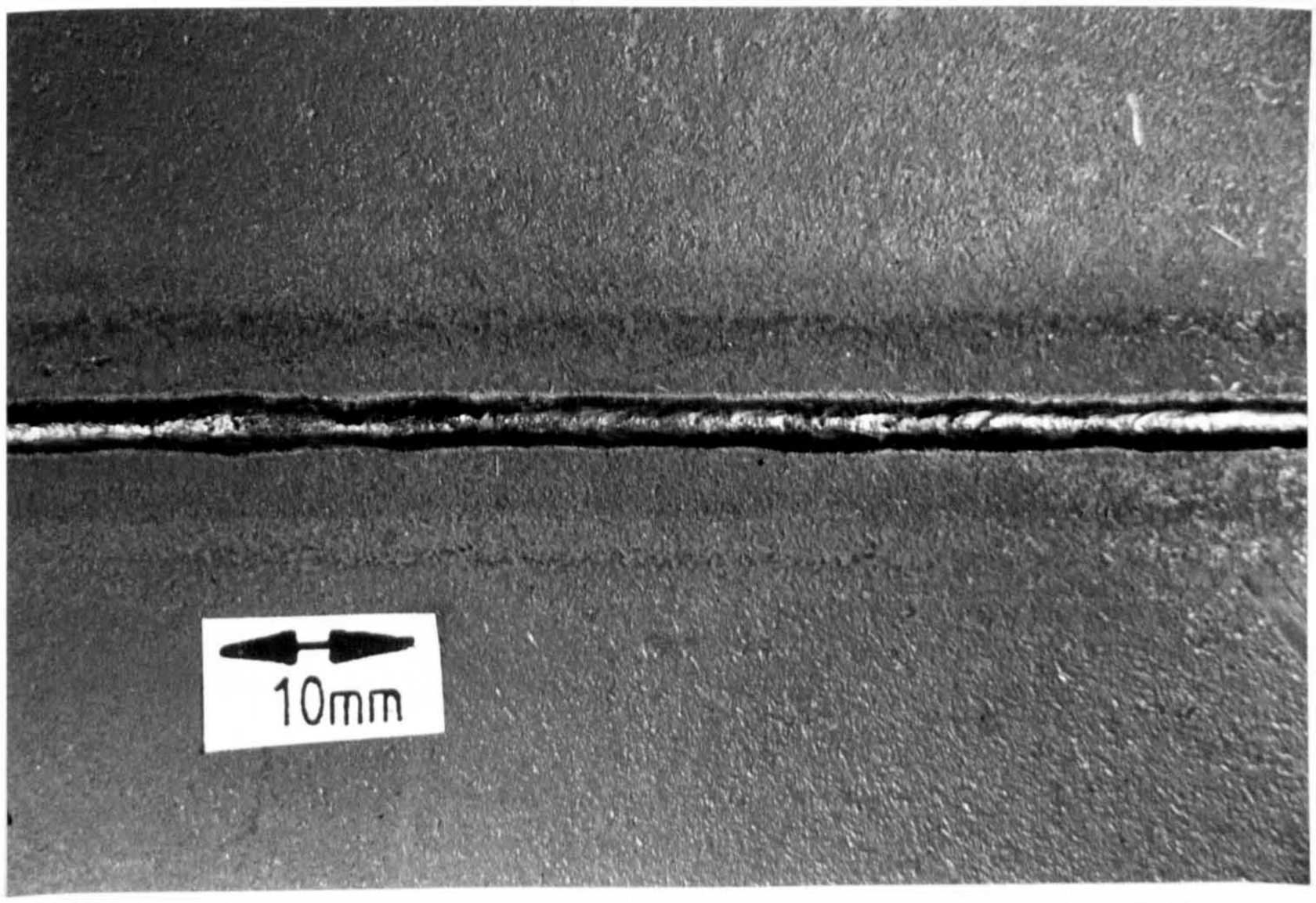

Figure 2.13b - Laser butt weld under bead surface profile

Fault	Reason	Remedies
Lack of penetration	1.Insufficient heat input	1.1 Increase incident power 1.2 Reduce traverse speed
	2.Too much energy absorbed nearer plate surface	2.1 Optimise height of focus 2.2 Optimise plasma control 2.3 Reduce filler input at surface
	3.Excess plasma above plate	3.1 Optimise focus 3.2 Optimise plasma control 3.3 Increase speed slightly
Excess penetration	1.Excess heat input	1.1 Reduce incident power 1.2 Increase traverse speed
	2.Molten pool/keyhole not absorbing sufficient energy	2.1 Increase wire feed rate 2.2 Defocus incident beam 2.3 Reduce plasma control slightly
Underfill	1.Insufficient joint material	1.1 Increase filler rate 1.2 Reduce traverse speed
	2.Excessive weld sag/ underfill at incident side	2.1 Increase traverse speed 2.2 Reduce plasma control 2.3 Defocus incident beam
	3.Lack of penetration/ underfill at the emergent side	3.1 As for "lack of penetration"
Undercut	1.Same as noted for "underfill"	1.1 As for "underfill"
	2.Excess heat input	2.1 Increase traverse speed 2.2 Reduce incident power 2.3 Increase filler rate
Lack of side wall fusion	1.Molten pool/keyhole not centred in joint-lack of fusion to one side	1.1 Align incident beam with joint centreline 1.2 Align plasma control jet with laser/joint centre line
	2.Joint gap wider than focused incident beam	2.1 Use filler wire as a beam interceptor to initiate process 2.2 Defocus beam
	3.Molten zone/keyhole not wide enough at a particular depth of penetration	3.1 Reduce the traverse speed 3.2 Increase incident power 3.3 Defocus or use beam spinning techniques

Table 2.02 - Potential laser butt welding faults, reasons and remedies

Fault	Reason	Remedies
Excessive reinforcement	1.Too much filler input (top bead)	1.1 Reduce filler rate
	2.Excessive penetration/ sag(Emergent bead)	2.1 See excess "penetration" and "underfill"
	3.Lack of penetration (top bead)	3.1 See "lack of pen."
Centreline cracking	1.Chemical composition of plate	1.1 Use filler wire with a composition to counter-act plate inadequacies
	2.Molten zone too large for a given joint restraint	2.1 Change filler input to give a lower cracking potential 2.2 Multipass joints
	3.Molten pool cooling too quickly	3.1 Change filler compost'n 3.2 Increase heat input
Porosity	1.Chemical composition of plate or filler	1.1 Use filler wire to counter plate inadequacies
	2.Inadequate or excessive plasma control	2.1 Optimise plasma control
	3.Unbalanced power intensities	3.1 Optimise heat inputs for the joint size 3.2 Optimise beam focus characteristics
	4.Joint preparation inadequate	4.1 Reduce impurities going into the joint eg from paint, grease etc
	5.Shielding gas incorrect	5.1 If not helium, check suitability 5.2 If helium, check purity. 5.3 Check that shielding is not being entrapped in weld pool
	6.Beam stability	6.1 Check for power, mode or directional variation

Table 2.02 continued

forming the joint.

As for the butt welds idealised conditions exist when the joint is perfectly clean and close fitting. Similarly, weld characteristics change as joint conditions deteriorate.

Plasma control can be achieved with a typical butt welding shoe as the top plate surface remains flat. Inherently the control of plasma will also affect weld cross-section, thus the gas jet could also be used to optimise the weld profile e.g. to obtain maximum width at the joint line.

Welding through a joint gap presents a slightly different problem. As the incident beam interacts with the solid top plate the initial part of the keyhole will be formed. At the joint gap, continuation of the keyhole will depend on the stability of the surrounding molten pool. If there is insufficient material dropping from the top plate to bridge the gap i.e. the keyhole will become open ended. The residual beam energy would then become defocused reducing the power density and the potential for re-penetration into the second member of the joint. By either increasing heat input or introducing filler material into the joint, the amount of available molten material can be increased, and a satisfactory weld profile maintained.

Alterations in the height of the focal positions could be used, like plasma control, to modify the weld profile. If maximum penetration is not the prime objective the focal height could be changed to modify the

weld aspect ratio. The limits on lateral beam movement are set only by the lap zone unlike the higher accuracy required to follow a butt line.

This type of joint is of particular interest when access is precluded to the back side of a lap joint, or a one sided production efficient joint is required. For these reasons the joint has been employed in the construction of "sandwich structures", both by using Nd-YAG lasers for work in thin sheet steel [53] and more recently using CO2 lasers for shipbased forms [88] .

2.4.3 Laser Keyhole Welds with Reinforcement or Smoothing Bead Additions

For "butt" and "through" welding the deep penetration property of keyhole welding is fully utilised. By comparison conventional welds used in ship construction often depend on the fusion of a fillet or large quantities of filler material adjacent to the joint. Deep penetration - other than that caused during the fusion process - is only achieved by preparing joint edges so that the infill and reinforcement material can be laid along the prepared and in-set edges.

By introducing filler material to a laser keyhole weld at a rate in excess of that required solely to fill a joint gap a smoothing bead or reinforcement can be deposited. For the fully penetrating butt weld the excess material could sag to the emergent side but for a blind keyhole weld the bead will build up behind the keyhole mouth producing a "keyhole reinforcement".

For appropriate joints, figure 2.14, in addition to penetration to the depth of the keyhole, a smoothing bead can be laid along the joint surface. Similarly, consecutive beads could be laid if large quantities of in-fill were necessary.

While this type of joint can be made under the idealised conditions already noted, the reinforcing beads formed are negligible. So to enable the joints to be reproducible under present shipbuilding fit-up criteria, the use of filler wire will be essential.

Plasma control would be achieved as for melt runs though the shoe would have to be designed to fit the relevant joint type. With excess filler being introduced to the mouth of a non penetrating keyhole, control of gas flow rates need assessing carefully to avoid plasma build-up above the joint. Similarly the shoe stand-off must give sufficient clearance to avoid contact with the formed bead.

2.5 LASER SKID WELDING

For the melt runs, butt and through welds described the incident laser beam was assumed to be perpendicular to the plate surface. For producing the keyhole weld with smoothing beads in a tee joint, the beam has to be introduced to the joint at an angle for the fusion zone to intersect both web and face plates. A specialised joint, combining the technology of both keyhole reinforcement, fully penetrating butt joints and through joints, the skid weld is produced when the incident angle made with the

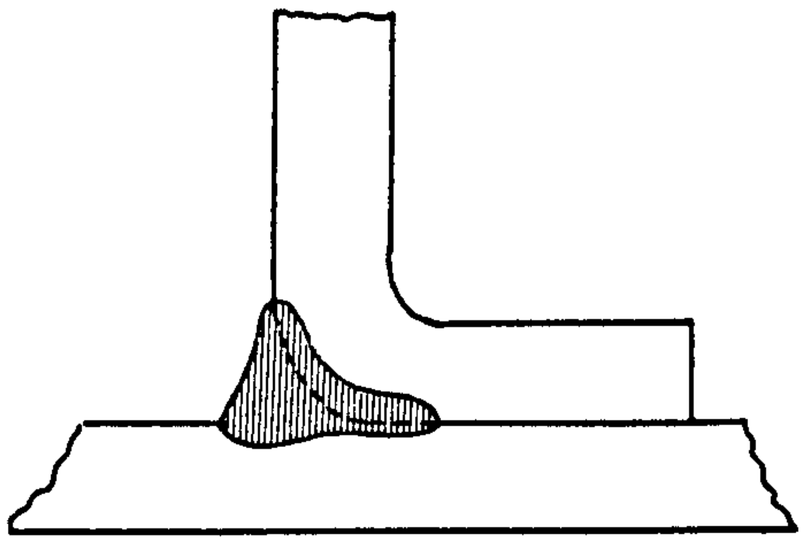

Angle bar T butt joint

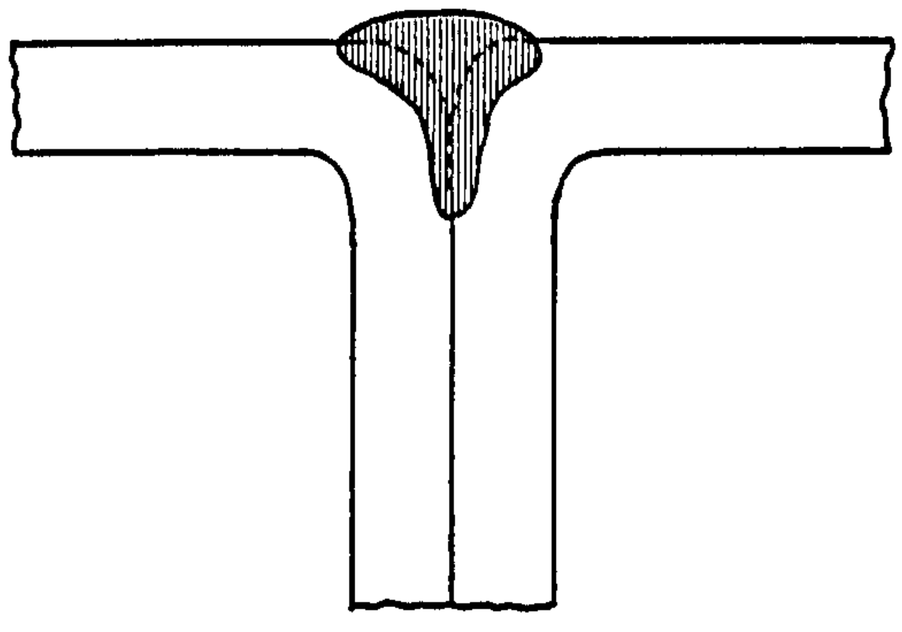

Flared T joint

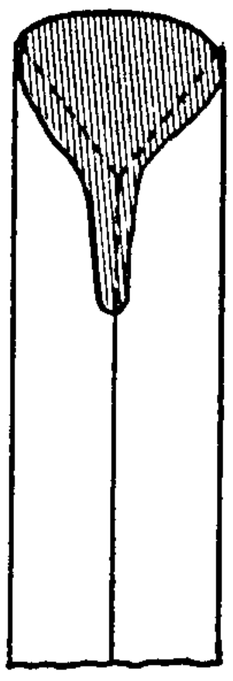

Lap edge joint

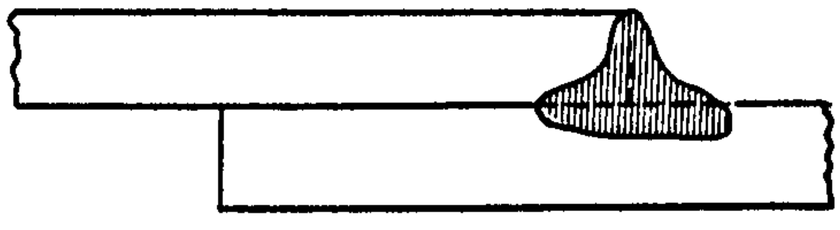

Lap fillet joint

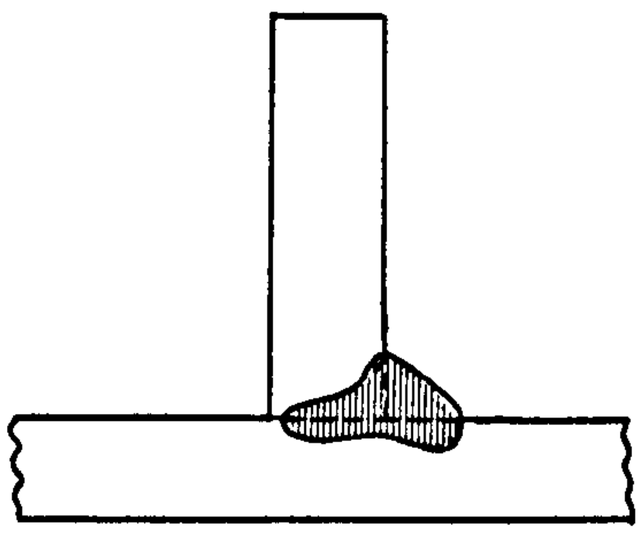

T butt with a single smoothing bead

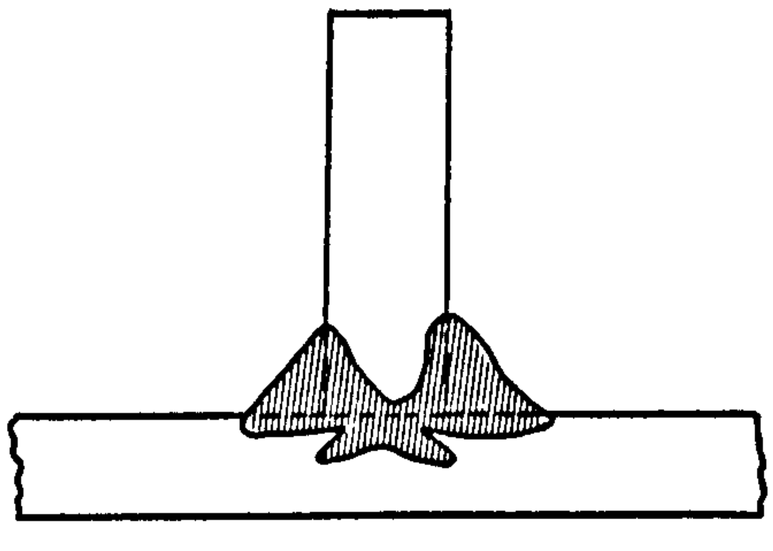

T butt with twin sided smoothing beads

Figure 2.14 - Laser keyhole welds with smoothing beads

face plate is minimised together with sufficient heat input for the keyhole produced fusion zone to be fully penetrating through the complete web thickness. To ensure joint integrity, smoothing beads will be required on both the incident and emergent sides of the joint. The term "skid weld" is thus derived from the representation of the laser beam "skidding" along the joint line of the face plate and web edge.

2.5.1 Principal Parameter Assessment

The skid weld, like the principal weld configurations, can be considered as a melt run with discontinuities. Therefore depth of penetration and consequently the thickness of web which can be joined is, a function of laser power and traverse speed.

Ideally, maximum penetration would be achieved if the keyhole was formed perpendicular to the web surface although in practice with a converging beam, there is a limiting angle to which the beam may be lowered towards the face plate before it impinges with its surface. Assuming a minimum angle, there will be an optimum height of impingement on the web plate to ensure fusion at the emergent end as opposed to the beam burying into the plate surface. Similarly if the beam is too high, lack of fusion could occur at the incident end or ultimately along the complete joint when a simple melt run would be formed in the web plate.

Beam positional limitations can therefore be considered for a particular joint/laser configuration, figure 2.15.

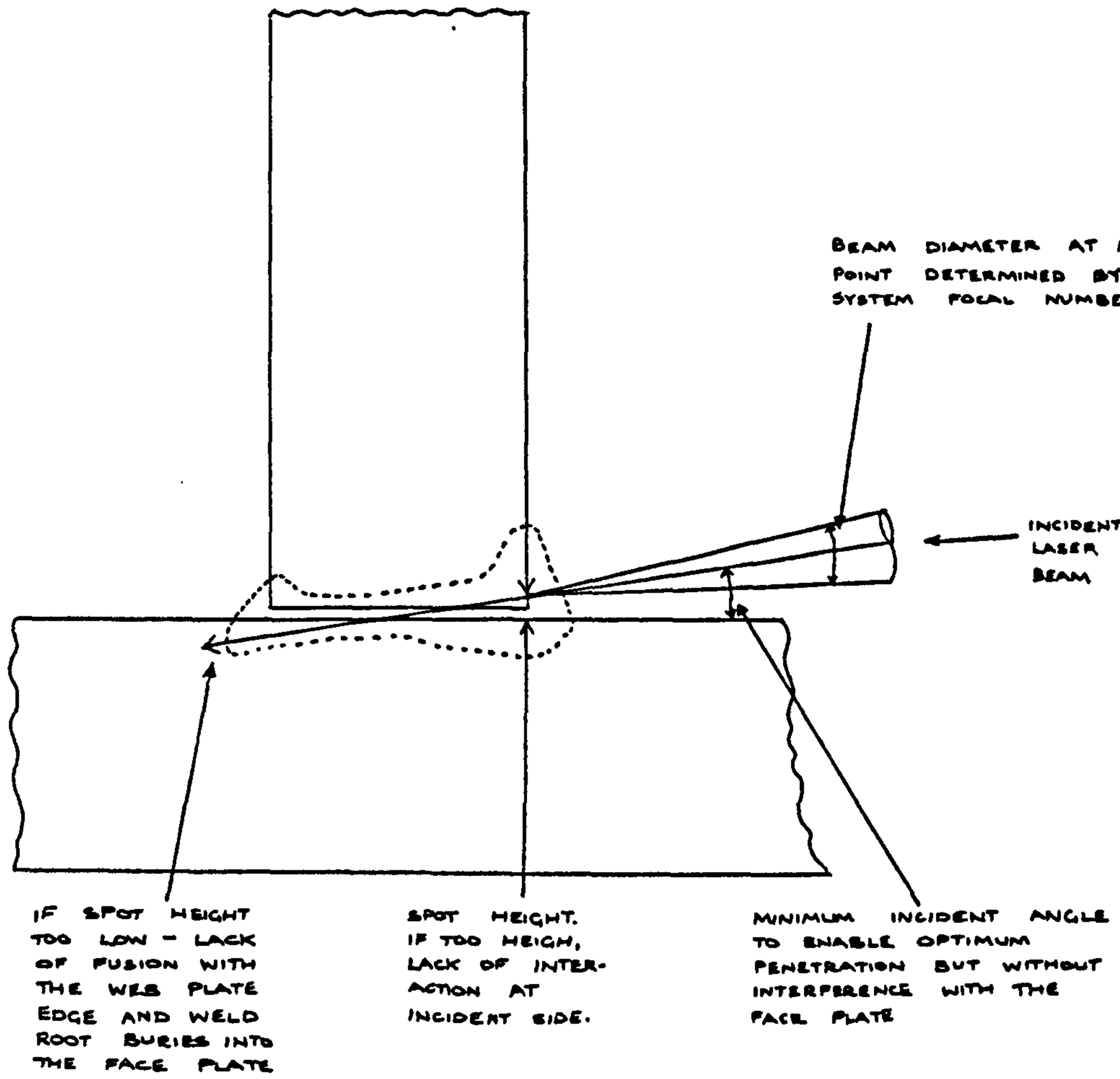

Figure 2.15 - Limiting beam positional considerations for skid welding

2.5.2 Plasma Control Requirements

The principles of plasma control for skid welding are similar to those for butt welding though the carrying shoe must be designed to fit the joint giving clearance to both the face plate and web.

Unlike butt welds, when control gases can escape to either side of the shoe , the skid web formsa funnel for the gas flow so that values of gas flow used for butt welding may not necessarily be the same for skid welding.

With the need to optimise spot height for a given incident angle, movement of the directional gas jet could be necessary, independently of the shoe height, so that the jet could be directed to the spot height chosen.

2.5.3 Filler Requirement

Again, satisfactory autogenous skid welds are only achievable with an idealised joint when no reinforcing bead is required. Hence in practice skid welds produced to shipbuilding requirements will need a filler input, both to form a satisfactory profile and where necessary to act as a beam interceptor.

Filler rates should be relatable to the joint gap and size of the beads produced on both incident and emergent sides. There could be a

limit to the amount of filler that can be fed into the joint depending on the rate of melting. For the emergent bead there will also be a dependence on the rate of transfer of molten material along the keyhole, i.e. the further the filler can be directed towards mid-plate thickness, the more even the filler distribution.

2.5.4 Laser Skid Welding - Summary of D.R. Martyrs Trials and Conclusions

In practice, the majority of Martyr's successful welds in tee section joints were dual sided keyhole welds with smoothing beads, the welds overlapping in mid-plate thickness to form a tee butt type joint. A small number of single pass fully penetrating skid welds were produced to show the potential of forming such a joint. Whilst the laser remained in the vertical position his samples were aligned to the laser as shown in figure 2.16a. An incident angle of 7 degrees was used for single pass welds where gaps of 1.5mm were joined and 13 degrees was used for dual pass welds where gaps to 3.4 mm were joined using the "interceptor" technique.

Welds were made on 6mm plate using about 4.5kW at the workpiece. Repeatability of incident bead (hence both beads for dual pass) was good. Very few single pass welds had reported good emergent beads with concentration solely on penetration.

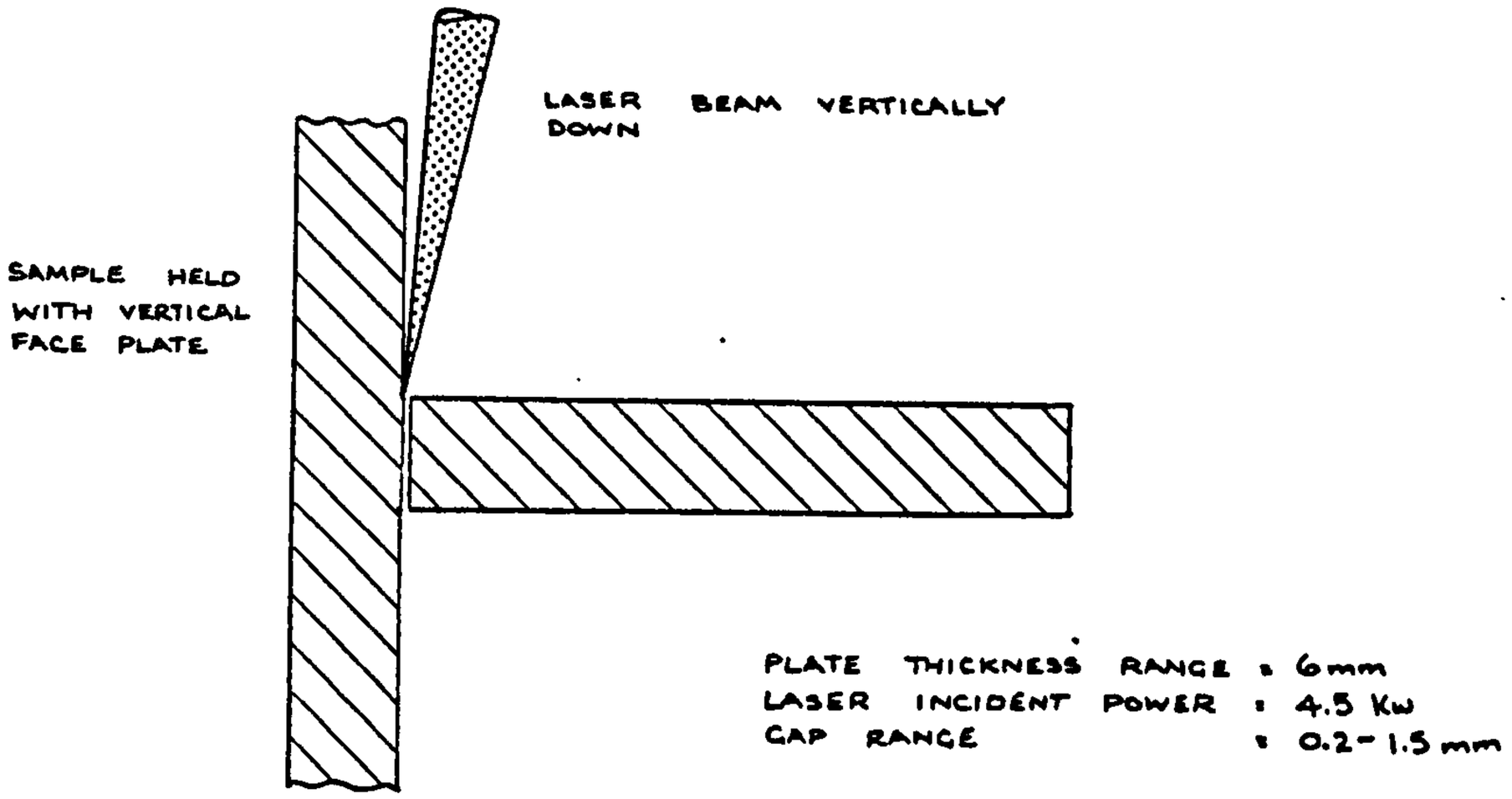

Figure 2.16a - Laser to sample orientation for Martyr's work

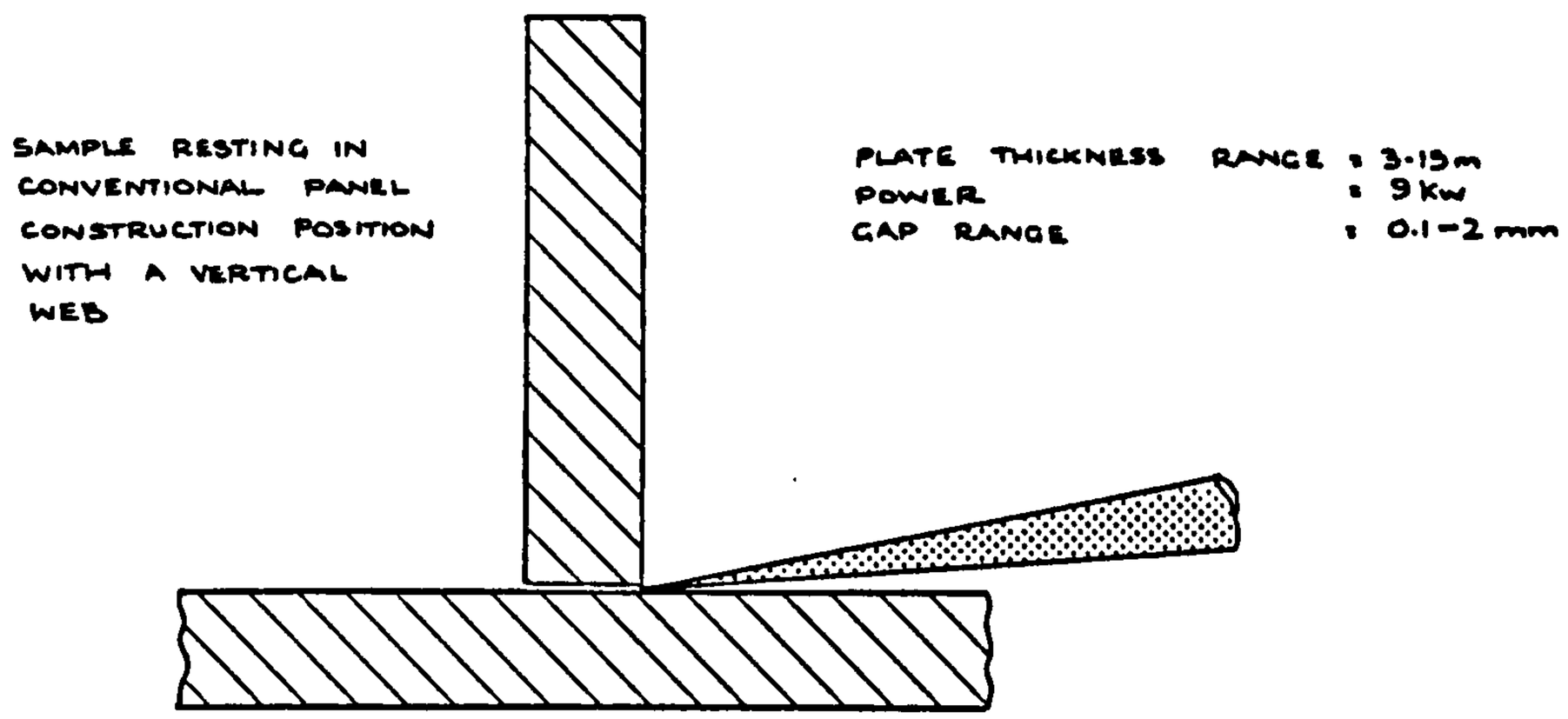

Figure 2.16b - Laser to sample orientation for Brooke's work

Painted joint surfaces did not appear to have any adverse effect on the resultant weld appearance though Martyr noted an increase in sparks emerging from the joint. He concluded that the paint seemed to be ejected from the bottom of the keyhole.

2.5.5 Laser Skid Welds - Review of Recent Literature

In comparison with plain butt joint laser welding, there are few references to the welding of tee joints. The majority concentrate on dual pass, double sided welds [23] [2] [89] [90] [91] [92] [93] [21] [24] [25] [94] [95] and only a few refer to single pass skid welds [23] [96] [97] . Many suffer by not giving the sample orientation or weld with a near vertical incident laser beam, as investigated by Martyr. Few refer to the use of filler wire.

Dawes et al [96] [93] give useful guidance on welding parameter settings though they have restricted their work to materials of 4mm thickness and 6kW laser power, without the use of a filler material. Welds were examined on a visual and macro basis but no mechanical tests were conducted to assess the weld characteristics.

Banas and Peters [23] provide basic parameters used both for double sided and a limited number of single sided skid welds on close fitting prepared joints. However, for structural acceptance, only one bend test result on a dual pass weld has been reported.

Hakansson [24] [25] presents the most evidence of testing the characteristics of tee joints welded by laser with a filler input. However these were all dual pass, double-sided welds. The tested joints generally compare favourably with a MMA welded control sample.

2.5.6 Laser Skid Weld - Reasons for further investigation in this Weld

The majority of laser welding research has been directed towards butt welds, primarily because of the ease of relating butt weld characteristics to the melt run. In fact readers of any laser welding literature should be cautious as to whether an author is describing plain butt or melt run data.

Martyr [3] concentrated on producing and testing plain butt welds to classification requirements and showed only the potential of producing laser welded tee joints.

Within the structure of a ship there are usually at least four times as many tee joint connections as plane butt connections. Hence in any shipyard application, the pay-back period for the same saving per weld length when applied to tee joints will be reduced in comparison to plane butt joints.

At present the majority of tee joints are made using twin fillet welds. Stiffened flat and slightly-curved panels, consisting of a number of butted plates and a lattice of stiffening sections, are produced

either on a jigged slab (predominantly within warship construction), or on an automated mechanised panel line (predominantly within merchant ship construction).

Although dual pass skid welding is becoming an established technique within laser welding research, a one-sided process would give greater flexibility in structural assembly. In addition a one-sided process increases accessibility and, if process speeds and power are balanced, reduce the process heat input and thereby minimise distortion.

For some structural applications welds are made only to seal a joint and do not necessarily add to the strength of a vessel. An example is in the nuclear industry where joints that could be contaminated internally if not welded, must be sealed. In this case a weld is further adding to the likelihood of distortion to a vessel. Similarly for light scantling vessels , e.g. patrol craft, scallops are made on stringers rather than leaving corrosion-raising zones between intermittent welds. A sealing laser weld could replace the need for costly scalloping and labour intensive intermittent welds.

CHAPTER THREE

WELDING TRIALS TO PRODUCE "SKID" WELDS IN TEE BUTT JOINTS

The basic principles of lasers and laser welding have been discussed. This chapter now describes the Author's practical laser welding programme and the necessary pre-requisites. Firstly the trial objectives are summarised.

3.1 OBJECTIVES OF LASER SKID WELDING TRIALS

The overall objective of the Author's work was to produce single-sided, laser skid welds for typical shipbuilding joint configurations, in plate thicknesses of 3 to 15 mm complying with the requirements of classification institutions. Therefore the principal objectives of the welding trials programme were set as follows:

1. Analyse laser welding parameters and their tolerances obtained from experiments to enable an operator to produce satisfactory and repeatable skid welds for typical ship production joint configurations in plate of 3 - 15mm thick with chemical compositions typical of those used in shipyards for building conventional surface vessels.

2. Produce sufficient welds in each joint configuration to enable non-destructive and destructive testing to be undertaken both to compare the weld properties with those required for conventional welds by classification institutions and to understand the effects of

changing welding parameters on the weld properties.

The following secondary objectives were included to detail the "typical" ship production joint configurations:

1. Analyse the effect of welding tee joints made up of plate surfaces and edge finishes, such as primer coatings, found normally in the shipbuilding process.
2. Analyse the effect that typical stiffener edge shape, such as the radius edge of a rolled section web, might have on the skid welding process.
3. Assess the effect of joint gaps on the skid welding process.

So that the maximum benefit could be obtained from trial information a tertiary set of objectives was formed:

1. Collect process parameter data so that procedural limits could be calculated, both to aid the weld property assessment and set workstation machinery tolerances.
2. Observe a typical prototype laser and its associated beam line working under trial conditions to assess factors which might affect equipment reliability when developed in a shipyard environment.
3. Collect working envelope data to be used as a basis for comparative process and economic evaluations.

3.2 PREREQUISITES FOR TRIALS PROGRAMME

3.2.1 Choice and Scheduling of Laser Welding Test Facility

The requirement to penetrate mild steel plate up to 15mm thick in a single pass, dominated the selection of a laser test facility. In addition the following favourable points were considered before approaching the UKAEA Culham Laboratory to investigate the possibility of using their CL10 laser facility for skid welding trials:

1. Continuity in experience of lasers and personnel following upon the work of Martyr.
2. Researcher operation of lasers giving hands-on experience.
3. Capacity and capability for producing the necessary focusing and shrouding equipment.
4. Opportunity to assess the CL10 as a potential design for use on a production panel line workstation.
5. Continuity of research information with topics projected for the Culham Laboratory coordinated Laser Users Club.

The facility, figure 3.01a, comprises the CL10 laser, figure 3.01b - a transverse flow machine with an unstable optical resonator giving a continuous wave output - which is connected to a remote workstation by a 20m beam line. The beam leaves the laser via an aerodynamic output window and is then columnated to compensate for the the natural divergence which would otherwise occur over the delivery distance. Having passed through a set of five beam bending mirrors to the focal

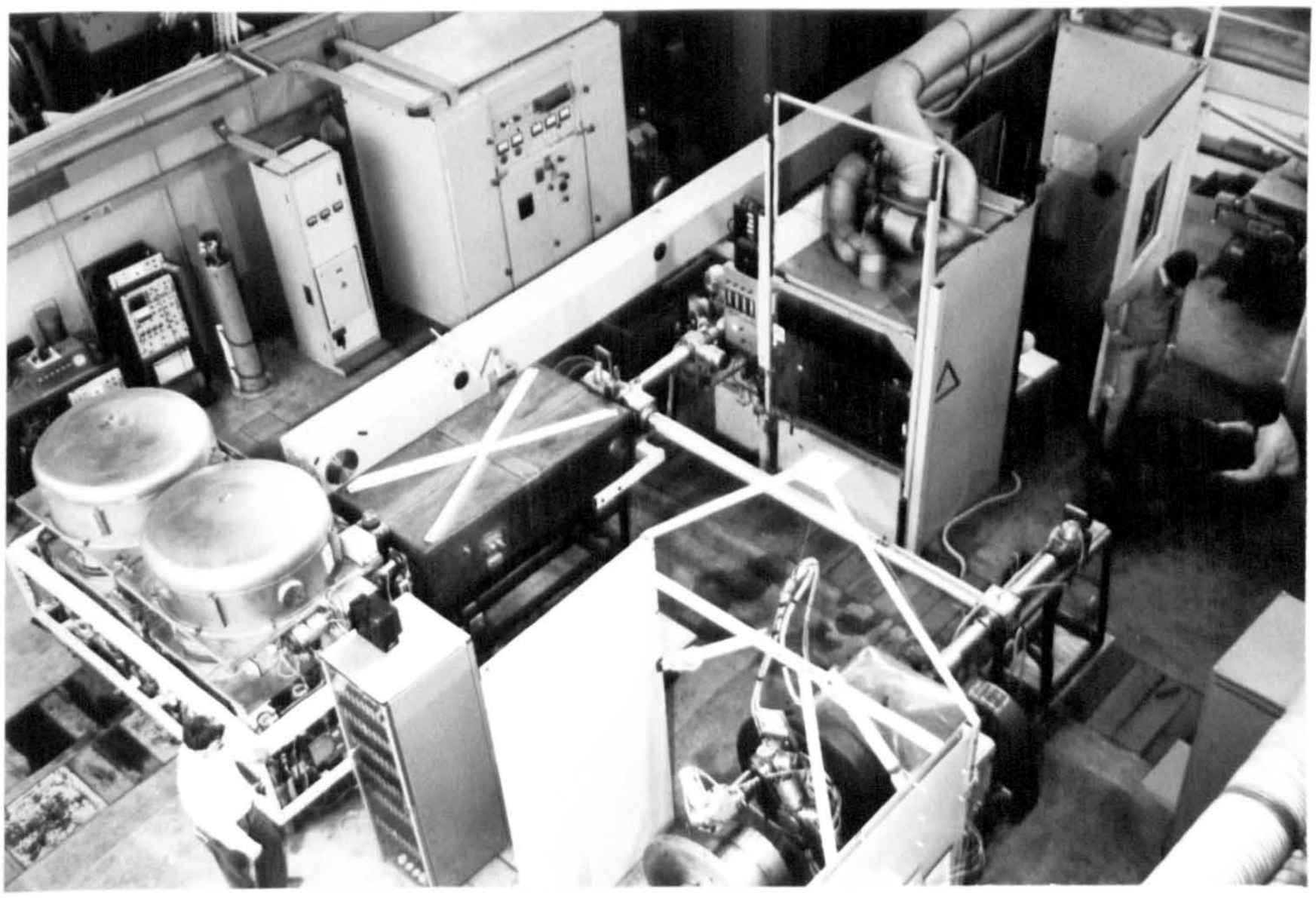

Figure 3.01a - CL10 laser processing facility, UKAEA Culham Laboratory

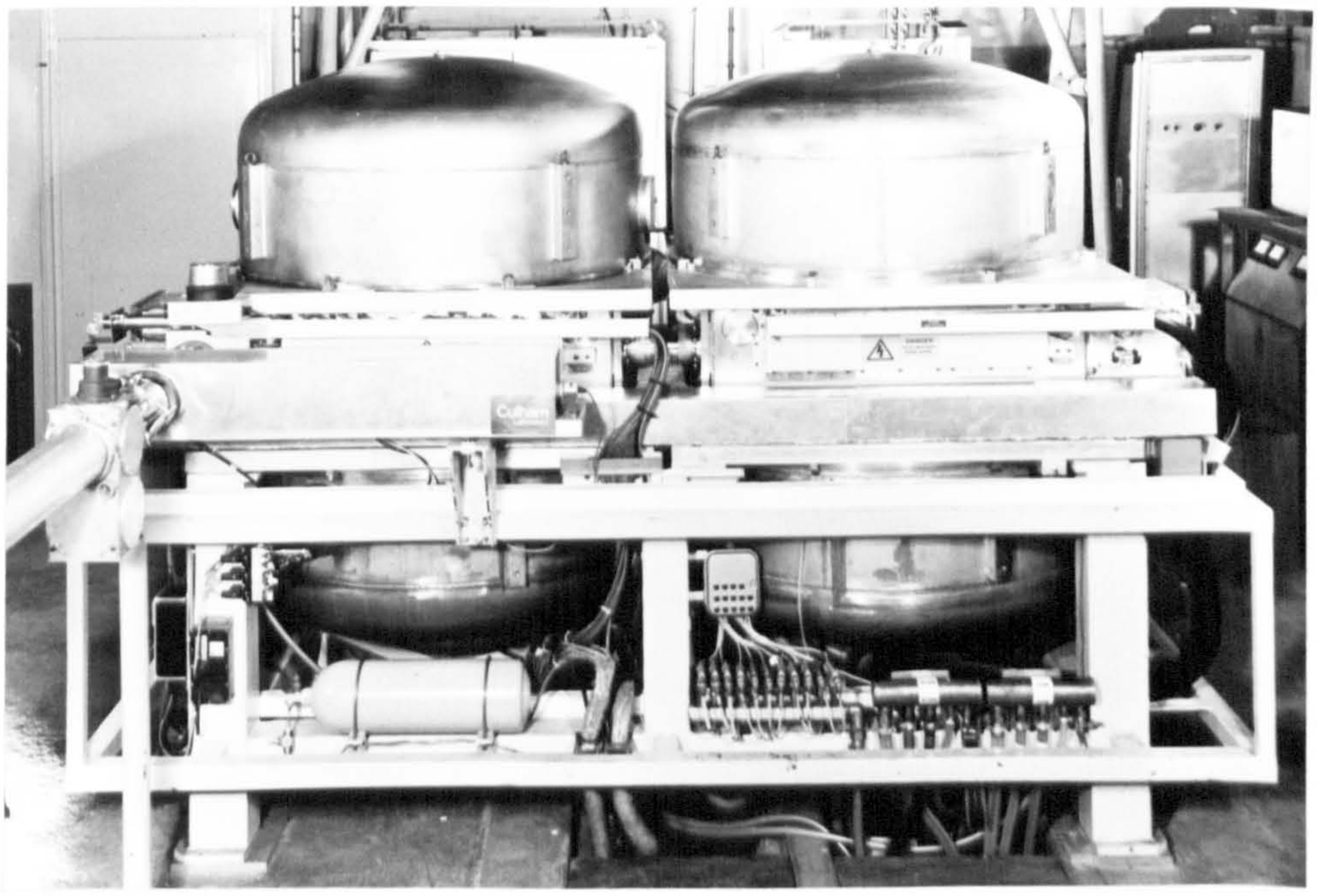

Figure 3.01b - Culham laboratory designed and built CL10 laser

position the beam is directed at the workpiece through a fixed nozzle while the workpiece is traversed, mounted on a Boko machine table.

The option on four weeks of laser time was arranged in advance and the design specifications for a specialised focus unit and shroud unit discussed and decided upon [98] . Specific trial dates were normally finalised one month in advance but this time scale fluctuated to fit around commitments of both parties.

3.2.2 Design of a Focus Unit for Skid Welding

The focus unit generally used with the CL10 laser incorporated an "Off-Axis Spherical" (OAS) focusing mirror geometry with a designed focal length of 300mm. For butt welding the incident beam is projected perpendicularly downwards on to the workpiece surface.

To enable single-pass, tee section skid welding, the focusing head had to be positioned for the incident beam to strike the joint at a shallow angle to the flange plate surface. Therefore the following changes had to be made to the usual focus unit and as shown in figure 3.02a-d.

1. Increase the focal length of the focusing mirror from 300 to 400mm so that the unit could be positioned beside the flange plate for projecting the laser beam at the required shallow angle.
2. Increase the outlet aperture to accommodate the resulting enlarged beam diameter at this point.
3. Facilitate head movement through 90 degrees from the vertical

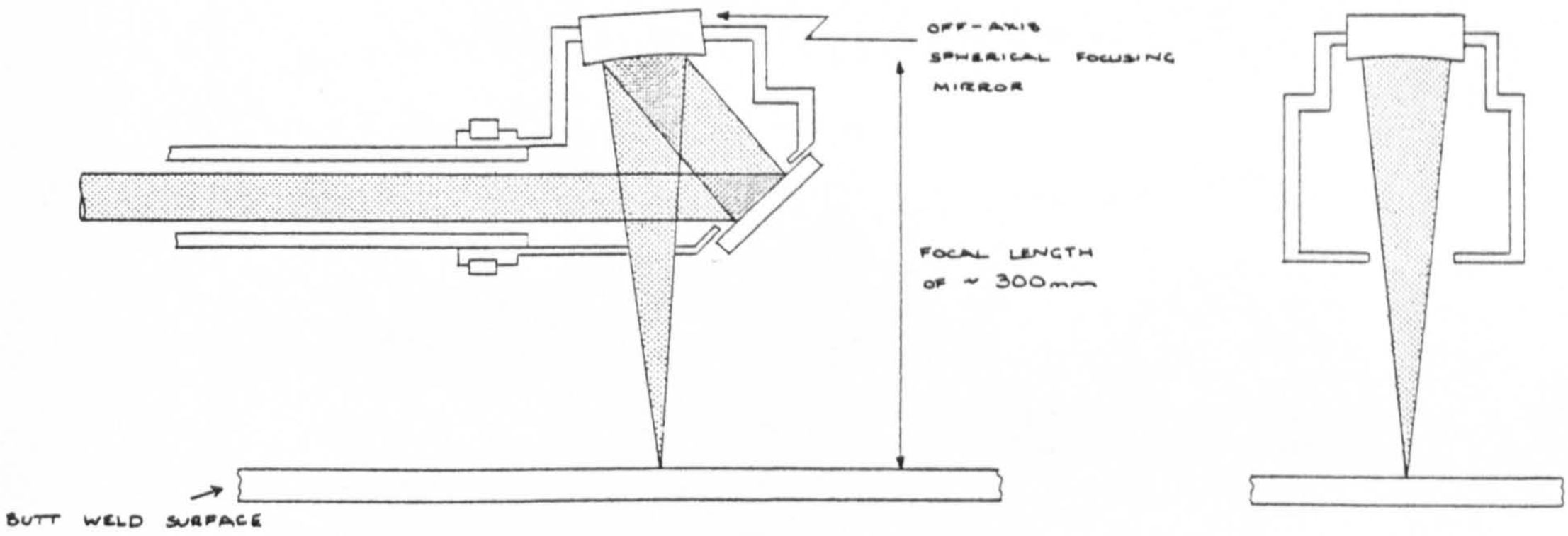

Figure 3.02a - Elevation of the focusing unit used for laser butt welding

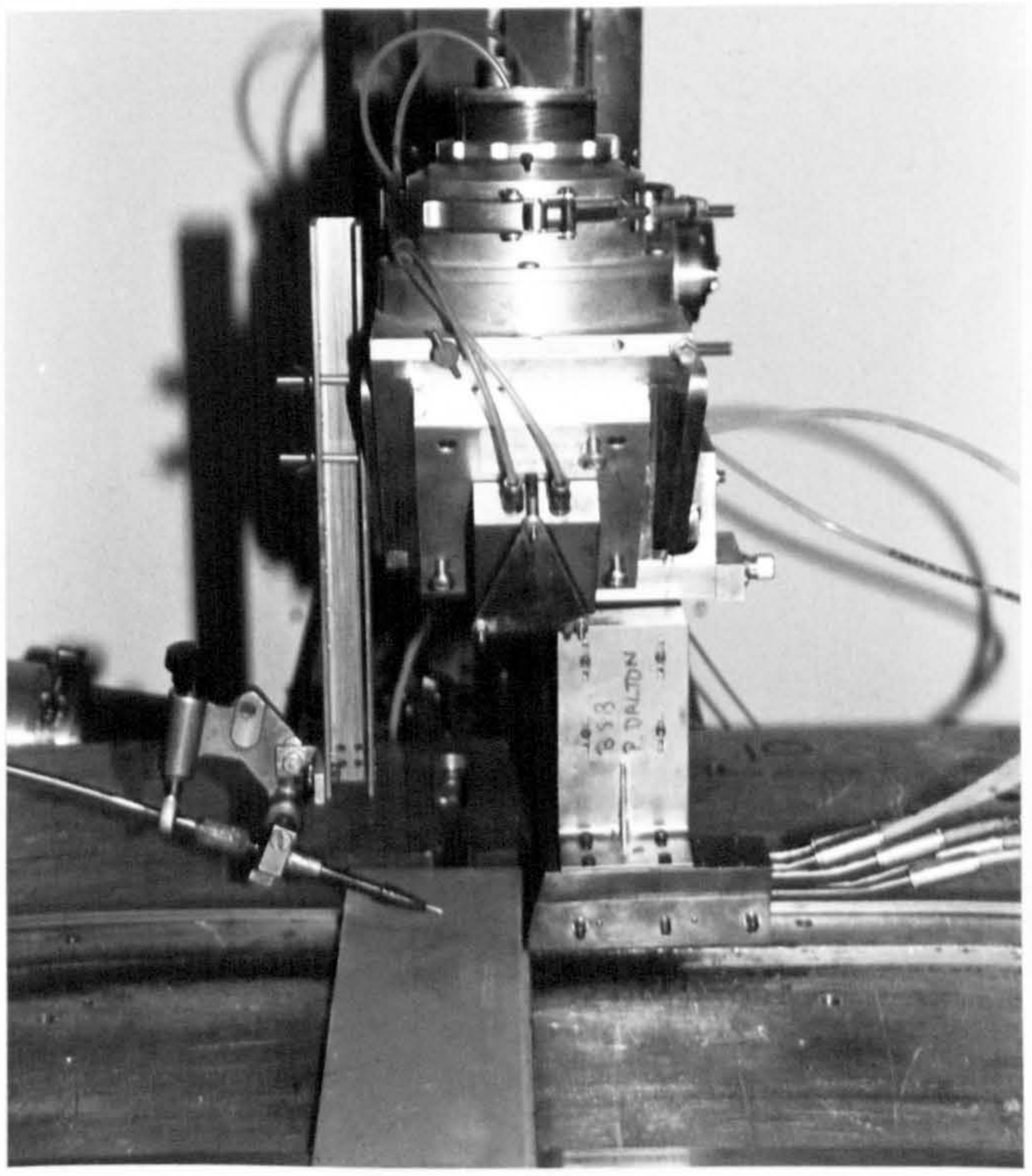

Figure 3.02b - Laser focusing head positioned for butt welding

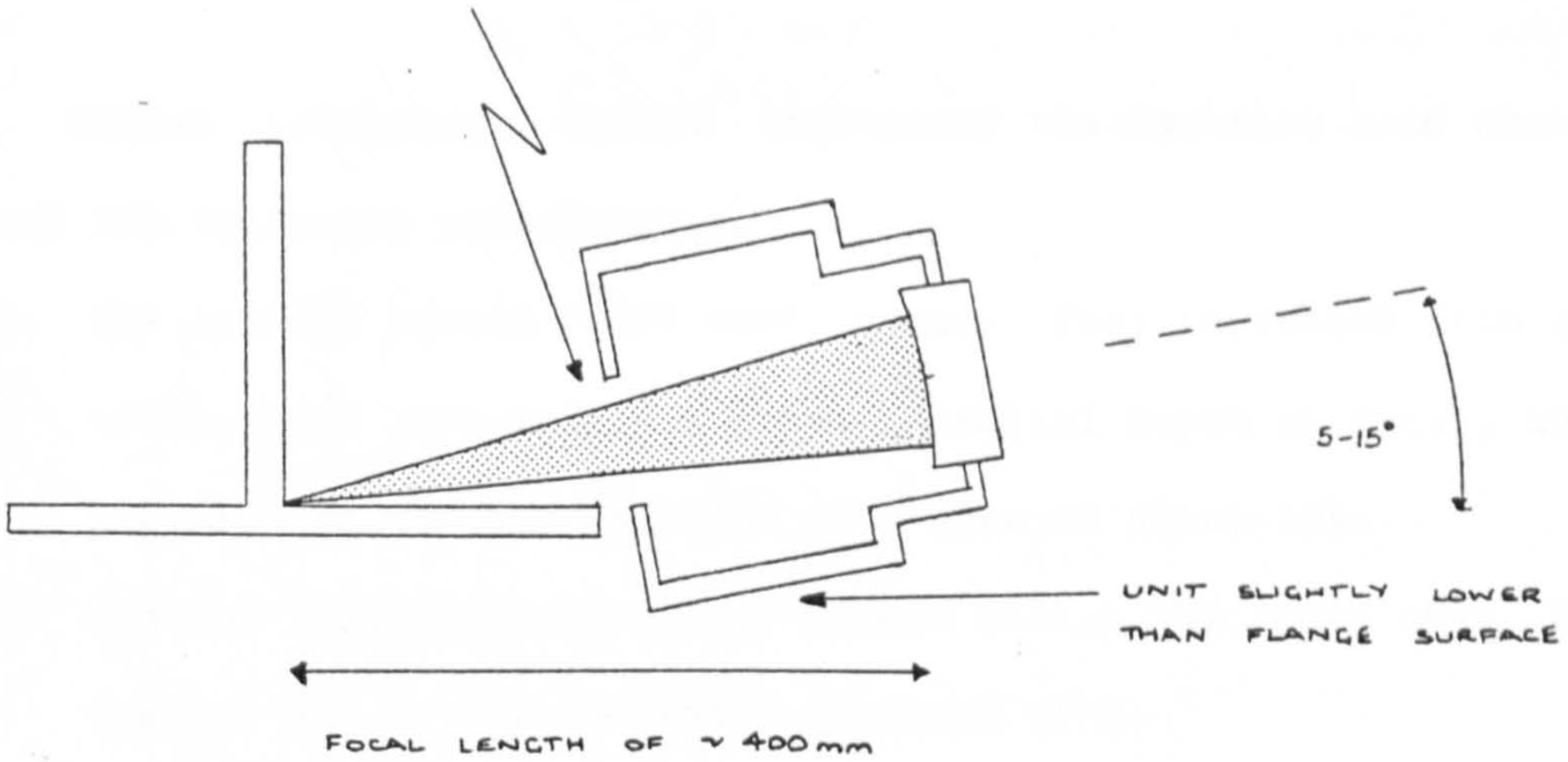

Figure 3.01c - Section of the focusing unit angled for laser skid welding

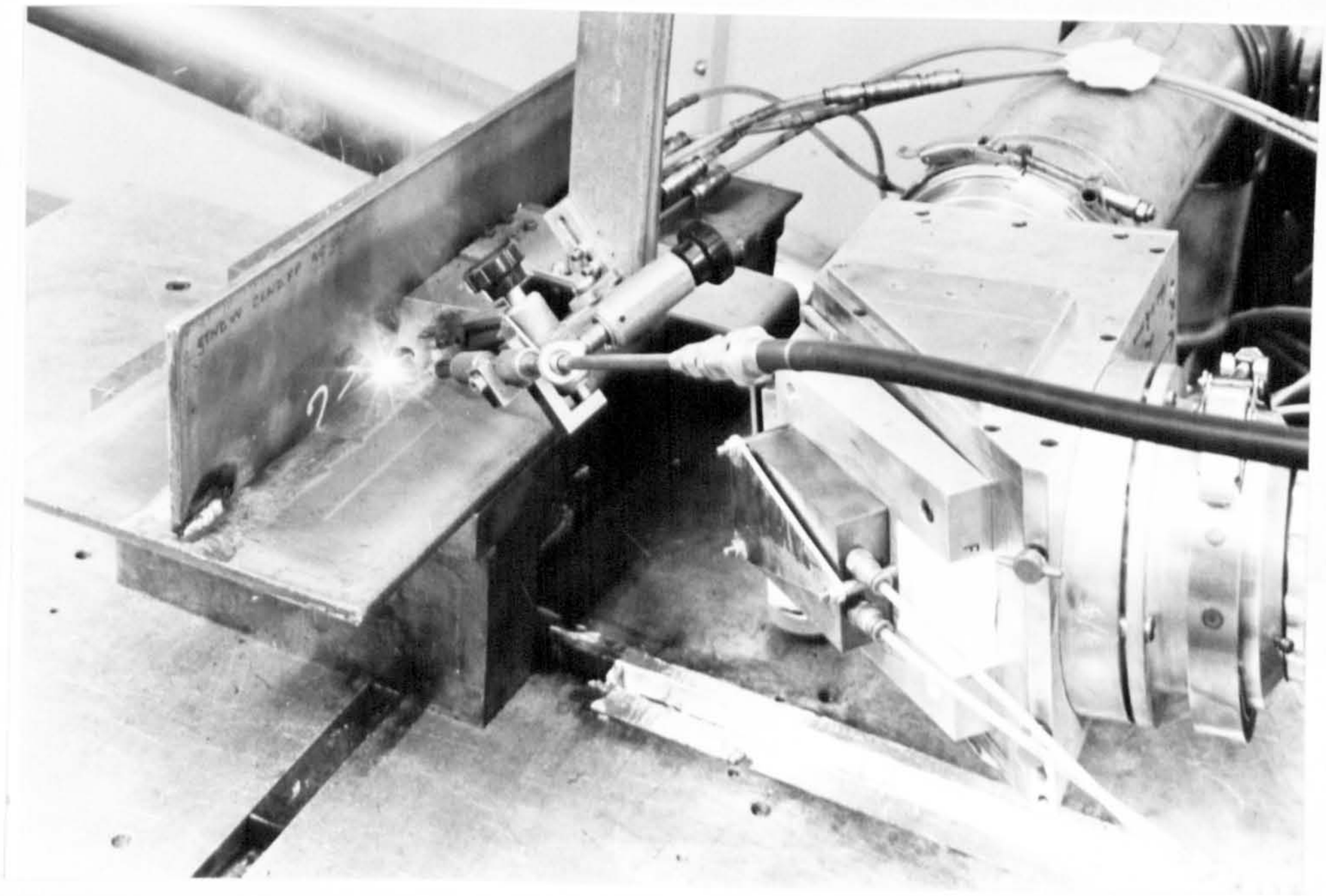

Figure 3.01d - Laser focusing head positioned for skid welding

position.

Culham Laboratory detail engineered the focusing head changes which had the following consequences:

1. The optical system focal ratio number (fno) increased from 8 to 9.5 which gave not only a greater potential depth of focus, but also an increase of the focused blur spot size of about 25%.
2. Greater likelihood of mirror damage within the focus unit from weld spatter due to the increased aperture size.

The completed actual unit proved successful for all the welding trials. A focus unit for a production machine would, however, need to be more compact to be positioned above the flange plate surface and have multiple degrees of freedom. For this a light-weight "Off-Axis Parabola" (OAP) type mirror in a manipulative head could be used.

3.2.3 Design of a Shroud Unit for Skid Welding

The skid welds developed and analysed by the Author were the first of their type to be produced using the CL10 laser. Therefore a suitable plasma control and shroud unit was required, taking into consideration the following criteria:

1. The shroud should comprise a plasma control jet, lens and trailing shroud similar to those used for butt welding, the jet and lens being directed into the joint of the web and the flange plate. Also the jet should also be easily replaceable to enable changes or

de-blocking.

2. The shroud should be able to withstand the heat radiation produced within a working distance of the 10kW beam and plasma formed at the joint. It was therefore to be made of copper and incorporate a water cooling system.

3. It should be capable of traversing adjacent to a tee section joint with the beam being introduced at an angle of between five and ten degrees above the flange plate, leaving adequate space for a weld leg length of 5mm or tackweld to form in the joint.

4. It should incorporate a means for enabling easy positioning accuracy to +/-0.25mm

The resultant shroud unit, figure 3.03 was used for all of the Author's tee section welds. It incorporated Culham Laboratory's existing shroud technology but had the gas outlets angled to correspond to the joint configuration.

However, by the the time of the second trial the Author observed that skid welds could be achieved without the use of the plasma control jet which tended to cause a disruption of the incident bead surface. This was possibly due to the funnelling effect caused by the joint configuration concentrating too much gas over the keyhole and disrupting the plasma stability.

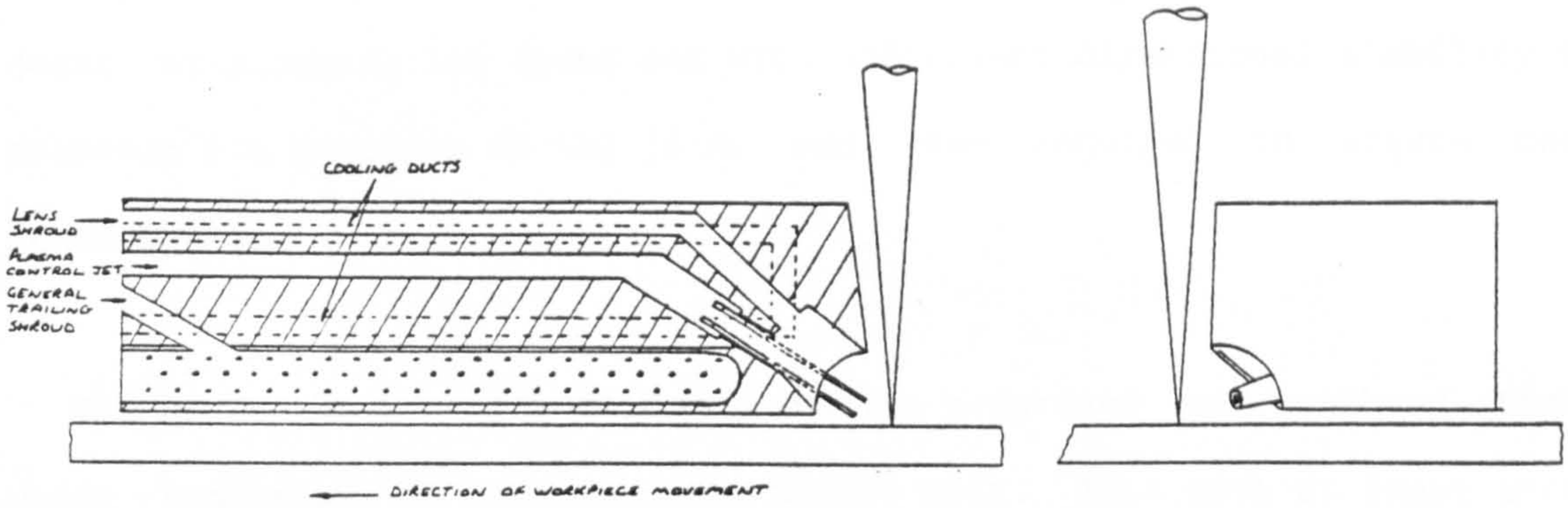

Figure 3.03a - Elevation of the skid welding shroud unit showing gas flow and cooling ducts

Figure 3.03b - Skid welding shroud unit with it supporting bracket

3.2.4 Wire Feed Unit Design

A wire feed device was required to supply filler material into the joint at a controlled speed and with sufficient directional stability to maintain its position in the joint and when required to ensure beam interception.

The arrangement in the CL10 workstation comprised an overhead frame which supported an articulating nozzle unit. This gave at least three degrees of movement for fine positional accuracy. The wire, usually a double-deoxidised mild steel type of diameters 0.9,1.0,1.2 or 1.6mm, was fed to the nozzle via a flexible cable from a standard MIG welding type drive unit [99] as shown in figure 3.04a. This enabled a large range of wire feed rates, from 10 to 200 millimetres per second. The unit could be controlled either locally at the drive unit or remotely for setting up and for controlling welding operations from outside the workstation.

The articulating nozzle arrangement, figure 3.04b, comprised a delivery tube with a replaceable end nozzle piece which could be slid towards or away from a target position. Horizontal and vertical axis screw adjusters could then be used for fine aiming of the nozzle at the required spot. If any large movements were necessary the supporting frame had to be adjusted.

To ensure the consistency of wire feed rates the drive unit and feeder cable were positioned to give the largest possible radius of curvature in

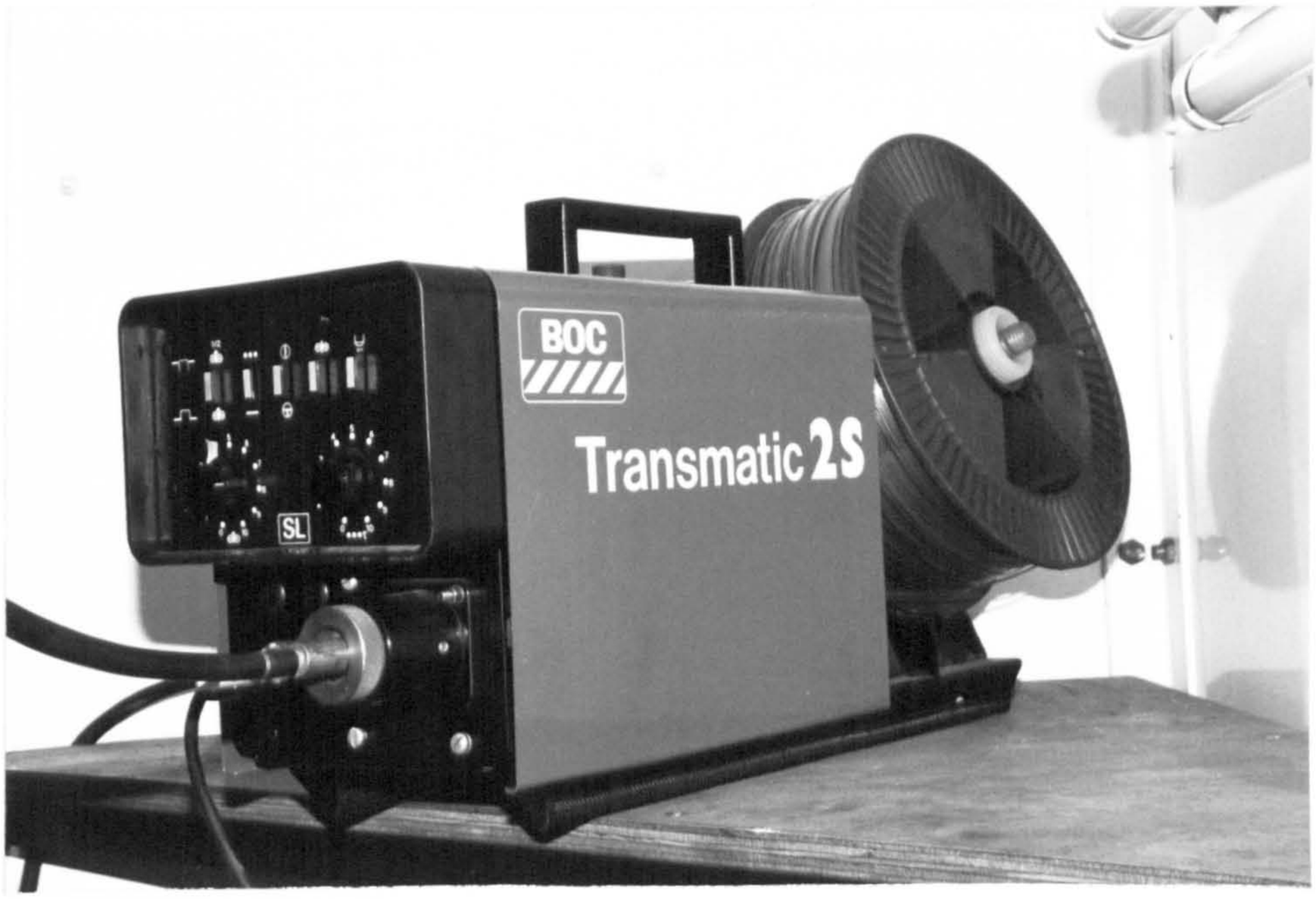

Figure 3.04a - MIG welding wire feed drive unit used for the skid welding trials

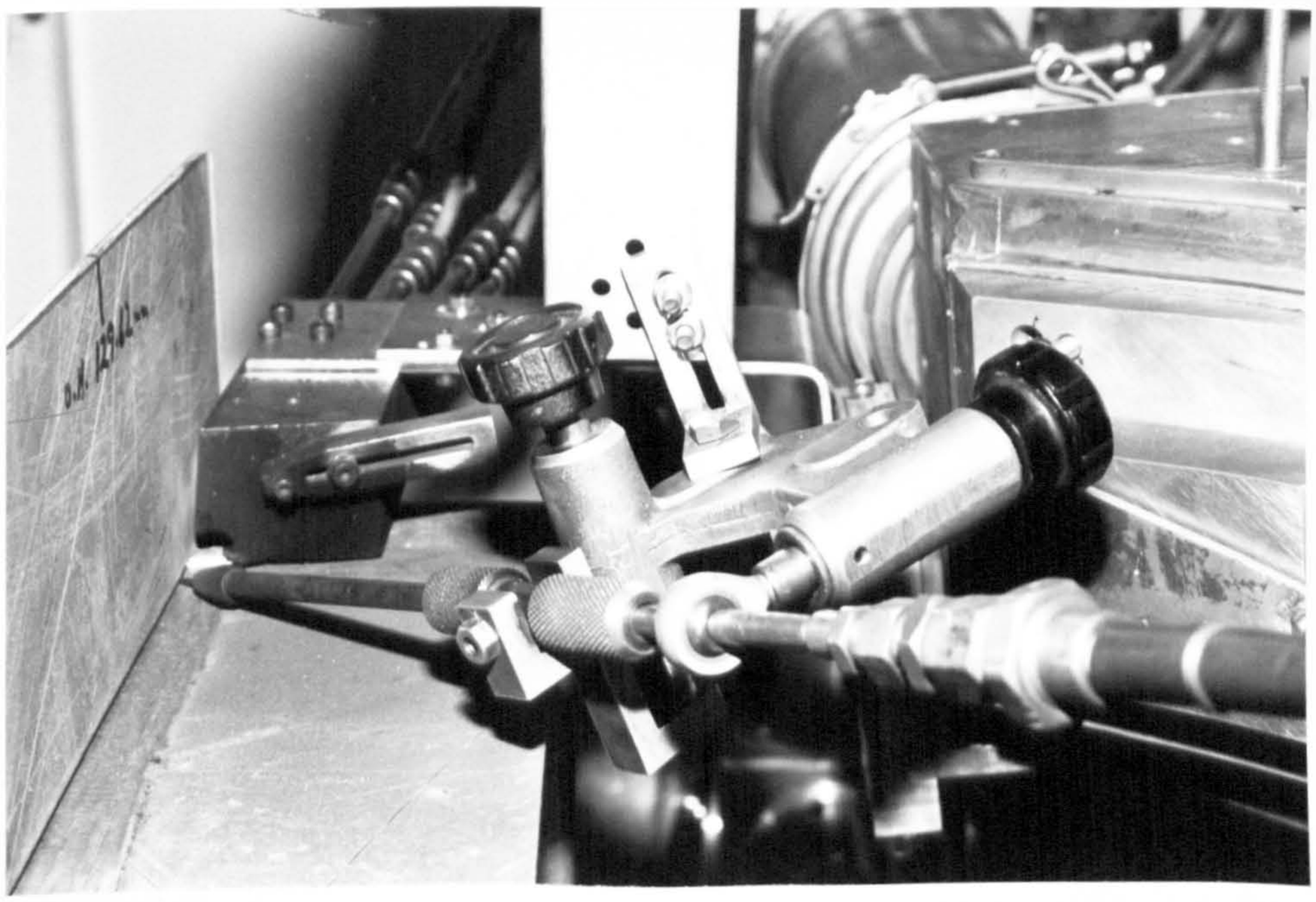

Figure 3.04b - Wire feeding arrangement at the workpiece

the flexible conduit between the drive unit and delivery nozzle.

3.2.5 Sample Support Table Design

As a consequence of the focus unit design, the tee sample flange plate needed to be positioned higher than the focus unit housing. Therefore the samples could not be placed directly on the machine table. Initially samples were raised on blocks but this often necessitated the use of shims between the sample and blocks to ensure positional accuracy.

A simple support jig was therefore designed, figure 3.05, to give greater flexibility and accuracy in positioning the sample and to facilitate the support of cruciform sections which were required for tensile and fatigue tests.

3.3 SAMPLE SELECTION AND PREPARATION

3.3.1 Plate Selection and Preparation

Material specifications as set by Lloyd's Register of Shipping and the Ministry of Defence (Navy) for surface vessel steel plate were analysed [100]. Assessment of their "Rules and Regulations for the Classification of Ships" [101] , and the "Naval Engineering Standards" [102] [103] [104] was followed by discussions with both organisations [105] [106] .

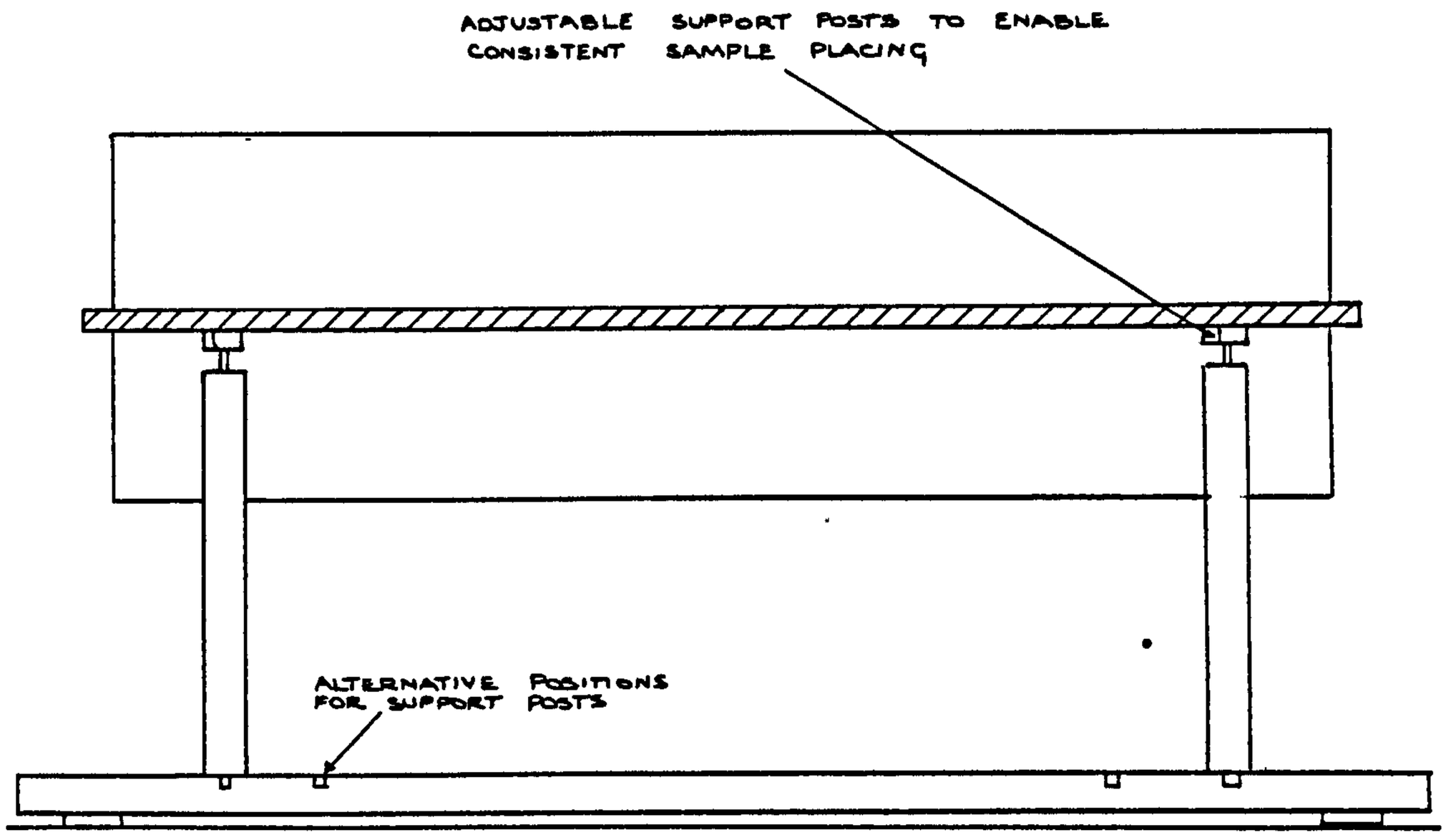

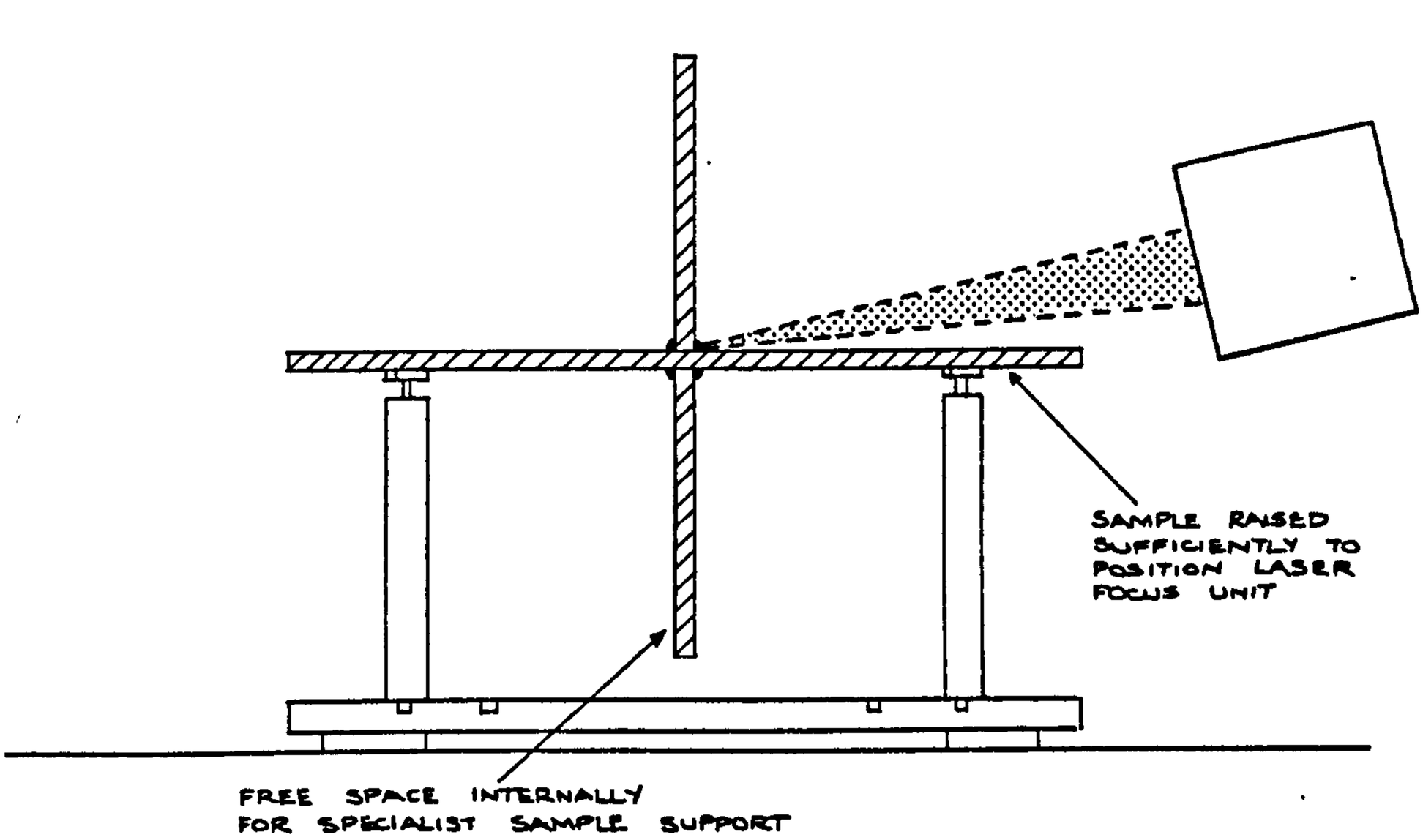

Figure 3.05 - Workpiece support jig with leveling adjuster mechanism

The discussions confirmed that the majority of surface vessels were being built from steel manufactured to the standards specified as Lloyds "Grade A" or BS4360: Grade 43A. British Standard material "50D" tends to be used for more specialist vessels such as LNG carriers or in the building of offshore structures. The MOD(N) also showed an intent to include BS4360:43D into future warship designs.

Grade A/43A steel was chosen as the datum specification for trial samples, being the material most widely used for merchant vessel and surface warship construction. However the specifications allow for a large variation in chemical compositions below a set maximum. Steel with extreme compositional levels can cause problems for conventional methods of welding therefore the Author endeavoured to use a cross-section of plates typically found within the shipyard.

All plate was shot blasted and primed, with either International Paints "Interplate 709/708" or Leigh's "Metaguard" both of which are used as primers dispensed from shipyard automatic spray systems, and having similar composition specifications. The specified dry coating thickness of 25um for these paints normally give a stockyard life of about 6 months.

Plate pieces were first cut on flame planer machines in local shipyards. For samples less than 150mm wide, a larger sample was flame cut then guillotined to minimise any heat distortion. Sample sizes were chosen to enable adequate weld run lengths for test sample extraction

between supporting tack welds while staying within the traverse length of the machine table. Flange and web plate widths were chosen to provide at least enough material to support the joint without distorting (150mm) and at most to be large enough for the extraction of samples to be fitted into specialist testing machines e.g. fatigue testing units (300mm).

3.3.2 Jig Construction

To enable the maximum utilisation of laser time, samples were pre-tacked. A jig was designed for constraining the plates during tacking so that inherent plate distortion could be removed and the joint held in the required configuration.

Figure 3.07 shows the jig in use having been constructed from available "scrap" material. Sizes were chosen to accommodate maximum projected sample size. A pivoting web support could be rotated through 30 degrees to enable angular web placing if required.

Plates were secured to the jig using "G" clamps, the plates being placed so that the centre of any curvature was adjacent to the jig centreline surface for the clamps to act near the plate edges.

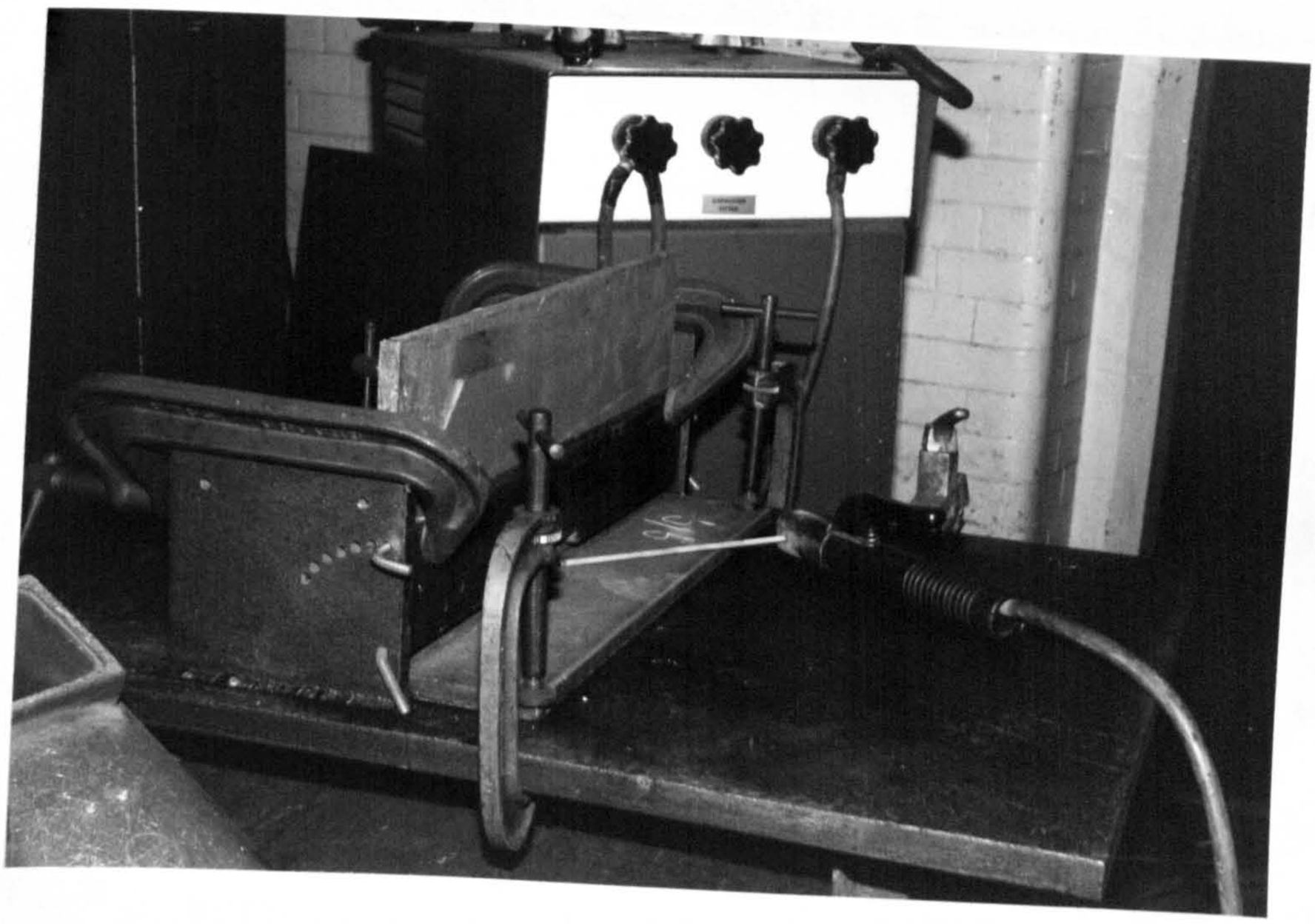

Figure 3.06 - Sample preparation jig with a sample supported for tack welding

3.3.3 Sample Pretacking

The web edge and flange face were prepared prior to tacking if required. When the joining of bare metal surfaces was required, paint was removed using a rotary grinder; excessive oxide deposits on gas cut edges were dislodged using a wire brush. Packing strips were placed in the joint to pre-set gaps.

Once clamped to the jig, Manual Metal Arc (MMA) tack welds were placed at both ends to one side of the web and in the middle to the other side.

The tack size was regulated to give maximum free joint and adequate strength for transportation. Tack fillet sizes were typical of those experienced in the shipyard (approximately 4mm leg length).

Samples were finally marked with a joint configuration and edge preparation code to enable easy recognition once at the Culham Laboratory.

By using pretacked samples laser utilisation was increased from 10 welds to 20 welds per day but the trial programme at Culham Laboratory became constrained by the selected configuration of the pretacked samples. Therefore detailed planning was necessary to fully utilise each set of trials.

3.4 PREPARATION OF LASER, BEAM LINE AND WORKSTATION PRIOR TO TRIALS

3.4.1 Laser Start Procedure and Stabilisation

The laser was started at the beginning of each day by Culham technicians. Although the required processing power (about 10 kW at the laser output to give 9kW on the workpiece) was normally reached in less than 30 minutes, beam alignment and power readings were considered unreliable until the laser had run for one hour to allow optics, gases and equipment to reach a stabilised temperature. During the first two trial periods time was wasted in attempting to align and use the system before the elapse of one hour. The beam appeared to "wander" within the system making the alignment procedure impossible. During subsequent trials faster start-up times were experienced with the system running at 10kW and alignment checked within 30 minutes.

Once satisfactory power and directional stability were achieved (the designed power stability for CL10 is +/- 300W after half an hour warm-up period [107]), the beam line and focusing optics were checked for beam transmission alignment.

3.4.2 Beam Line Alignment

A Helium Neon (HeNe) laser producing a very low power red light was used to check system alignment. The HeNe beam was projected into the main beam path at right angles via a 45 degree mirror which was switched into the beam line for the alignment process. At the same time the 10kw beam was deflected into the calorimeter for power measurement and dumping with a safety shutter closing off the line from the CO2 laser source.

Prior to entering the main beam line the HeNe beam passes a set of perpendicular cross wires which consequently form a silhouette in the beam spot profile. At each deflection of the beam path, the mirror used for folding the beam was removed and replaced with a perspex target plate. The position of the HeNe spot cross wires was then compared to the target zones scribed on the perspex. A difference in target position or noncircularity of HeNe spot indicated that the previous optical component optic in the beam path needed adjusting to align the spot to the target.

For the final alignment check at the workpiece a simple paper target was placed over the output aperture to view the spot position relative to the aperture sides and ensure its central position.

3.4.3 Beam Diameter and Intensity Distribution Measurement

Using the power of the beam to heat or char a material surface is the simplest method of examining the power intensity profile of an unfocused or partially focused beam. The surface area affected will depend however on the laser power and exposure time. Most commonly used is a shallow burn in an acrylic material (e.g. Perspex, Plexiglass, Lucite) with a short exposure time to the laser, typically one second.

A perspex plate was positioned in a holder perpendicular to the beam line ensuring that it was large enough to accommodate the likely beam profile area. Alignment was checked using the HeNe laser.

At the same time as the main beam was projected on to the perspex, a jet of air or inert gas was blown across the surface to stop the vapour being given off from igniting, as the flames would absorb some of the incident beam energy, figure 3.07.

A number of prints were taken at the laser output, before the workstation and at the workpiece to show how the beam intensity profile changed over the beam line length; to estimate beam diameter (for estimating the system focal ratio - f number) and to assess the effects of any system hardware interactions on the beam e.g. beam clipping at any apertures would show up as a fringing pattern on the shallow burn.

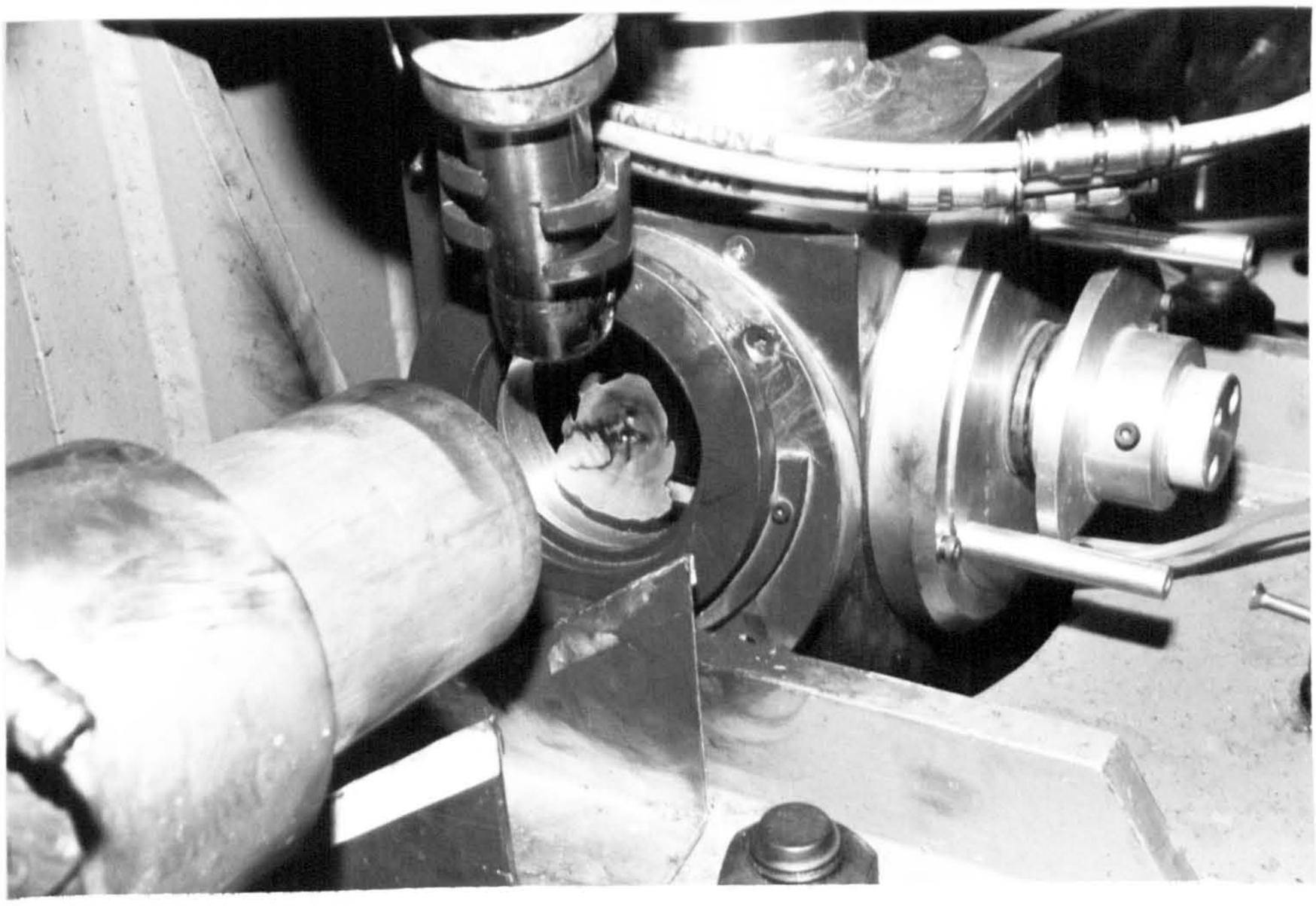

Figure 3.07 - A shallow beam print made in way of a beam line folding mirror

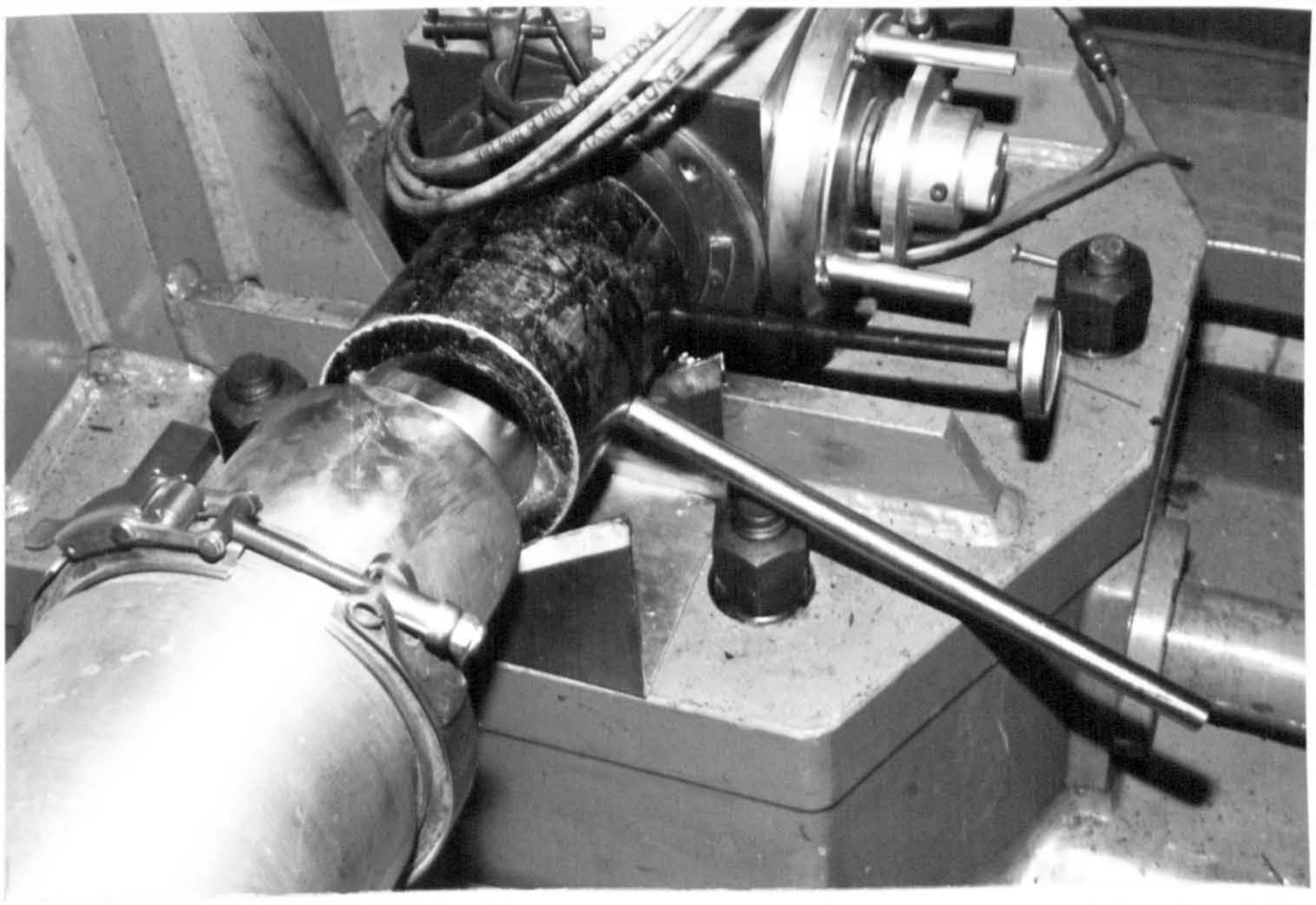

Figure 3.08 - A Joule Stick positioned in the beam line for power measurements

However, this method of beam quality assessment could not be conducted concurrently with any actual production processing. For this, on-line beam analysis equipment would be required, such as a laser beam analyser [108] or use of a hole matrix grating linked to appropriate sensing devices [109] .

3.4.4 Power Measurement

The two most common methods of power measurement use either an absorption bolometer - often known as a "Joule Stick" - or a constant flow "Calorimeter". For both methods the complete beam must enter the apparatus (although there are calorimeters that will monitor a split beam) hence they cannot be used whilst processing is in progress

To use a joule stick the apparatus is positioned into the beam line, figure 3.08 the HeNe laser being used to ensure centring of the beam into the conical measuring surface. The main beam is then switched into the beam line for a set time period, usually 10 seconds. A temperature-sensitive gauge indicates rise in temperature, the power being deduced using a calibration factor with this reading. Operators should ensure that a joule stick with an operating range as near to the likely power is used to ensure optimum accuracy. The joule stick measurement of 10kW is be accurate to +/-100 W.

If a Calorimeter is incorporated into a beam line it may have a dual role as power measurement device and beam dump. A laser system is

usually purchased with a calorimeter designed for the appropriate beam size and output power, the beam being directed into the inside conical surface by a deflecting mirror moved into the main beam path. Thermocouples measuring the difference in water temperature into and out of the device are then linked to a calibrated electronic display. Air may be used as the circulating fluid for devices designed to measure powers of less than 500W.

Once the beam was aligned, power measurements were taken using a joule stick and the calorimeter. Although for the majority of trials the two readings coincided for the power at the laser output because of fluctuations in the water supply to the calorimeter inaccuracies developed in the calorimeter read-out during the progress of a day of trials. However, joule stick measurements at mid-day and day-end normally showed that the initial power had been maintained.

3.4.5 Wire Feed Alignment

The wire feed nozzle supporting frame was constructed in the workstation prior to the trials and only repositioned if a large movement of the nozzle was necessary.

The fine-positioning screw movements on the nozzle unit were set to half travel while the frame was aligned and secured to give greatest flexibility of movement once fixed. A tacked test sample was placed on the welding stand for guidance purposes so that the nozzle could be

placed to within the required position limits of the fine adjustment movement.

The wire feed conduit was secured, where possible, to workstation structure to give a maximum radius of curvature and to reduce conduit vibration. A loose cable could have contributed to disturbed incident beads or porosity in emergent beads because of instabilities caused in the keyhole.

3.4.6 Shroud Unit Alignment

The shroud unit was first aligned parallel to the traversing direction of the machine table so that when welding was in progress, with the sample also aligned to this datum, they would not collide. Similarly, set distances would remain constant. The shroud unit offset distance from the focus unit was made relative to the position of the focused spot with an allowance made for stand-off from the joint surfaces (2mm) to avoid any collisions with tack welds, figure 3.09.

3.4.7 Focus Unit Positional Alignment

For plane butt welds the focus unit normally directed the incident laser beam vertically downwards to the plate surface. For tee butt skid welds a shallow angle of incidence relative to the flange surface was needed. This was achieved by rotating the focus unit about the beam line axis to the required angle (normally 7 degrees) which was then checked

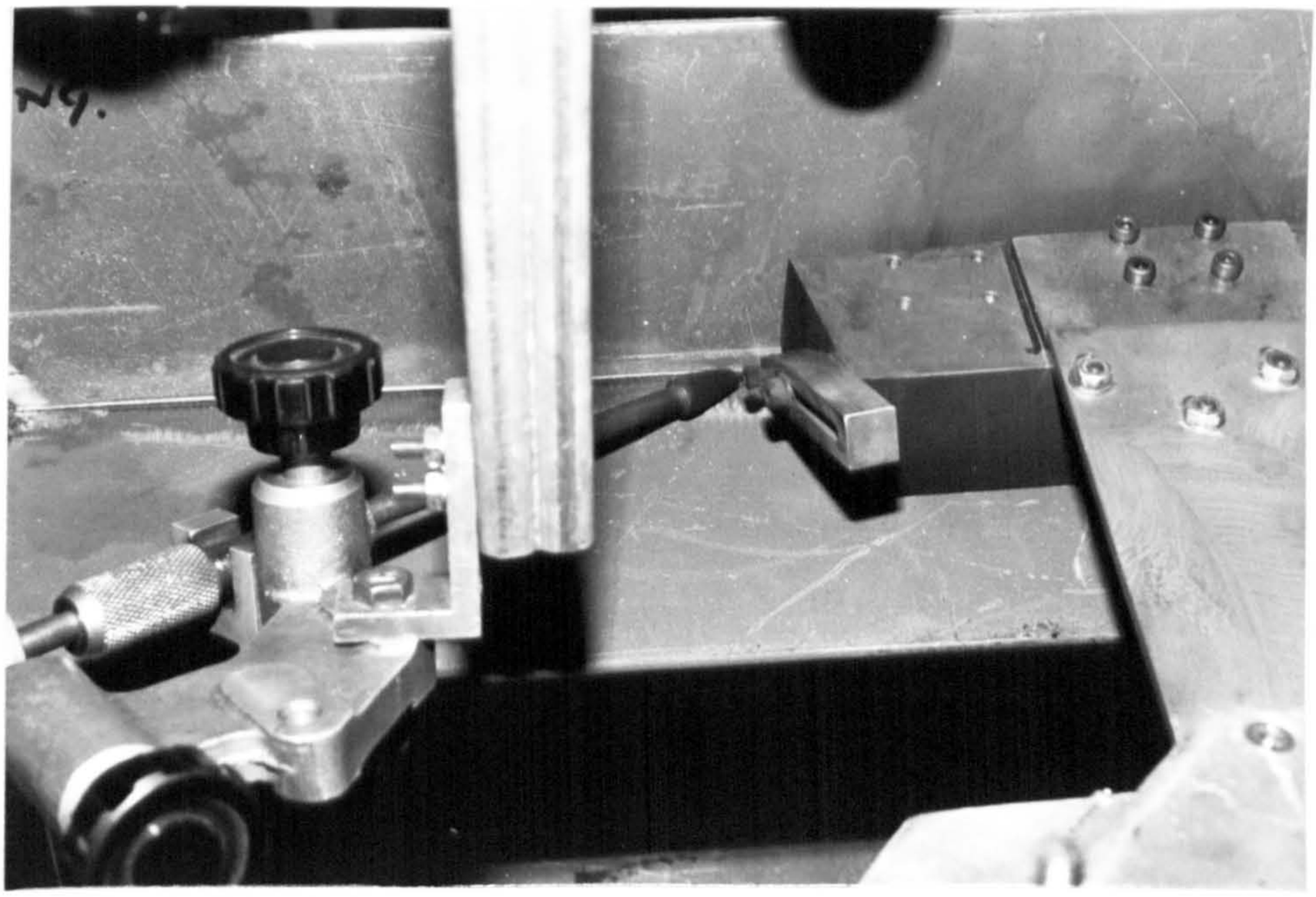

Figure 3.09a - Position of the gas shroud unit for skid welding as viewed from above

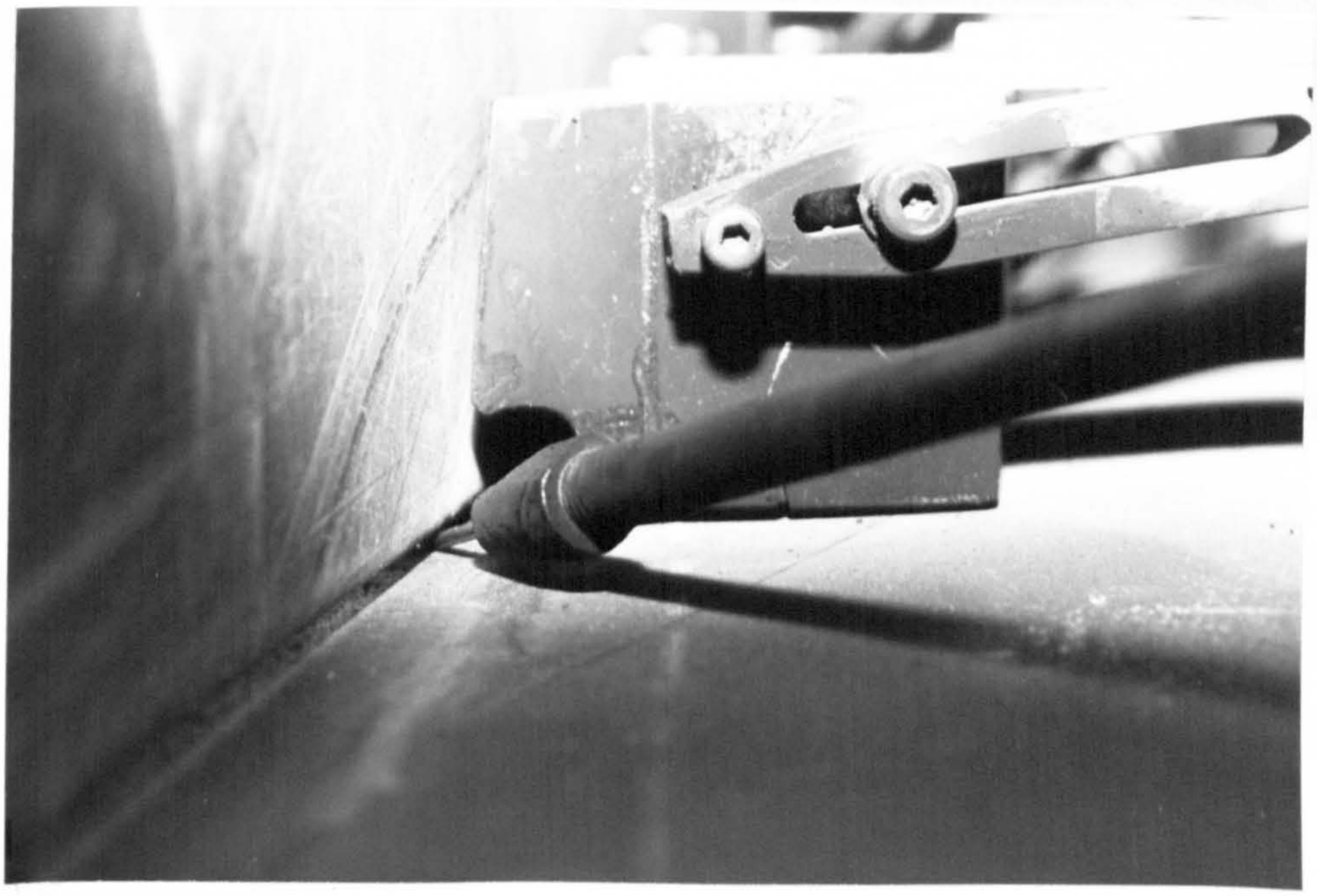

Figure 3.09b - Position of the gas shroud unit viewed from infront

using a spirit level.

A check was also made at this stage to ensure that the CO2 beam and the alignment HeNe beam were coincident. A plate was positioned vertically at the assumed focus spot position. After a short pulse of the CO2 beam (0.5 second) the position of the frozen keyhole within the small melted zone was checked against the projected HeNe beam spot.

3.4.8 Focus Position Assessment

The position of the CO2 beam's point of focus may be assessed using the CO2 beam itself or by comparative approximations using the HeNe beam. Various methods of varying complexity have been used by other authors [110] [108] [111] [112] [113] .

During the skid welding trials a first indication of the focus position was gained visually by inserting a target surface e.g. a piece of plain paper into the HeNe beam. By moving the target along the beam away from the focus unit the zone of minimum diameter was located. This process was helped by the characteristics of the off-axis system. At the point of focus the axial orientation of the elliptical "blur spot" rotated by 90 degrees so that this transition position could be located, figure 3.10.

After this initial assessment, the focal position for a CO2 laser beam to penetrate a certain plate thickness may be optimised by making melt

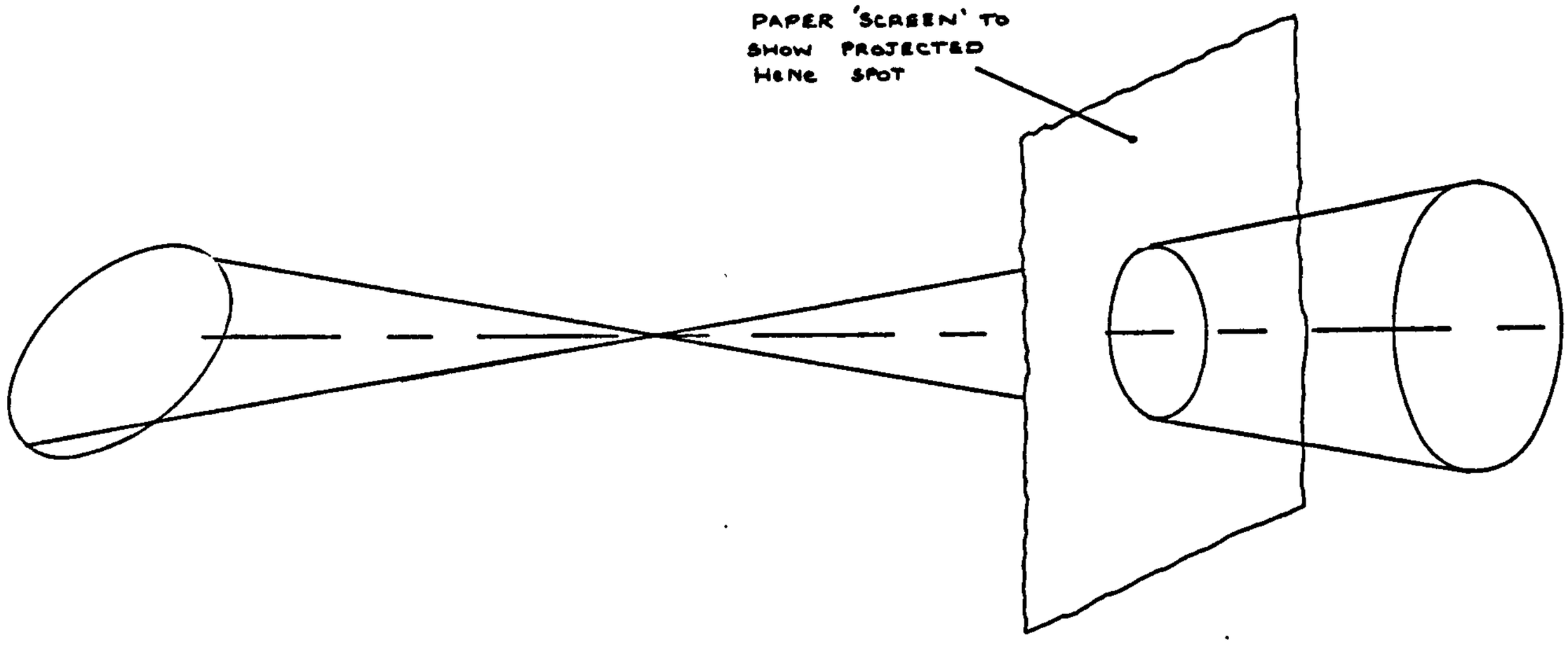

Figure 3.10 - Effect of the off axis focused beam to assist in identifying the relative position of the beam focus

runs at a traverse speed high enough to just show penetration with the estimated focus positioned on the plate surface. By moving the estimated focus position into and out of the plate for consecutive runs and observing the resulting penetration difference, an optimised focal position for the particular plate thickness may be found.

3.4.9 System Calibration

Power measurements as indicated on a digital display connected to the calorimeter were calibrated by comparison with the joule stick measurements. By taking readings of power at the laser output and at the workpiece, beam line power losses could be assessed. An average loss of 1.0kW (2% loss at each of 5 folding mirrors) was considered normal. However slight misalignment or dirt on the beam line mirrors at times caused losses of up to 1.3kW.

Wire feed rates as set on the MIG welding type wire feed drive unit (divisions of 1 to 10) were calibrated against wire output rates measured at the feed nozzle by operating the system for a fixed time interval, normally 10 seconds and measuring the length of wire extruded.

Traverse speeds were set from a dial with divisions of 0 to 1100 in units of 50. This was calibrated by timing the table movement over a set distance, which excluded times for acceleration or deceleration. The resulting graph was then used to derive trial settings.

3.5 PRACTICAL WELDING PROCEDURES

3.5.1 Parameters to be Considered for each Weld Run

Table 3.01 shows the the main processing parameters that had to be set, positioned or checked for each weld run and their basic effect. Some, such as beam angle, would remain constant throughout a trial period whilst others had to be specifically set for each weld run. Usually only one parameter was actually changed between consecutive welds.

3.5.2 Workpiece Positioning in Workstation

Pre-tacked samples were placed either directly on the machine table or on a supporting stand, depending on the joint configuration.

When many melt runs were made in a single plate in the flat position, plate wrap-up increased with each consecutive run. Consequently the plate was unstable when placed directly on to the machine table surface. Therefore melt run test pieces rested on supporting bars with the proposed melt position aligned over the table's under plate shroud gas channel.

Melt runs in the horizontal vertical position were made in the web of a pre-tacked tee section sample, with the flange plate positioned on the machine table or on the welding stand. The focusing unit, angled to 7 degrees was raised to allow beam interaction at the required height on

PARAMETER		EFFECTS
INCIDENT LASER POWER	]	HEAT INPUT DETERMINING PENETRATION
WORKPIECE TRANVERSE SPEED	]	
LASER SPOT HEIGHT	]	DIRECTION AND POSITION OF FUSED WELD ZONE
INCIDENT ANGLE	]	
WIRE FEED RATE	-	SIZE OF FUSED AND REINFORCED ZONE
WIRE FEED ANGLE	]	POSITION OF INTERCEPTION WITH WELD ZONE/LASER BEAM. DEPTH OF INSERTION INTO A JOINT
WIRE FEED STANDOFF	]	
SHROUD GAS	-	DEGREE OF PROTECTION TO FUSION ZONE
PLASMA CONTROL	-	CONTROL OF THE PLASMA DENSITY AT THE KEYHOLE

Table 3.01 - Parameters considered for each weld run and their principle effects

the web plate. The sample was aligned, at the relative focal distance, parallel to the table traverse direction.

For laser butt welding, pretacked samples were placed on the machine table with the joint line over the centreline under-plate shroud channel. The table was then moved until the HeNe spot was positioned on the joint line at one end. Then, by traversing the sample under the spot, the joint could be adjusted to ensure the spot remained aligned along the joint length.

Two 20mm square bars were clamped longitudinally over the butt weld sample pieces. This reduced any plate distortion induced during cutting to give consistent beam focal heights and free passage of the welding shroud. The disadvantage of clamping the plates is that during the heating process the weld itself will yield due to the fixture of the plates so that comparative joint wrap-up measurements will be affected.

Pre-tacked tee section samples for skid welding were positioned on the welding stand and placed on the machine table within its traverse limits but without the use of any restraining clamps, figure 3.11a-b.

With the plasma control shroud aligned parallel to the machine table's traverse path at the required focal distance, the tee sample could then be positioned parallel to the shroud. A 2mm gauge was used to check the offset distance between the shroud and the flange plate. The accuracy of alignment was checked by traversing the sample and monitoring the shroud

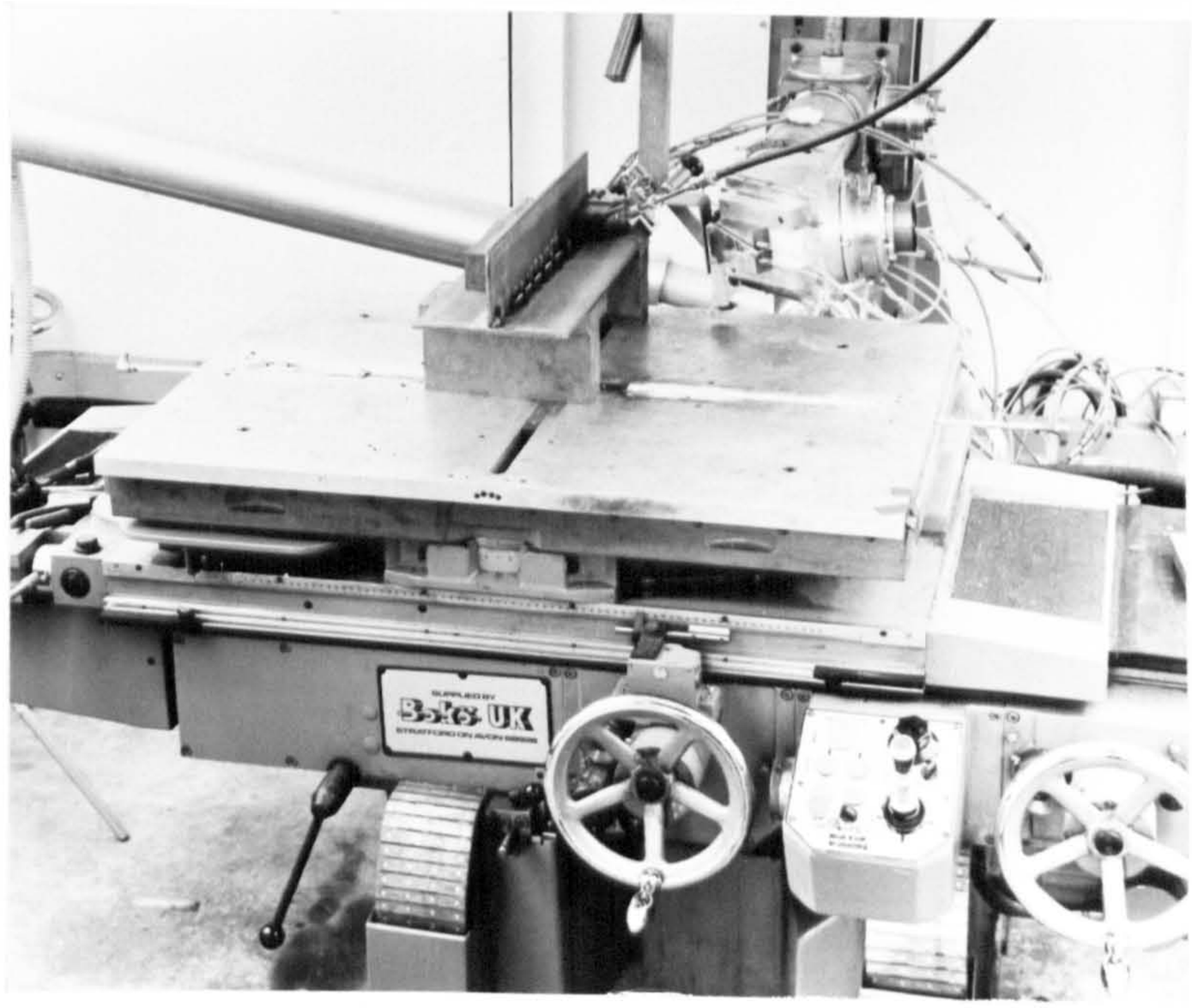

Figure 3.11a - A pre-tacked tee joint sample positioned on the welding stand and aligned to the worktable datum

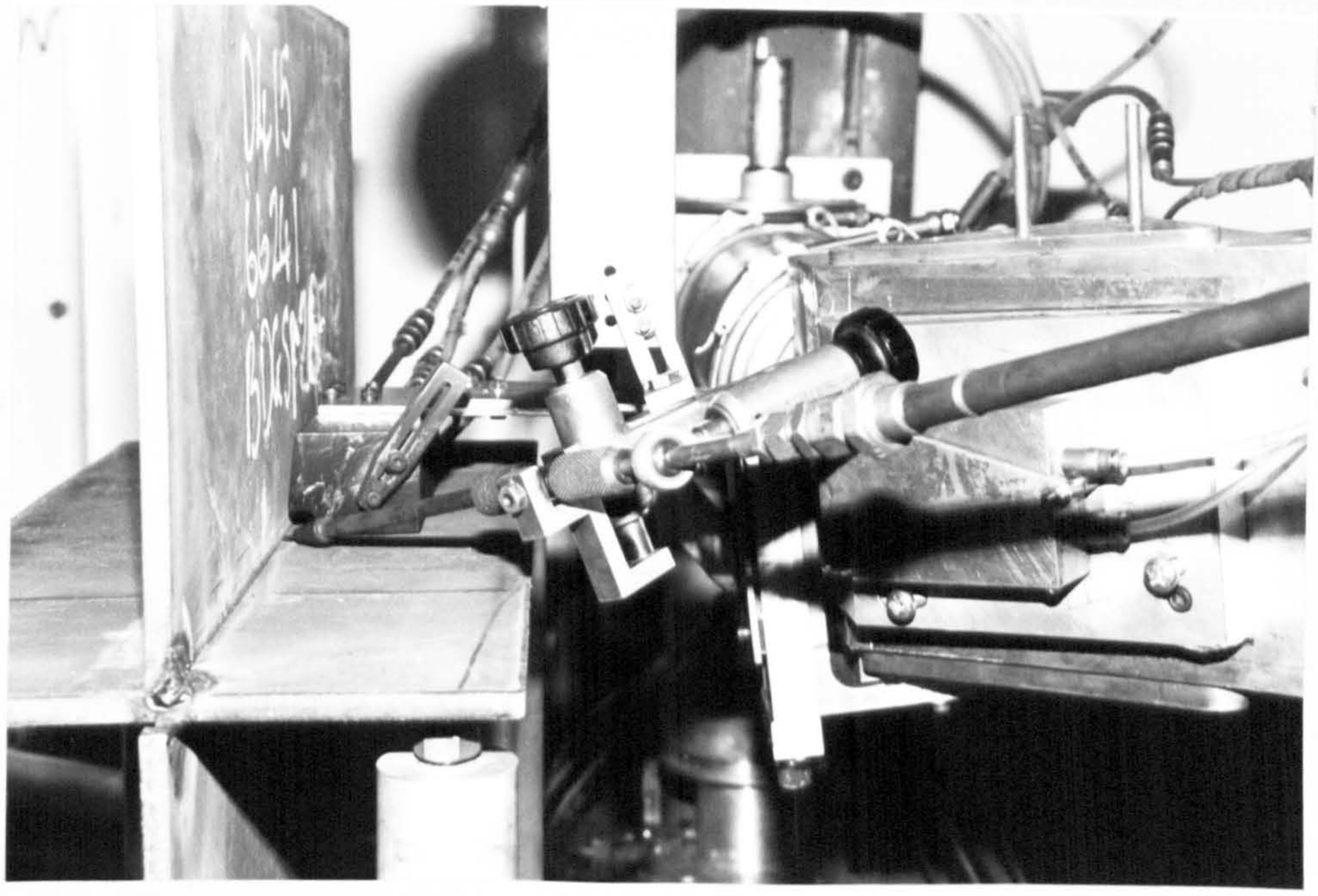

Figure 3.11b - A pre-tacked cruciform sample postioned on the welding stand with the plasma control unit positioned parallel to the joint line

and plate gap along the proposed joint path.

Vertical alignment was dependent on obtaining the required height for the incident laser beam. This was achieved at one end of the sample by raising or lowering the focus unit, measuring the height of the focused HeNe spot on the web surface. After traversing the sample to align the beam with the opposite end any changes in the relative sample and spot height could then be made by altering the stand's support adjusters. The accuracy of the alignment could again be checked by traversing the sample, monitoring any change in the required spot height.

3.5.3 Plasma Control Jet Positioning

For melt runs, butt welding and through welding the welding shroud unit is usually positioned relative to the joint line aiming the gas flow from the plasma control jet to impinge on to the focused beam spot on the plate surface [3] [68] . For a particular design of shroud unit with a feed jet angle, this can be easily related to a given stand-off distance of the jet from the plate surface.

For tee section welds, with vertical and horizontal alignment considerations , the Author used an indicator needle mounted on the front end of the shroud to point to the interaction plane of the jet nozzle. This could be then moved into line with the laser spot, figure 3.12 a-b.

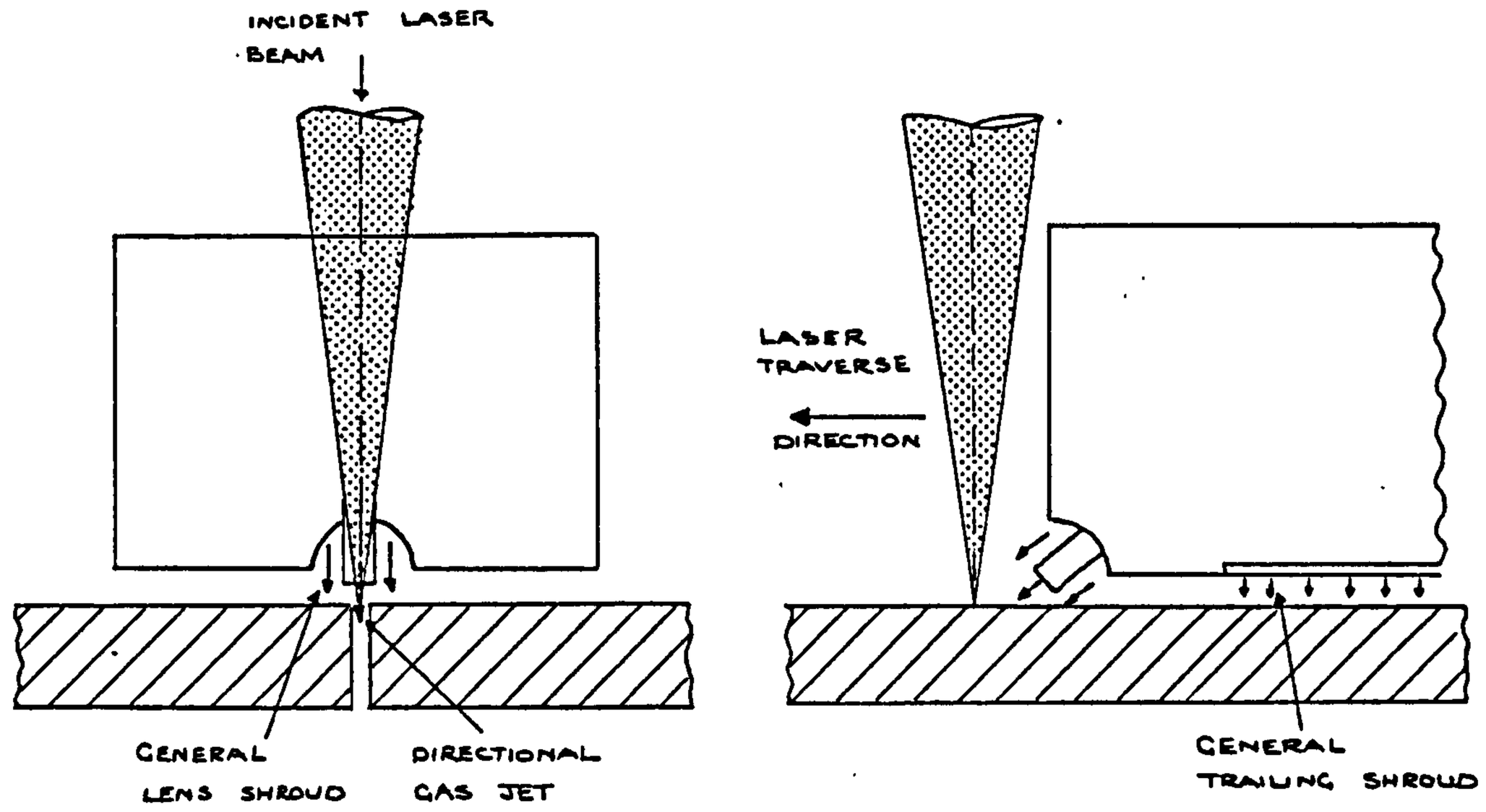

Figure 3.12a - The shroud position relative to the joint line for butt welding

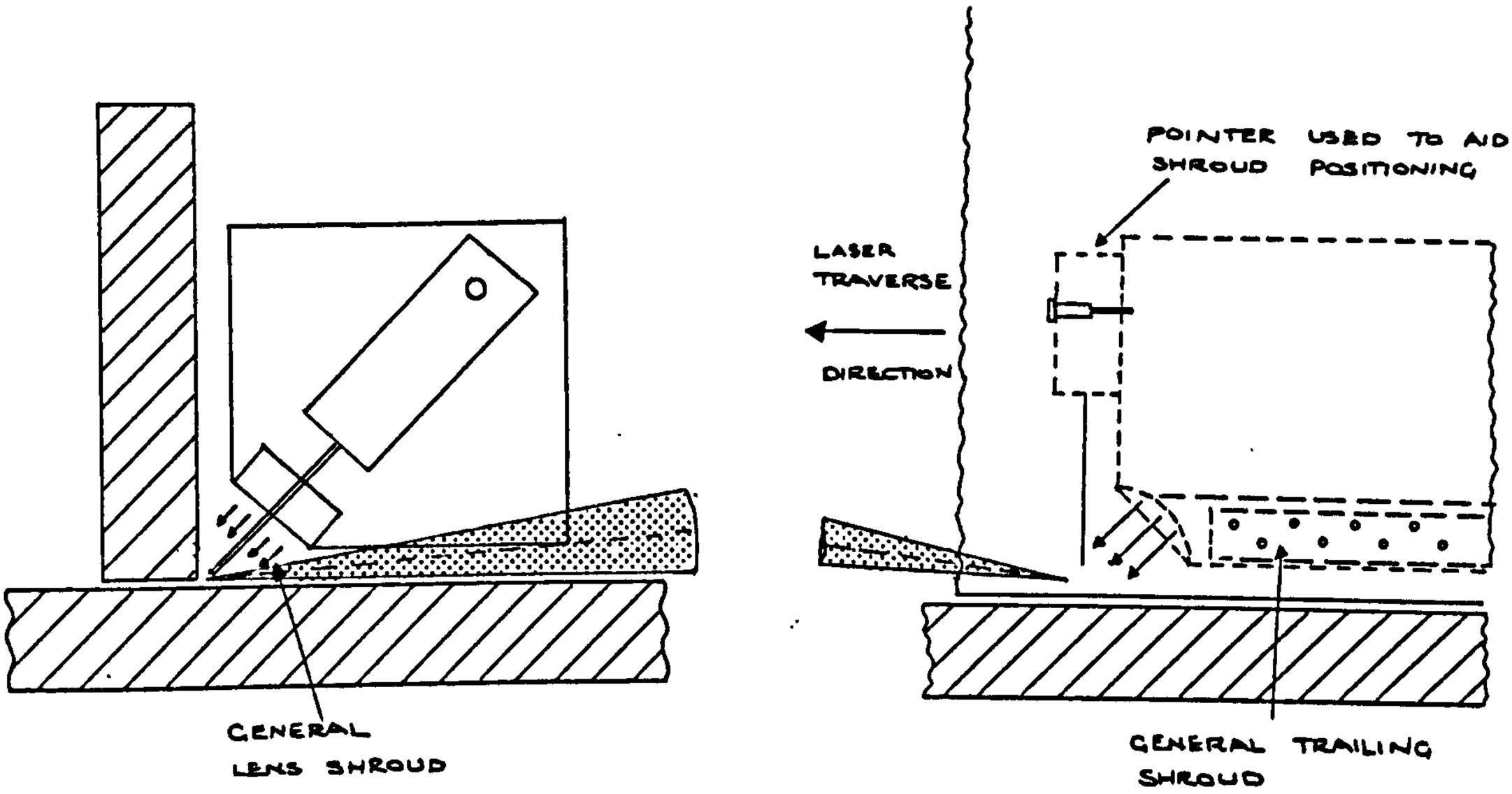

Figure 3.12b - The shroud position relative to the joint line for skid welding

Although the plasma control jet was not used after the second trial period, the indicator was still used to ensure consistency in positioning the shroud, especially for the lens gas flow on to beam interaction point.

3.5.4 Filler Feed Positioning

For butt welds, when the filler must enter the weld along the joint line, there are two degrees of freedom; the angle subtended by the wire nozzle and plate surface and secondly the distance between wire/plate surface interception and laser beam/plate interception, figure 3.13a.

For tee section welds, however, there are four degrees of freedom - as shown in figure 3.13b. Angular positions were generally fixed for any one trial leaving the linear movement to be finalised between consecutive welds. Equal subtended angles of 45 degrees were used as a starting position, linear distances being set to aim the wire directly at the laser spot. A slight radius of curvature of the wire had to be considered when making final adjustments. A 20mm length of "stick-out" was usually left between the nozzle end and the joint, to avoid over-heating the nozzle tip.

For joints with gaps or when the web edge shape allowed, e.g. for a radiused section, the wire could be inserted further into the joint. By increasing the stand-off for the position of insertion, the interception point of the laser and wire occurred further into the joint to give the

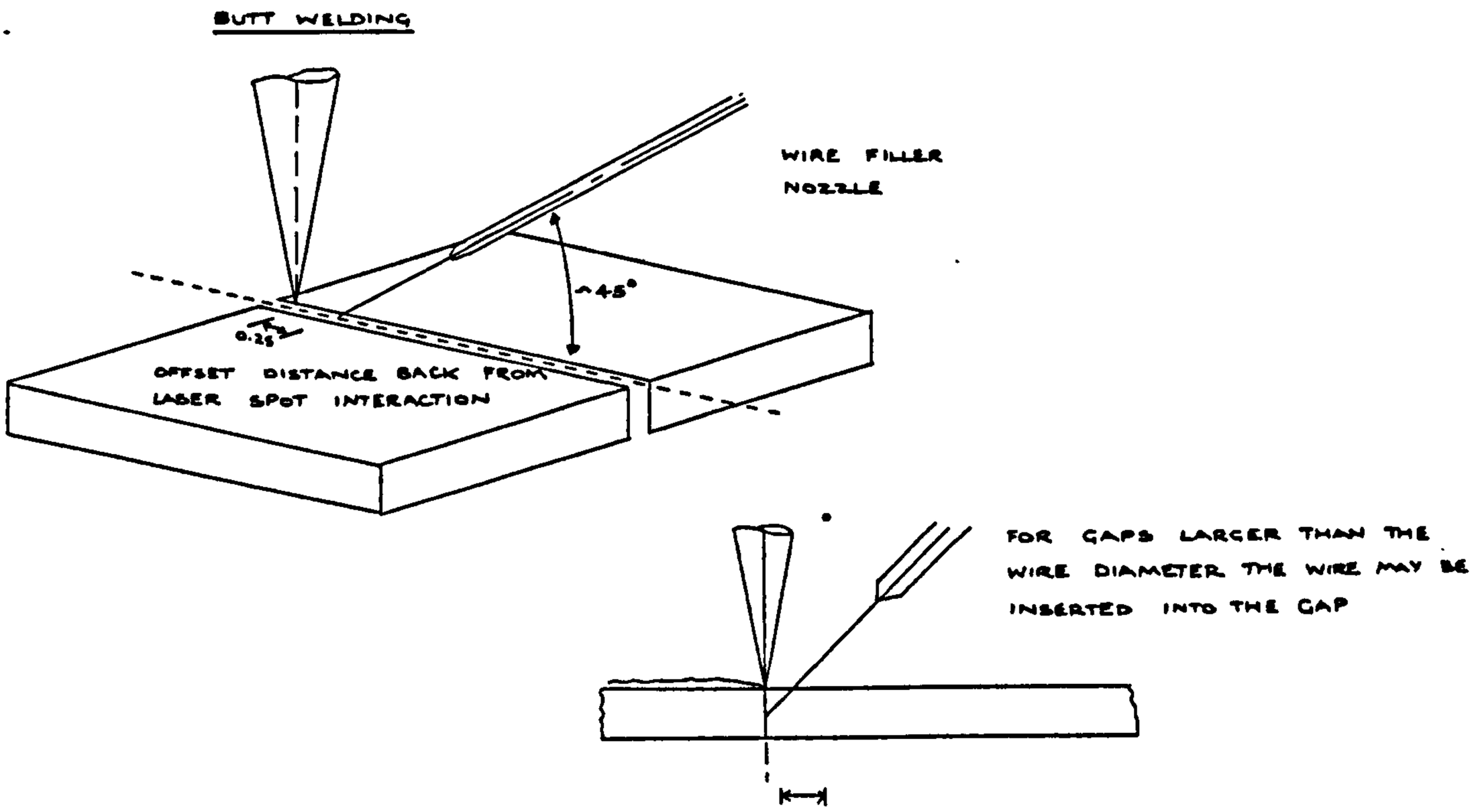

Figure 3.13a - Position of the filler wire for butt welding

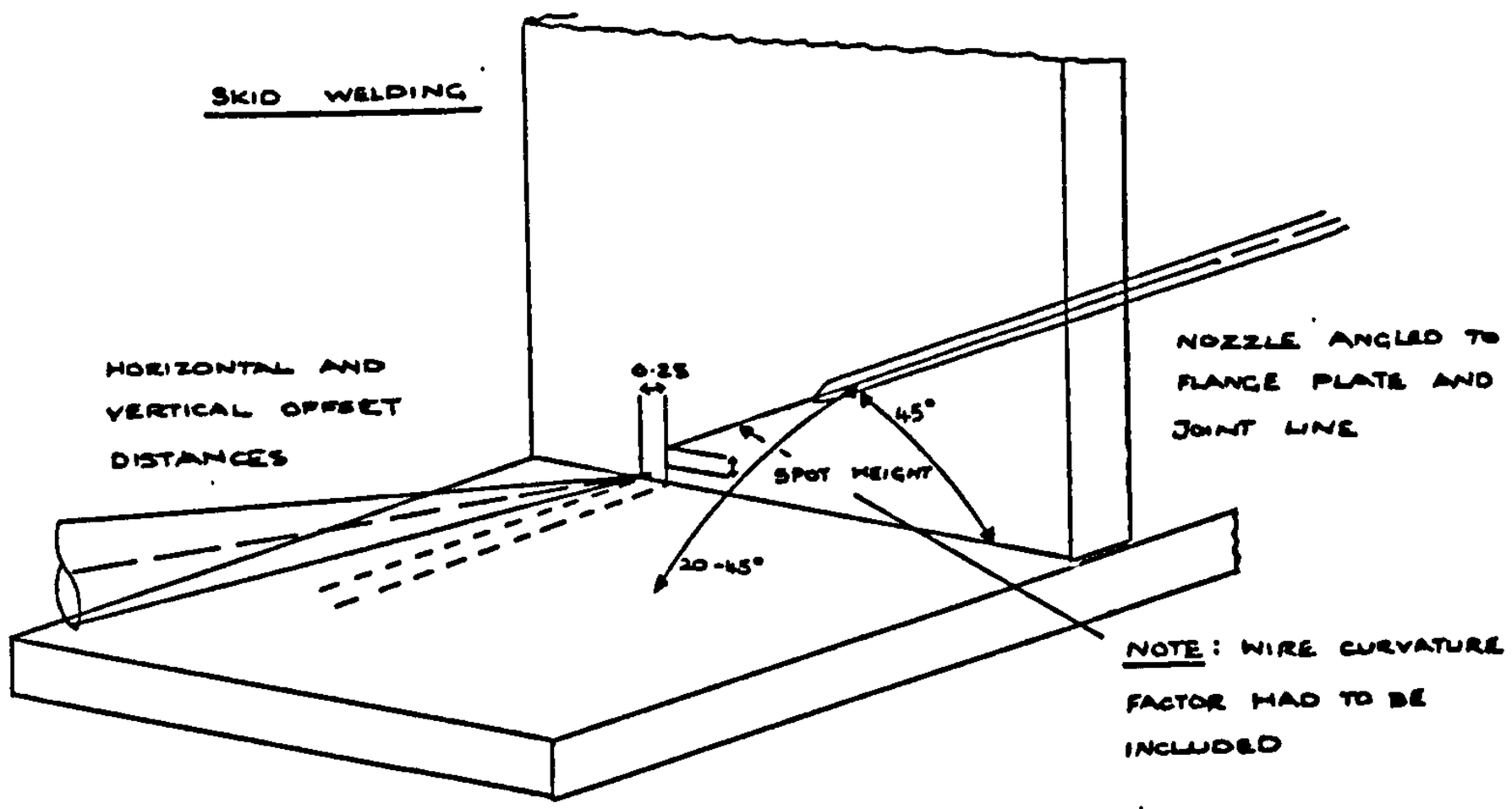

Figure 3.13b - Position of the filler wire for skid welding

potential for improving the flow of filler material throughout the joint.

3.5.5 Interlocks

Culham Laboratory have set an example to high power laser users in establishing safety procedures well in advance of any British Standard directives. Before the CL10 beam can enter the workstation, the electronic control system checks the following interlocks - door closure, excess smoke or temperature.

A mechanical key system is also used to preclude the use of overhead gantries and to ensure door locking and shutter positioning while the laser is in use. All interlocks, both mechanical and electronic, figure 3.14a-b. have to be engaged before the main CL10 mechanical shutter is released thus protecting the beam line from any accidental exposure to the 10kW beam.

The laser is also protected by similar interlocks to ensure correct functioning through the monitoring of gas pressure, gas bottle content, water supply, temperatures and pressures. Gas bottle level indicators give an audible warning allowing 30 seconds for changing to the next bottle otherwise interlocks operate to shutdown the laser. If any interlock fails an indicator light shows on the laser controller in addition to the audible warnings.

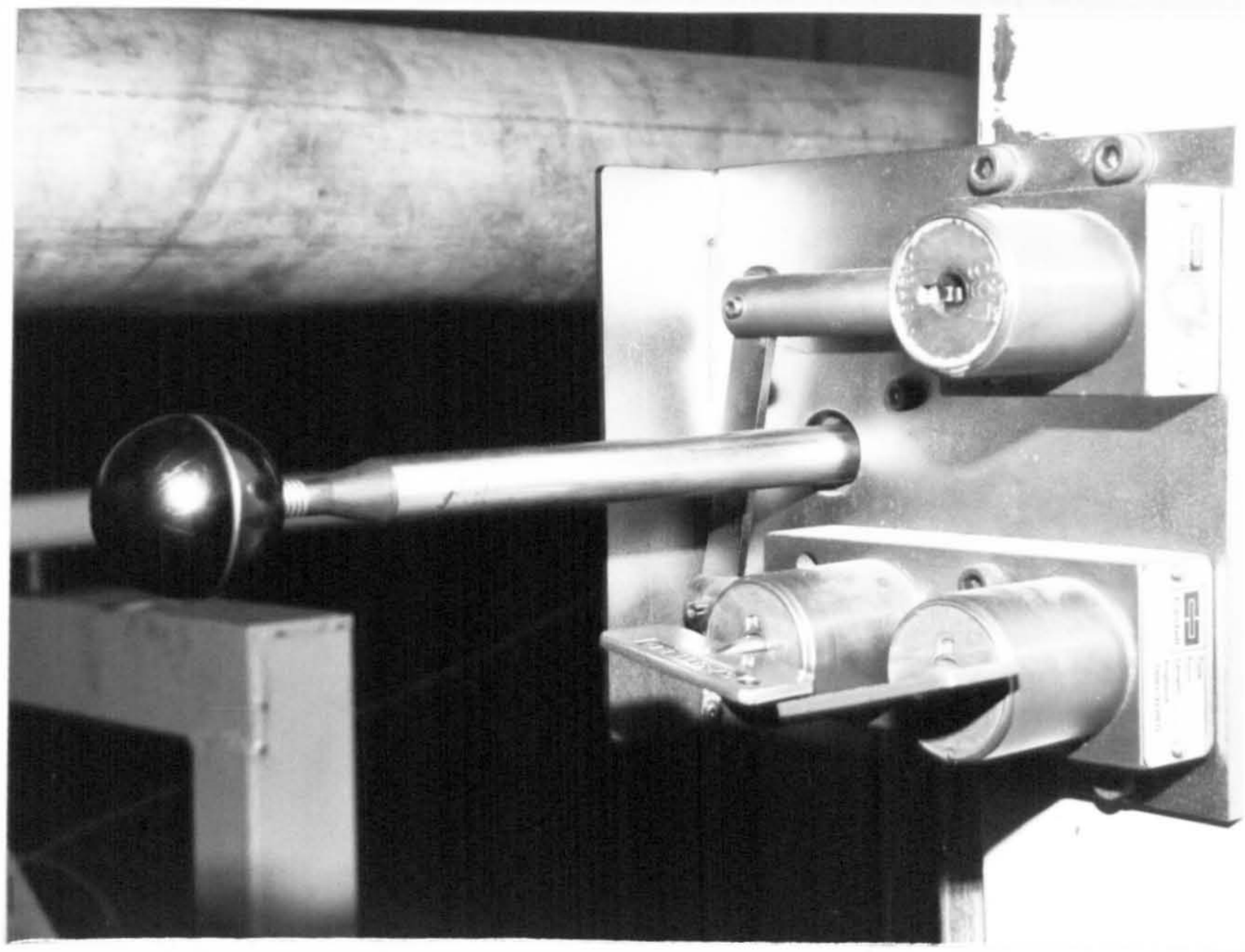

Figure 3.14a - Mechanical key interlocks controlling access to the workstation and the beam line shutters

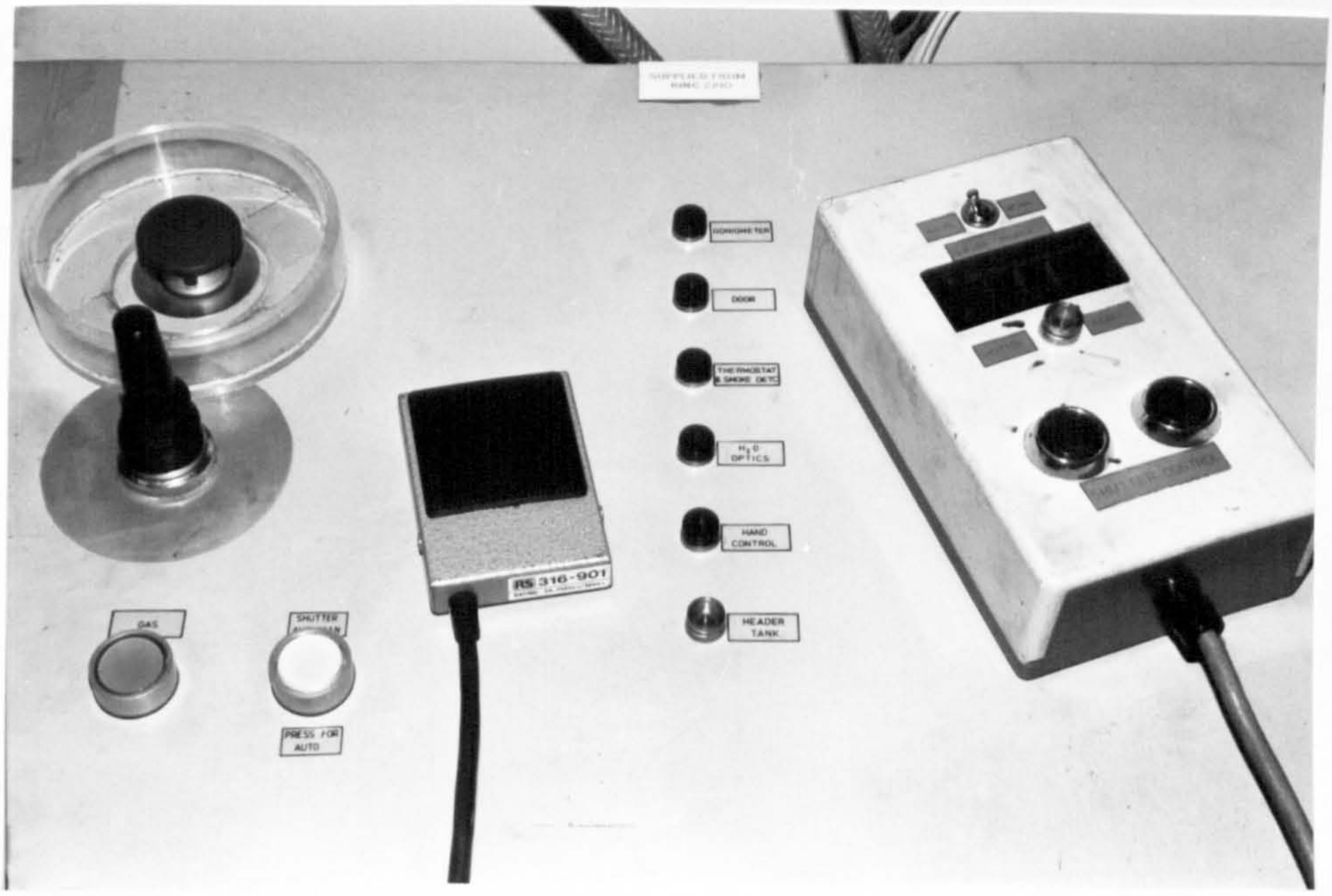

Figure 3.14b - Workstation control panel with a display of electronic interlock identification warning lights in the middle

3.5.6 Operation of the Laser System for each Weld Run

After positioning the workpiece, aligning the shroud and wire feed units , setting the traverse speed and wire feed rate, the workstation door was closed. The relevant interlocking keys could then be exchanged to prepare the system for operation.

Plasma control jet and shroud gas pressures were set from regulators on the workstation control panel although the actual gas bottles were only fully activated just prior to a weld run in order to economise on gas consumption.

Any changes to laser power, taking account of losses within the beam line, had to be made at the laser controller although this would normally be kept constant for a trial period. After switching the control system from the "align" mode, when the HeNe laser was projected into the beam line and a warning signal sounded, the CL10 laser shutter could be activated.

The workstation table traverse control was operated just prior to opening the laser shutter. This stopped an uncontrolled hole from being "drilled" into the joint while the sample remained stationary.

After the initial few seconds of traverse time, when either the autogenous keyhole was allowed to form and stabilise or, due to an excessive gap, the beam penetrated the joint without forming the keyhole,

the wire feed was activated using a remote pressure switch.

As the laser neared the end of the proposed weld run, the wire feed was stopped first so that the continuing laser action severed the wire from the weld pool. If not, the wire froze into the solidifying weld pool, wire cutters being needed to release the wire nozzle unit.

As a reversal of the start procedure the laser shutter was closed before traverse motion ended to avoid cavity "drilling". The workstation could then be opened for the sample to be inspected and dismantled.

During the run, the process could be observed through the workstation door viewing panel; a double-skinned perspex window. The gap between the skins provided a means for a water release interlocking system. The welding action could be observed both audibly and visually so that characteristics could be noted, potentially dangerous situations foreseen and the system stopped when required. However,during a particular weld run, once the workstation door was closed only shielding gas pressures could be changed and the wire feed stopped or started.

3.5.7 Sample Identification

Each weld run, or melt run, was given a unique identification. This remained with the weld for all scheduling, testing and documenting activities. The code identified the type of joint, plate thickness, edge preparation and consecutive number.

3.6 TRIAL PROGRAMME SCHEDULING

3.6.1 Review of Processing Variables

The analysis of both the laser weld and the laser beam's characteristics in the two preceding chapters enabled the Author to assess the variables which were likely to affect the laser skid welding process, tables A3.01 a-e, Appendix A-1. If analysed fully, even with the restricted number of variables chosen for examination, the total number of weld runs would need to be in excess of 9 million. Hence a refinement process was required which took account of the following factors:

1. Technology available for monitoring the variable.
2. Time scale of any valid experimentation.
3. Previous evidence of testing a variable for similar joint configurations.
4. Non-applicability of testing a variable to the project objectives.

3.6.2 Selection of Programme Priorities

Examination of the welding process variables showed two dependent sectors applicable to producing skid welds for shipbuilding applications. Experiments to produce skid welds in various joint configurations and orientations would show the wide applicability of the process. However this would only be possible if the process itself was tolerant for the

weld to be easily and repeatedly produced in the first instance. If not, experiments to assess the variables affecting the process tolerance would be more important.

The first skid welding trial (Trial 1) was used to assess the likelihood of easily producing joints in many joint configurations, based on assumptions made from the conclusions of Martyr [3] when using the CL5 laser. However, the results showed that the skid welding process was not as tolerant as had been expected when using the 10kW laser. Therefore, for each plate thickness the trials programme was first directed to understanding the welding process and mechanism before investigating any further joint configurations.

3.6.3 Trial Schedule Development

Plate thickness was the prime variable for the trial programme. After initial tests on 10mm thick plate, trials were conducted on thicker plate up to 15mm and thinner plate down to 3mm. The scheduled number of runs to assess processes parameters reduced for each subsequent plate thickness as the process became more fully understood. However, when tests conducted on the weld showed any detrimental properties when compared with classification requirements, further trial runs were made using alternative input parameters for the same material thickness.

While plate thickness and the effect of prime joint configurations dominated the trial scheduling in advance, the detailed programming of

each trial depended on experience gained from a previous trial and the results of basic tests conducted on the welds produced. Figure 3.15 shows the resulting trial programme with a detailed listing of the trials conducted presented in Appendix A-2.

3.6.4 Dominant Milestones in the Welding Programme

The results of Trial 1 affecting the test programme emphasis have already been noted. Whilst the Author had contemplated experiments to complete welds in multiple orientations, instead the initial trials showed the supreme importance of understanding the welding process more fully. Further discoveries which affected the overall programme scheduling should also be emphasised.

Trial 2 confirmed that skid welding to a painted flange plate was not as simple as had initially been hoped. Compared with welding to a non-coated plate, the process became inconsistent with mass formation of pores. Therefore subsequent initial parameter surveys for varying plate thicknesses had to be conducted on non-coated plate, with experiments on coated surfaces attempted as a secondary priority.

The effect that laser spot height might have on the resulting weld profile was also confirmed during Trial 2. The tolerances observed meant that an accurate assessment of this parameter was necessary for each plate thickness tested. This was especially so with the implications of assessing the positional tolerances for a multi-axis welding head to

TRIAL SESSION	FAM	1	2	3	4	5	6	7	8	9	10	11
DATE / PLATE THICKNESS	AUG 83	OCT 83	JAN 84	APR 84	MAY 84	AUG 84	SEP 84	OCT 84	JAN 85	FEB 85	MAY 85	OCT 85
3												
6											BUTT	
8												
10	BUTT	BUTT									BUTT	
11												
12												
15											BUTT	

Figure 3.15 - Programme of laser welding trials at UKAEA Culham Laboratory

ensure the repeatability of satisfactory joints.

The effect that the use of the plasma control jet had on weld stability was particularly noticed during Trial 3. In fact, for the plate thickness and range of traverse speeds used (10mm and 8-14mm/second resectively) the use of the jet served only to disturb the weld stability, possibly because of the funnelling effect of the joint configuration on the general shroud gases. The incentive to produce all the "final" welds without the jet gas input was high as this would reduce the need for a complicated directional nozzle axis.

Satisfactory welds were produced in 8mm plate during Trial 4 so that subsequent welds in this thickness could be attempted on different joint configurations or for structural proving tests and the basic parameter assessment widened to complete the thickness range.

During Trial 5 preparations were made for Trial 6 when welds were produced for fatigue tests to be overseen by a representative of Lloyds Register of Shipping. Flange plate wrap-up was monitored so that a small amount of pre-set (one degree) necessary to have a flat post-welded joint, could be introduced before the welding trials.

The first power reductions were made during Trial 7. While the power had been kept constant at a level considered to be the maximum constant power available at the start of the project, 9kW(WP), tests on the first 6mm plate used (plate P6/01/CS) had shown a tendency for excessive

hardness as tested by a Vickers Pyramid Hardness machine ie >350 Hv. Therefore an initial attempt was made to create effective changes by changing input laser parameters. The samples produced, while in fact showing higher hardnesses for reduced heat inputs because of faster cooling rates, indicated the relevance of attempting to correlate weld properties to input parameters.

The experiment also emphasised how, by observing the balance between any plasma build-up at the incident side to that at the emergent side as heat input varied, the balance of the weld beads may also be assessed.

During Trial 8, in addition to increasing the scope of samples appropriate to testing for confirmed welding parameters, initial surveys in 12mm and 15mm plate were attempted. These showed how, as plate thickness tended to the available penetration depth for a particular heat input, there was a reduction in the capacity to control the profile of the emergent bead. This was due to the reduced volume of material melted on the emergent side and subsequently a lower rate of flow of molten material, causing both small and improperly fused emergent beads.

The opposing view of the heat input, plate thickness balance was found during Trial 9 when welding was attempted on 3mm plate. Even by using the maximum traverse speed of 40mm/second for 9kW(WP) power, satisfactory emergent beads could not be formed. Observation of the plasma balance showed how all the input energy was being dissipated on the emergent side in a totally uncontrolled manner. However, by reducing the power to

5kW(WP) a balanced system could be regained.

During Trial 10 butt welds were produced using similar heat input parameters to those of tee section welds in the same plate thickness. While the project was designed for the testing of tee section welds, butt welds were produced to help compare weld toughness as would be required for testing conventional welds. In addition the Author also produced initial procedures for laser filler butt welding to 15mm thickness on the unprepared, gas cut edges using 10kW of laser power.

Finally, Trial 11 was used to test procedures deduced from theoretical analysis and observations from previous trials. Therefore the Author could provide a basis for predicting both the procedures necessary and the tolerances for production skid welding processing and an assurance of the potential weld quality available.

A log was written during each trial [114] . This was compiled in a computer data file so that a case history, with all subsequent test results added, could be kept for each weld by a compact and easily retrievable method.

After listing the identification number, the relevant parameter details, laser power, traverse speed, joint preparation and wire feed rate were entered. As the trials progressed the Author appreciated the value of descriptive observations made during a weld; hence short comments were progressively introduced.

Results of property testings were then added to the file, many in a coded form not only to save space but also to introduce a standard format for the property specifications.

Therefore the full set of logs present a concise and factual description of the project trials, not only for the Author but in a form which could be used easily as progressive records for the further development of the process.

CHAPTER FOUR

SKID WELDING PARAMETERS, PROCESS EFFECTS AND TOLERANCES

The practical skid welding trials were conducted as described in Chapter 3. For each trial emphasis was placed on assessing the effect of varying a fixed set of parameters on the resulting joint. As trials progressed the inter-relationships between parameters became more obvious. This helped not only in the understanding of the process, but also confirmed the relevance of highlighting parameter effects and tolerances. This was achieved in order to secure an early and reliable feedback of design specifications for the development of a prototype skid welding workstation facility.

For ease of understanding the Author has separated the parameters assessed under related category headings. The importance of the inter-relationships explained in each section should not be underestimated. It should be remembered also that the results relate to trials conducted using a particular laser, a particular beam line and manipulative focusing unit, and a particular workstation providing its own unique optical, physical and environmental characteristics. Whilst parameters affected by the working system, identified by the present level of developed laser beam technology have been noted, the philosophy behind each parameter assessment should be considered in parallel with the assessment itself when relating the results to those gained or predicted on other systems.

4.1 LASER POWER AND SKID WELDING TRAVERSE SPEEDS

Heat input, the quotient of laser power and welding traverse speed, directly affects potential weld penetration and fusion zone size. Furthermore, as material coooling rate is a function of heat input (the greater the heat input, the slower the cooling rate for a particular joint configuration) then the structural properties of the weld will also be influenced. Therefore usually laser power and welding traverse speed should be considered together.

Various authors [115] [116] [117] have made comparisons of the relationships of power and speed by measuring the penetration of blind melt runs produced by different lasers. Generally they conclude the following:

1. Penetration depth is proportional to incident power at any one speed.
2. Maximum penetration is a function of laser power raised to a constant power, equation 4.01.

$$amax = k \cdot Pwp^{k_1} \qquad (4.01)$$

where tmax = maximum penetration (mm)

P_{wp} = laser power (kW)

k = constant

k_1 = constant

The values of k and k_1 as assessed by Kaye [117] for the CL10 laser

are given as 3.03 and 0.8 respectively.

3. Penetration depth is exponentially dependent on the traverse speed.

The different constants of proportionality derived by each author will probably be due to the differing beam characteristics of each laser, focus spot size, beam mode and power stability, and to the effectiveness of the plasma control methods employed.

Having decided to use the Culham Laboratory designed and located CL10 laser for processing trials, a preliminary assessment was made of its welding capability. Curves of "blind" melt run penetrations against traverse speed for varying powers using CL10 have been produced by Kaye et al [117], figure 4.01a. In order to compare welding procedures for each trial plate thickness by assessing the heat inputs required to produce equivalent depths of melt run penetration, Kaye's results were replotted to form a graph of input power against the heat input required to produce the set penetration, figure 4.01b. This shows that for each penetration depth, as laser power reduces so the heat input required to produce a set penetration increases exponentially to a point when the keyhole becomes unstable (traverse speed of between 4 and 5mm/second). This increase in heat input (or reduction in speed for a particular power) will be due to a reduction in the heat transfer efficiency because of the increasing effect of plasma interaction absorbing beam energy above the joint surface and the increasing loss of heat to the parent plate.

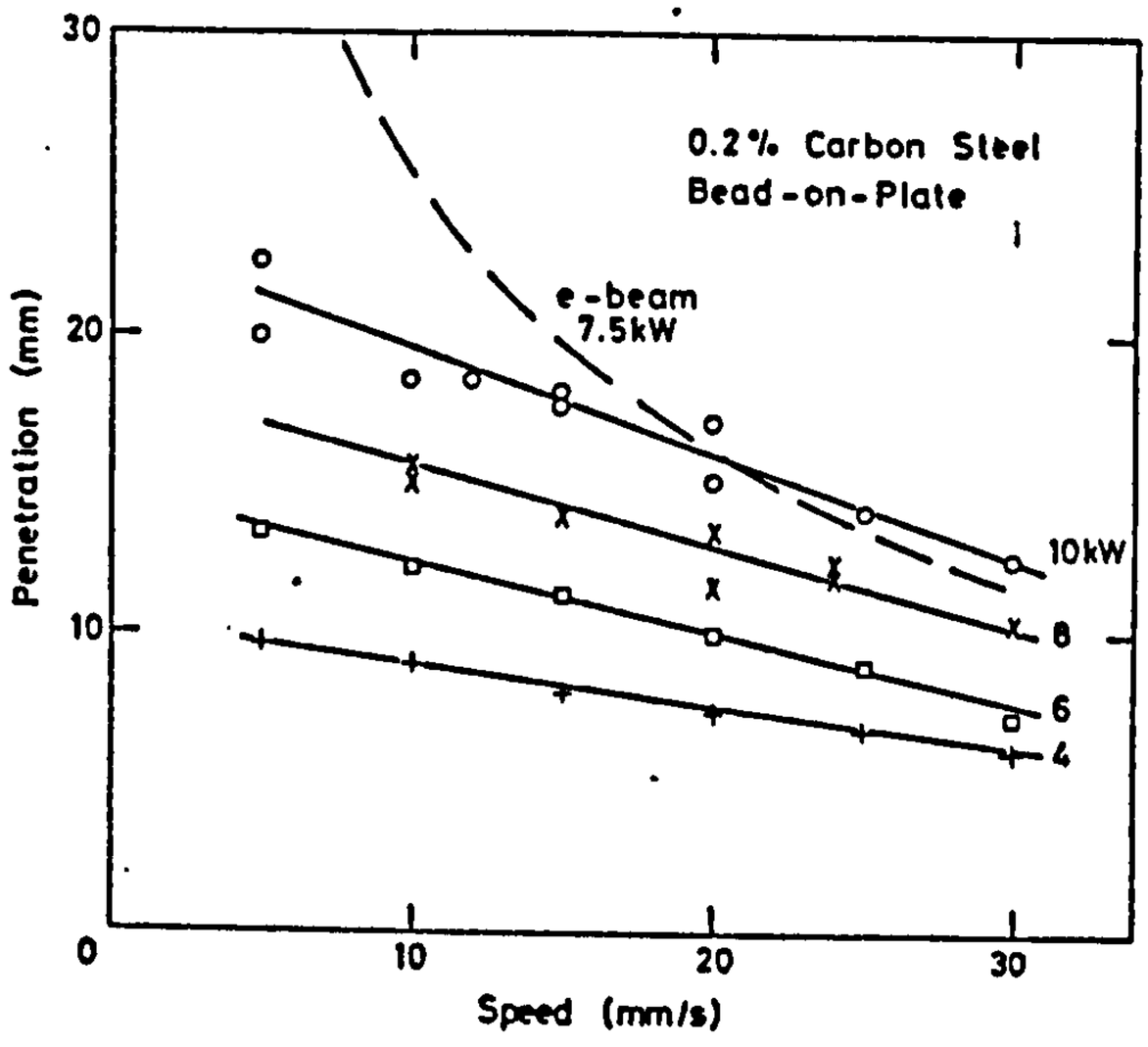

Figure 4.01a - Blind melt run penetration using the CL10 laser (after Kaye et al [117])

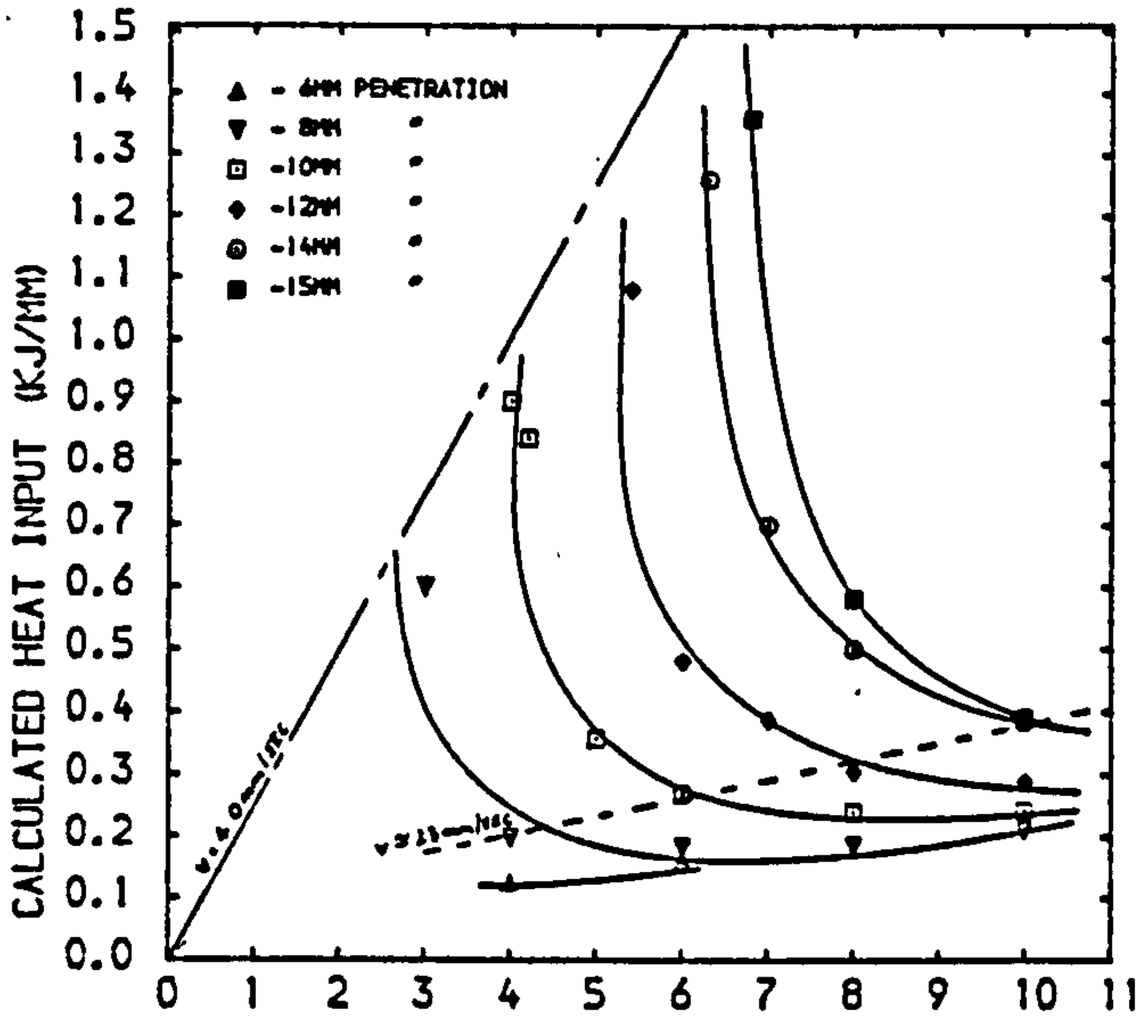

Figure 4.01b - Heat inputs needed to enable blind melt run penetrations of 6-15mm at various powers using a CL10 laser - data from Kaye et al

For the particular laser system used, the traverse speed at which the required heat input appears to rise sharply is at about 23mm/second. This also shows that ideally there is a minimum power level that should be employed to ensure efficient welding to a particular depth of penetration without an excessive loss of processing efficiency.

For skid welds using filler wire when small smoothing beads are required on the incident and emergent sides of the joint, overall penetration must include the "leg" length of these beads in addition to the web plate thickness.

Therefore, if there is a requirement for smoothing beads with a leg length of 2mm on each side of an 8mm web joint, a penetration capability of 12mm would be required.

A factor must also be introduced into a comparison intended to account for any change in processing efficiency due to a change from the blind melt run situation of the curves provided and that of a penetration joint with gaps and an open keyhole root. Melt runs produced by the Author were assessed to calculate the melt efficiency of production. Whilst melt efficiencies of 48% were obtained for blind melt runs, full penetration efficiencies averaged 26% - a reduction factor of 46%.

By assuming similar processing efficiency as the melt runs, the minimum power required to enable equivalent skid welding penetrations without excessive power loss in the joint could be estimated. Similarly

by assuming 46% reduction in efficiency between the melt run and the skid weld an estimate could be made of the likely trials processing speed achievable, table 4.01.

The results indicate that for skid welding plate thicknesses of greater than 10mm, although penetration may be achieved using the 10kw laser, the effect of increasing plasma interaction and reduced tolerances could be a problem in achieving the required skid weld penetrations.

However, during trials the majority of weld runs were made using 9kw at the workpiece(WP) this being the maximum power which the operator could guarantee to provide at the workpiece. With about 2% loss of power in each of 5 mirrors in the beam line, this required the laser to produce 10kw - at the laser output (LO) consistently. Power was only reduced from the 9kW(WP) either to assess the effect of reduced power on weld properties (6mm plate), or when, with the machine table traverse speed at its maximum limit of 40mm/sec., a lower heat input was required to produce satisfactory joint profiles (3mm plate).

4.1.1 Traverse speeds for skid welding flat plate webs

For each web plate thickness, skid welds were produced using a range of traverse speeds and various laser beam spot heights. An upper speed limit was set when full emergent bead penetration failed; the lower speed limit was set when the leg length of the emergent bead,together with any "extended" fusion zone, became greater than the incident bead leg length.

Web plate thickness (mm)	Estimated penetration to form smoothing beads (mm)	Power for equivalent blind melt run penetration (kW)	Speed to gain req'red pen't'n assuming 46% power loss (mm/sec)
6	10	6.5	18.4
8	12	8.0	15.1
10	14	9.0	11.9
12	16	10.5	8.6

Table 4.01 - Estimates of the minimum processing powers to avoid excessive heat losses and an estimate of potential processing speeds

Initial trial speeds in 10mm thick plate, when, to include penetration for smoothing bead formation a total penetration of 14mm would be required, were calculated from table 4.01. However, once the first speed survey had been conducted and processing efficiency was found to be nearer 50% for the skid welds in 10mm plate, the results were taken into consideration when assessing the likely speed range to be used on other plate thicknesses.

Joints with a nominal gap (0.1-0.5mm) were used with a filler rate calculated to fill the gap and supply sufficient material to form the set size of sealing beads.

Figure 4.02a-b show appropriate criteria determined for skid welding plate thicknesses from 3mm to 15mm with nominal gaps. Figure 4.02a shows the traverse speed envelope for skid welding 6-15mm plate with 9kW(WP) laser power•figure 4.02b shows the speeds used for skid welding 3mm plate when the power was reduced to 5kW to reduce a susceptibility to the formation of porosity in the emergent bead. A comparison of typical weld profiles, both as external views and macrographic sections is presented in Appendix B, figures B4.01-4.06.

From a visual assessment of the external shape of each weld produced, an acceptance tolerance envelope has been constructed within which the Author would consider that visually sound welds could be produced with balanced smoothing beads. The effect of welding at speeds above and below this band is noted. The most apparent parameter settings which

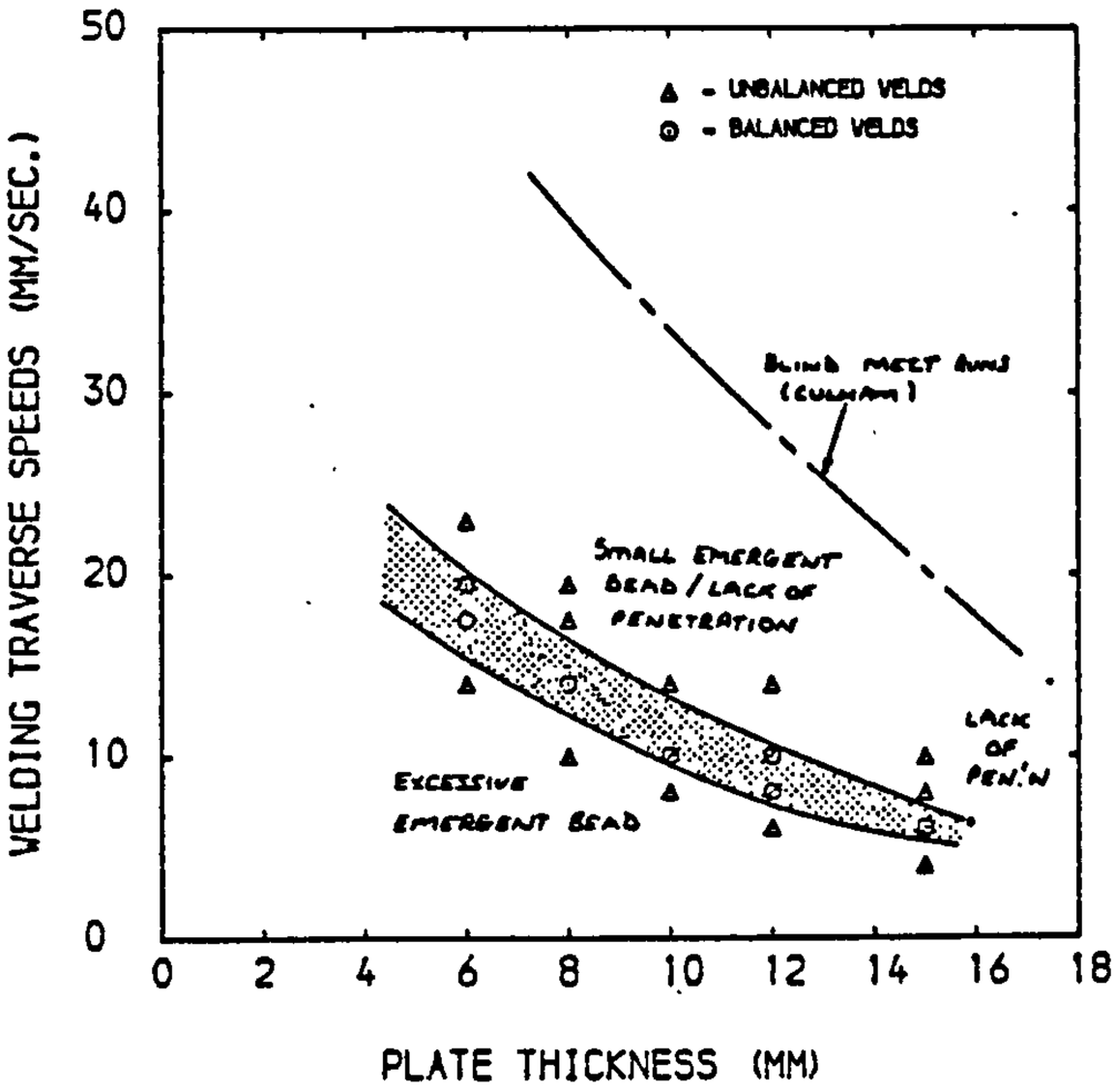

Figure 4.02a- Traverse speed envelope for skid welding flat plate tee section joints using 9kW(WP) for 6-15mm plate

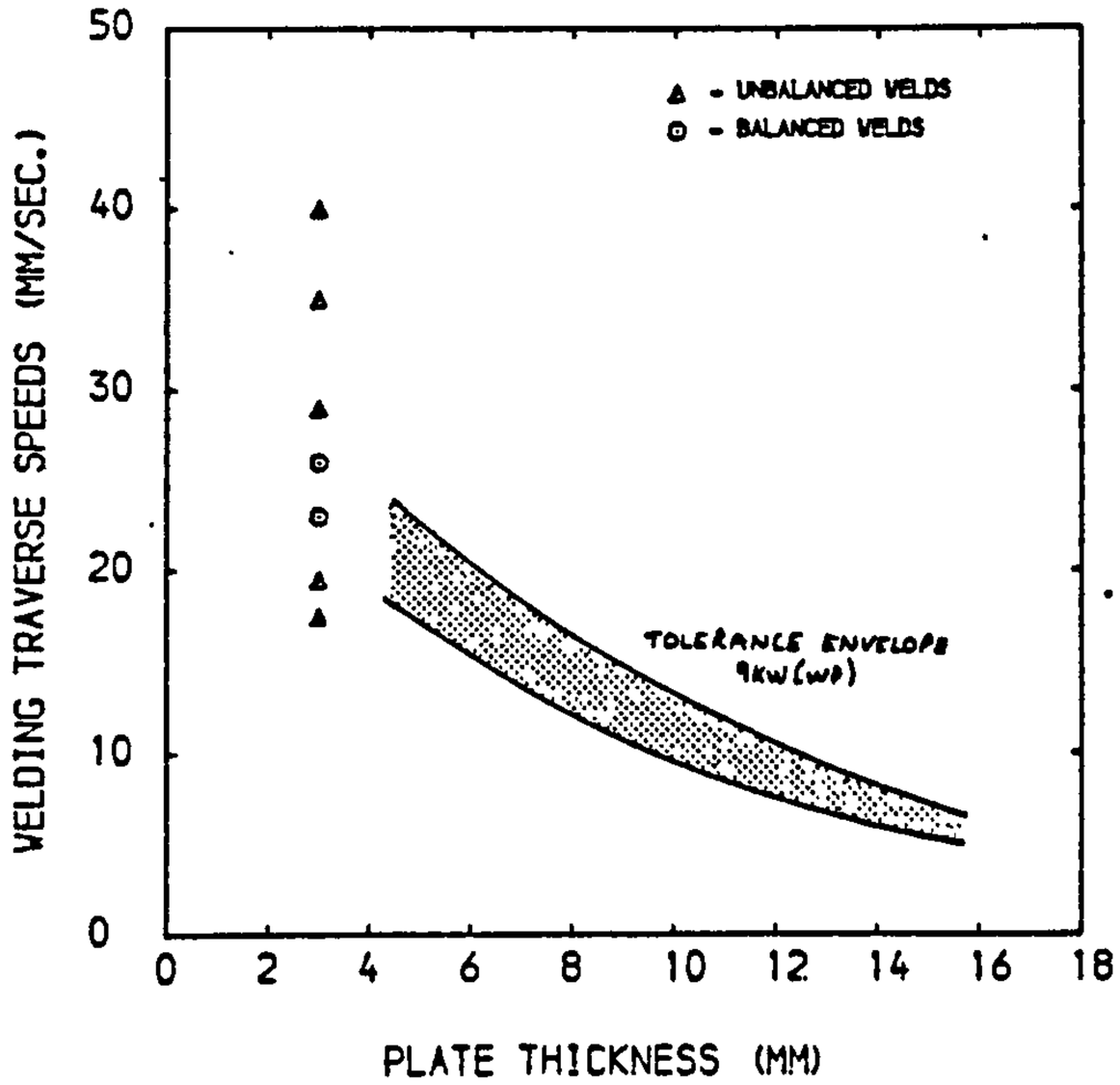

Figure 4.02b- Traverse speed envelope for skid welding at powers lower than 9kW - 3mm plate,5kW(WP)

gave balanced weld profiles within the tolerance envelope for nominal gap welds were designated "optimum" for the given conditions so that when welding with a changed joint configuration eg with a rolled section web plate, comparisons could be drawn.

While consistent results were obtained using 9kW(WP) for welding 6mm up to 10mm plate thickness with visually balanced smoothing bead profiles, for 3mm plate the power had to be reduced to 5kw in order that levels of porosity in the emergent bead could be controlled.

Whilst satisfactory joints were produced for 12mm and 15mm plate, the tolerance envelope was much narrower. Emergent beads became less smooth and inconsistent along a weld length for particular parameter settings. The apparent change in the process was also characterised by a change in the plasma balance - the intensity of the plasma at the incident side compared with that of the emergent side observed during the welding process itself.

While plates of less than 10mm were being welded at appropriate traverse speeds to produce visually acceptable balanced beads, a steady and intense plasma light was observed both on the incident side where the beam struck the joint and at the emergent side, figure 4.03. As traverse speed increased and resulting emergent bead reduced in size, so the plasma light was more dominant on the incident side, similarly as traverse speed reduced, so the emerging plasma dominated.

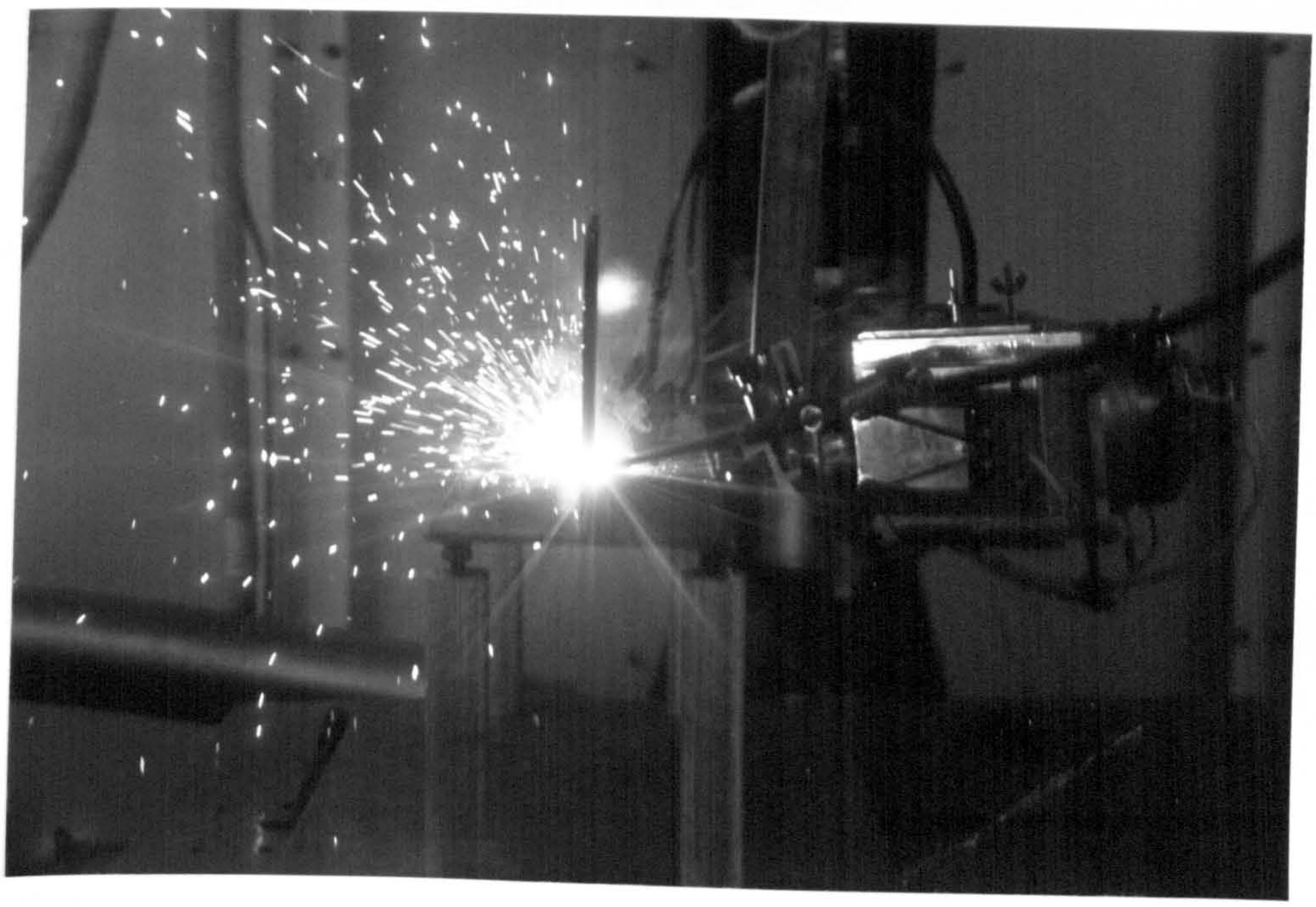

Figure 4.03 - Balanced plasma on both the incident and emergent side of an 8mm joint during skid welding

However, for web plate thicknesses above 10mm there was a tendency for the emerging plasma to become intermittent. The characteristic of the light fluctuated from the intense plasma light which obscured any view of the forming weld bead, to a bright glow when the flow of molten penetrating bead material could be clearly seen i.e. the light was much less intense. At times there would be no emerging light. Also as the light intensity reduced on the emerging side, so the intensity increased on the incident side. The resulting weld profiles tended to fluctuate, showing variations in penetration and inconsistencies in the volume of material flow to form the emerging bead.

The reasons for these apparent process fluctuations could be attributable to three factors:

1. The laser power is insufficient to maintain a sufficiently stable zone of the keyhole at a depth into the plate to form a consistent emergent bead.
2. For the given laser beam incident angle and a set spot height on the low side (so as not to risk any lack of fusion of the incident bead with the face plate surface) the natural line of the keyhole is to bury into the face plate prior to the web plate back edge. In consequence less energy is released from the root of the keyhole to create a properly fused emergent bead.
3. Filler wire input compounds the effects of "1" and "2" above. The thicker material requires proportionately greater quantities of filler material to fill a gap. Also, material must flow further from the front of the joint to form the emergent bead. As soon as a small

processing variation reduces penetration, e.g. slight beam instability or gap changes, a build-up of filler may occur nearer the keyhole mouth. Beam absorption at this point will increase and penetration will reduce still further. Full penetration is then regained once the beam has traversed over the material built up.

The fluctuations can be stopped by increasing spot height above the face plate. The natural line of the keyhole root lies nearer the face plate surface at the web plate back edge hence increasing the opportunity of heat flow to help form the sealing bead. However, with the increased spot height there is then a risk of lack of fusion between the incident bead and face plate surface.

This apparent limitation to producing skid welding joints of web plate thicknesses greater than 10mm may be overcome by the following actions:

1. Increase laser power to ensure more consistency in the stability at the root of the keyhole.
2. Devise optics to supply a narrower divergency in the incoming beam to enable angles of incidence of less than 7 degrees to be used.
3. Increase the width of the molten zone using a defocused beam or beam spinning so that full fusion can be ensured at both incident and emergent beads.

4.1.2 Effect of joint gap on skid weld traverse speeds

Having established appropriate traverse speeds for welding joints with nominal gaps, these speeds were then used as the starting point for welding joints with observed gaps. The best spot height found for welding each plate thickness with a nominal gap was used for joints with gaps until the gap distance became greater than twice the spot height. After this height, a spot height of half the gap distance was employed to ensure efficient interaction of the laser beam and intercepting filler wire.

If a successful weld was not produced at the initial settings, traverse speed was reduced on subsequent welds until a fully fused joint was produced, preferably with visually balanced smoothing beads.

Filler input was initially hand calculated to fill the joint gap volume and produce smoothing beads. However, at a later stage the a program, named "SKIDFILL" was designed and written (explained in detail in section 4.2) to calculate the filler input rate compensating for changes in penetration for each plate thickness.

Figures 4.04a-b show the parameters used for skid welds run with joint gaps of 1.0mm and 2.0mm and the tolerance envelopes found for enabling the production of visually satisfactory weld profiles. Similar to the nominal gap envelopes, these were determined from visual inspection of the welds, comparing smoothing bead sizes for respective parameters to

determine the limits of the parameter settings.

Generally an increase in joint gap required a reduction in traverse speed to enable a satisfactory joint to be formed. For thinner plate e.g. 6mm, there was greater tolerance and speeds nearer the nominal gap "optimum speeds" could be used. This was because of the excess power available to penetrate the relatively thin plate not being efficiently utilised for a nominal gap hence giving excess capacity for bridging a larger gap.

However, for plate thicknesses greater than 12mm, the opposite was true. The reduction in tolerance found while welding nominal gap joints was compounded for gap joints due to the increased amount of filler material entering the joint. This material tended to absorb the laser power at the incident side with a resulting reduction of material flow to form the emerging bead.

For plate less than 12mm thick, the presence of a joint gap was found to be advantageous in producing a well balanced joint profile. This was especially true when the joint gap was sufficient for the filler wire to be inserted into the middle of the joint to ensure interception of wire and laser beam as far into the joint as possible. By this method, very well balanced smoothing beads could be formed with a good transfer of material to the emergent side, figure 4.05. The balance of the process was confirmed when observing the weld in progress. A balanced plasma could be observed to each side of the joint web.

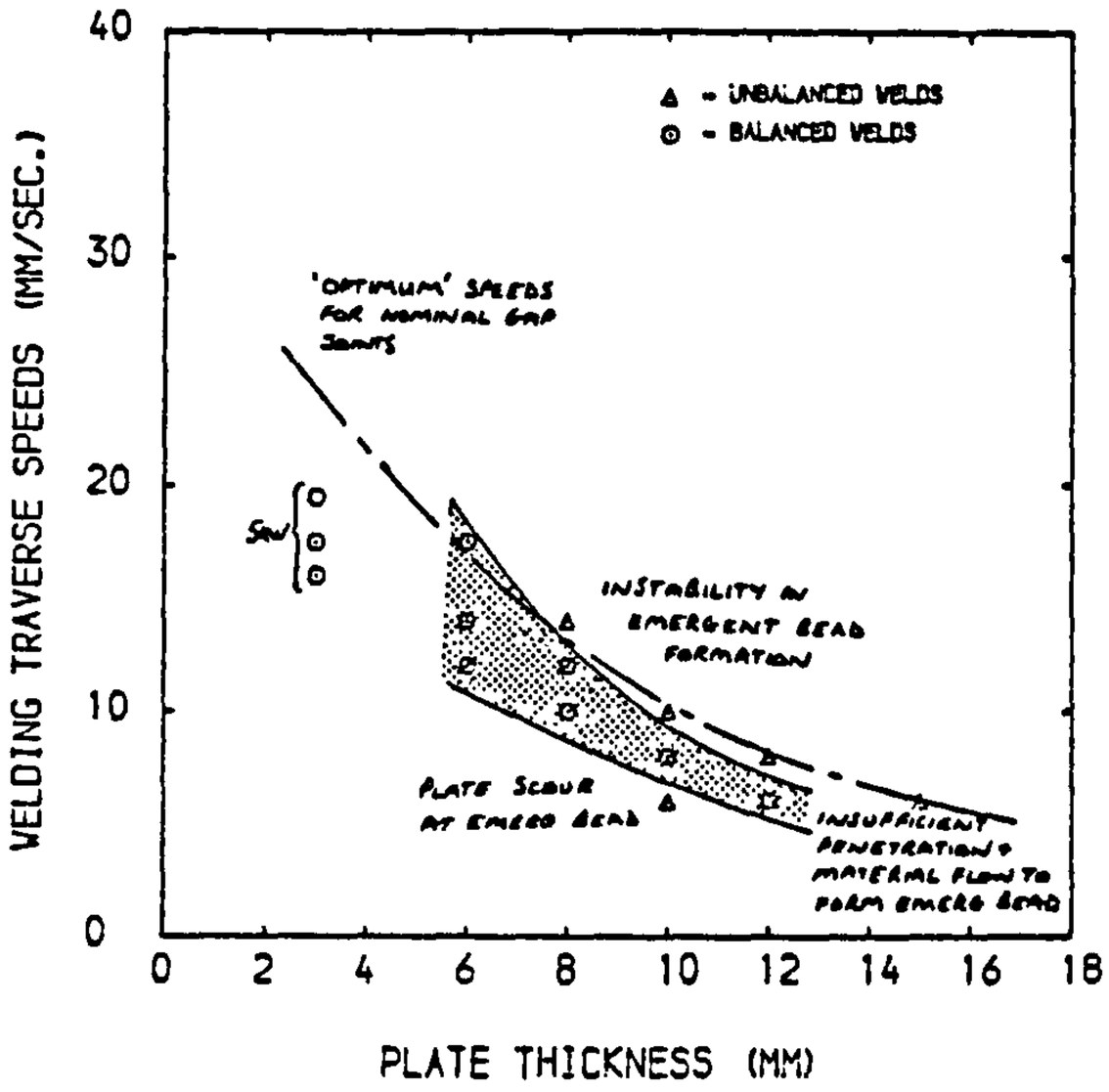

Figure 4.04a - Traverse speed envelope for skid welding gap joints (1mm gap) : laser power 9kW(WP)

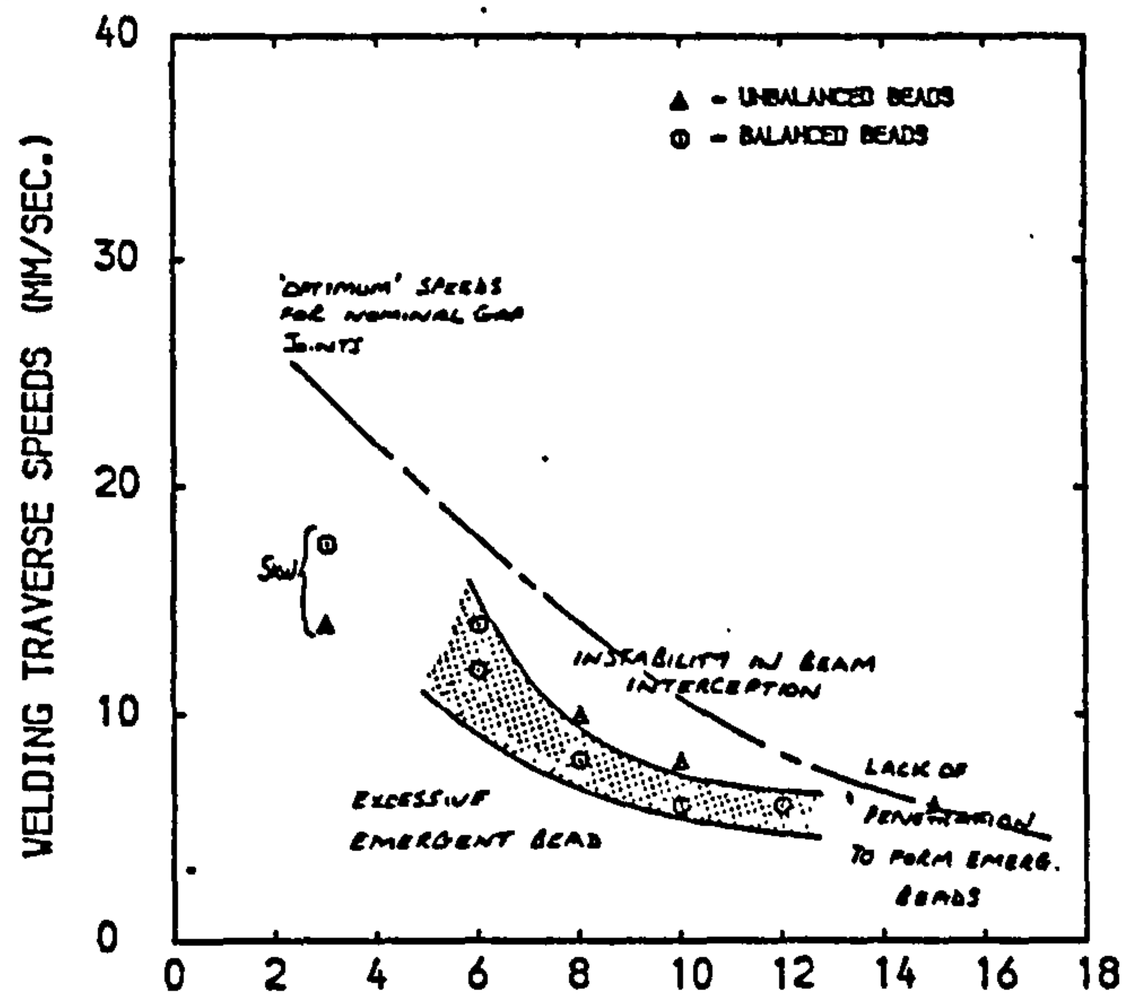

Figure 4.04b - Traverse speed envelope for skid welding gap joints (2mm gap) : laser power 9kW(WP)

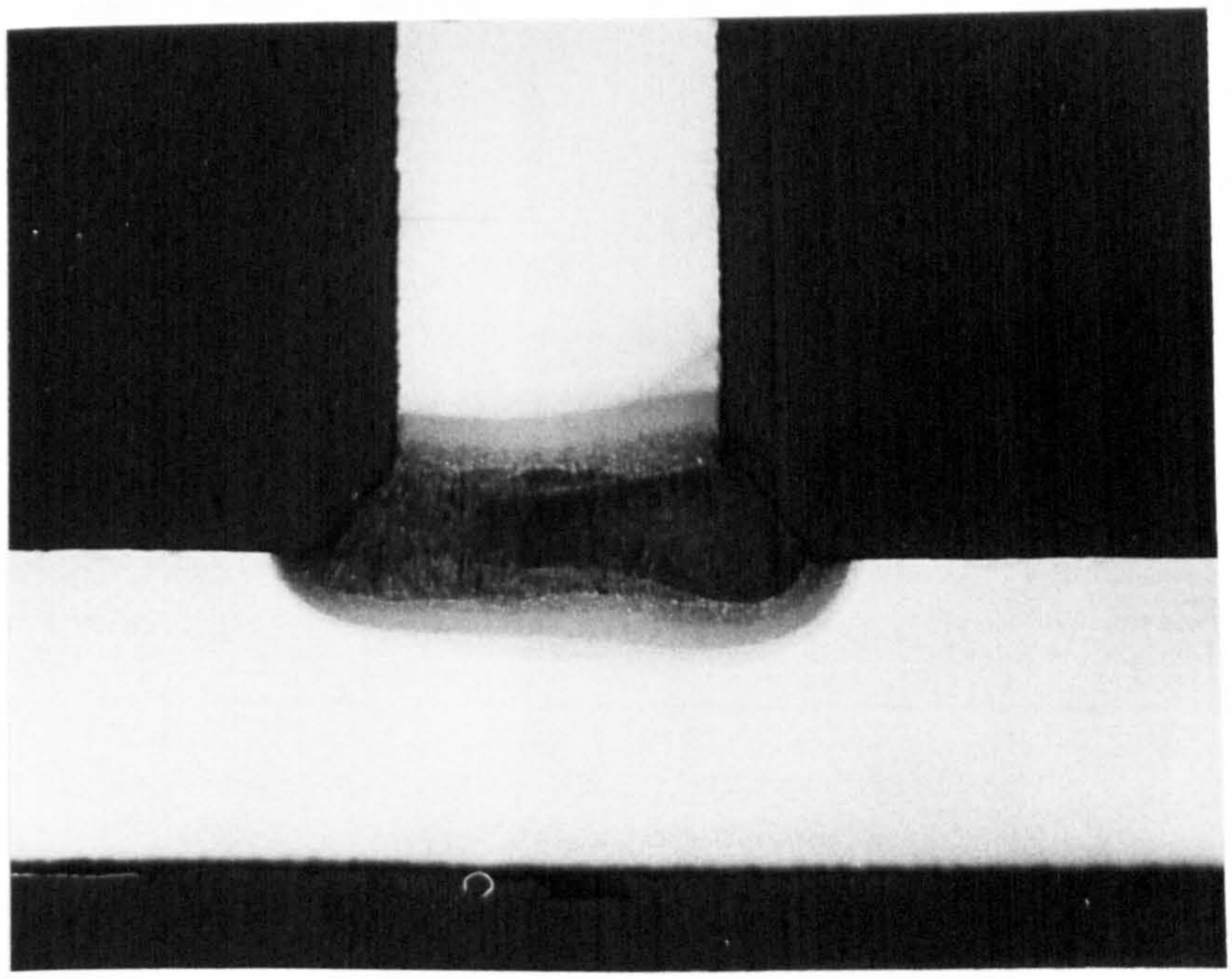

Figure 4.05 - Skid weld produced in a joint in 6mm thick plate containing a gap of 2mm and showing well balanced beads (X4.8)

A precautionary safety note should be made clearly at this stage. For the finite time before wire and laser beam intercept (about one second during trials) the raw beam projects clear through the joint gap. Although the quickly diverging beam failed to penetrate the face plate surface behind the joint web there was sufficient power density at the workstation wall, approximately one metre away, to burn the painted surface. Therefore, when full absorption of the beam into the joint cannot be guaranteed, either for a direct or errant beam, a procedure will have to be devised to ensure personnel safety. This would not only need to be applicable to the skid welding situation but also for the butt and through welds conducted in the down handed and other orientation. Such a procedure has been described in Chapter 7.

4.1.3 Effect of plate edge shape on skid weld traverse speeds

Although the majority of welding trials were conducted using flat plate edge joints a set of comparative trials were run using rolled section flat bar. A representative set of bars was purchased from local shipyards for trials in each plate thickness.

A procedure similar to that used for gap-effect trials was used to assess the effect of a radius edge in the production of the laser skid welded joint, changing speeds and filler rates.

As shown in figure 4.06 satisfactory joints could be made at the speeds of flat plate joints with nominal gaps for plates of less than

10mm thickness. Above this thickness welding capability reduced quickly. While incident beads could be adequately formed, the flow of material to form the emergent bead reduced. This was compounded in that sufficient material was being supplied to the incident side to "fill" the radius section on the emergent side. However, as penetration reduced, the excess material remaining on the incident side served only to absorb the beam energy still further. For plate thicknesses of less than 10mm the presvence of the radius appeared to help joint production in that, similar to the gap joints, the wire could be inserted nearer to the joint centre-line hence aiding material flow to form the emergent bead.

4.1.4 Effect of plate coatings on skid weld traverse speed

Following from the conclusions of Martyr [3] , Trial 1 was conducted using coated plate assuming that within the skid welding process the products of paint combustion would be ejected from the emergent side. However, after inconsistent results during trial 1, further investigation confirmed that primer coatings on the plate surface affected weld reproduction and often initial production of a skid welded joint.

The most noticable effect during this welding process was a dramatic increase in the sparks being ejected from the emergent side and a significant "spluttering" noise from the process. The resulting weld was generally characterised by mass surface porosity in the emergent bead.

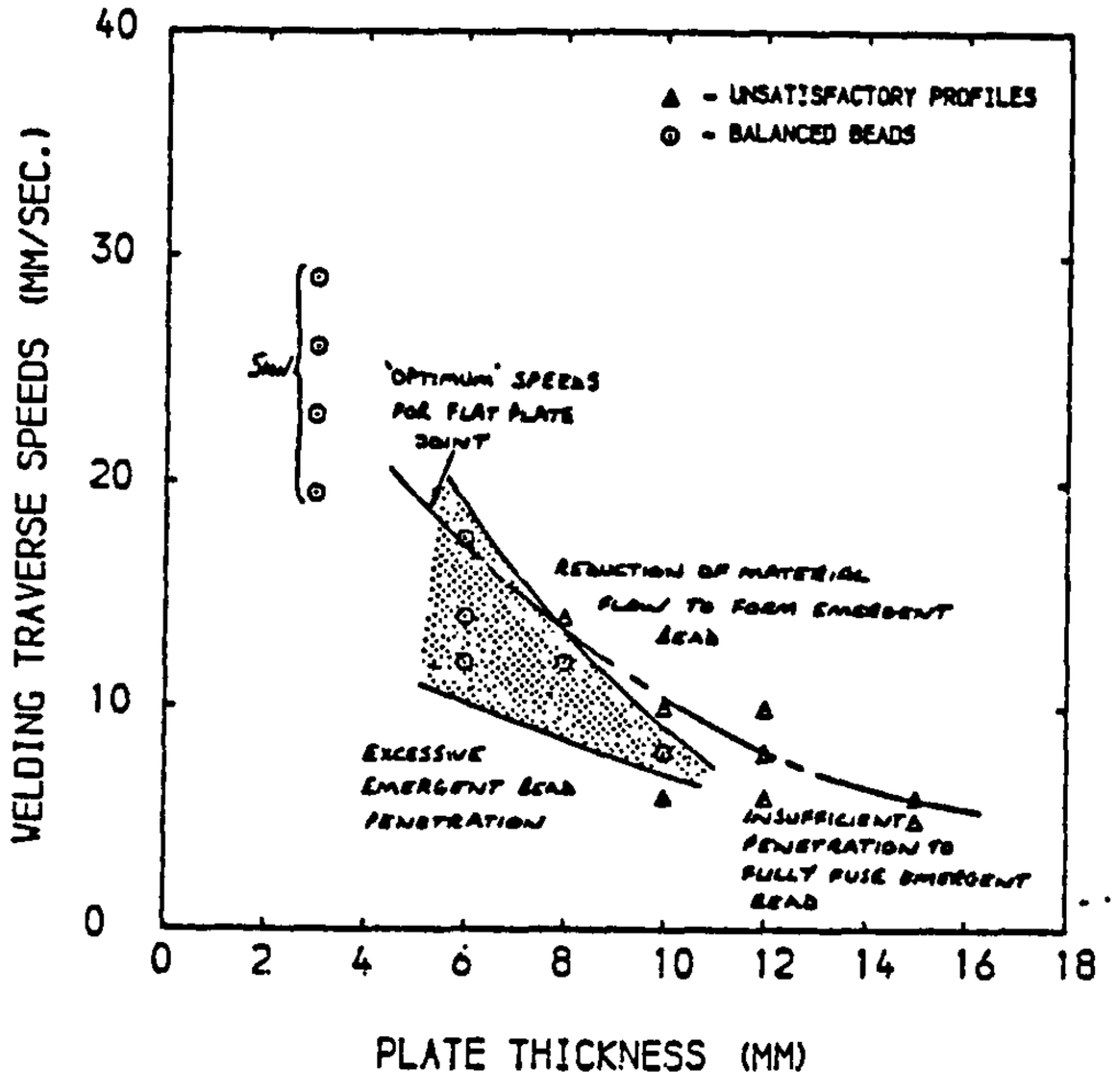

Figure 4.06 - Traverse speed envelope for skid welding rolled section tee section joints ; laser power 9kW(WP).

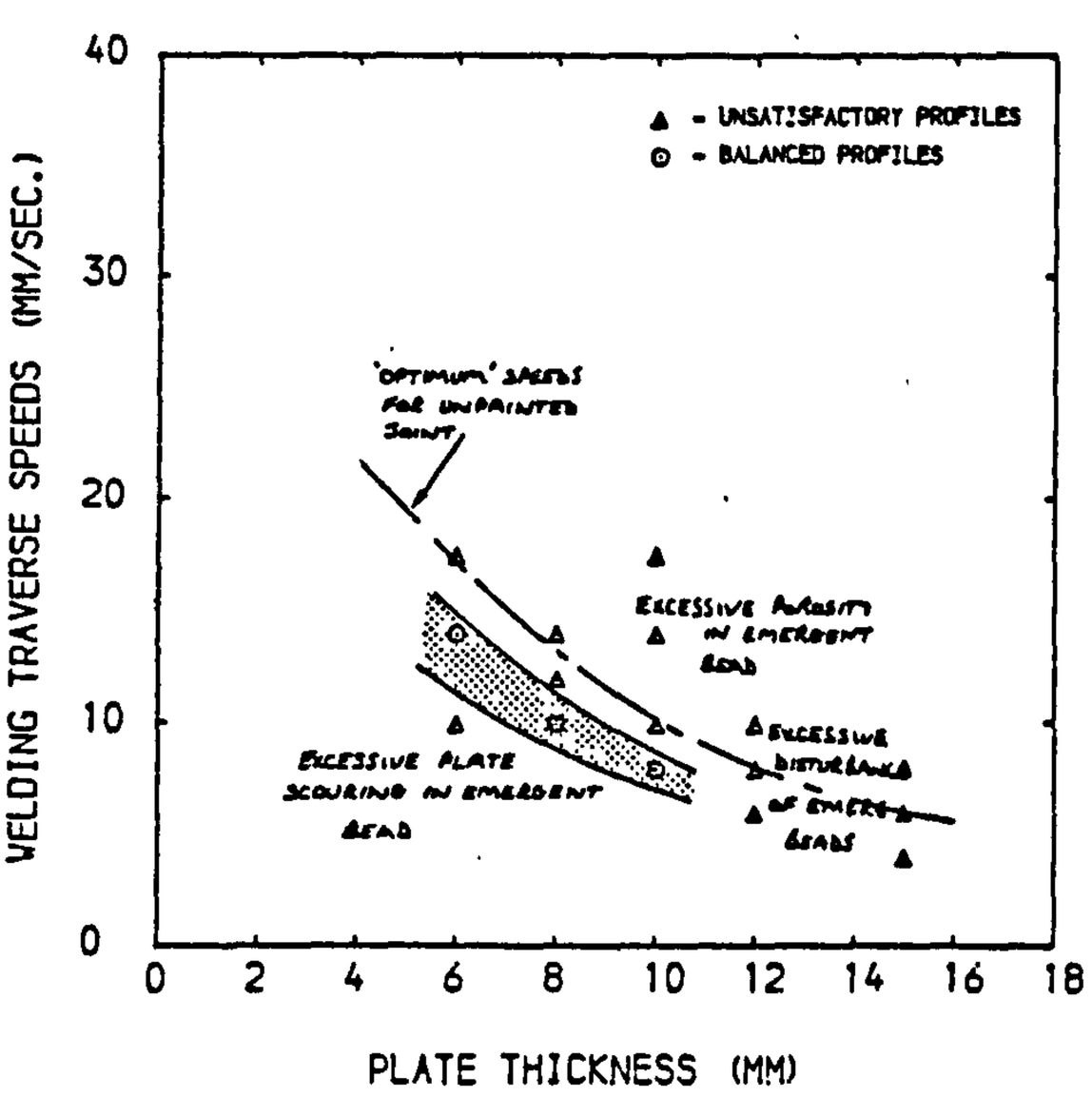

Figure 4.07 - Traverse speed envelope for skid welding tee section joints with primer on the plate surface ; laser power 9kW(WP).

By reducing traverse speed by about 20% some more consistent results could be obtained for plate thicknesses up to 10mm. For greater thicknesses the inconsistency remained. In addition there was a tendency for "blow-backs" from the incident bead. There appeared to be a gaseous build-up, indicated by an increase in the incident plasma, which then exploded from the incident bead. As a result a cavity was left within the incident bead surface.

For the plate thicknesses where satisfactory joints were formed, the speed tolerance envelope appeared to be narrower compared to that constructed for non-coated joints. As traverse speed was reduced the tendency for plate "scouring", creating undercut at the toe of the emergent bead, increased. This was due to an increase in the volume of gas ejected from the keyhole root, disturbing molten material which would normally be absorbed in forming the smoothing bead.

The detrimental effect of primed surfaces on both laser and conventional processing has been reported by other authors [118] [51] [119] . While the effects of primers vary depending on constituents and application, a product to give consistent welding characteristics remains to be found.

At present only MMA and gravity welding is used to produce fillet welds on primed plate with any confidence within shipyards. Generally surface paint is removed by mechanical grinding or isolated shot blasting(pencil blasting) prior to the use of any semiautomatic or

automatic welding process.

If sufficient tolerance cannot be gained for using the laser on painted plate, the laser itself provides an alternative energy source for clearing the painted surface. By defocusing the beam and traversing the designated cut path at speeds in excess of 12m/minute a controlled zone of paint can be removed. This method of surface scorching has been proposed for marking plate surfaces to inscribe datum lines and even operator instructions on plate piece parts. The Author has witnessed also a two-pass method for laser cutting coated plate, the first scorching the surface to remove a narrow region of paint and the second path making an efficient high speed cut. This technique could similarly be used for welding applications when the region to be welded would be cleared of paint by traversing the defocused beam at a speed of 9-12m/minute.

4.1.5 Effect of skidwelding through tack welds

Trials were conducted to assess how the presence of a tack weld on the joint line affected the formation of a continuous skid weld. Tack welds were placed firstly on the incident side and secondly on the emergent side of the joint. With the latter case, no detrimental effect was found as the emergent bead fused with the tack fillet. However, a tack weld placed on the incident side caused a reduction in weld penetration as the interaction point of the incident laser beam and joint material was above the joint line and power was absorbed prematurely. Introduction of

filler wire compounded this effect as filler deposits built up on the incident side.

To counteract this problem, the Author developed a laser tack weld which did not depend on the presence of any filler wire. By reducing the flow of the shrouding gas from 35l/min to 10l/min, increasing the incident beam angle to 45 degrees, and traversing for a distance of only 20mm, the initial excess of plasma and molten material as the beam first struck the plate was sufficient to fuse the plates even with up to 3mm gaps present. The fused material remained within the bounds of the web plate thickness and therefore was not detrimental to subsequent continuous skid welding.

4.1.6 Traverse speeds for skid welding at powers less that 9kw

Although satisfactory welds were produced in 6mm thick plate using 9kW(WP) of laser power, there was an occasional tendency for small pores to be formed in the emergent bead. In addition, for the plate composition initially used (C=0.199) hardness values in excess of 350Hv were encountered in the HAZ. Therefore a set of trials was conducted to assess the effect of reducing heat input, by reducing input power for set traverse speeds. Figure 4.08 shows how traverse speed needed to be lowered once laser power reduced below 7kw in order to maintain a satisfactory joint profile in 6mm plate. Conversely, there was no change to joint profile from increasing power above 8kw also and the tendency for slight emergent bead porosity seemed to increase. However, as heat

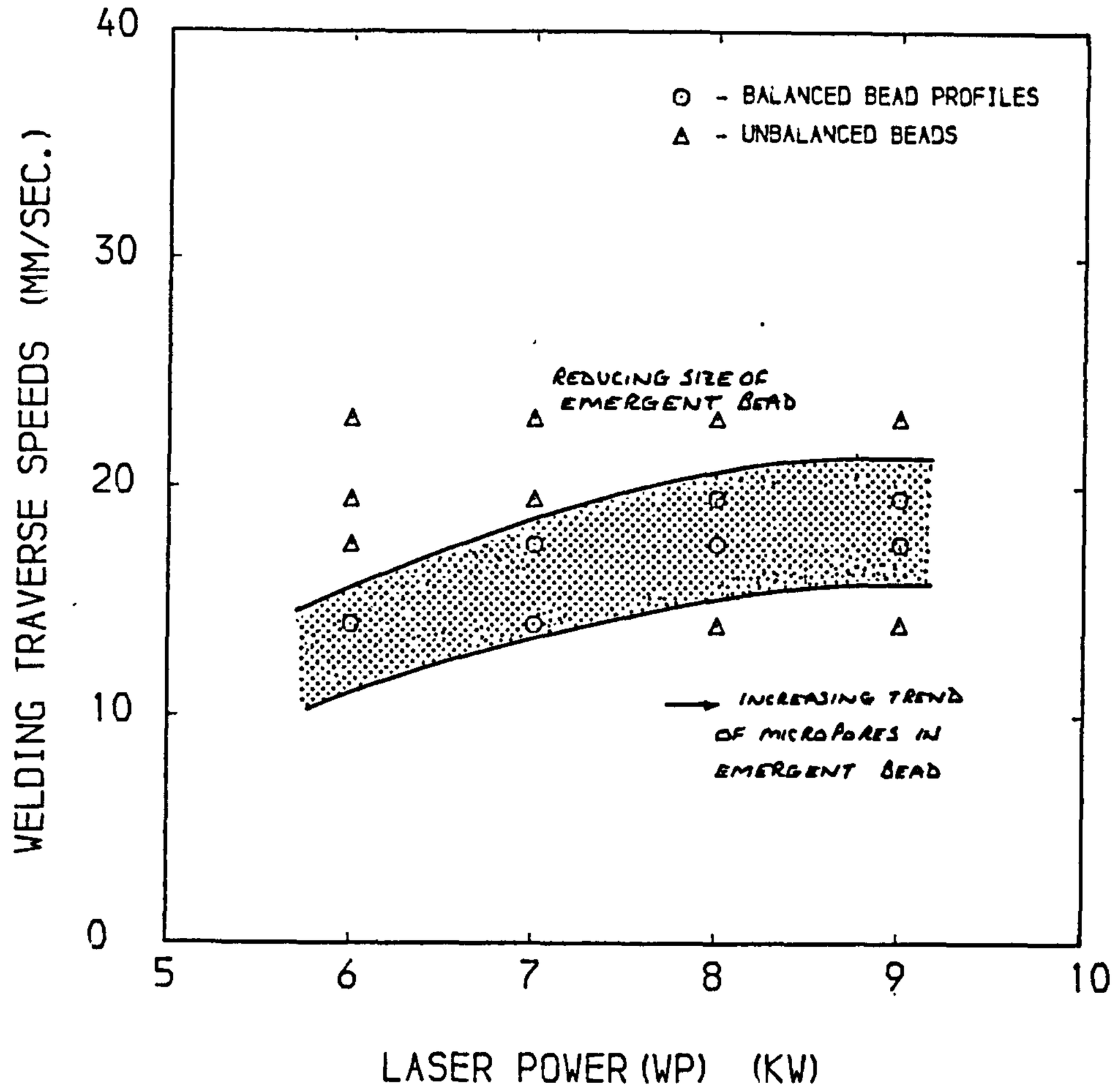

Figure 4.08 - The effect of reducing laser power from 9kW(WP) on traverse speed maintaining a visually acceptable joint ; 6mm plate.

input increased and the weld cooling rate reduced, so the HAZ hardness increased as described further in chapter 6.

For powers of 7-8kW(WP) the plasma balance could be more easily achieved whereas at 9kw the plasma appeared to be less easily balanced, even at high speeds.

The effect of applying 9kw (WP) to 3mm plate also resulted in mass porosity. Even at the maximum traverse speed of the worksupport table (40mm/second) large emergent pores remained. After intermediate trials at 7kw and 6kw power was reduced to 5kw before consistent results were obtained.

4.1.7 Correlation of laser power and traverse speed to joint shapes

Welding procedures have been assessed in terms of tolerance envelopes. In order to help correlate weld shape characteristics, welds were assessed in terms of the non-dimensional factors "X" and "Y" deduced by Hablanian [87] relating traverse speed, laser power, joint penetration and average width together with material heat functions. By comparing shape characteristics of the skid welds against the theoretical optimum, process efficiency could be calculated more accurately so that future predictions could be made for the particular joint configuration and orientation.

Fusion zone area, depth of penetration and average weld width were measured on both melt runs and skid welds macrograph sections. Values of the normalised functions X and Y were then plotted against comparative curves of optimum values of melt ratio and heat transfer efficiency.

An initial comparison for melt runs, figure 4.09, shows how blind melt runs, with melt ratios in excess of 50% representing heat transfer efficiencies of nearly 100%, may be achieved. As traverse speed is reduced to the range found for balanced skid welding with a fully penetrating melt run, heat transfer efficiency drops to 50%.

Figures 4.10 and 4.11 show similar comparisons made for skid welds in various plate thickness and with gaps increasing from a nominal gap to 2.00mm in each plate thickness. Results show how heat transfer efficiency is maintained within the 40-50% range. The effect of gaps is marginal, increasing efficiency nearer to 50%. This is probably due to the ability to insert the wire more centrally in the joint thereby reducing the plasma reaction at the mouth of the keyhole which would otherwise absorb or reflect incident radiation.

The effect of varying input power for a particular plate thickness has been assessed also, not only by analysing the heat transfer efficiency but also by calculating each individual melt ratio after first measuring directly the area of the molten zone. Having used the same traverse speed range (14.0-23.0mm/sec) for each power level, figure 4.12 shows how, while the majority of values of heat transfer efficiency remains in

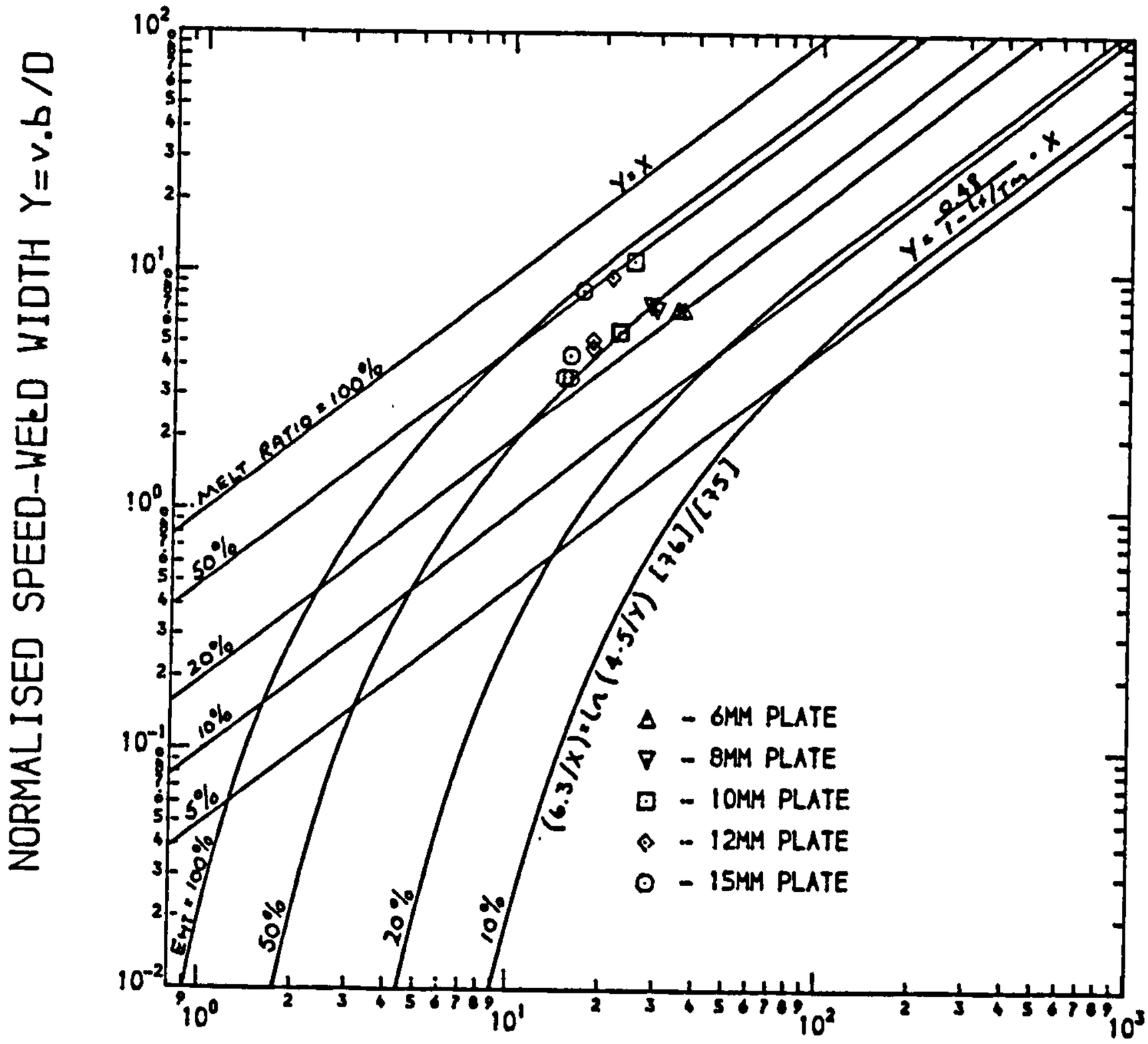

Figure 4.09 - Normalised efficiency analysis for melt runs showing the differential for blind and penetrating melt runs.

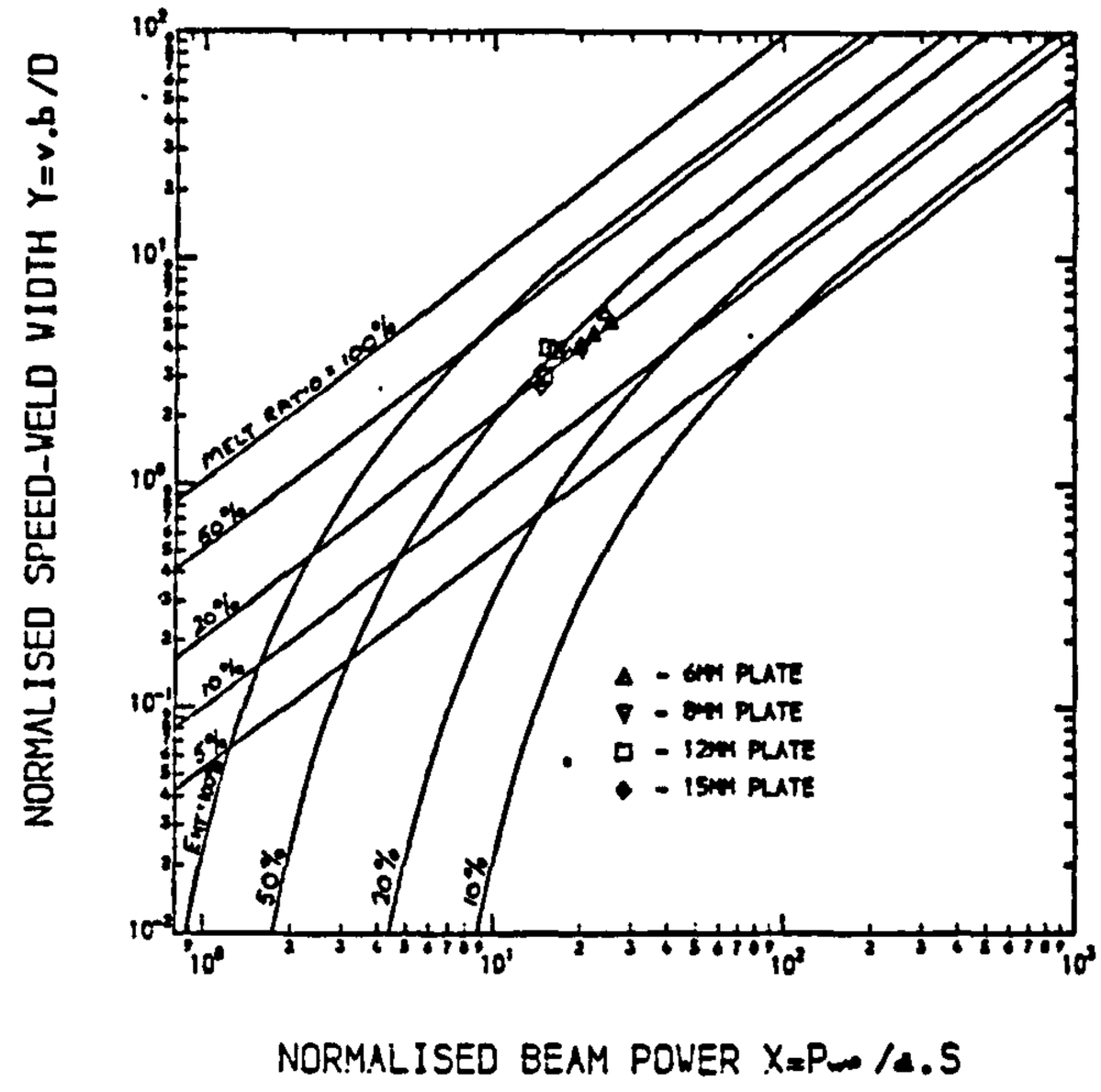

Figure 4.10 - Normalised efficiency analysis for skid welds in various plate thickness ; laser power 9kW(WP), various traverse speeds.

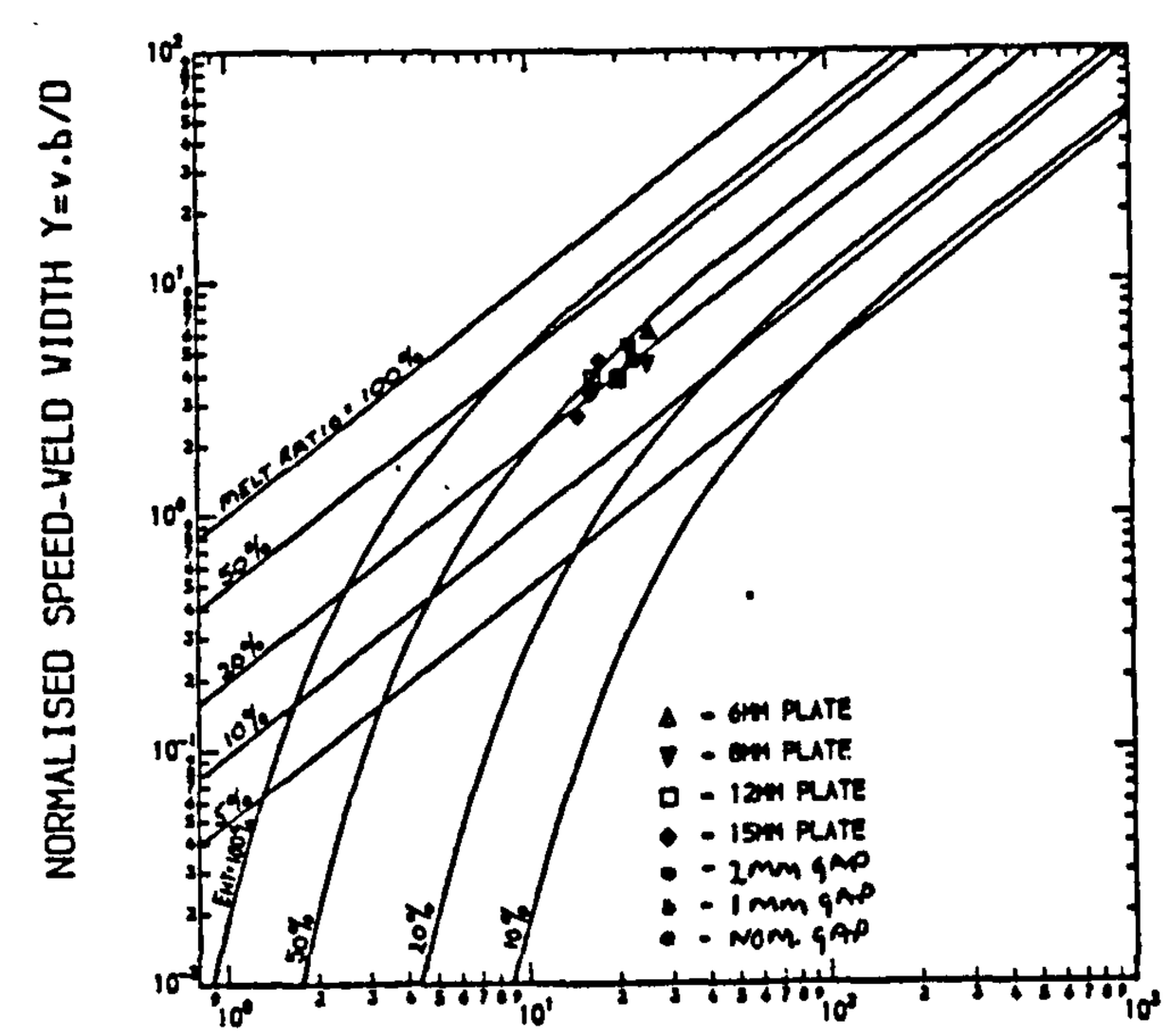

Figure 4.11 - Normalised efficency analysis for skid welds of varying joint gaps ; laser power 9kW(WP), various traverse speeds.

the band 40-50%, optimum efficiencies in excess of 50% were obtained from powers of 7kW as opposed to 9kW.

The assessment of melt ratios, figure 4.13, shows how as heat input reduced melt ratio increased. However, for each heat input an optimum power could be identified to provide highest processing efficiencies. This confirmed the view expressed whilst examining the melt run characteristics, figure 4.02, that for a particular penetration, complete optimisation of the process would require an assessment of laser power in addition to just changing traverse speed, in order to effect a change of heat input.

The efficiency factors calculated for the skid welding process can now be substituted into the equations used to calculate heat line source penetrations (Equations 2.12 and 2.13) so that, in the absence of an on-line penetration sensing device, weld penetration may be predicted. Figure 4.14 shows a comparison of predicted values; heat transfer efficiency equal to 100% and 45% to show optimum penetrations and predictions for skid welds respectively against actual penetrations for melt runs and the scatter band for trial skid weld penetrations.

Comparison between the calculated optimum penetration (Heat Transfer Efficiency = 100%) and the blind melt run penetrations shows good correlation until penetrations reach 15mm. As predicted from figure 4.02 disproportionately high heat inputs would be required to secure penetrations to greater depths as process efficiency decreases, i.e. heat

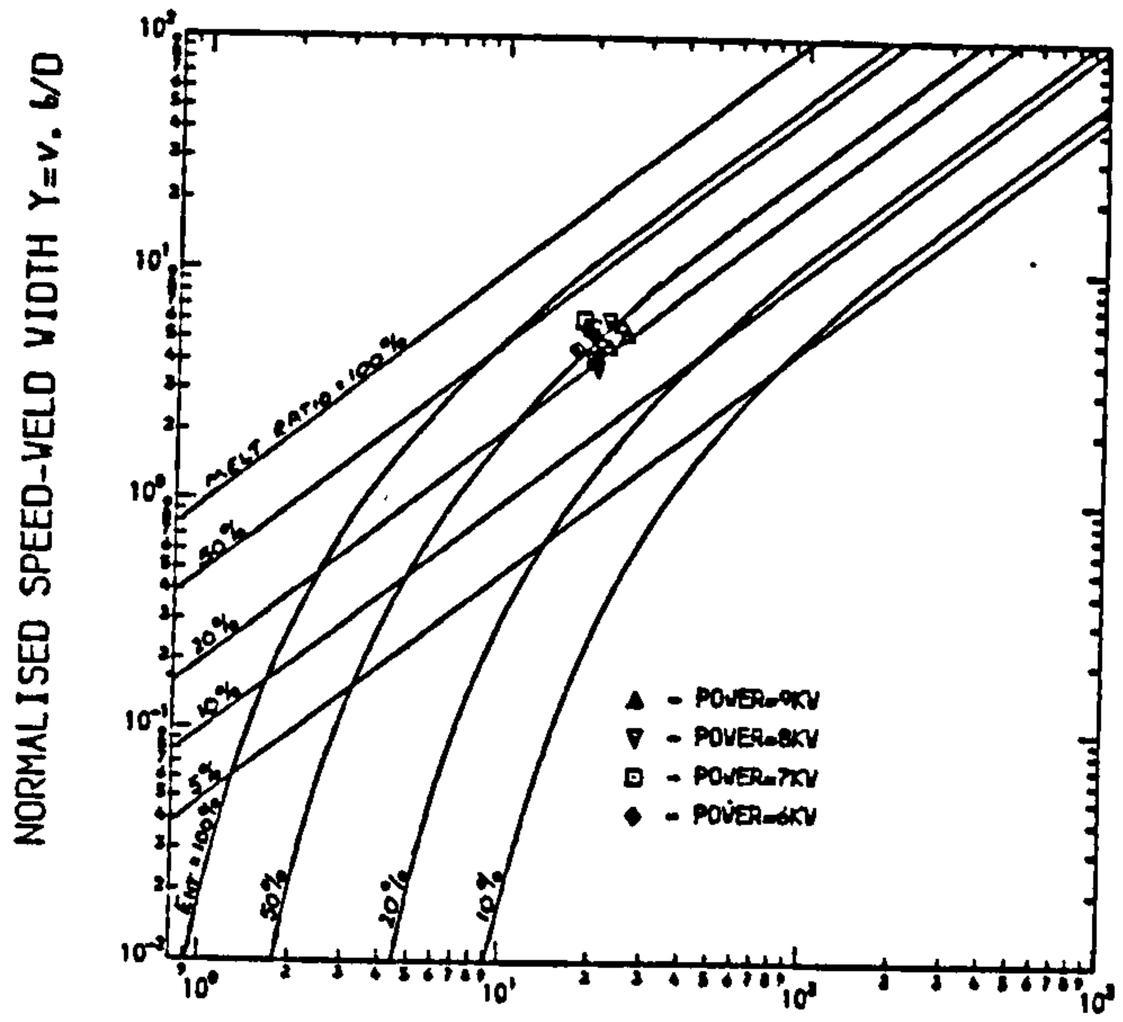

Figure 4.12 - Normalised efficiency analysis for skid welds in 6mm plate using various power inputs.

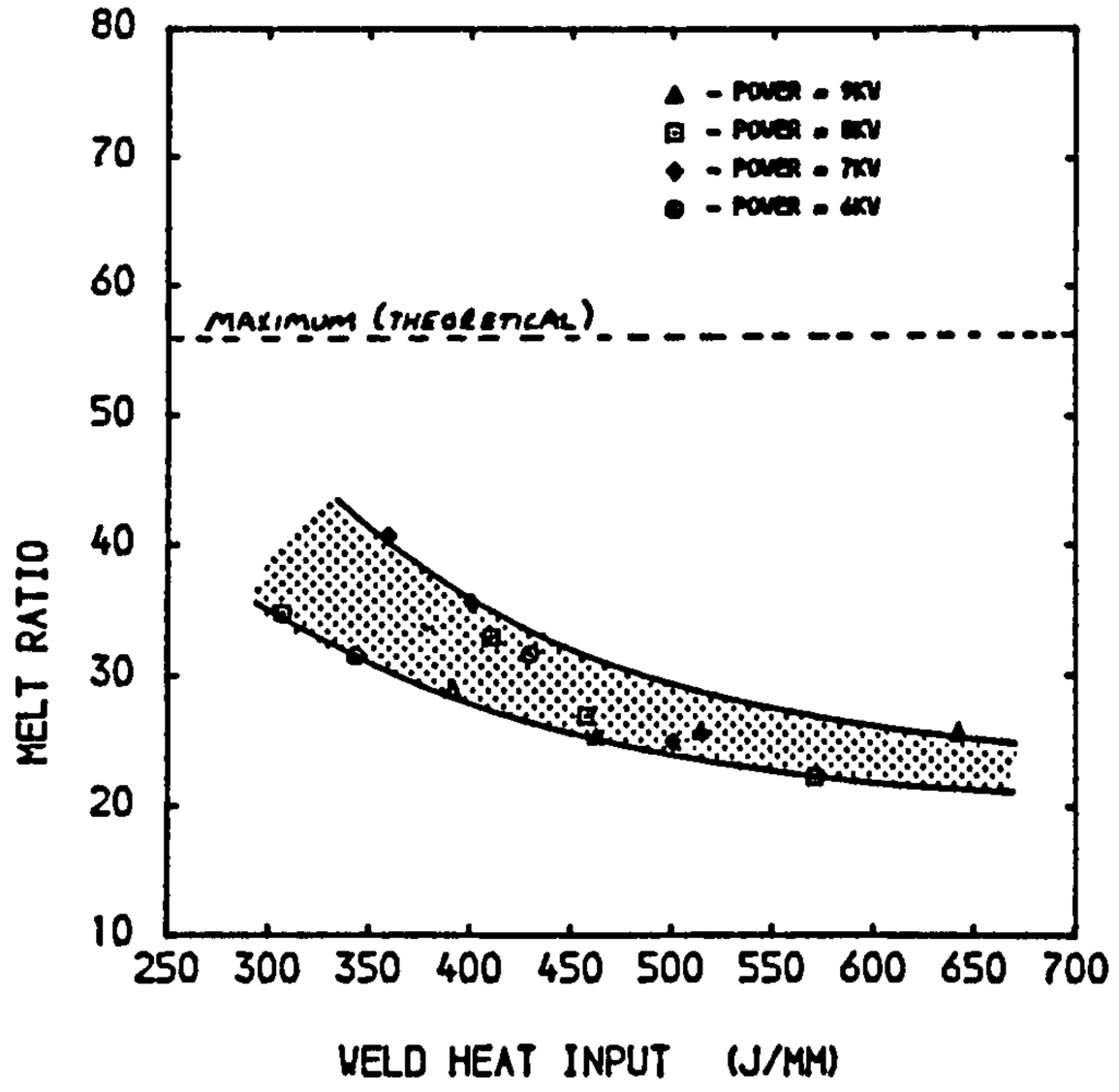

Figure 4.13 - Melt ratios of joints in 6mm plate calculated with respect to the weld zone area for various heat inputs.

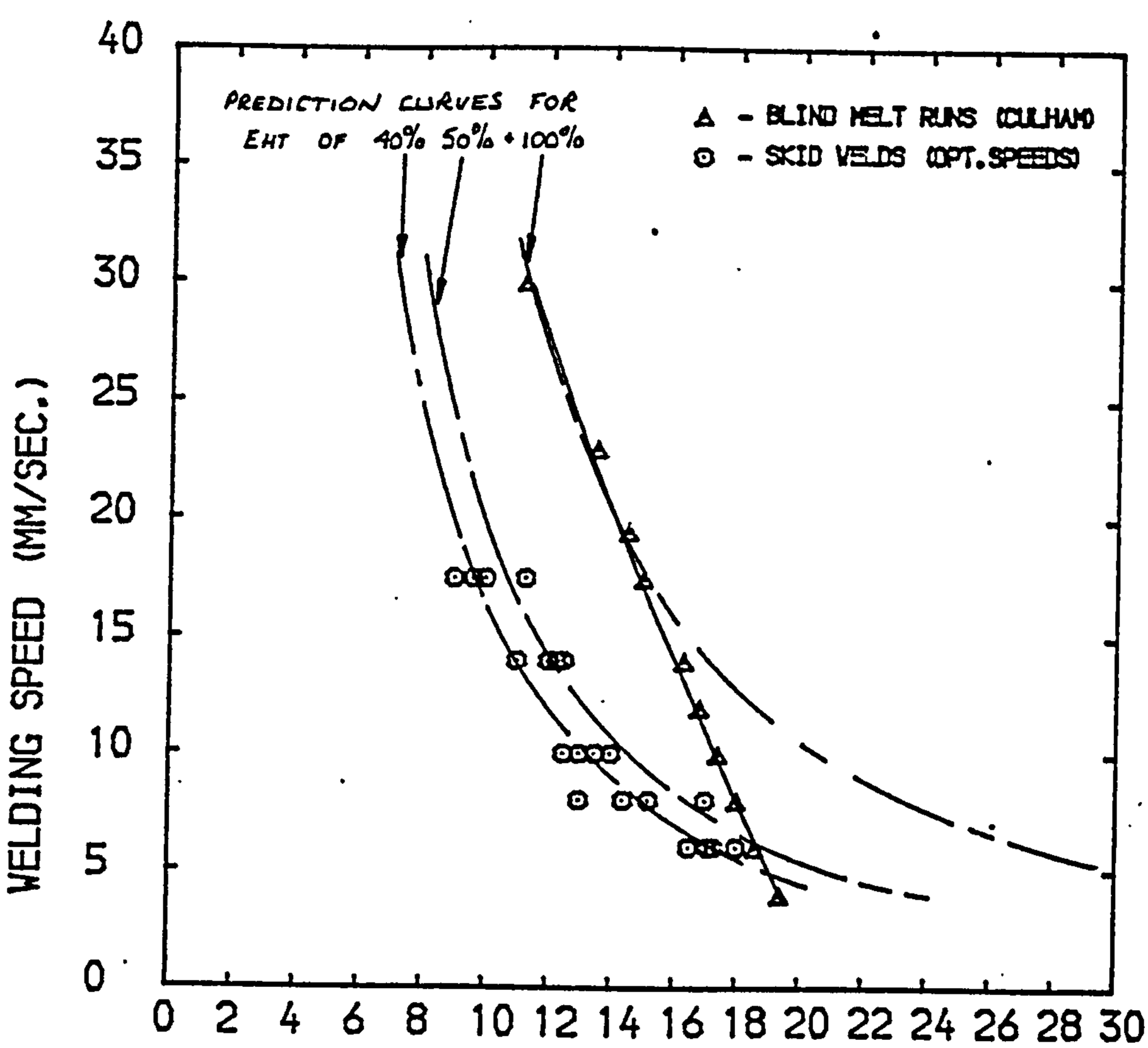

Figure 4.14 - Comparison of predicted and actual weld penetration for skid and blind melt runs using a laser power of 9kW(WP).

transfer efficiency reduces. Consequently the melt run curve moves to lower contours of heat transfer efficiency.

Comparison between the calculated skid weld penetrations (Eht=45%) and actual weld penetration shows good correlation with variations of +/- 1.0mm, representing efficiency variations of +/- 5%, for use in subsequent filler rate calculations.

4.2 FILLER WIRE INPUT

4.2.1 Assessment of filler wire input rate

The general philosophy used by other authors [120] [3] [121] [122] for calculating the rate of filler input into a laser welded joint has been to equate the volume of wire input directly to the volume of the joint gap and assume negligible loss of material. As the product of the wire cross-section area and wire rate must be proportional to the product of the joint gap cross-section area and welding traverse speed, i.e.:

$$FILo \times (\pi \times d^2/4) = v \times (h \times G)$$

then:

$$FILo = 4v.(h \times G)/(\pi \times d^2) \qquad (4.02)$$

where :FILo = Basic filler rate (mm/second)

v = Weld traverse speed (mm/second)

h = Plate thickness (mm)

G = Joint gap (mm)

d = wire diameter(mm)

During Trial 1 equation 4.02 was used to calculate filler rates for skid welds. While the joint zone in way of the web was adequately filled there was insufficient material to form any smoothing beads, leaving unsound joint profiles.

Measurement of the cross-section for the incident side of these rather straight sided welds in 10mm plate, showed that a bead with a leg length of 0.35h i.e. half the usual maximum expected leg length for a twin fillet tee section weld, could be produced.

Assuming concave radiused bead surfaces, the total cross sectional area factor for beads on both incident and emergent sides is given by equation 4.03 as follows:

$$\text{Total bead c.s.a.} = (4 - \pi).l^2/2$$

where l = bead effective leg length(mm)

Substituting 0.35 x h for l and resolving gives:

$$\text{Smoothing bead area factor} = 0.053 \times h^2 \quad (mm^2) \qquad (4.03)$$

Similarly for rolled section web plates an additional factor had to be added proportional to the area lost by the radiused edges, as shown in equation 4.04:

$$\text{Rolled edge factor} = (4 - \pi) \cdot q^2 / 2$$

$$=0.429 \cdot q^2 \quad (mm^2) \qquad (4.04)$$

where q = radius of rolled section plate edges (mm)

Therefore adding the factors, equation 4.03 and 4.04 into equation 4.02 gave a basic formula for calculating the filler rate for skid welding. Assuming the capacity to produce smoothing beads on only one side of the joint "FIL1" or on both sides "FIL2" the rates are given by equations 4.05 and 4.06 respectively.

$$FIL1 = 4.v.\{(h \times G) + (0.026 \times h^2) + (0.429 \times q^2)\} / (\pi \times d^2) \qquad (4.05)$$

$$FIL2 = 4.v.\{(h \times G) + (0.05 \times h^2) + (0.429 \times q^2)\} / (\pi \times d^2) \qquad (4.06)$$

where FIL1 and FIL2 are provided in mm/second.

Equation 4.06, "FIL2" rate, was used as an initial rate for trials on each plate thickness. Good balanced weld profiles were obtained in joints of 6 and 8mm thickness. Once the rate had been used at the "optimum" welding speed (the speed shown from traverse speed trials to enable a balanced weld to be formed) a filler rate survey was conducted.

As filler rate increased for a constant traverse speed the spatter produced from the emergent bead increased, leaving a mass of solidified metallic globules on the face plate. At the same time the incident bead became "humped" i.e. convex,both wasting filler material and creating a likely prospect for reduced fatigue life. As filler rates were increased

still further, filler material tended to be melted on to the incident face plate, subsequently increasing the incident plasma. This resulted in the emergent bead reducing in size i.e. too much power was being absorbed in "melting" the filler wire subsequently reducing weld penetration.

As filler rate was reduced, the weld profile tended towards the straight sided joint experienced when using the "FILo" filler rate. At the same time as effective penetration increased the plate scouring also increased, creating an undercut zone at the emergent bead. Two interlinked factors contributed to this effect. Firstly the reduced filler input reduced beam absorption on the incident face hence a larger proportion of the energy was available to be absorbed into the plate at the emergent side. Secondly there was less available material to in-fill the increased affected zone.

When the FIL2 equation was used for welding plate thicknesses greater than 10mm, build-up of filler material on the incident side effectively reduced penetration to the emergent side creating instability in bead formation. Reducing the filler rate to FIL1 and below enabled penetration to be increased but reduced smoothing beads to be formed.

The filler trials in 12mm and 15mm plate thickness confirmed the inadequacy of the FIL2 equation to take account of power available to melt sufficient material to the required depth of penetration and form a certain size of smoothing bead, especially on the emergent side of the

joint.

This showed that in order to balance the amount of wire entering the joint with the available space to be filled, the weld penetration and average weld width had to be taken into account. Therefore, in the absence of any proved penetration monitoring device, equation 2.12 and 2.13 were used to predict the "potential penetration" and weld pool width. Potential penetration could then be compared with the actual joint thickness. Also, by assuming that the smoothing bead effective leg length could extend no further than the weld's average width, smoothing bead sizes could be calculated more accurately. Therefore by equating the incident bead leg length to the average width and by adding the joint plate thickness, the minimum penetration required to form a joint with a smoothing bead on the incident side may be calculated. The emergent bead leg length may then be equated to the difference between minimum and potential penetration. If sufficient power is available an emergent bead equal in size to the incident bead may be formed.

The resulting cross sectional area of smoothing beads may then be used in the basic filler rate equation together with the cross sectional area of material calculated to fill the joint gap.

This interactive method of filler rate determination was used as a basis in writing the "SKIDFILL" computer program (Appendix B-2) which was then used to provide filler rate and bead size information for latter welding trials.

During Trial 11 skid welds were made in plate thickness of 6, 10, and 12mm with various gaps to verify the SKIDFILL program, the filler rate calculated being designated as the "FILLY" rate. Comparative runs were made to assess the accuracy of program predictions and the tolerance of gap measurements influencing results. Figure 4.15 shows a tolerance envelope for acceptable welds bounding the actual FILLY predictions for a set gap joint giving good correlation.

The program can also be used to estimate the size of the smoothing beads, for particular input parameter. For a given power and traverse speed the likelihood of having balanced beads can be predicted. Figure 4.16 shows calculated bead sizes for skid welding in 6mm, 10mm and 15mm thick plate for varying traverse speed. While balanced beads can be formed for the 6mm plate at the optimum traverse speeds determined during the trials, the size of emergent beads in the 15mm plate is clearly reduced. This is due to the lack of potential penetration using 9kW(WP) of laser power.

A comparison between the initial FIL1/FIL2 predictions and FILLY predictions for welds at optimum trial speeds is shown in figure 4.17. While the two predictions coincide for plate thickness below 8mm, as plate thickness increases the excessive values produced by the FIL2 calculations confirm the problems involved with excessive filler rates for plate thicknesses greater than 10mm in initial trials.

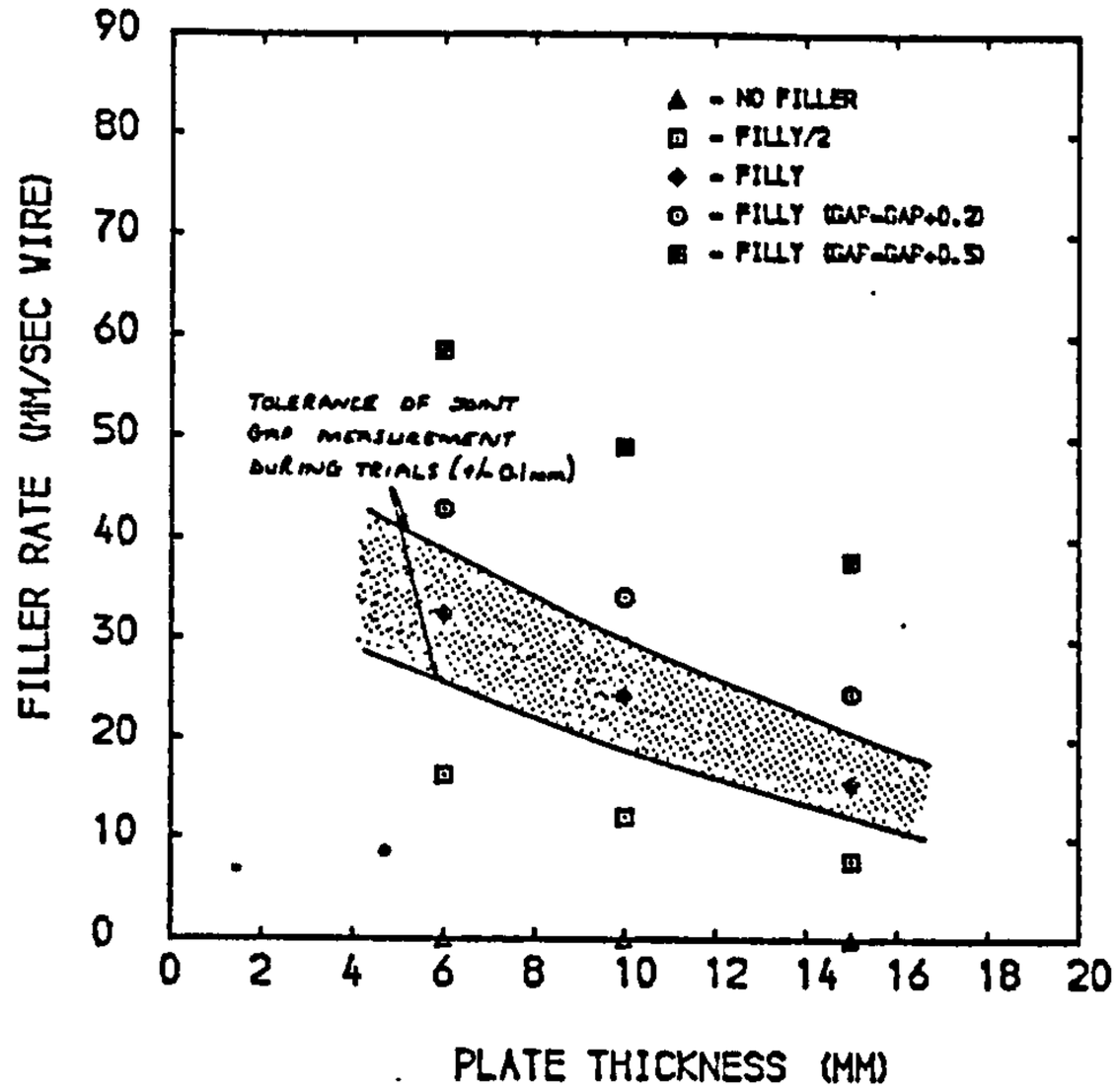

Figure 4.15 - Filler rates calculated by the Skidfill program for various joint gaps as measured. Actual rates used for a nominal gap shown.

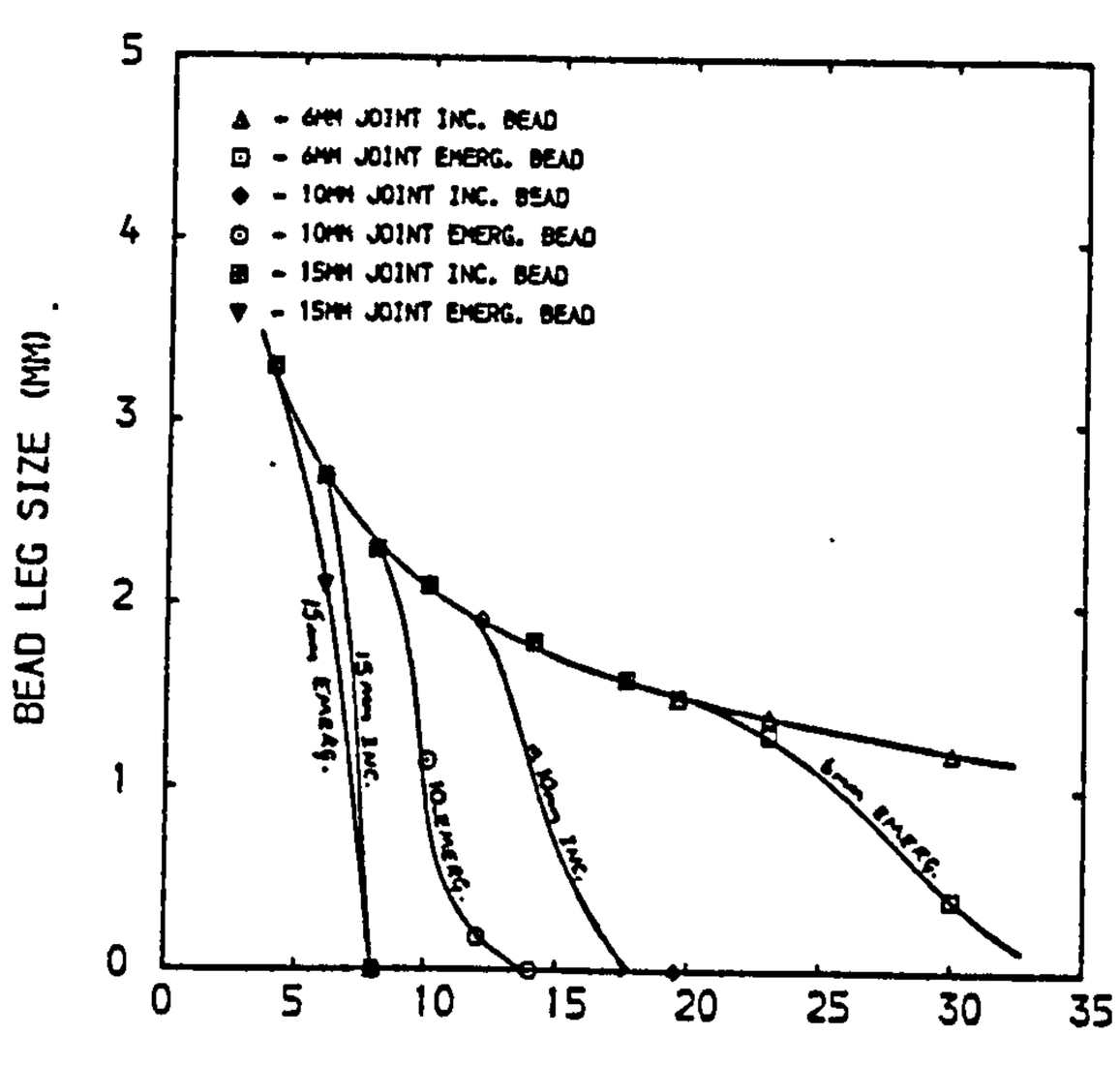

Figure 4.16 - Predictions of smoothing bead sizes for various speeds in 6,10 and 15mm thick joints; laser power 9kW(WP).

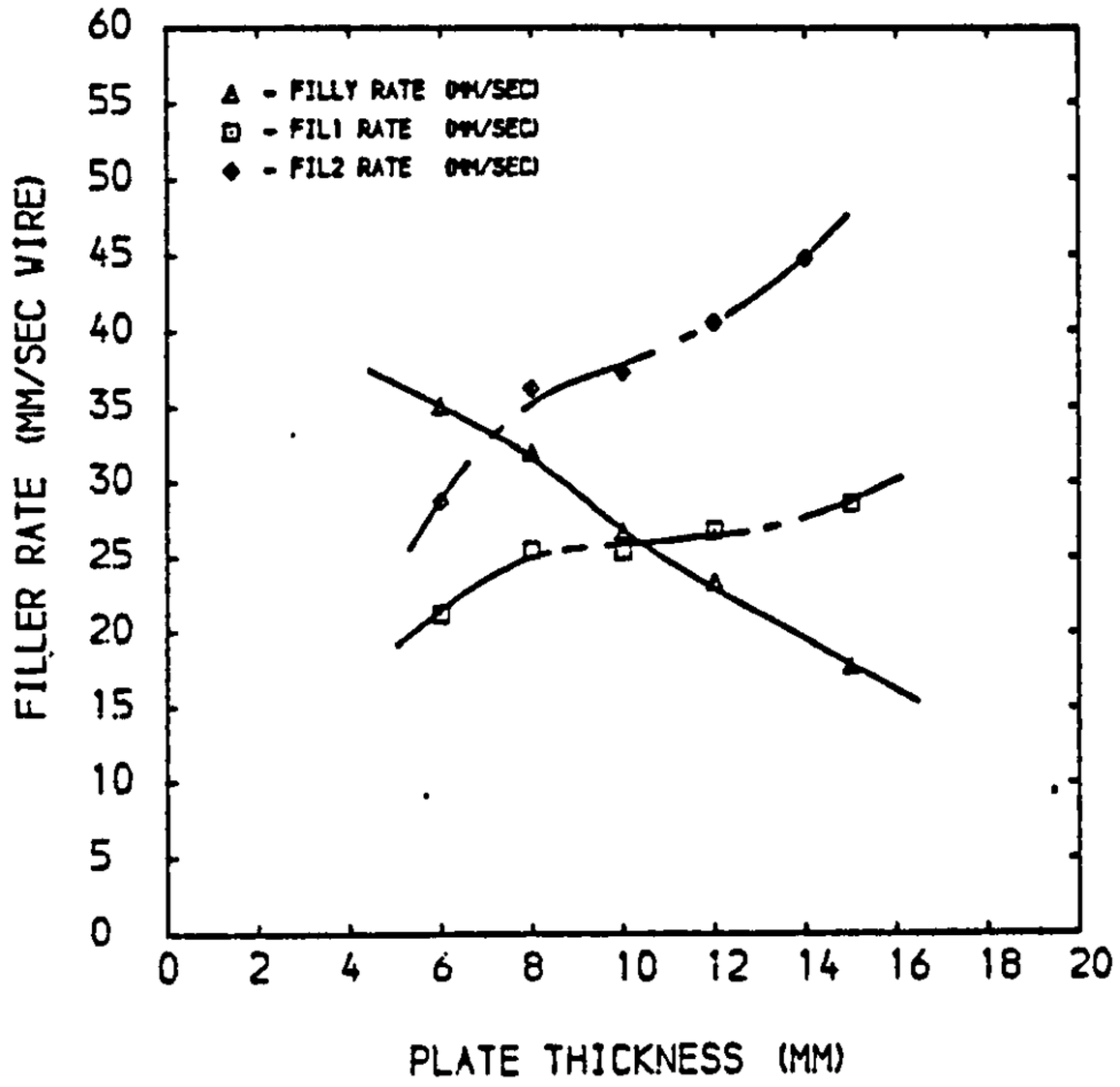

Figure 4.17 - Comparison of FIL1/FIL2 and FILLY predicted filler rates for each plate thickness welding at the recommended production speed.

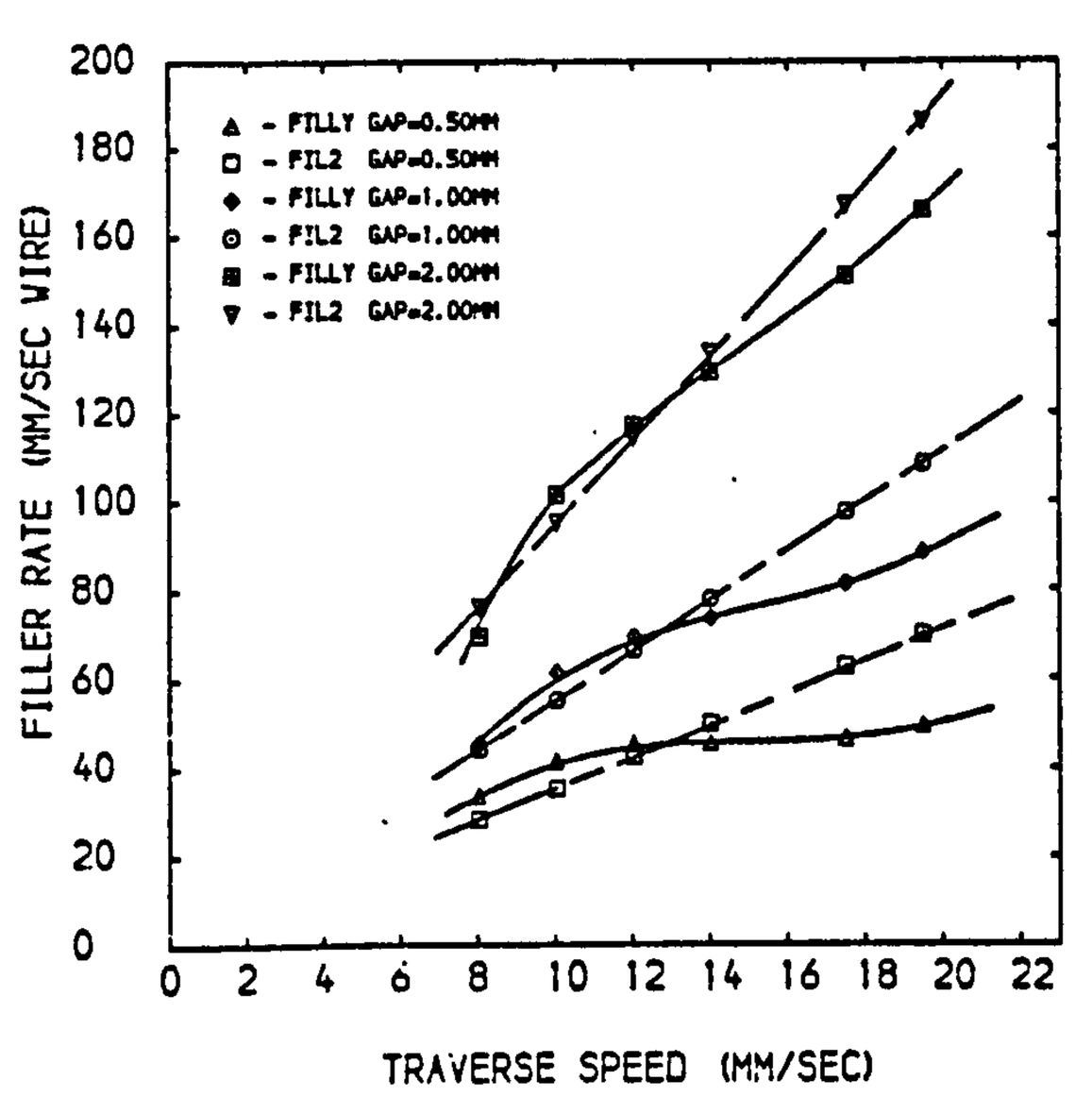

Figure 4.18 - Variations between FIL2 and FILLY prediction of weld filler rates in 8mm plate with various joint gaps.

Figure 4.18 shows how the discrepancies between FIL2 and FILLY rates for 8mm plate vary with increasing traverse speed for various joint gaps. For FIL2 predictions the filler rate increase is proportional with increasing speed using a fixed size of smoothing bead. In contrast the FILLY predictions for a nominal gap remain relatively constant. Although an increase in filler rate would be expected to compensate for the increased speed, penetration and weld width obviously reduce so that the reduction in smoothing bead size compensates for this increase. However for larger gaps, the volume of wire entering the joint to fill the gap dominates hence the filler rate increases.

The trials have shown the importance of the filler rate calculations for producing well-formed single sided skid welds and the important inter-relationships between traverse speed, input laser power and filler rate. If the rate is too low, excessive penetration will lead to undercut in the emergent bead or underfill to the incident bead; if too high, excessive build-up on the incident side can reduce penetration for the subsequent formation of an emergent bead. While penetration into 12mm and 15mm may be achieved using 9kW(WP), controllability of the emergent bead is obviously reduced.

In order to increase the potential for achieving good balanced emergent bead profiles in 15mm plate thickness joints and minimum power requirement of 15kw would be needed.

4.2.2 Filler Wire Thickness

Wire diameters of 0.9, 1.0, 1.2 and 1.6mm were used during the trials, (mostly the largest size). A compromise judgement is made in selecting the best size. The thinner wire could be directed further into the centre of progressively narrower gaps enabling the interaction point to be near the middle of the joint and help provide a more balanced joint. However greater accuracy was required in placing the wire as its inherent curvature increased the tendency for the wire to jump from the joint or interception zone.

The larger wire, while facilitating good directional stability, could not be aimed between the edges of small gaps. Therefore, wire diameters of 1.0 or 1.2 would be advised for production welding procedures.

4.2.3 Filler Wire Alignment

Initial welds were conducted with the filler nozzle directed at angles of 45 degrees to plate faces and laser beam, the wire being aimed to the leading edge of the HeNe alignment spot. When gaps of greater than 1.0mm were encountered, the insertion angle of 45 degrees with respect to the face plate surface was too large to facilitate efficient insertion of the wire into mid-joint. Consequently the nozzle was lowered and found to be best at an angle of 15 degrees to the face plate but maintaining the angle of 45 degrees subtended with the laser beam. This arrangement was maintained for both close fit and gap joints.

The position of wire insertion relative to the HeNe spot changed depending on joint fit-up and plate thickness in order to aim the wire as near as possible to the joint centre. For nominal joint gaps the wire was aimed to the HeNe spot leading edge on the plate surface. When joint gap permitted, the wire was aimed to a position in front of the HeNe spot, as detailed in table 4.02, in order that beam interception was initiated in the joint centre.

While the changes in wire insertion angle enabled well-shaped emergent beads to be formed, changes of +/- 10 degrees between trials did not have any noticable effect on general weld profile. However accuracy in aiming the wire was more important and the result more dramatic. Movement in excess of +/- 0.5mm in initially setting up the wire into the HeNe spot often resulted in a joint failing to be produced with the wire "jumping" from the molten zone or from the joint gap.

4.3 LASER BEAM SPOT POSITIONING AND FOCUS

The two most important factors influencing the position of the weld in relation to the joint line are the angle and height at which the focused laser beam strikes the plates. This will determine the position of the keyhole, the surrounding molten pool and the extent of the fused material which includes the smoothing beads to either side of the web plate.

Plate Thickness (mm)	Distance of wire insertion point infront of HeNe spot, assuming 45~ angle (mm)
3	1.5
6	3.0
8	4.0
10	5.0
12	6.0
15	7.5

Table 4.02 - Filler wire/plate surface interaction point infront of the leading edge of the HeNe spot for varying plate thicknesses

4.3.1 Incident Beam Angle

Ideally, penetration to a maximum depth through a web plate would be achieved with the beam striking the surface at right angles. However, the presence of the flange plate in a tee section joint configuration precludes such operation, not only because the flange plate interacts with the beam path but also because of accessibility for the focusing optics.

Compact, lightweight focusing optics are now being developed for manipulative beam delivery heads to direct beams into "tight" corners. However the lowest beam angle becomes dependent on the minimum "safe" angle for a system with a particular focal number and associated included angle of divergence so that the incident beam does not impinge in any way with the flange plate before striking the joint.

Previous authors [23] [93] [3] have used beam incident angles to the face plate varying from 5 to 10 degrees for single pass welds and up to 15 degrees for dual pass welds. After initial trials the present Author endeavoured to maintain a single angle, varying only the spot height.

Figure 4.19 shows the total included angle beam divergence for various focal number systems. For the system used, with a focal length of 400mm and a raw beam diameter of about 45mm giving a focal number of nine , a minimum "safe" angle of seven degrees was selected for the trials. This was not only to ensure minimal heating effects between the incoming beam

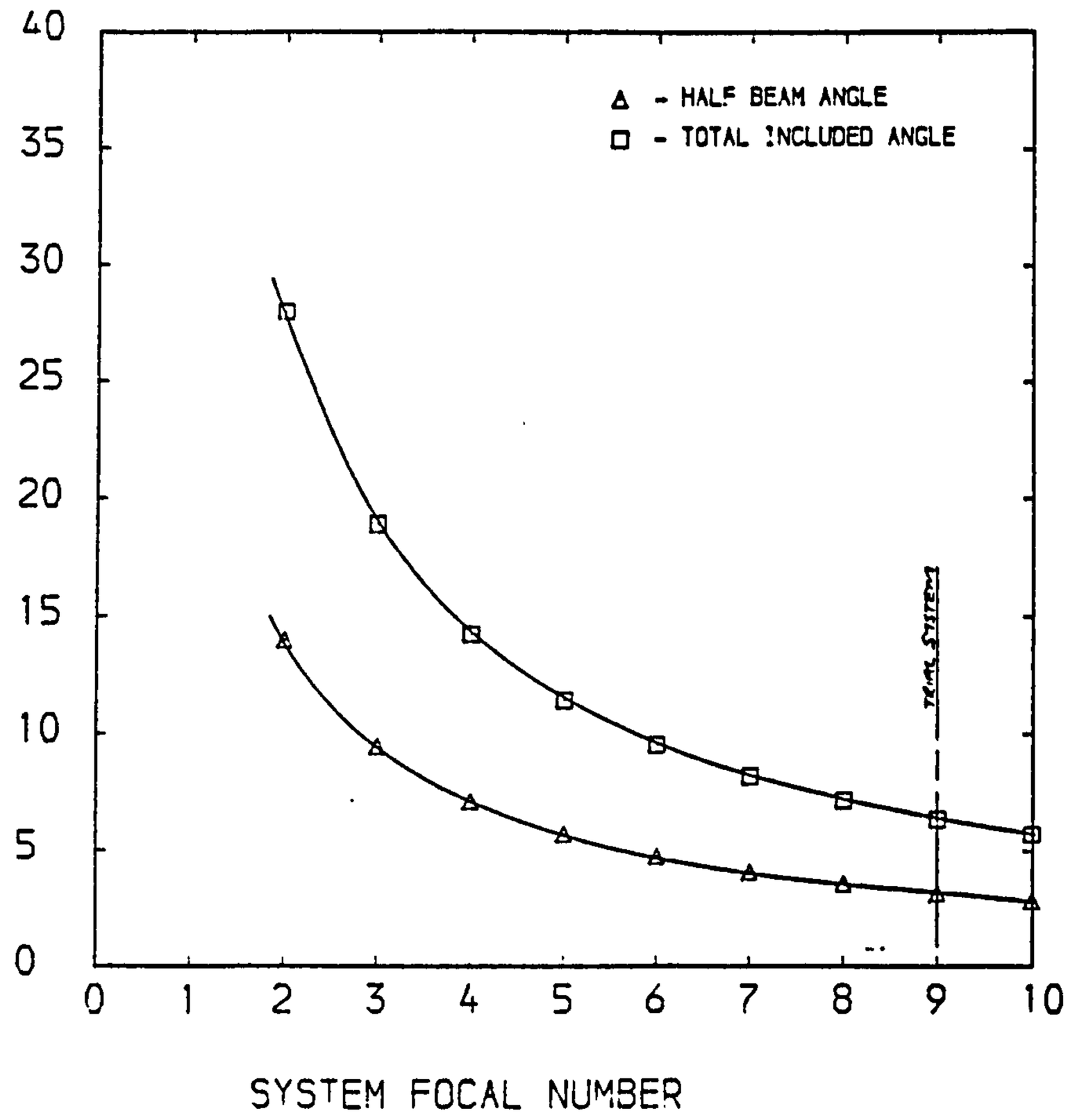

Figure 4.19 - Total included beam angle for laser beams of various focal numbers.

and the adjacent plate but also to give adequate tolerance to use the process on systems with shorter focal number systems if required.

The 7 degree beam incident angle was used for each plate thickness allowing single sided skid welds to be perfected. A steeper angle of 13 degrees was used for double sided tee-section joints to ensure that the second pass did not penetrate the surface of the first pass incident bead. It was used also for trials on 3mm plate tee section joints in an unsuccessful attempt to reduce porosity when using 9kW(WP) as the working power.

Crucial to the success of producing adequate emergent beads during skid welding is the theory of the formation of the molten zone path with respect to the incident beam angle i.e. whether the beam deflects upwards with respect to the joint line. Dawes [96] discusses this "so-called skid welding effect" refuting the idea that the beam could be redirected by a reflection mechanism along the joint line [97] . However, no positive explanation is provided by him or other authors.

To assess the necessity for investigating changes in beam angle or spot height to enable full fusion, the ideas of beam bending had to be explored.

The verification was possible using CL10 with 9kW input power into 8mm plate to gain penetrations greater than the joint zone requirements, as shown in macrograph sections, figure 4.20a-c. For welds in 8mm plate,

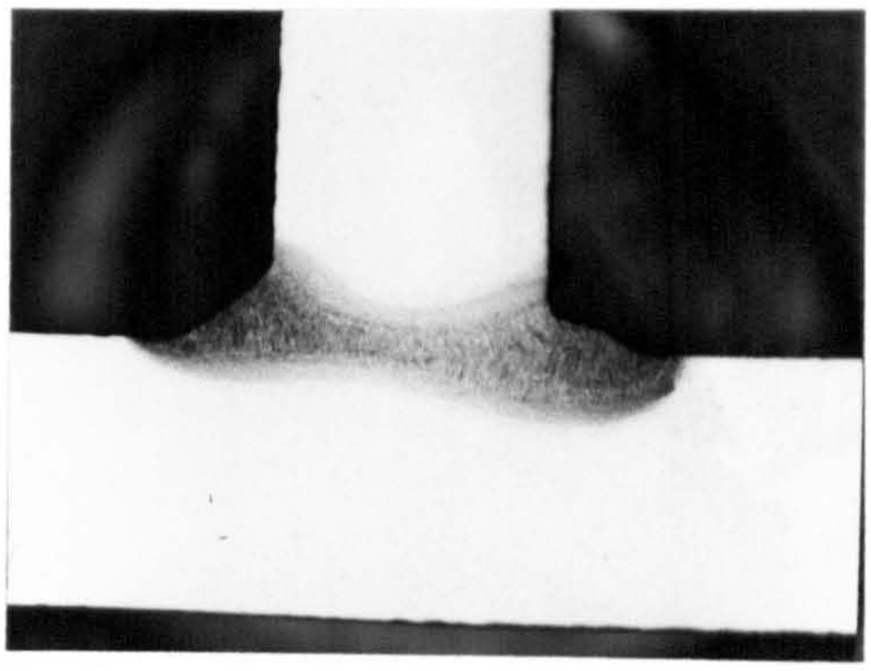

Figure 4.20a - Balanced beads formed ; Traverse speed 14mm/sec.

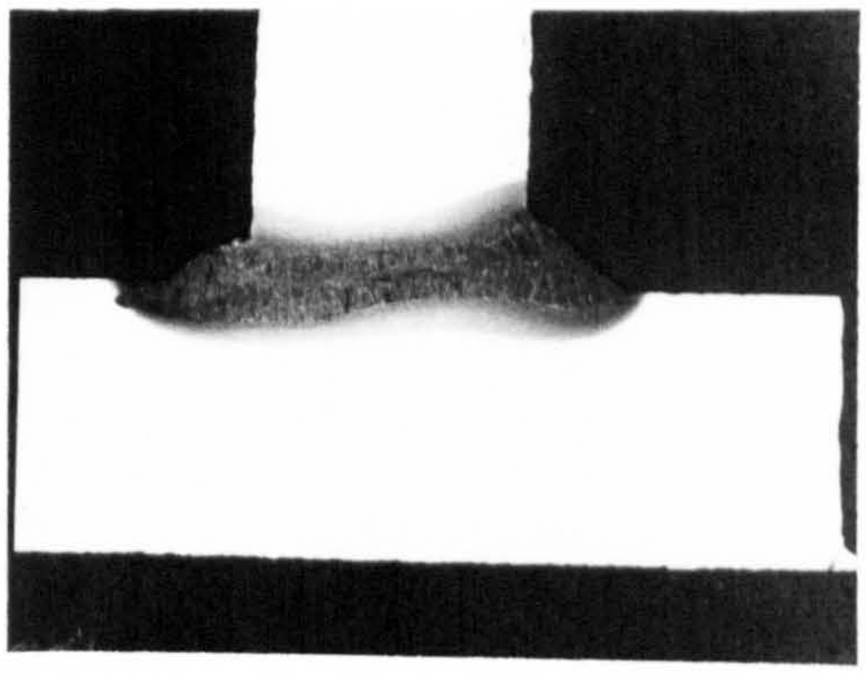

Figure 4.20b - Balanced beads but evidence of a heat affected root tip ; traverse speed 12mm/sec.

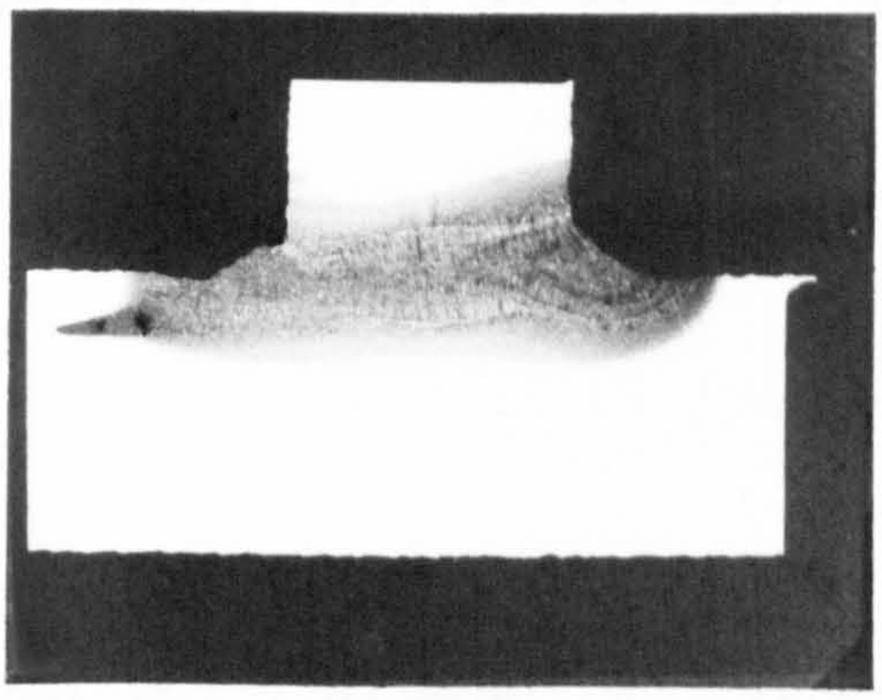

Figure 4.20c - Flattened emergent bead with a penetrated root tip ; traverse speed 10mm/sec.

tee joints were produced at speeds of 14.0, 12.0 and 10.0mm/second respectively. Whilst figure 14.20a gives the impression of the emergent end of the laser path having deflected upwards, figure 14.20b shows a small heat affect zone tip area in line with the laser beam line of incidence. By reducing speed further, figure 14.20c a keyhole root is seen clearly even though the upper part of the emergent bead still appeared to deflect upwards.

Certainly while viewing the welding process the mass sparks and plasma coming from the emergent side of the joint would indicate that at least a proportion of the energy in the keyhole is released upwards, figure 4.21.

The predominant keyhole path is along the laser beam line of incidence. However, once the molten pool formed around the keyhole root extends to the joint line surface, the vapour pressure of gas inside the keyhole is sufficient to penetrate into the fully molten zone and escape upwards to the atmosphere. Once penetrated, this "side-shoot" or extension to the keyhole will form its own associated surrounding molten zone which subsequently forms the emergent bead.

In perfecting a fully fused and smoothed emergent bead the penetration and depth of the keyhole root should be sufficient to allow a stable keyhole extension to be formed. Penetration should not be too great so as to leave a heat affected or molten root zone creating a potential stress raiser within the plate.

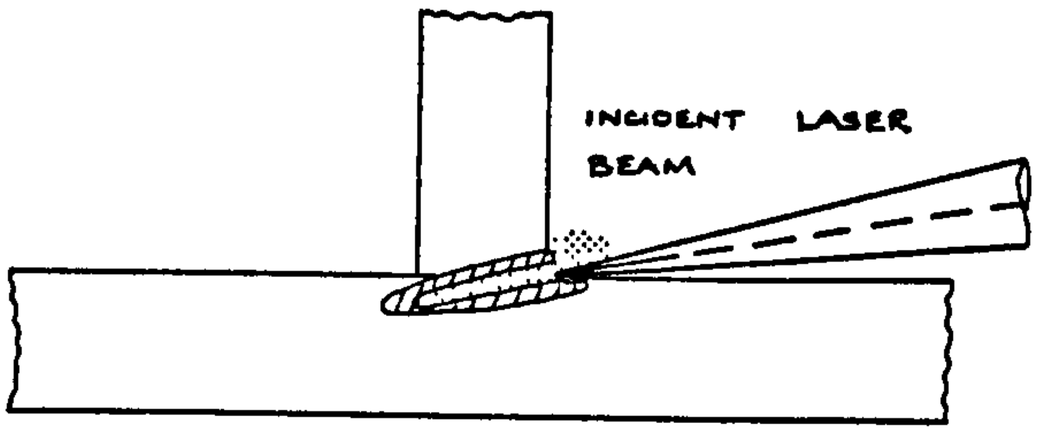

a) Molten pool surrounding keyhole fails to affect emergent edge. Spot height too low and keyhole root buries in face plate.

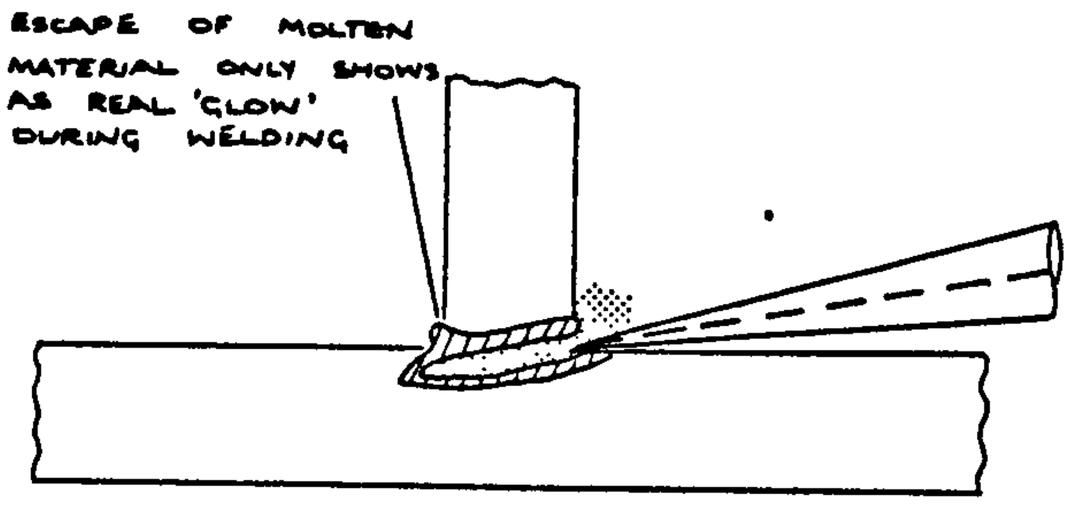

b) Spot height raised. Molten pool extends to emergent position but insufficient for keyhole to break through.

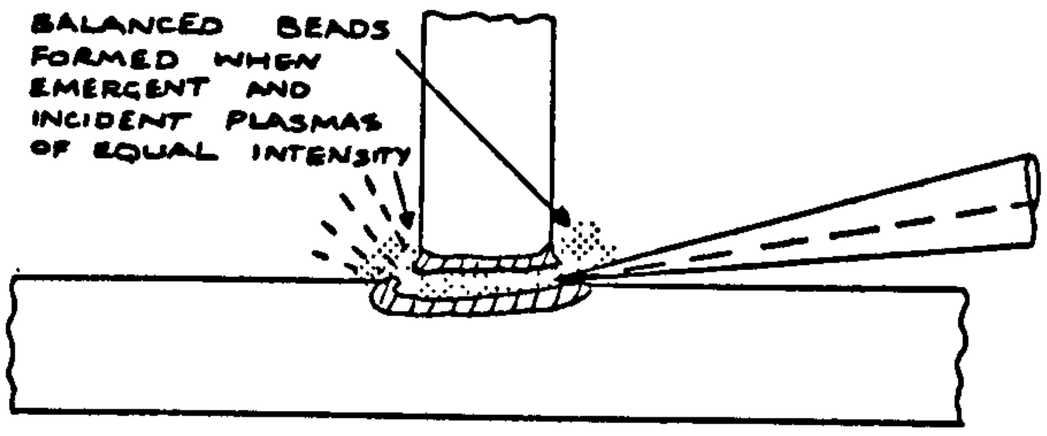

c) Spot height raised further. Molten pool extends into emergent zone. Vapour pressure sufficient to open up "extension keyhole" and allow emergent plasma cloud to form.

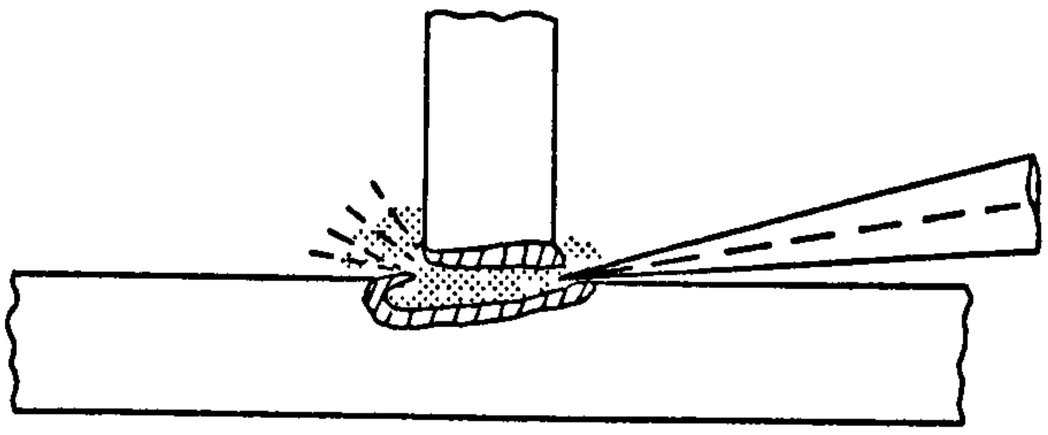

d) As for "c" but slower speed increases penetration leaving an enlarged root zone.

Figure 4.21 - Formation of the keyhole side shoot to form a fully fused emergent bead.

Therefore, while the process does not appear to depend on a reflection mechanism, the incident beam angle should be maintained as shallow as possible so that the keyhole root can be adjusted to a position just below the plate surface by simply altering the spot height and thus enable the keyhole extension to be formed.

Although the angle of the focusing head was set carefully during the trials to the required angle, slackness in the focus mirror mount adjusting screws sometimes created slight angular movements within the head setting. Comparative measurements showed angular differences of +/- 0.5 degree from the set angle. Therefore, by including visual deviations a tolerance of +/-1.0 degree was realised for set angles.

Angular variations within this limit would not be considered critical for weld formation where balanced beads could be formed e.g. for plate thicknesses below 10mm, using 9kW. However for greater thicknesses, any variation in angle could cause a destabilising of the "keyhole side-shoot" producing a fluctuating emergent bead profile.

4.3.2 Incident Beam Spot Height

Once the minimum "safe" angle had been determined for use throughout the skid welding trials the dominant parameter affecting the melt zone position with respect to the joint line became the incident bead spot height.

During Trial 1 the author followed the practice of Martyr [3] in his initial attempts to form single sided skid welds, when the beam was aimed to impinge on the jointline. However, Dawes [96] had shown how spot height affected the profile of autogenous welds at powers of 5kW.

Initial trials, varying spot height on 8mm plate joints (Trial 2), emphasised the effects of changing spot height. Macrograph sections taken from the autogenous welds, figure 4.22a-e also show the effect of excessive spot height (2.0mm). Although forming an incident bead there is some lack of fusion between the web and face plate. The sample produced at 2.5mm spot height was found to be totally unfused.

For each plate thickness the effect of changing spot height was assessed in parallel to the changes to traverse speed. Spot height was assessed by aiming the red HeNe spot on to a rule positioned on the web plate surface. With a spot diameter of 0.5mm, positioning the spot to incremental height increases of 0.25mm proved somewhat subjective. Even so, an estimated accuracy of +/-0.25mm was considered sufficient for the trials programme.

Figure 4.23 shows the spot heights investigated for each web plate thickness and the tolerance envelope for the production of balanced weld profiles. The comparative curve, showing idealised spot heights, was produced geometrically. The calculation used, equation 4.07 assumed beam angle of incidence of 7 degrees and a penetration depth at the emergent position of 0.25mm giving an allowance to ensure face plate fusion.

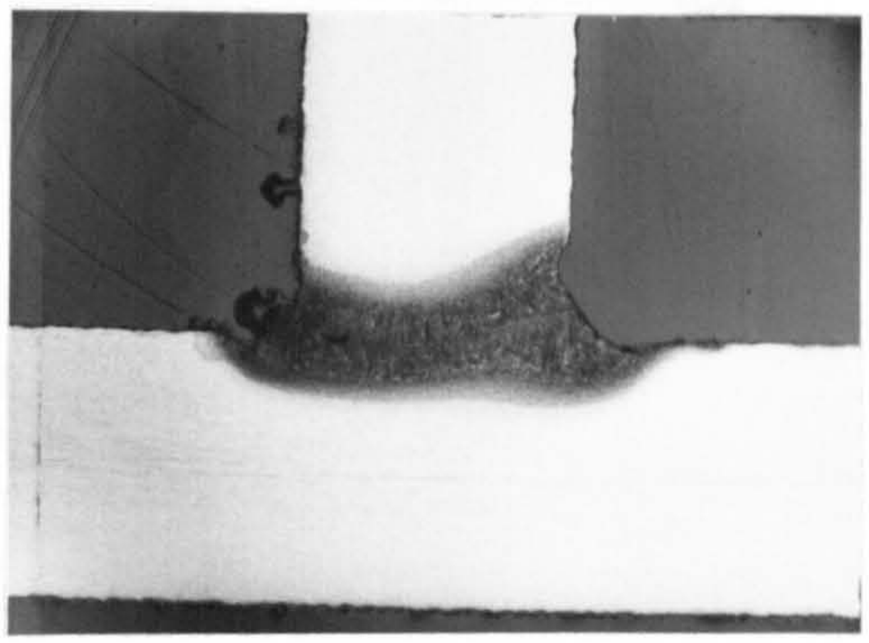

a) Spot height = 0.0mm
Balanced fusion but
rough emergent bead

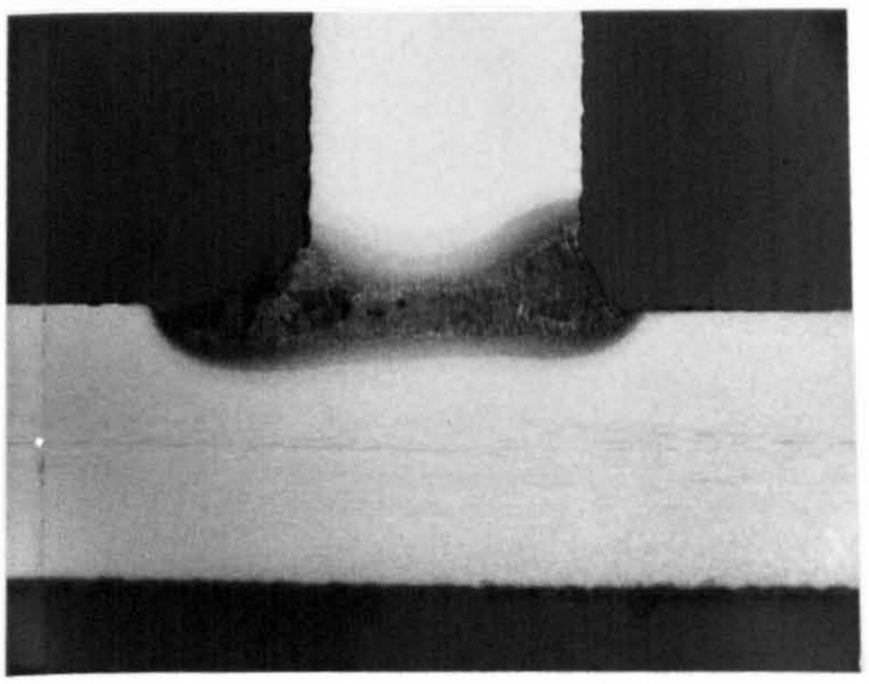

b) Spot height = 0.3mm
Emergent bead forma'n
but porous

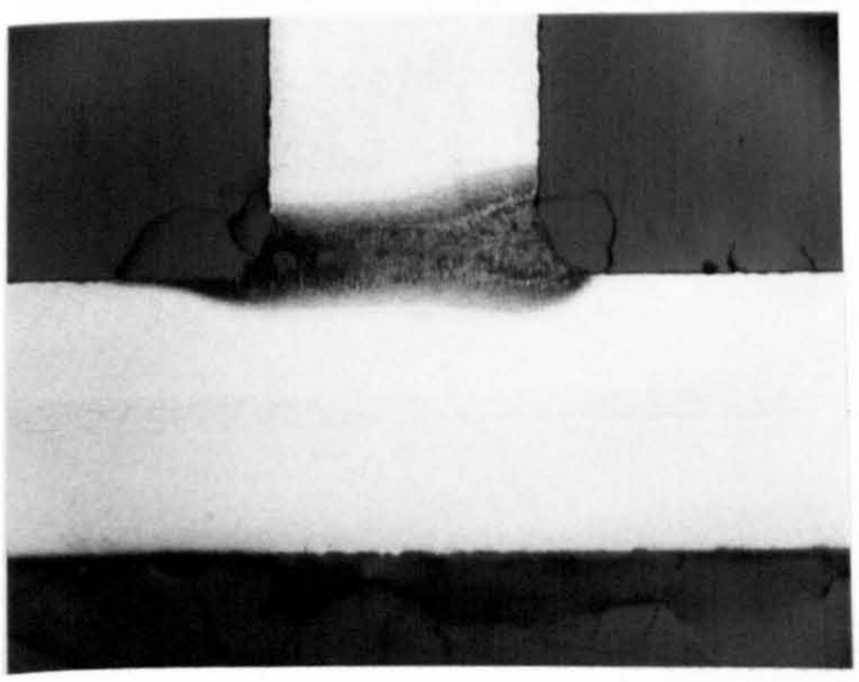

c) Spot height = 0.5mm
Fusion zone mainly
_n web plate, emerg.
side scouring

Figure 4.22 a-e - Effect of the laser spot heigt on autogenous skid welds ; 8mm plate thickness.

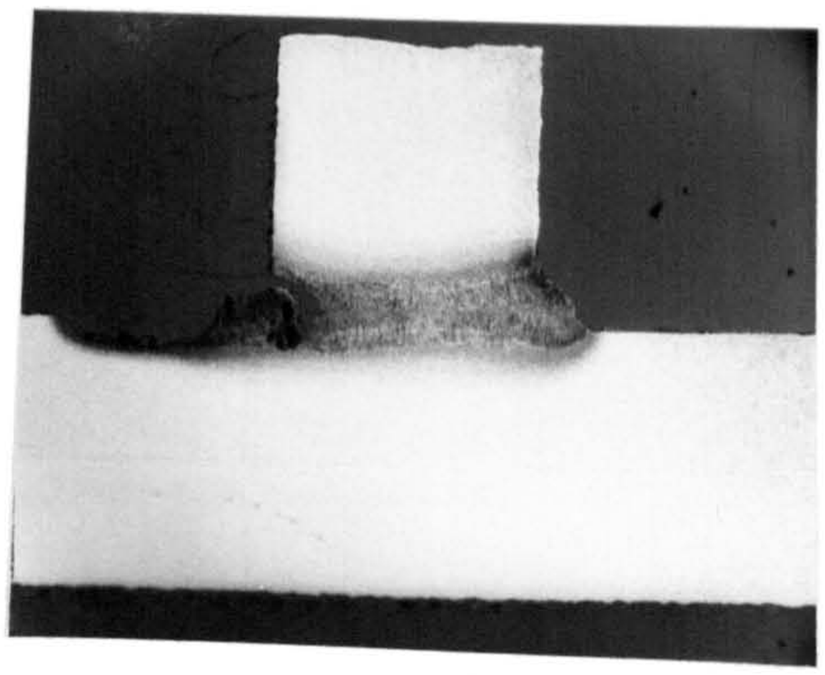

d) Spot height = 1.0mm
Large scouring of emergent plate surface

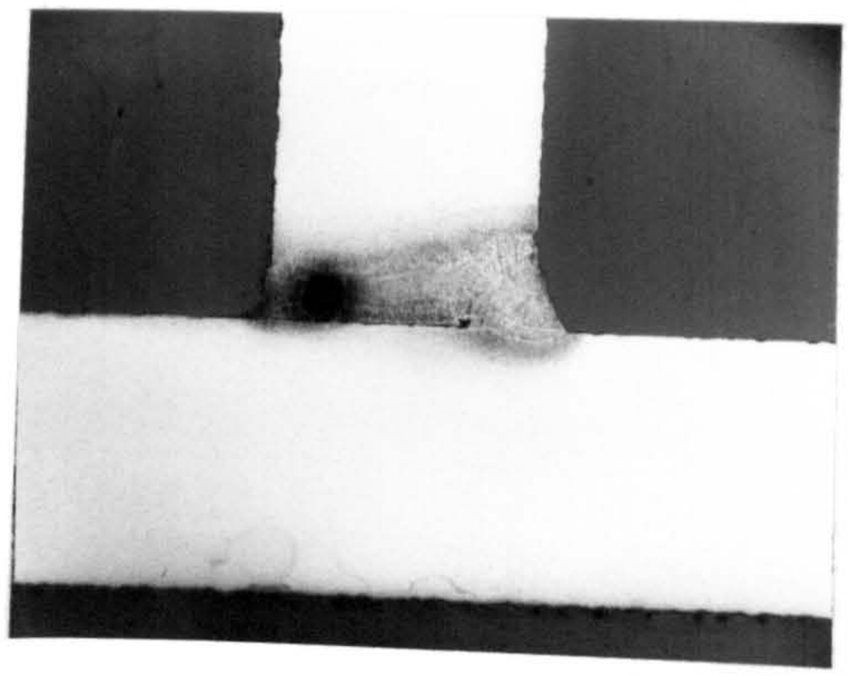

e) Spot height = 2.0mm
Incident bead fused but lack of fusion further into the plate

Figure 4.22 continued.

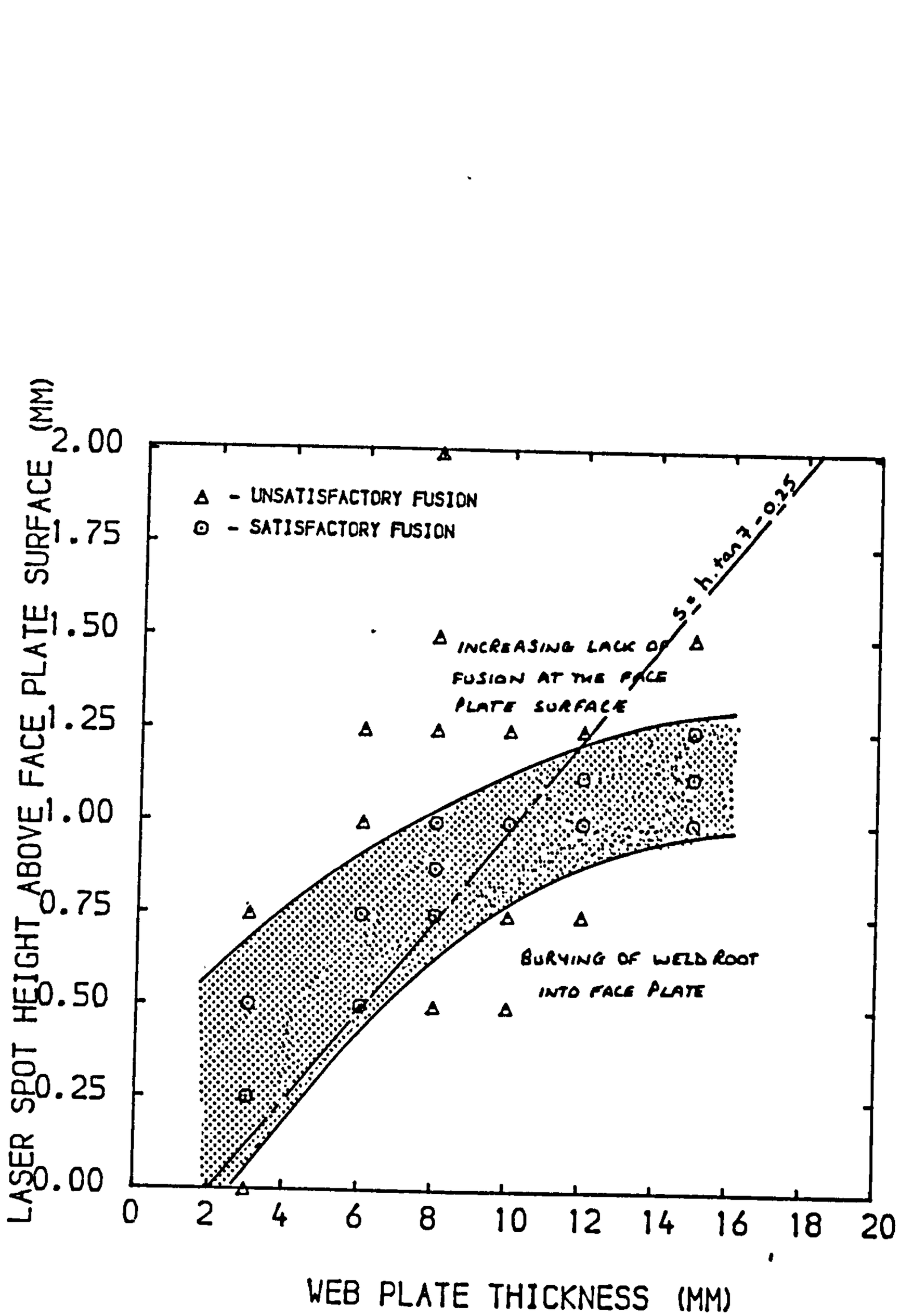

Figure 4.23 - Comparison of tested spot heights, the tolerance envelope and a plot calculated heights from equation 4.07

$$s = h \cdot \tan 7 - 0.25 \qquad (4.07)$$

where: s = spot height (mm)

h = web plate thickness(mm)

The resulting tolerance envelope produced after assessing the soundness of the range of welds produced at varying spot heights both visally and ultrasonically, shows how, for plate thickness of 10mm and below, there is good correlation between the idealised and actual weld paths emphasised by the relatively large tolerances available (about +/-0.5mm). Above 10mm web plate thickness tolerances reduce as the "actual" curves fall below the idealised, a maximum height being reached when the tendency for lack of fusion at the incident bead increased, figure 4.24. At the same time, as filler rate was being reduced to ensure sufficient penetration, the incident bead tended to become vertically flat, reducing its "smoothing" capacity. Increased tolerance could possibly be gained by the use of beam spinning techniques, commonly used in electron beam welding with limited trials for laser butt welding [74] .

The visual appearance of welds with excessive spot heights were often deceptive, with a well-shaped incident bead and a rounded emergent bead with no tendency for undercutting. During the welding process, the emergent plasma was normally stable and balanced and hence a good weld could be expected. Only after ultrasonic scanning and macrographic

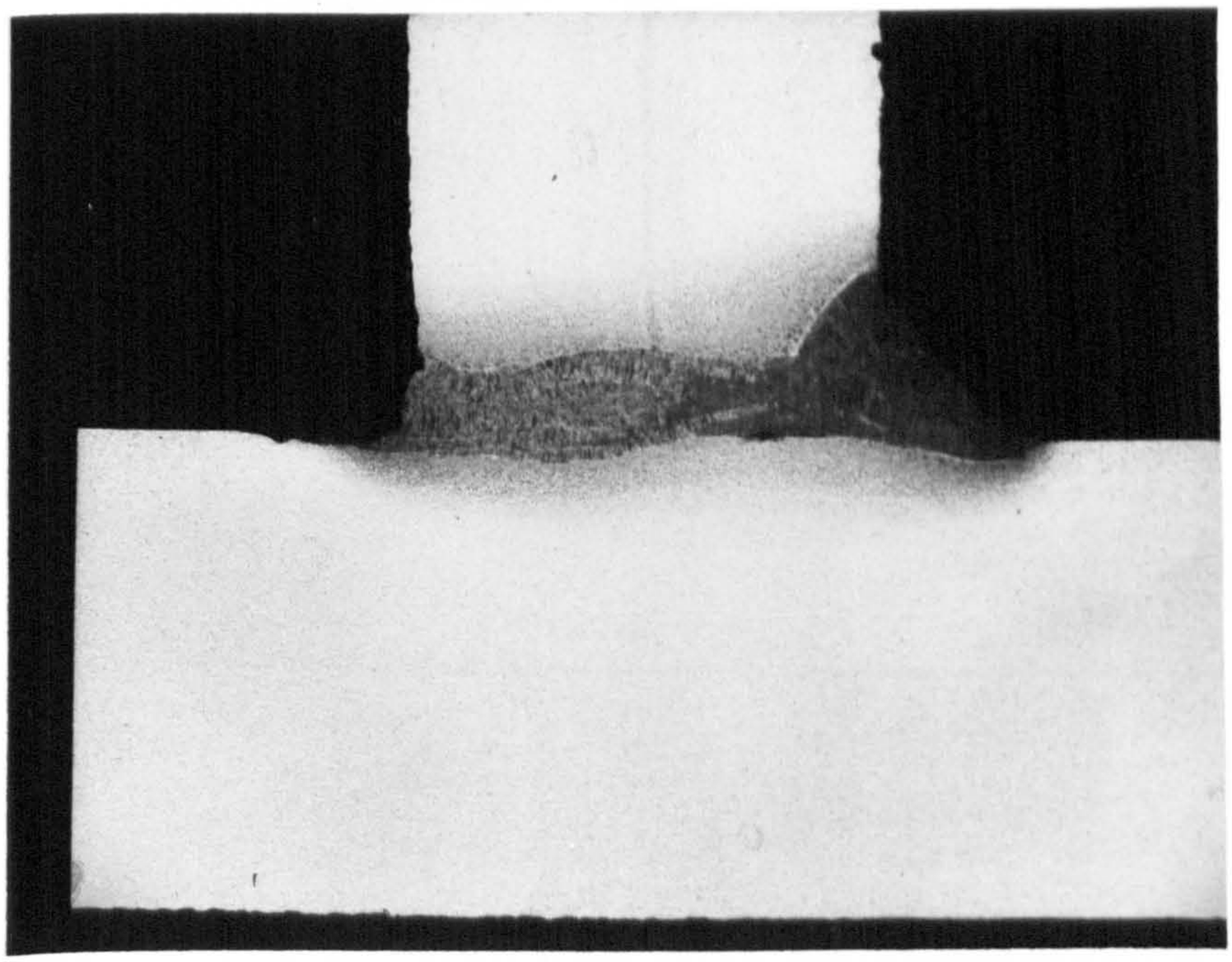

Figure 4.24a - Skid weld in 8mm plate, excessive spot height causing a lack of fusion next to the incident bead.

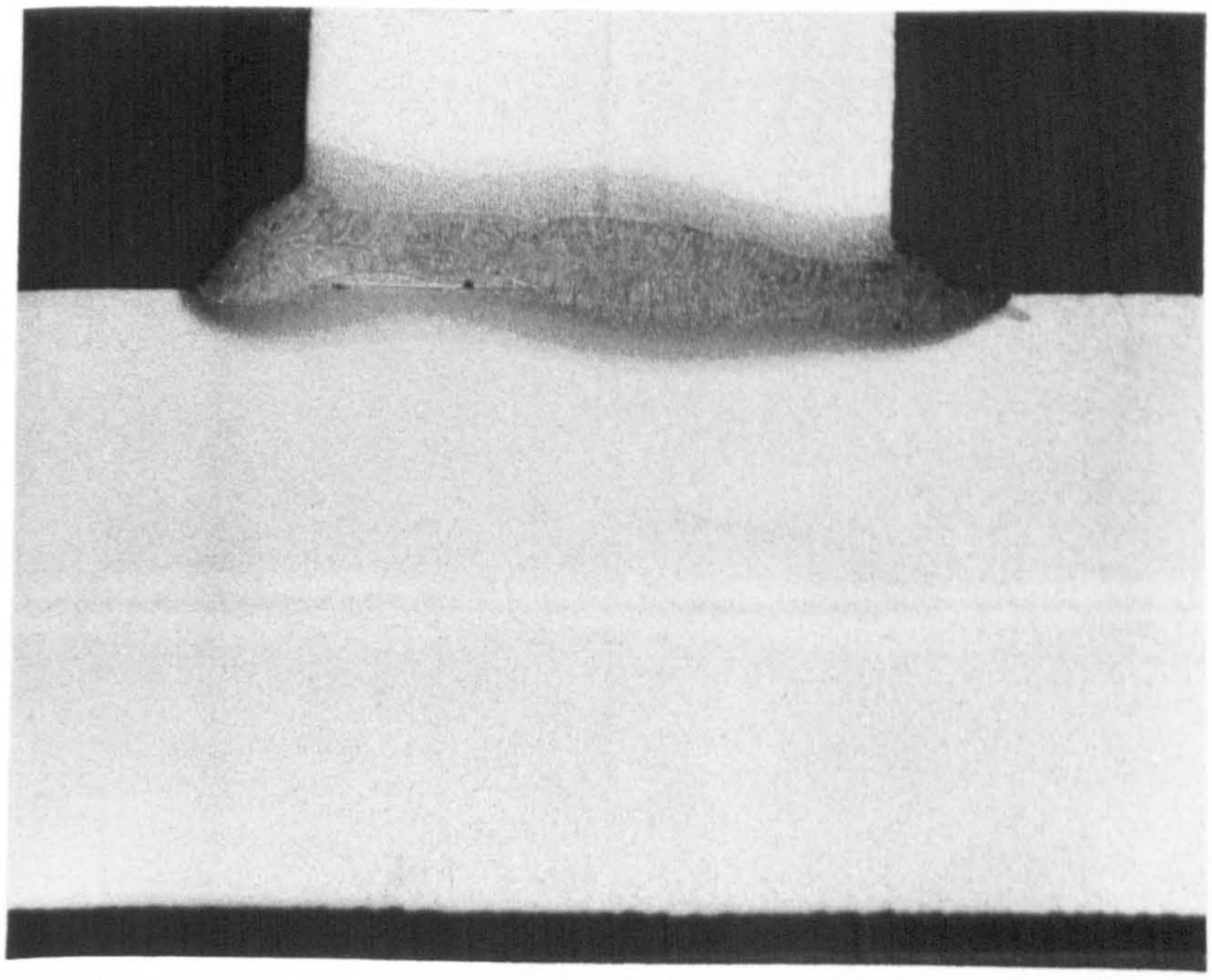

Figure 4.24b - Skid weld in 12mm plate, excessive spot height causing a lack of fusion next to the incident bead.

sectioning was the lack of fusion discovered.

It was observed that good stability resulted from the reduced interaction of the keyhole and molten pool into the face plate. The welding mechanism was nearer to that of a butt weld with the actual keyhole root opening to the atmosphere rather than being absorbed by the face plate.

As spot height increased to the upper limit with a lower than "optimum" traverse speed e.g. spot height of 1.0mm, traverse speed of 10mm/second for 8mm plate nominal gap, there was also a tendency for open porosity to occur in the emergent bead. This appeared to occur because of instability within the keyhole root energy firstly being absorbed into the face plate, then to the atmosphere, open pores being formed as a result of the transitions. This type of porosity could be reduced by either increasing or decreasing traverse speed and by reducing spot height so that power would be absorbed into the face plate.

For plate thickness above 10mm, the lower limit of acceptability occurred when the emergent bead "buried" into the flange plate without any penetration, either via a keyhole extension or flowing molten material to form a sealed emergent bead. While similar observations were made for web plate thicknesses below 10mm, the lower limit was also influenced by the shape of the incident bead. As spot height decreased, e.g. below 0.75mm for 8mm plate the incident bead became horizontally flatter to the face plate as shown in figure 4.25.

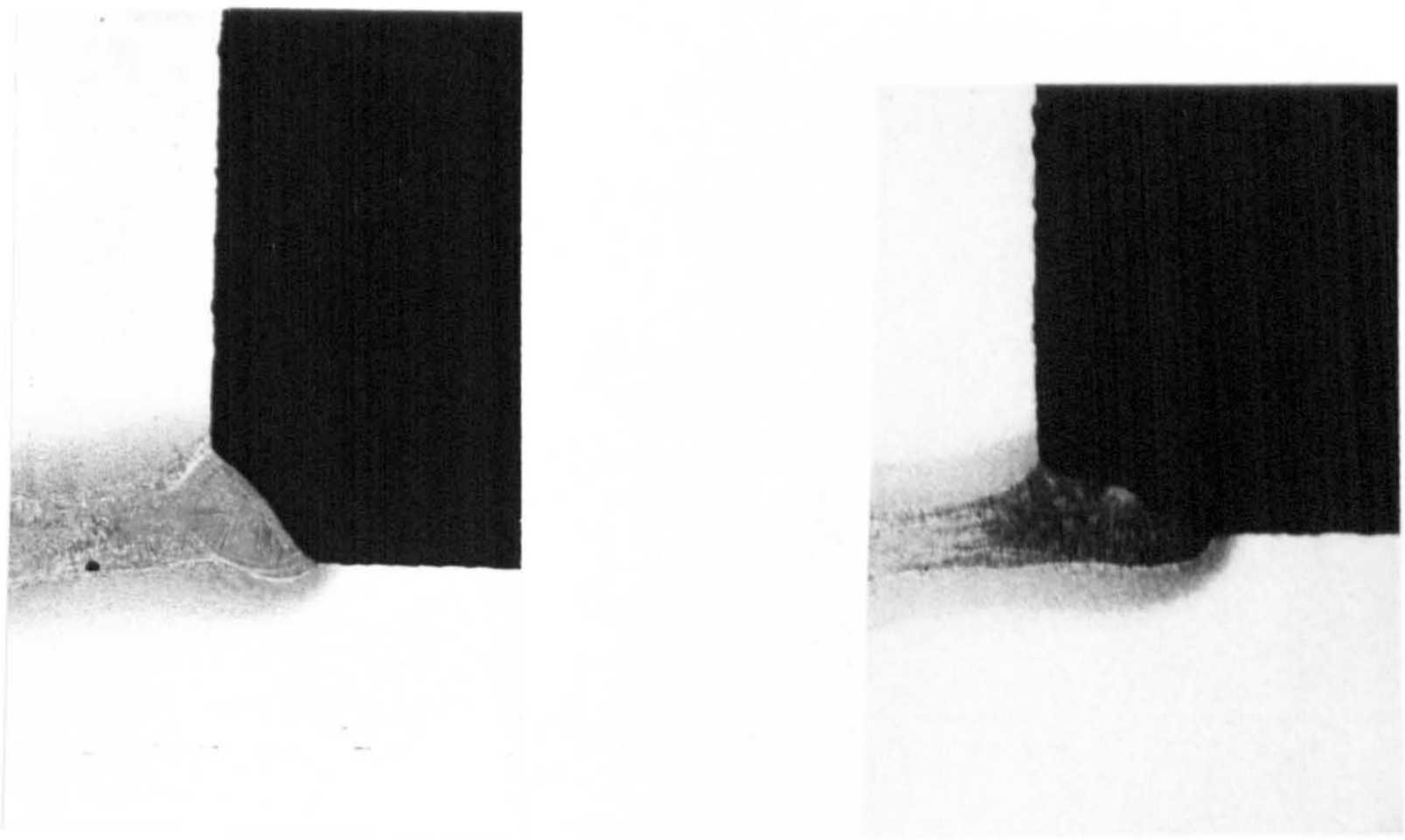

a) Spot height =1.0mm
Bead face angle = 48°

b) Spot height = 0.5mm
Bead face ange = 20°

Figure 4.25 - Comparison of incident bead face angles for varying spot heights.

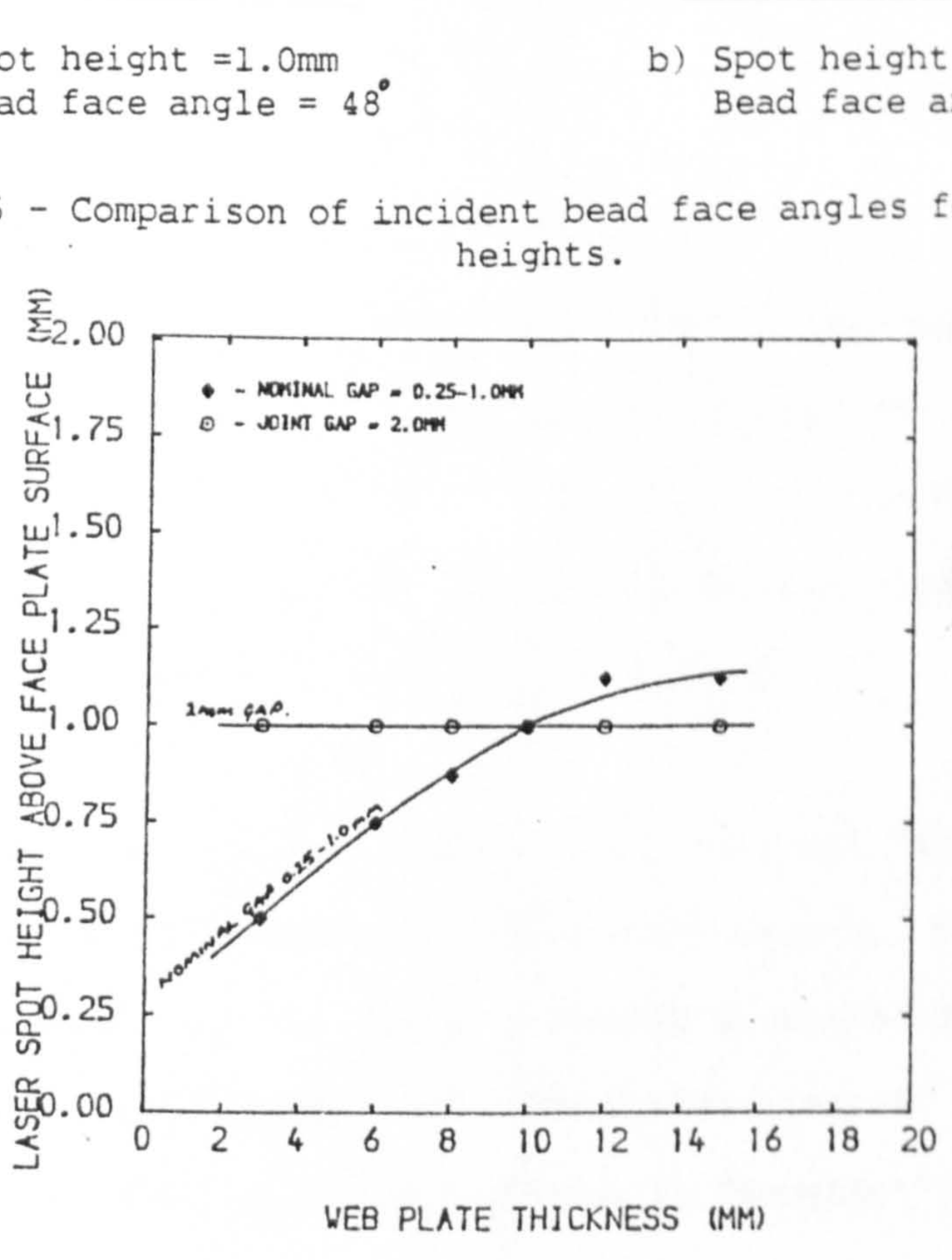

Figure 4.26 - Laser spot heights for use in skid welding joint of varying gaps ; laser power 9kW.

The above mechanisms were also observed for joint gaps below 1.0mm when the wire was inserted to the front of the joint line. Once joint gap increased to a value greater than 1.0mm when the wire could be aimed to intercept the beam at mid-joint, spot heights were found to need increasing to mid-joint height in order to ensure beam and wire interception. This is reflected in the curves of spot height for varying joint gaps shown in figure 4.26. The beam was aimed to mid gap with the reduced traverse speed and consequently the result was a wider melt zone width ensuring good fusion.

4.3.3 Beam Mode

Few authors refer to the effect of beam mode on welding characteristics, confining themselves to relating their welding results to one particular laser. There have certainly been more investigations assessing the effect of beam mode on cutting performance when a stable Gaussian mode is preferred for precision cutting.

Beam modes for the skid welding trials were all "as produced" by the CL10 laser but as seen from the shallow beam prints, figure 4.27, the mode at the workstation was characterised by a central peak surrounded by an inconsistent ring distribution, though when tested adjacent to the laser output the mode was characteristically "doughnut" shaped.

Beam prints were taken at the start, middle and end of each trial day. The general shape remained consistent and there was no apparent

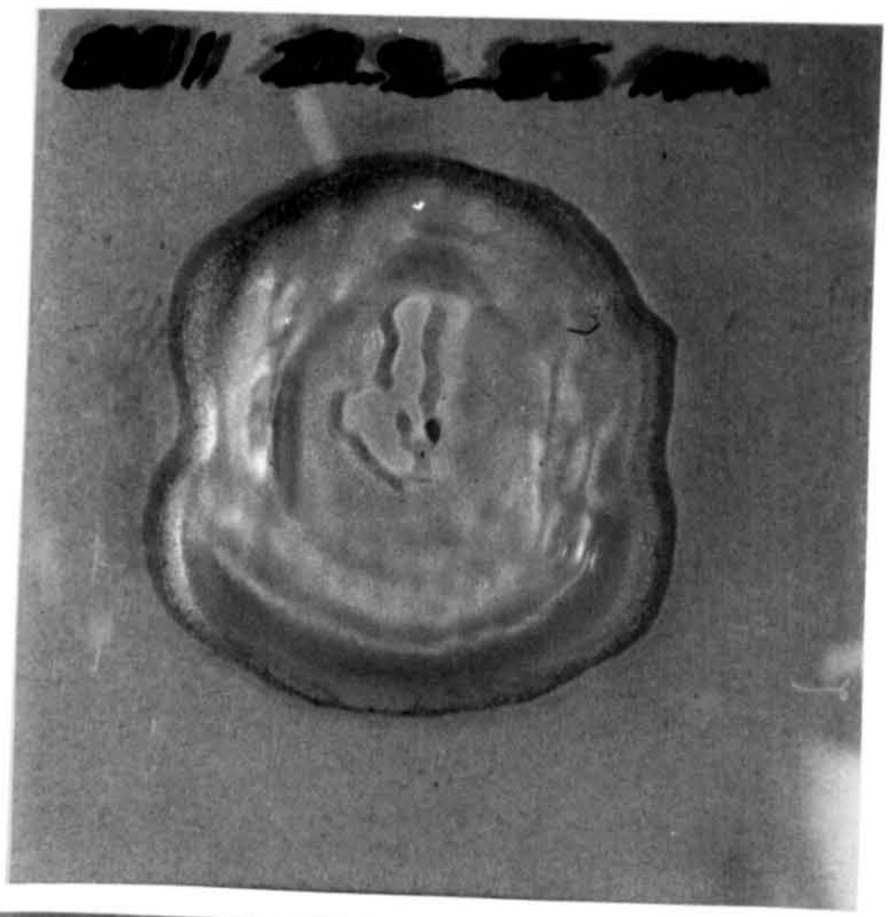

a) Laser output
(doughnut shape)

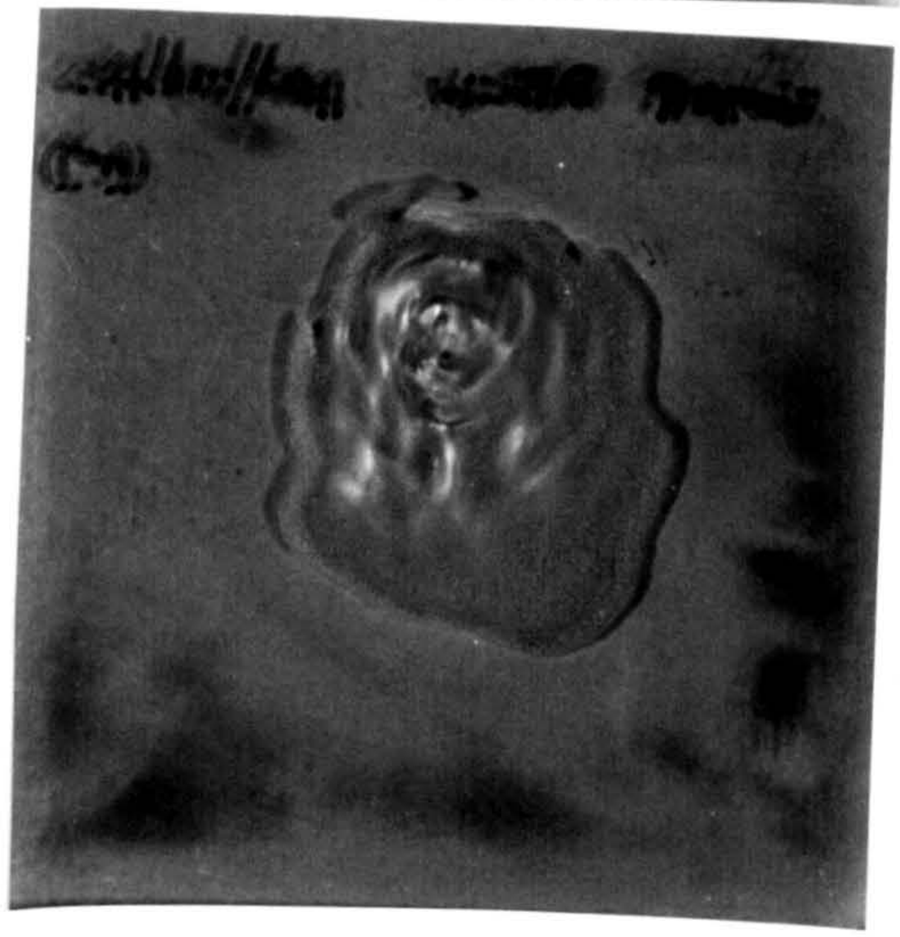

b) Prior to work-
station; central
peak starting to
form

c) At workpiece;
diverged with a
central peak

Figure 4.27 - Beam prints taken at various positions within the beam line from the source to the workstation.

difference in welding performance. This is not to say that the mode, or more importantly, the stability of the mode, might affect weld characteristics. Certainly fluctuations in the mode, affecting the focused spot power densities, could affect keyhole stability and penetration. The longest fluctuations in welding performance would be noticed when existing parameter tolerances are narrow. Therefore for welding, and single sided skid welding in particular, stability of the mode is more important than the nature of the mode.

4.3.4 Focal Depth of Operation

Melt runs were produced using various focal positions (the datum set by visually setting the HeNe spot focus on the plate surface) to find the optimum focal position for penetrating each plate thickness.

While results fluctuated by +/-2.0mm with respect to the plate surface, a single datum was preferred for the majority of the trial programme. Therefore the majority of welds were produced for each plate thickness with the HeNe spot focus positioned on the web plate surface.

While this particular focal position proved satisfactory for producing each thickness of joint, a survey was conducted in 6,7 and 12mm plate (Trials 10 and 11) to assess the parameter tolerance required to maintain or even improve joint formation.

The trial in 7mm plate (Trial 10) proved inconclusive as, by moving the focal position, the spot height had inadvertantly been moved, so that results assessed on bead profile changes due solely to focal changes could not be made.

The trial using 6mm plate (Trial 11) showed a tolerance of -5mm (into the plate) and +15mm(out of the plate) after which penetration for emergent bead formation became disturbed. Certainly by increasing the focal distance the tendency for undercut to occur in the emergent bead reduced. Similarly as the focus was initially moved further into the plate, together with slight undercut, open porosity increased due to a more effective and vigorous action of the focal spot deeper into the plate.

By contrast, the tolerance for movement in focal position welding 12mm plate (Trial 11) reduced to +/-5mm, limited by reductions in penetration. Lack of fusion found within many of the welds also emphasised how, for the larger plate thicknesses (above 10mm) small parameter changes could easily reduce process reproduction due to narrow tolerance envelopes found in each parameter.

4.4 PLASMA CONTROL AND WELD SHROUDING

Plasma control techniques have been used by the majority of authors not simply to stop beam absorption above the joint, but also to improve weld penetration [68] . However, for the process to be accepted commercially the use of expensive Helium for plasma control needs to be minimised. More recently authors have shown, primarily for butt welding, that it is possible to make quite satisfactory joints with less complex plasma control devices [69] .

While mainly helium is used as the control gas for deep penetration welding, further investigations are being made by other researchers in the use of Argon, Carbon Dioxide and Nitrogen [123] . It is interesting to note that for conventional welding there is a trend to include higher proportions of helium in shielding gas mixes for high precision tasks e.g. high integrity TIG welding of nuclear containers.

The price of helium (£3.5/1000 litres for a medium sized user) is high compared with, for example, carbon dioxide used for semi-automatic MIG welding costing nearer 25 pence/1000 litres. The use of a directional jet for plasma control would also lead to operational tracking problems if applied to a multi-axis welding head. Therefore the author attempted to minimise the use of the plasma control jet during welding trials, accepting that a penalty may be paid for not obtaining "optimal" penetration.

4.4.1 Gas Flow Rates to Achieve Plasma Control and Weld Shielding

During Trial 1.0 gas rates were put at the same settings to those used for butt welds, table 4.03. Whilst very disturbed incident beads were experienced during this trial a specific survey of shielding gas rates, Trial 2.4 showed how gas flow through the plasma control jet could be reduced to zero, The gas flow through the "lens" served to control the plasma and act as a general shroud.

Comparison of results from Trial 1 and 2 indicated that the tee joint shape had been acting as a "funnel", concentrating the combined gas flow over the weld keyhole. This disturbed the plasma stability and resulted in irregular weld beads.

Thus the only time that the plasma control jet was employed was during Trial 9 in an attempt to reduce the large incident plasma created when welding 15mm plate at slow speeds (>6mm/second). Therefore, although the presence of a plasma control jet may still have some advantages in refining the process when traverse speeds are low, welding thick plate, these would be easily outweighed by the disadvantages from the reductions in process flexibility.

Apart from the above instance, the lens shroud was used as a combined plasma control and concentrated general shroud. Trial 2 tests showed that in 8mm plate, a lense gas flow of 20L/min was required to give repeatable and good weld profiles. Although welds were formed at lense

Weld Configuration	Plasma control "Jet" flow (L/min)	"Lens" general molten pool shroud (L/min)	Trailing shroud gas flow (L/min)
Butt	20	50	(100)
Skid	0	35	(100)

Table 4.03 - Comparison of plasma control and general shroud gas flow rates used for butt and skid welding

gas flows of 10l/min the results were incapable of reliable repetition and as gas flow reduced to 4.0l/min the increase in incident plasma caused a reduction in weld penetration and excessive porosity in both incident and emergent beads.

The effect of increasing lens gas rates from 20 to 40 litres per minute were analysed, in Trial 4. Although profile variations and changes in joint hardness were marginal a lens gas flow rate of 35l/min was selected to ensure consistency in joint production and properties.

The trailing shroud gas flow rate was maintained at 100 l/min for the majority of trials. For weld lengths when no trailing shroud gas was employed, either during sections of standard welds or for a specific test (Trial 6) the most noticeable difference in appearance was a dull grey discolouration of the weld surface as opposed to the usual clean shiny appearance. No obvious change was found in weld properties, therefore it is expected that the general trailing shroud unit could be removed, in addition to the plasma control jet, as it is only performing a generally "cosmetic" role at present.

4.4.2 Position of Plasma Control Unit

The plasma control/shroud unit was placed with a nominal spacing of 2.0mm from both the web and face plates. The distance of the unit back from the laser focused spot was set initially for the gas flow from the plasma control jet to interact with the laser spot position on the plate

surface.

For tee section welding, by abandoning the use of the specific plasma control jet and making use of the joint "funnelling" effect greater tolerances were available. The unit was not moved closer to the laser spot than described above for fear of beam interaction with the unit. However, the unit was moved away from the "spot" by at least 5.0mm before concern was experienced for an increase in the incident plasma and resulting joint profile deterioration.

The trials have shown how, for commercial use, an essentially simple plasma control device could be used when producing skid welds. For the trials, the off-axis general shroud was employed. However, the tolerance of the results would indicate that the use of a co-axial device would be possible. This would give a general gas flow around the incident beam to provide an adequate general shield and control to the incident plasma.

With this simplified form of weld shielding, a multi-axis beam delivery head would not be restricted by a directional plasma control device, thereby increasing process adaptability and acceptability. Similarly, gas flow may be kept to a minimum and thus increase cost effectiveness, not only by reducing gas consumed, but also by reducing maintenance costs for the simplified equipment.

4.5 SUMMARY OF LASER WELDING PARAMETER SPECIFICATIONS AND TOLERANCES

From the parameter details provided in this chapter the Author has developed the computer program "SKIDWELD" (Appendix B-3) to provide operators of a prototype skid welding workstation with initial parameters for skid welding of ship production type joints as experienced during the trials. The program runs interactively, the operator entering the joint variables, the output providing a listing of the principal processing parameters, figure 4.28. The parameter determination may subsequently form the basis of software for the closed loop control of a prototype workstation. In addition table 4.04 has been compiled to summarise typical parameter specifications and their tolerances, to be considered within the design of the prototype workstation for the production of skid welded joints.

In order to maintain processing parameters within the given tolerances, the most important functions that should also be specified are those of joint finding, tracking and gap assessment. This creates the link between the experimental programme where set joint configurations have been presented for welding and a capacity to produce the weld, repeatably, in the ship production environment.

However, as noted in the introduction to the chapter, the interpolation of results obtained from one particular system to another system should be treated with care to gain accurate weld profile and property reproduction. If this is to be assured, in addition to joint

```
**********************************************************************

                    SKIDWELD
                    ========

INTERACTIVE PROGRAM TO DETERMINE THE INITIAL PROCESSING  PARAMETERS
FOR HIGH POWER LASER SKID WELDING OF TEE SECTION  JOINTS IN SHIP
RODUCTION

**********************************************************************

AFTER EACH VARIABLE INPUT, PLEASE PRESS "RETURN"

JOINT SCANTLING AND CONFIGURATIONS>>>>>>>>
------------------------------------------

ENTER WEB PLATE THICKNESS(MM)
8

ENTER JOINT GAP(MM)
0.5


IF PRIMED PLATE ENTER  "1",  IF NOT ENTER  "0"
0

IF R.S. WEB PLATE ENTER  "1", IF SQUARE EDGE FLAT PLATE ENTER "0"
0

FILLER WIRE INPUT REQUIREMENTS>>>>
----------------------------------

ENTER FILLER WIRE DIAMETER (MM)
1.6

REQUIREMENTS OF LASER POWER (AT THE WORK PIECE)>>>>>>
-----------------------------------------------------

IF 9KW ENTER "9", IF ADVISED POWER REQUIRED ENTER "0"
9

**********************************************************************

                SKID WELDING PARAMETERS
                =======================

SUMMARY OF INPUT VARIABLES
==========================

 WEB PL.     JOINT      LASER      ROLL SEC.  SURFACE      WIRE
THICKNESS    GAP        POWER      RADIUS     COAT         DIA.
  (MM)       (MM)       (KW)       (MM)                    (MM)
-------------------------------------------------------------------
  8.00       0.50       9.00       0.00       CLEAN        1.60

INITIAL PARAMETERS REQUIRED FOR SKID WELDING
============================================

TRAVERSE    SPOT      INCIDENT    FILLER      PLASMA    LENSE     TRAIL
 SPEED     HEIGHT     ANGLE       RATE        JET      SHROUD    SHROUD
(MM/SEC)    (MM)     (DEGREE)   (MM/SEC)    (L/MIN)   (L/MIN)   (L/MIN)
-------------------------------------------------------------------------
 14.00      0.88       7.00        52.32      0.00      35.00     0.00

TO RE-RUN THE PROGRAM ENTER 1; TO EXIT , ENTER 01
```

Figure 4.28 - Typical output from the SKIDWELD program presenting principal skidwelding parameters

Parameter	Remarks	Max.	Min.	Tolerance (+/-)
Laser beam generation:				
Laser power at workpiece (continuous)	Projected for welding in 15mm thick tee joint (Kilowatts)	20	0	100
Manipulator/ focusing head:				
Traverse speed	Welding (mm/sec)	50	0	0.5
	Paint surface etching (mm/sec)	200	0	0.5
Laser beam director from tracked joint position	Height above web plate ie spot height (mm)	+3.0	-1.0	0.1
	Angle above flange plate (deg.)	+20	0	0.5
Laser beam focus	Assume F9 system; distance away from web plate (mm)	+20	-10	1.0
Gas shrouding:				
Flow rate	Helium to a co-axial unit(L/min)	100	0	2.0
Filler input:				
Feed rate	Assuming 1.0mm dia. wire(mm/sec)	300	0	0.5
Wire position	Distance along joint from the laser spot position (mm)	10	0	0.1
	Distance perp. to joint (mm)	1.5	0	0.1
	Angle to face plate (deg)	45	0	2.0
	Angle to laser beam (deg)	45	7	5.0
Joint monitoring:				
Gap sensing	Sensing to joint gap to maintain above factors (mm)	3.0	0.1	0.05

Table 4.04 - Summary of skid welding parameter specifications and tolerances.

sensing, on-line process monitoring and feedback would be essential. Processing diagnostics could include monitoring the incident beam to ensure positional and modal consistency or an assessment of the plasma characteristics to assess penetration functions.

The monitored output would then be compared against standard output characteristics for the production of satisfactory welds, thereby forming a means for fed-back adjustments to be facilitated and ultimately a method for on-line quality control and safety monitoring.